Catalytic membrane reactor for waste water treatments
Ali Abusaloua

▶ To cite this version:

Ali Abusaloua. Catalytic membrane reactor for waste water treatments. Other. Université Claude Bernard - Lyon I, 2010. English. NNT : 2010LYO10122 . tel-00703265

HAL Id: tel-00703265
https://theses.hal.science/tel-00703265

Submitted on 1 Jun 2012

N° d'ordre :122   Année 2010

THESE DE L'UNIVERSITE DE LYON

Délivrée par

L'UNIVERSITE CLAUDE BERNARD LYON 1

ECOLE DOCTORALE de Chimie

DIPLOME DE DOCTORAT en Génie Chimique

(arrêté du 7 août 2006)

soutenue publiquement le 9 Juillet 2010

par

Ali ABUSALOUA

Réacteur catalytique membranaire pour

le traitement d'effluents liquides

Directeur de thèse: **Anne GIROIR-FENDLER**

Koffi FIATY

JURY

Madame **GIROIR-FENDLER Anne**

Monsieur **DUPREZ Daniel**

Monsieur **FIATY Koffi**

Monsieur **IOJOIU Eduard**

Monsieur **KADDOURI Abdel-Hakim**

Monsieur **VALVERDE Jose Luis**

9 Juillet 2010

ACKNOWLEDGEMENT

I would like to take this opportunity to extend my deepest gratitude and special thanks to my supervisor, Dr. Anne GIROIR- FENDLER, of the Lyon I University.

Dr. GIROIR- FENDLER has a sharp eye for tracking the details and superb analytical skills; that have been instrumental in the success of my thesis.

I need to reiterate my deep gratitude to my supervisor, Dr. Anne GIROIR- FENDLER, for accepting to guide me during the completion of the PhD program after the death of my former supervisor Dr. Sylvain MIACHON.

Also I wish to extend my sincere gratitude to my co-supervisor Dr. Koffi FIATY of the Lyon I University. Dr. FIATY has a keen eye for spotting the details as well as excellent analytical skills, which have been paramount in the success of my thesis. In addition, Dr. Koffi FIATY provided insight in membrane reactor modelling, partial differential equations manipulations and MATLAB programming.

My deep gratitude and special thanks goes to my former supervisor the late Dr. Sylvain MIACHON who passed away after two years of a valiant struggle with disease. Dr. MIACHON still lives on scientist in my memory forever. I continue to abide to his invaluable recommendations on being an astute. I wish to express my condolence to Dr. MIACHON family, and to our team of research (Engineering) in IRCELyon.

My gratitude also is extended to Dr. J-A. DALMON. Dr. DALMON has moved on to retirement a few months ago.

I am also grateful to my colleague's in-group meeting (WATERCATOX), particularly, and beside Dr. J-A. DALMON, Dr. Nolven GUILHAUME, Dr. Marc PERA-TITUS and Dr. Mohamed ALAME, for providing fruitful discussions.

Special thanks to all my colleagues in IRCELYON, who have been very supportive during my years as a doctorate student. They have show always concern for my progress and my well being. Some of who, over the years, have become good friends.

Special acknowledgment is also given to Libyan Embassy-Paris for funding this research thesis. The Libyan scholarship Funding enabled the purchase of materials, instruments, and software for the research thesis.

Last but not least, I am greatly indebted to my mother, my father, my wife and my family for their understanding, patience and support during the entire period of my study.

''À ceux qui m'ont appris à monter l'escalier de la vie avec patience et sagesse

ma mère et mon père ''

A mon épouse Zuhira et

mes enfants Abdulalhadi, Fatima, Mohamed, Kawala, Hammam

Je dois avouer ma reconnaissance devant cet aboutissement,

qui n'aurait pu se faire sans le soutien de ma femme

et de mes parents

CONTENTS

11

LIST OF FIGURES

LIST OF TABLES

INTRODUCTION

INTRODUCTION

Water is the most abundant chemical component within the biosphere. It is also the most important. Almost all life on Earth uses water as the basic medium of metabolic functioning. Water's abundance make it ideal as a universal solvent for cleaning and flushing away all manner of waste from human activities. In addition, water possesses several unique physical properties that are directly responsible for the evolution of our environment and the life that functions within it. Water resources have been critical to human society since people discovered that food could be produced cultivating plants. The cities and towns which arose from east Egypt to Mesopotamia (Modern day Iraq) following the Agricultural revolution, about 3500 B.C., required a ready supply of water for domestic as well as agricultural needs [1].

Sustainable water management is one of the critical issues to be addressed in the coming decades. Particularly due to growing populations and countries undergoing industrial expansion, which have triggered primed the need for increased water supply and distribution [2]. A main aspect of sustainable water management is the treatment of wastewater.

The amount of toxic wastewaters and sludge generated by industrial and domestic sources is approaching 500 million metric tons per year [19], also over fourteen million different molecular compounds have been synthesized during the last century and about one hundred thousand can be found in the market [17]. Furthermore, in conjunction with future minimization and rigorous effluent quality control, the Environmental protection agency (EPA) have proposed that some compounds be eliminated up to 99.99 % and use of enclosed treatment facilities [189]. In addition, it must be noted that increased environmental constraints and unfavourable public opinion have challenged the continuation of conventional waste management techniques. To accomplish these objectives, novel waste treatment and process concepts are needed. The widespread application of modern technology to the supply of abundant water for unrestricted municipal, industrial, and agricultural uses, or conservation has greatly increased the competition for limited sources of easily accessible water. Engineers, biologists, sociologists, geographers and many other specialists are all intimately involved in researching and predicting all aspects of water and wastewater management.

The main objective of this work is:

1. Experimental work for wet air oxidation of aqueous compounds solution (selected model compounds) on catalytic membrane reactors.

2. Theoretical modelling of kinetics and hydrodynamic behaviour for catalytic membrane reactors.

 The model compound solutions tested were formic acid, acetic acid, oxalic acid, and phenol.

These experiments were performed on a Watercatox bench setup by using different types of catalytic membranes (monometallic, bimetallic, or trimetallic catalytic membranes). Different combinations of active phase metals loaded these membranes. The metals examined include Pt, Pd, and Ru from the noble metal group and Cu, Fe, Ni, Zn and Co from the transition metal group

1 BIBLIOGRAPHIC STUDY

1.1 WATER POLLUTION

Water quality and the treatment of effluents from all industrial operations remain the major environment focus. Water pollution occurs when the discharge of waste impairs water quality or disturbs the natural ecological balance. Industrial processes can address environmental issues at three stages in the life cycle of the industrial process. The basic process can be initially designed as non-polluting as possible, by minimizing the generation of harmful by products; or those by products generated in the process can be removed through installation of appropriate pollution control equipment; or substances released to the environment can be remediate. The last option is always the most expensive [5]. The contaminates which cause problems include disease-causing organisms (Pathogens), organic matter, solids, nutrients, toxic substances, colour, foam, heat, and radioactive materials.

Water pollution is an imprecise term that reveals nothing about either the type of polluting material or its source. Pollution of our water resources can occur directly from sewer outfalls or industrial discharge (point sources) or indirectly from air pollution or agricultural or urban runoff (non point sources). Wastewater can be divided into four broad categories, according to its origin namely domestic, industrial, public service and system loss/leakage. Among these, industrial wastewaters occupy a 42.4 % of the total volume and domestic a 36.4 % [45].

1.2 WASTEWATER TREATMENT PROCESSES

Since the end of the last century, with an increased awareness of the potential harmful effects of the hazardous materials present in many industrial wastewaters, the destruction of the toxic pollutants from the aqueous effluents has become mandatory.

The principles of wastewater treatment can be mapped according to Henry [1], for their effluent requirements, water quality, and pollution control regulation. Effluent requirement is the primary objective of wastewater treatment is to remove or modify those contaminates detrimental to human health or the water, land, and air environment. Water quality improvements had become widespread by the beginning of this century in the technology of making water safe for public use thought Europe and North America. Pollution control regulation has often been said that the solution to the pollution is dilution. There is logic in the statement. Where small quantities of sewage discharge into relatively large rivers or water bodies, incidents of contaminated water supplies or hazards to public health are less

dangerous if compared to the original contaminants, This because of the dilution of the contaminates and the natural purification that take place.

Therefore, the development of highly efficient techniques for the treatment of such organic contaminated wastewater is crucial. The suspended, colloidal, and dissolved contaminants (both organic and non organic) in wastewater may be removed physically, converted biologically, or changed chemically, or may be removed physically and changed chemically in the same unit as in catalytic membrane reactors which suggested recently by Dalmon et al [144,146-154,158-159,162-167]. The classification of wastewater treatment processes was also reported [2]. The classification that we will present here based on later references with some modification to energy intensive processes

1.2.1 PHYSICAL PROCESSES

Gravity settling is the most common physical process for removing suspended solids from wastewater. Ideal settling is the settling of discrete particles for water treatment also occurs with the removal of grit from wastewater while non-ideal settling. In ideal settling tanks, uniform flow (plug flow) was assumed, undisturbed by eddy currents or wind, and sludge that stayed settled. In fact, because of turbulence - particularly at the tank inlet and outlet short-circuiting of the flow, dead spots in the tank, and the movement of sludge collectors, the behaviour actual settling tanks deviate from idealist.

1.2.2 BIOLOGICAL TREATMENT

Most of the organic constituents in wastewater can serve as food (substrate) to provide for microbial growth. This is the principle used in biological waste treatment, where microorganism converts organic substrate, mainly bacteria (with help of protozoa), to carbon dioxide, water and more new cells.

1.2.2.1 AEROBIC/ANOXIC PROCESSES

In aerobic processes (i.e. molecular oxygen is present), heterotrophic bacteria (those obtaining carbon from organic compounds) oxidize about one-third of the colloidal and dissolved organic matter to stable end products (CO_2+H_2O) and convert the remaining two-thirds into new microbial cells that can be removed from wastewater by settling.

1.2.2.2 ANAEROBIC PROCESSES

In anaerobic biological processes (i.e. no oxygen is present), two groups of heterotrophic bacteria, in a two-step liquefaction / gasification process, convert over 90% of the organic matter present, initially to intermediate (partially stabilized end products including organic acids and alcohols) and then to (CH_4+CO_2).

1.2.3 CHEMICAL PROCESSES

Many chemical processes, including oxidation, reduction, precipitation, and neutralization, are commonly used for industrial wastewater treatment. For municipal wastewater, precipitation and disinfection are the only processes having wide application. Chemical treatment alone or with other processes is frequently necessary for industrial wastes that are not amenable to treatment by biological means. The most fundamental operations, which can be classified under chemical and physical-chemical processes of water and wastewater treatment, are: neutralization, adsorption on activated carbon, treatment by ionic exchange and wet air oxidation. Catalytic wet air oxidation is emerging as economically and ecologically promising technique to convert refractory organic compounds, such as phenol, into carbon dioxide or harmless intermediate, mainly fatty acids, which can later be treated biologically [21].

1.2.4 ENERGY INTENSIVE TECHNOLOGIES

The synonym of energy intensive processes is advanced oxidation processes (AOP) because it utilizes an external energy source to enhance the oxidation performance of a process such as electrical energy source in (electrochemical oxidation), radiation energy source in (photochemical oxidation), or ultrasound energy sources in (sonochemical oxidation).

1.3 MEMBRANE SEPARATION PROCESSES

There are five types of membrane processes, which are commonly used in water and wastewater treatment: electro dialysis, micro or nano-filtration, ultra filtration, and reverse osmosis. A membrane is defined as an intervening phase separating two phases forming an active or passive barrier to the transport of mater. Through these processes dissolved substances and/or finely dispersed particles can be separated from liquids. Membrane processes can be operated as: dead-end filtration mode and cross-flow filtration mode.

1.4 SELECTION OF WASTEWATER TREATMENT PROCESS

In recent decades, much attention has been given to all the existing processes of water treatment ranging from incineration to biological treatment, passing through aqueous oxidation catalytic processes. Not all of the available physical, biological, and, energy intensive, membrane separation, and chemical processes have been described, nor are all of the processes mentioned required in every wastewater facility. Choosing one of the available processes depends on three major variables, namely the concentration of chemical oxygen demand (COD) present in a given stream of water, the quantity of water needed to treat and the costs involved in such a process. The optimal selection of a treatment technology is a difficult task because it depends on several factors. The first attempt to study the suitability of water treatment technologies according to COD content was made by Andreozzi [34] where the criteria that have presented based on COD concentration of the effluents. Figure 1 shows the suitability of water treatment technologies according to COD content
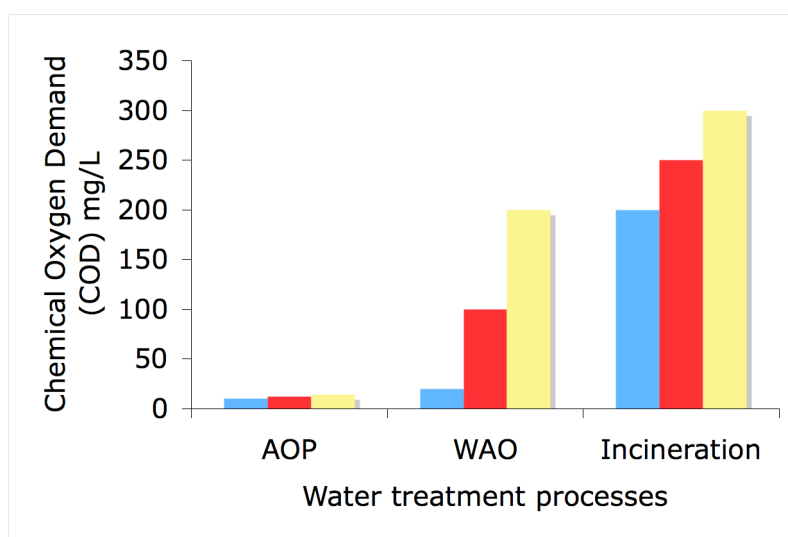
Figure 1: Suitability of water treatment technologies according to COD content

All existing wastewater treatment technologies have been studied for remediation of several model and real effluents. Among all alternative technologies that have been developed, the most important being the liquid phase chemical oxidation. Other alternative technologies such as adsorption on activated carbon and thermal incineration are still used for treatment of refractory effluents.

Several CWAO processes have studied by optimizing, different oxidants used, different catalyst types, different reactor configurations, or operating conditions applied. The optimization of the operating conditions effect in CWAO performance have been investigated by several authors [74-78]. Through oxidation processes, supercritical oxidation process can be done at temperatures and pressures higher the critical temperature and critical pressure of water. Supercritical oxidation is proved as a powerful for CWAO processes but it has accused by high operating cost due to high energy required.

The optimization of oxidant effects in CWAO performance was investigated by testing several types of oxidants, such as air, pure oxygen, hydrogen peroxide, or ozone but the attention always drawn toward the less expensive oxidants [31]. Using external energy source such as further enhances the effect of oxidants in CWAO performance:

i.   Electrical source as in electrochemical oxidation of dyeing [36], electrochemical oxidation of phenol [89, 90], or pulsed corona streamer oxidation [38].

ii. Radiation source as in photochemical oxidation [187].

iii. Ultrasound source as in sonochemical oxidation [37].

The application of these techniques for the destruction of aqueous organic wastes have been tried on bench and pilot plant scale, but they are not used commercially because of their high operating costs, low treatment capacity and low concentrations [37, 38, 89].

Thermal incineration (gas phase oxidation-combustion) is the other well established technology for the treatment of concentrated and toxic organic waste streams, but this technique has accused for the emission of toxic by products such as dioxin and furans [15].

The optimization of catalyst type is investigated by testing either homogeneous or heterogonous catalysts (mono or bimetallic catalysts for example). This means then, the water treatment facilities from a design and operational standpoints vary, but they do rely on overlapping and even identical unit processes. We may organize water treatment into different general areas. Figure 2 shows general areas of water treatment.
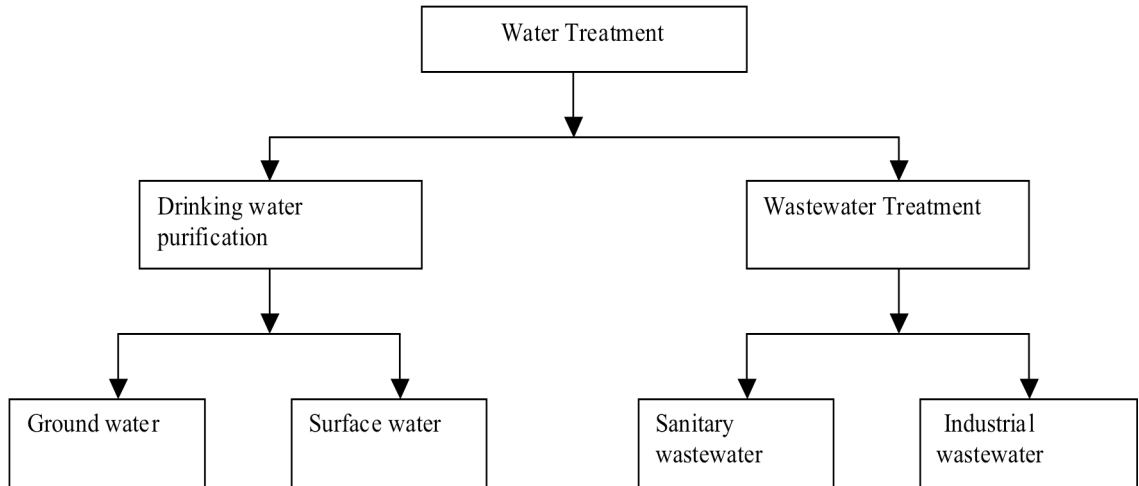
Figure 2 : General areas of water treatment [11].

In this light, costs can be significantly reduced by the use of suitable catalysts able to promote the wet oxidation under milder operating conditions and shorter residence times.

1.5 OVERVIEW OF WAO PROCESSES

Wet air oxidation (WAO) is an attractive destruction method for the treatment of waste streams which are too dilute to incinerate or too concentrated for biological treatment. Oxidation is a process widely used for water treatment by which the pollutants are removed or converted into more biodegradable substances.
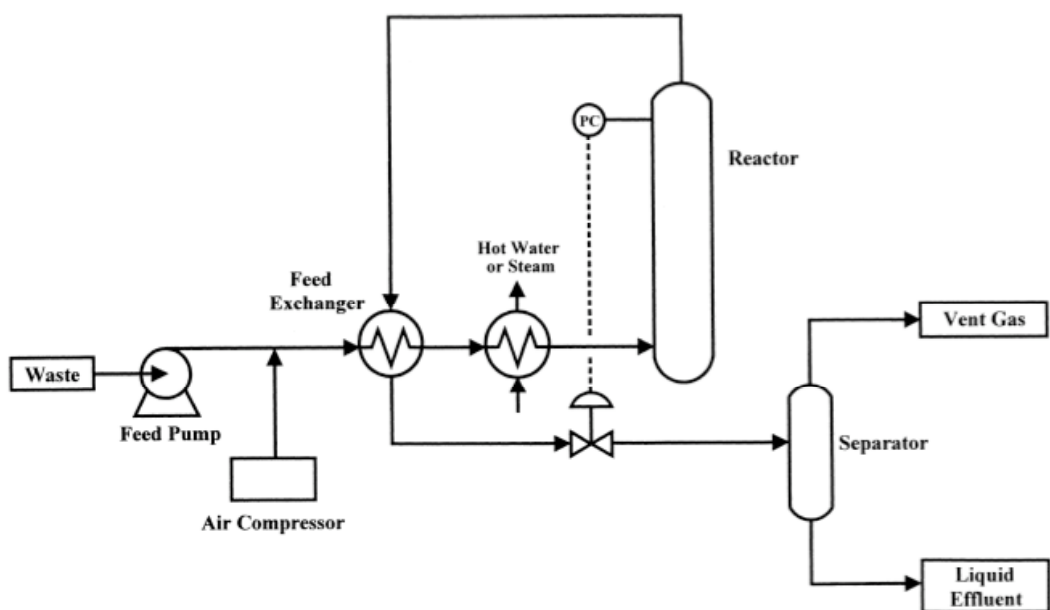
Figure 3: Flow diagram of wet air oxidation process [21]

28

The origins of WAO can be traced to the Strehlenert Process of wood technology patented in (1911) and to the Zinc sulphide oxidation process of hydrometallurgy patented in (1927) as reported by Levec [21]. WAO has been introduced by Zimmerman [14] as primary industrial applications for treating spent pulp mill liquor. Figure 3 shows a basic flow diagram of a WAO process.

WAO process without catalyst may be prohibitively expensive when used to achieve complete oxidation of all organic material present to carbon dioxide and water. Catalytic wet air oxidation (CWAO) processes, (oxidation of organic pollutants in wastewaters by using oxygen or air over solid catalysts) has been offered as an alternative to non-catalytic wet air oxidation in mid seventies. CWAO processes can be done with homogenous or heterogeneous catalysts. Katzer and co-workers (as reported by Levec [19]) were the first who evaluated the catalytic liquid phase oxidation (CWAO) as a potential wastewater treatment technology and offered a process scheme

Figure 4 shows wet air oxidation related processes. CWAO process has developed to minimize the severity of operating conditions in WAO processes. On the other hand, the catalytic wet air oxidation (CWAO) technique is economical and technologically viable for abating or reducing the toxicity of moderately concentrated, toxic, non-biodegradable organic compounds.
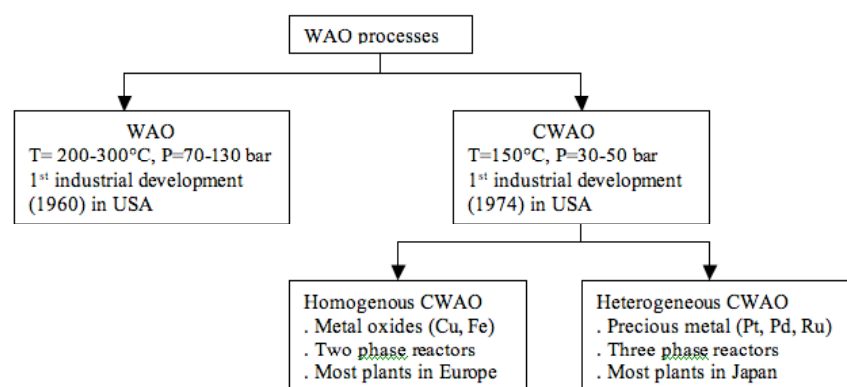
Figure 4 : Wet air oxidation related processes [19]

29

There are several publications, which have reviewed the various aspects of WAO. Zimmerman [14] discussed the WAO process, process conditions, and its application in treatment, and recovery of chemicals from pulp and paper mill effluent.

Kolaczkowski et al. [24] have published an excellent review covering the historical development, treatment of municipal sludge, pulp and paper mill effluent, and chemical industry effluent by WAO, catalytic WAO, use of oxidizing agent other than oxygen, various available reactor designs and processes, construction materials and cost comparison to other processes.

Imamura et al. [27,29] have extensively reviewed the (WAO) catalytic as well as non catalytic of various organic compound solutions, and the oxy desulphurization of coal using WAO. They also discussed the engineering aspects of WAO along with the wastewater treatment methods such as biological and chemical treatment. They have compared the performance of a variety of equipment used for gas-liquid reactions.

Mishra et al. [22] published a very good review that summarise all WAO reviews published prior to 1995. They discussed in detail WAO of pure compound solutions, carboxylic acids, phenols and substituted phenols, cyanides and nitrites. They also discuss industrial applications of WAO, energy and resource generations.

Li et al. [189] have compiled the kinetic parameter for WAO of various organic compounds under sub critical and supercritical conditions. On the basis of these data they proposed a generalized kinetic model for WAO of organic compounds.

Luck [15,18] reviewed the industrial processes of homogenous and heterogeneous CWAO, recent developments in industrial processes of CWAO and discussed a simplified kinetic model for wet air oxidation reactions based on lumped scheme.

Pintar et al. [20] have studied the catalytic processes for the purification of drinking water and industrial effluents. Bahrgava et al. [26] published a very comprehensive review in WAO and catalytic wet air oxidation (CWAO), they discussed in detail four main aspects of WAO and CWAO (i) The chemistry of WAO and CWAO (ii) Reactors suitable for wet air oxidation (iii) Important aspects of CWAO catalysts (iv) WAO of industrial effluents.

Cybulski [23] discussed CWAO processes and the feasibility WAO reactors by using monolithic catalysts. Levec et al [21] discussed CWAO in general; they discussed catalysts used, oxidation kinetics, oxidation processes, and a biodegradability/ toxicity of CWAO effluents. Kolaczkowski et al [24] have outlined the operational principles for all WAO

processes also he has presented schematic flow diagrams for several industrial WAO processes.

1.6 INDUSTRIAL WAO PROCESSES

Nowadays, there are more than 400 wet air oxidation plants operating around the world. The majority being dedicated to the treatment of sewage sludge, spent activated carbon and the rest for the treatment of industrial wastewaters effluents from petrochemical, chemical and pharmaceutical plants [21]. Table 1 shows Industrial WAO processes for wet air oxidations. Several companies have developed CWAO technologies relying on utilizing either homogenous or heterogeneous catalysts.

1.6.1 HOMOGENOUS WAO PROCESSES

Several homogeneous (CWAO) processes have been developed in the recent decades, all processes rely on homogenous catalyst based on transition metals which need however to be separated and recycled to the reactor or discarded.

- Zimpro process

The Zimpro process reactor is a co-current bubble column, with or without internal baffling depending on the desired mixing conditions. The reactor operates at temperatures between 420 K and 598 K and pressures of 2.0 to 12.0 MPa depending on the degree of oxidation required and the waste being processed [31]

- Bayer Loprox process

The Bayer Loprox (low pressure wet oxidation) process is especially suited to the conditioning of wastewater streams prior to biological treatment. In the 1970s, research conducted by Bayer found that wastewater containing compounds difficult to treat biologically could be pre-treated at mild conditions in a wet air oxidation process. These mild conditions would partially oxidize organic substances in the wastewater producing an effluent better suited to subsequent biological treatment [31]

- Wet peroxide oxidation process

The Wet Peroxide Oxidation (WPO) process has been developed in France by the Institut National des Sciences Appliqués (INSA) and the IDE Environnement SA [31]. The

wet peroxide oxidation process uses a liquid oxidizing agent (hydrogen peroxide) instead of a gaseous one (oxygen), eliminating mass transfer limitations. This process is an adaptation of the classical Fenton's reagent (combination of hydrogen peroxide and Fe $^{2+}$), but uses temperatures of around 373 K and pressures 0.5 MPa.

Table 1 Industrial WAO [45]

Process	Waste	Reactor	P (MPa)	T (°C)	Catalyst
Zimpro	Ind. &Sewage sludge	Bubble column	20	280-325	none
Vertch	Sewage sludge	Deep shaft	<11	< 280	none
Wetox	-	Stirred tanks	4.5	200-250	none
Kenox	-	Recirculation	-	< 200	none
Ciba-Geigy	Industrial	-	-	300	Cu^{2+}
LOPROX[1]	Industrial	Bubble Column	5-20	< 200	Fe^{2}
NS-LC	-	monolith	4	220	Pt-Pd/ TiO_2-ZrO_2^{+}
Osaka	Cyanides	slurry bubble	7	250	ZrO_2 or TiO_2
Kurita[1]	ammonia	-	>100	-	Supported Pt

[1] This process uses nitrite as oxidant

1.6.2 HETEROGEONOUS **WAO PROCESSES**

Two CWAO technologies have been developed in the late 80's in Japan by Nippon Shokubai (NS-LC process) and Osaka gas. Both processes rely on heterogeneous catalysts based on precious metals deposited on titania or titania-zirconia supports. The NS-LC process involves a Pt-Pd/TiO_2-ZrO_2 honeycomb catalyst. The Osaka Gas CWO process is based on mixture of precious and base metals on titania or titania-zirconia supports (honeycomb or spheres) [19].

1.7 OVERVIEW OF CWAO PROCESSES

An overview of the current state of art in CWAO, kinetics and reactor design configuration are attempted to outline both the progress done in the field of CWAO and the open key aspects to be addressed by future research work [105]

The reviews of the related research work done in the field of CWAO suggests that several catalyst types and reactor design configurations have been used by numerous authors to destroy a number of model compound pollutants or real effluents in aqueous phases at bench and pilot scale.

1.7.1 MONOMETALLIC CATALYSTS

Several types of catalysts were studied in recent years. There are many important aspects of catalysis and issues related to the use of catalysts in CWAO processes.

The types of catalyst that have been tested for wet air oxidation (WAO), were the most often with metal oxides (mainly Cu or Fe salts or oxides in homogenous catalysts) [73,82,88] or supported precious metals (mainly Pt / Pd / Ru in heterogeneous catalysts) [61,80,87,102,118,135] or activated carbon without any additional active phases [25].

For heterogeneous catalysts, these aspects include catalyst preparation and characterization, catalyst stability, deactivation, and catalyst regeneration, where as for homogenous catalysts, aspects such as the oxidation state of the metal ion, the type of counter anion, solubility and separation from treated effluent are important [24].

1.7.2 CATALYST STABILITY AND DEACTIVATION

All catalysts have an activity life period through its operation time. Catalyst deactivation can be observed due its physical, chemical, or thermal nature as a result to operating conditions that applied in the system. There are several reasons for catalyst deactivation such as poisoning, coking, fouling, practical failure, or sintering. Table 2 shows causes and results of catalyst deactivation.

Table 2 Causes for deactivation [41]

Type	Cause	Result
Chemical	Coking, Poisoning	Loss of surfaces, plugging loss of active sites
Physical	Fouling Particle failure	Loss of surface, Bed channelling, plugging
Thermal	Sintering Compound formation Phase change	Loss of surface Loss of surface and component Loss of surface

In some cases the reasons of catalyst deactivation are reversible, and then catalyst can be regenerated [41,215].

The stability and possible deactivation of a catalyst in WAO has a significant impact on the cost of CWAO processes [26]. Catalyst deactivations can occur by several mechanisms, which have been described by Bartholomew [121].

The deactivation due to formation of heavy polymers through studying CWAO of aqueous phenol over MnO_2/ CeO_2 has been observed by Hamoudi et al. [95].

Santos et al. [122] have observed catalyst deactivation due to copper leaching in CWAO of phenol aqueous solution over copper catalyst.

Barbier et al. [62] have reported that the degradation of acetic acid is due to formation of carbonate species on the catalyst surface during the reaction. Moreover, the formation of carbonates is depended on the type of support (titanium, zirconium, or ceria). Also, they have suggested that when ceria or ceria doped zirconium supports were used, the formation of carbonates is less due to the unique stability of an elevated oxygen transport capacity coupled with the ability to shift easily between reduced and oxidizes states (i.e. Ce^{+3} - Ce^{+4})

Besson et al. [28] have presented a detailed description about deactivation of metal catalysts in CWAO of liquid phase organic reactions. Due to catalyst deactivation problems that encountered in CWAO processes, several research groups have been motivated to look for another catalyst preparation techniques due to catalyst deactivation phenomena by metal sintering or aggregation in supported metal catalysis systems.

1.7.3 BIMETALLIC CATALYSTS

In several publications [172, 208, 210, 215], the preparation of bimetallic catalysts has been described. It is one possibility to avoid metal sintering or aggregation. Layer by layer adsorption of polyelectrolyte/ nanoparticle films is another option to avoid metal sintering or aggregation [174].

Fortuny et al [214] have explored the ability of bimetallic (Cu-Co, Co-Fe, Cu-Mn, Cu-Zn) catalysts supported on alumina for WAO of aqueous phenol solutions at 140° C and 9 bars in packed bed reactor operating in trickle flow regime. Lifetime tests were conducted for 8 days, severe deactivation during first two days, later; the catalyst presents steady state activity until the end of the test. The catalyst deactivation is related to the dissolution of the metal oxides from the catalyst surface due to the acidic reaction condition.

Michaud et al [207] have studied bimetallic catalysts (Pd-Pt) supported on alumina prepared by co impregnation for complete hydrocarbon oxidation. Deffernez [204] has studied several types of bimetallic catalysts (Bi-Pt, Ru-Pd, Pt-Ru) supported active carbon for the selective oxidation of glyoxal into glyoxalic acid in aqueous phase. Kim et al [209] have studied the bimetallic catalysts (Pd-Pt) supported on alumina for oxidation of real effluents from textile plants (reactive dye solutions) in presence of 1% H_2. Zhang et al [211] have studied the bimetallic catalysts (Pd-Pt) supported on alumina for wet air oxidation of real effluents from paper and pulp mill plants (black liquor). Barbier et al [104] have studied bimetallic Pd-Ru catalyst supported on alumina or ceria / alumina for WAO of aniline or ammonia at 150-250 °C and 20 bar. The greatest interest of CWAO compared to the classical biological one is that the selectivity toward molecular nitrogen is much higher (90%). With the bimetallic Pd-Ru/CeO_2 alumina catalysts, the optimal ammonia conversion is obtained at 200 °C

Sinfelt as reported by Ponec [215] is the first one who has introduced the term "bimetallic" and he has discussed why this term has got the preference for the classical term – alloys. An alternative is to polish a little the ancient term of alloys and use the definition that by alloy catalysts we mean those, which contain alloys in the working or precursor state of the catalysts. As far as the signification of alloys is concerned, authors of a recent monograph arrived after inspection of literature to the following conclusion: alloy is most conveniently defined as a metallic system containing two or more components, irrespective of their intimacy of mixing or, precise manner of mixing [215]. Alloys can form a continuous series of solid solutions (monophasic alloys) or segregate under the critical temperature into two

phases (biphasic alloys). Elements of a very limited solubility can still form the "surface alloys". There are a number of studies oriented toward characterization and morphology analysis of bimetallic catalysts. Rousset et al [208] have studied and characterized Pt-Pd bimetallic catalyst clusters in both free and supported phases. They observed a sequential evaporation of Pd atoms in the mixed clusters consistent with a palladium segregation process. This tendency has been also observed on supported particles from which the structure and the compositions are determined by high-resolution TEM and EDS analysis.

Batista et al [213] have studied bimetallic (Pd-Cu) catalysts with different Pd: Cu atomic ratio (2:1,1:1,1:2) prepared by successive impregnation and the bimetallic material has been characterized by XRD, EDS, TEM, and EXAFS analysis. It is found that both surface compositions and bulk structure of the bimetallic particles varied with the Pd: Cu atomic ratio, while the size of particles did not change significantly. Pd: Cu with 2:1 atomic ratio exhibited the highest selectivity in a liquid-phase nitrate reduction.

Kim et al [212] have prepared Pt-Ru bimetallic catalysts by reverse micro emulsions for fuel cell catalysts. The results show that the particles diameters are between 2-4 nm, and these nanoparticles have a high active surface area and stability. The bimetallic Pt-Ru catalyst prepared by this method has higher activity for reformat gas oxidation. Romanenko et al [205] have studied the influence of ruthenium addition on sintering of carbon-supported palladium. It is shown that the introduction of ruthenium in the composition of palladium catalysts results in the increase of their sintering stability. Jhung et al [206] have studied bimetallic Pd-Ru supported on activated carbon for hydro purification of terphathalic acid. Breen et al [210] have studied Pt-Ru bimetallic catalysts supported on activated carbon for liquid phase hydrogenation of 2-butanone at 30°C and 3 bar. The activity of this bimetallic catalyst was more than of the sum of the monometallic Pt or Ru catalysts.

1.8 WAO REACTORS

Several authors have classified three phase reactors such as Smith [7], Fogler [8], Cybulski [23], Kolaczkowski [24], Eftaxias [25], and Bhargava [26].

Torres [43] has classified three phase reactors to the following types:
1. Conventional or classical reactors
    i.   Fixed bed reactors.
    ii.   Fluidized bed reactors.
    iii. Trickle bed reactors.

iv.   Reactor with mechanical agitation.

2. Non classical reactors

i.   Monolith like reactors some times named micro reactors [23]

The effective and economical viability with which the CWO process is applied to industrial problems is highly influenced by the choice of reactor concept and its detailed design, this mainly due to multiphase nature of CWO reactions [24]. In WAO without catalyst, the oxygen transfers from gas phase to liquid phase play a dominant role in the reaction rate. For slightly soluble gases, gas phase mass transfer resistance can be neglected in compared to the resistance in the liquid side; over all mass transfer is effectively controlled by liquid phase resistance [26].

Extensive kinetic models have been developed for CWAO reactions from simple lumped schemes to very detailed reaction scheme, including simple empirical power laws, to mechanistic Langmuir-Hinshelwood kinetics. The CWAO reactors can be mapped according to the open literature for their applicability to convert several model pollutants and real effluents as most work has done by utilizing conventional or classical reactors [25,39,87], recently by testing monolithic reactors [23].

1.8.1 WAO in conventional reactor

There are two main conventional reactor types that were mostly used for CWAO [23]:

. Packed-bed reactors (fixed-bed, fluidized bed, or trickle-bed)

. Slurry reactors (agitated ones or bubble slurry columns)
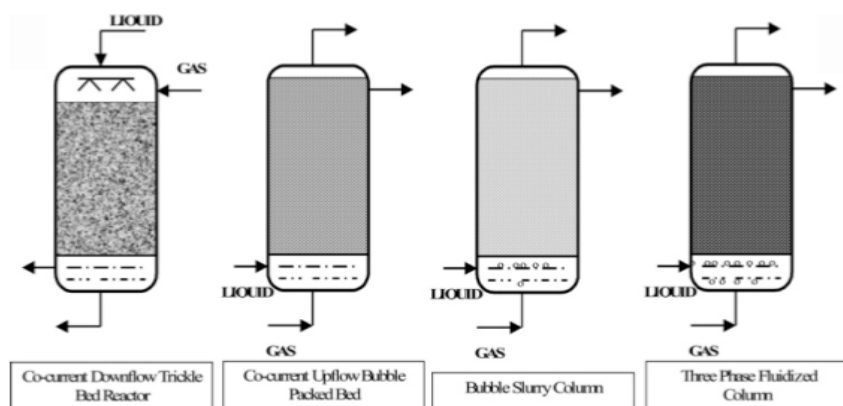
Figure 5 Conventional three phase reactors [23]

Among all types of the conventional reactors that usually utilized in CWAO processes, several authors have reported that trickle bed reactors are the most suitable for CWAO of aqueous organic phases [23].

1.8.2 CWAO ON MONOLITHIC REACTORS

Several authors have studied monolithic catalysts and reactors for three-phase application for CWAO. Cybulski [23] presented a very comprehensive study in the feasibility of monolithic catalysts and reactors. Ismagilov [51] have studied the monolithic catalyst design, the prospects of application for environmental protection in several countries of the world in USA, in EU, and especially in Russia. Luck [53] tested monolithic like reactors for CWAO of waste streams containing bio solids. The reactor performance was optimized through using several flow rates and several COD concentration. Klinghoffer [70] tested the monolithic reactor for CWAO of acetic acid at various flow conditions. The monolithic reactor performance was optimized through operated in the bubble train flow regime. The kinetics of acetic acid oxidation also studied in the presence of monolithic Pt/ γ-Al$_2$O$_3$ catalyst.
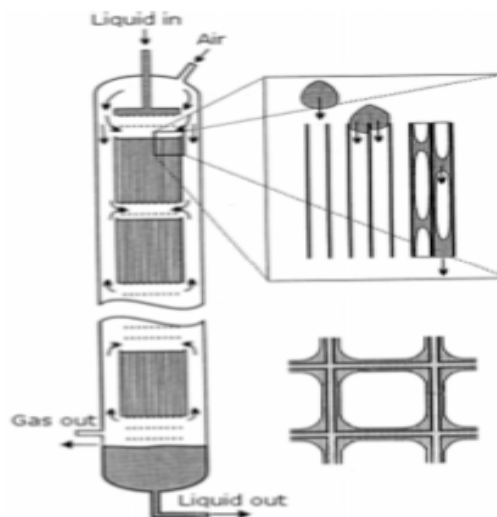
Figure 6: Monolithic Reactors type used for CWAO processes [24]:

1.9 WAO OF CARBOXYLIC ACIDS

Wet air oxidation of carboxylic acids have been studied extensively as they are somewhat difficult to oxidize, and, hence, usually it appears as an intermediate compounds to achieve complete oxidation toward CO_2 and H_2O. CWAO with homogenous or heterogeneous catalysts can be done at relatively low temperatures and short residence times in compared with WAO without catalyst

Table 3 provides a summary of some reported studies in CWAO of carboxylic acids.

Table 3: CWAO of some carboxylic acids

Catalyst		Polluted Model	Reactor type	T (C) P (bar)	Ref
Active phase	Support				
Cu-Zn	Glass bed	Formic acid	Fixed bed	204-240 C 40	**61**
Pd	alumina	Formic acid	Fluidized bed	100-150 C 10-40 bar	**59**
Pt	Carbon	Formic acid	Slurry reactor	10-20 C 6 bar	**57**
Mn, Co, La	Zinc aluminates	Acetic acid	packed bed	250-280	**7**
Cu, Mn	Ceria-zerconia	Acetic acid	Fluidized bed	100-247 50	**64**
Ru	Carbon	Acetic acid	Batch	200-300 7-15	**66**
Ru	CeO_2, TiO_2, ZrO_2	Acetic acid	Batch	200 5-20	**65**
Ru	CeO_2	Acetic acid	Batch	170 – 190 15	**67**
Pt	CeO_2 ZrO_2/CeO_2-Pr	Acetic acid	Batch	200 20	**62**
Pt	CeO_2, ZrO_2/CeO_2Pr	Acetic acid	Batch	200 20	**69**
Ru	CeO_2 ZrO_2 ZrO_2-CeO_2 TiO_2 - CeO_2	Acetic acid	Batch	200 40	**71**
Pt	Al_2O_3	Oxalic acid	Batch	40-50-80 C 1bar	**72**
Ru	CeO_2	Maleic acid	Batch	160-200 20	**86**
Pt	Al_2O_3	Formic acid Oxalic acid Maleic acid	Batch	80 1	84
Ru	TiO_2	Formic acid Acetic acid	Trickle bed	55-250 50	87
Ru	TiO_2	Acetic acid Succinic acid	Slurry reactor	180-200 3-18	85
Pt, Pd, Ru	Carbon nanofiber	Formic acid	Fixed bed	60-220 10	157
Ru	Carbon	Acetic acid Propionic acid Buteric acid	Stirred	200 6,9	81
Ir	Carbon	Buteric acid IsoButeric acid	Batch	200 6,9	80

The activity of CWAO catalysts was tested in different types of conventional reactors using model compounds or real effluents. CWAO of phenols, carboxylic acids, and some real industrial effluents in conventional reactors are reviewed, and it will be presented with their catalyst types and operating conditions.

Scrutiny of the past literature reveals that the major parts of CWAO of refractory carboxylic acids were tested based on precious metal supported catalysts.

In Table 3, Gallezot et al [66] have studied wet air oxidation of acetic acid on Ru supported on active carbon or graphite. The results suggested that Ru supported on graphite is more active than Ru supported on active carbon for wet air oxidation of acetic acid.

Lee et al [84] have studied $Pt/\alpha Al_2O_3$ for WAO of malice acid, formic acid and oxalic acid under high pressures and atmospheric pressure.

Parkas et al [83] have utilized the catalysts Pt/TiO_2 and Ru/ZrO_2 in oxidation reactions of succinic acid. The catalyst Pt/TiO_2 was more active than Ru/ZrO_2 and more stable in oxidation reaction of succinic acid.

Beziat et al [85] have studied the catalytic activity of (2.8wt %) Ru/TiO_2 for oxidation of succinic acid, acrylic acid, acetic acid and cyclohexanol. They have concluded that high conversions of organic acids was achieved, also the catalyst is stable.

Oliviero et al [86] have studied maleic acid oxidation on 5% Ru/CeO_2 /HAS5.

They have demonstrated that easy conversion of maleic acid oxidation as an example of refractory short chain carboxylic acids.

Barbier et al [62] have studied the oxidation of acetic acid in the presence of variety active metals supported on γ-Al_2O_3, CeO_2, and TiO_2. Their activities have classified in the following order: Ru $\langle$ Ir $\langle$ Pd $\cong$ Fe $\cong$ Cu $\langle$ $\cong$ Ni $\cong$ Co $\cong$ Cr.

Gomes et al [79, 80 and 81] have studied the catalytic activity of Pt/active carbon for oxidation of C_2-C_4 carboxylic acids. The supports γ-Al_2O_3, CeO_2, TiO_2, and ZrO_2 also have utilized with active supported noble metals.

1. 10 CWAO OF PHENOL

Catalytic wet air oxidation is emerging as economically and ecologically promising technique to convert refractory organic compounds, such as phenol, into carbon dioxide or

harmless intermediate, mainly fatty acids, which can later be treated in conventional wastewater treatment units [21]. Phenol wastewater is extensively produced from many industries, conferring a heavy burden to the environment. Phenol and its derivatives are known to be detrimental to human health and aquatic life and they will give water a particularly disagreeable taste and odour even at low concentrations [117]. Therefore, phenol-contaminated wastewaters require specific treatment prior to their discharge. Numerous studies have been conducted in the last three decades on the CWAO of phenols because phenol is found in aqueous end pipe effluents from several industrial units such as petrochemical, coke, paper, shale oil, and plastic industries. Table 4 summarize some reported studies CWAO of phenols

Table 4: CWAO of Phenols

Catalyst		Polluted Model	Reactor type	T (C) P (bar)	Ref
Active phase	Support				
Ru	TiO_2	Phenol	Trickle bed	55-250 50	**87**
Cu-Zn	Al_2O_3	Phenol	Semi-batch slurry	105-130 4.6-13.1	**115**
Cu, Zn	γ-Al_2O_3	Phenol p-clorophenol P-nitro phenol	Semi-batch slurry	130 5.6	**32**
Cu, Zn	γ-Al_2O_3	p-clorophenol P-nitro phenol	Fixed bed	150-190 30	**116**
Ru-CeO_2	Carbon	Phenol	Batch	160-200 20	**91**
Cu, Ni, Al	LDHS	Phenol	Trickle bed Semi batch	140 8.9	**109**
Cu	γ-Al_2O_3	Phenol	Fixed bed	140 44,4	**107**
Cu, Ni Cu Al_2O_4 Ni Al_2O_4	γ-Al_2O_3	Phenol	Semi batch	140 44.4	**108**
A carbon Cu	γ-Al_2O_3	Phenol	Trickle bed	140 46.4	**112**
Cu	γ-Al_2O_3	Phenol	Trickle bed	140 46.4	**111**
Al-Fe	Pillared clays	Phenol	Batch	70 1	**129**
Al-Fe	Pillared clays	Phenol	Continuous	18-70 1	128
A Carbon	-	Phenol	Trickle bed	120-160 1-2	126
Ru	ZrO_2	p-clorophenol	Batch	50	101
Pt, Pd, Ru	$Ce_{0.33} Zr_{0.63}Pr_{0.04}$	p-clorophenol	Batch	50	102
Pt, Pd, Ru	Carbon nanofiber	Phenol	Fixed bed	180-240 10	157
Cu, Zn, Co	-	Phenol	Batch Batch recycle	150-210 30	
Fe-Co	-	Phenol	Batch	40 1$	130

Pintar et al [21] have studied the activity of transition metals Cu, Zn supported on alumina for CWAO of phenol. The catalytic activity for oxidation of phenol compounds has classified by the following order: Phenol ⟨ p-chlorophenol ⟨ p-nitrophenol.

The catalytic activity of copper for phenol oxidation has decreased rapidly due to formation of polymers on the catalyst surface [32, 115, and 116].

Fortuny et al [112] have studied the catalytic activity of phenol oxidation on copper or active carbon. The activity of active carbon was decreased due to combustion of carbon even at low temperatures. The combustion carbon reduces oxygen partial from 9 bars to 2 bars.

Aljandre et al [107 and 109] have demonstrated that the catalyst $Cu/MgAl_2O_3$ relatively stable when used in trickle bed reactor for phenol oxidation, but when used in slurry reactor the activity was decreased probably due to formation of polymers. This behaviour of $Cu/MgAl_2O_3$ was not observed for Cu-Ni/ $MgAl_2O_3$ catalyst.

Li et al [101 and 102] have studied the oxidation of chlorophenols on Ru/ ZrO_2, Pt, Pd, or Ru supported on $Ce_{0.33} Zr_{0.33} Pr_{0.04}$. they have demonstrated that Ru/ZrO_2 was active in the oxidation of 2-chlorophenol. The catalyst 3% wt Ru/ $Ce_{0.33} Zr_{0.33} Pr_{0.04}$ was found active for oxidation of 3-chlorophenol and 4- chlorophenol. The activity of 3% wt Ru/ $Ce_{0.33} Zr_{0.33} Pr_{0.04}$ is better in compared with the activity of Ru/ ZrO_2 catalyst.

1.11 CWAO OF REAL EFFLUENTS AND MISCELLANEOUS COMPOUNDS

The majority of studies conducted on CWAO have focused on the CWAO of several model compounds (26); relatively very few studies have been conducted on CWAO of real effluents such as dyeing and printing wastewater, olive oil mill effluents, and detergents wastewater, Table 5 shows CWAO of real effluents and other pollutants

Table 5: CWAO of real effluents and other pollutants

Catalyst		Effluent	Reactor type	T (C) P (bar)	Ref
Active phase	Support				
Pt, Pt-Pd	Al$_2$O$_3$	B5, B19, R198	Batch	200 2.3	118
Ru	ZrO$_2$ CeO$_2$	D0, E1	Batch slurry	190 54	114, 113
Cu, Fe	Carbon nanofiber	TWW	Micro reactor	120-160 6.3-8.7	120
Cu-Zn, Pt, Pd, Ru	Al$_2$O$_3$	LAS	Semi Batch slurry Continuous	300 10	119
A carbon	-	Phenol+ 4-hydroxy Benzoic acid	Batch Fixed bed	130-160 10-20	123
Pt, Ru	ZrO$_2$ TiO$_2$	p-hydroxy-phenyl Acetic acid p-hydroxy benzoic acid	Batch	140 50	97
Pt, Ru	ZrO$_2$ TiO$_2$	P-comaric acid	Batch	140 50	96
Ru	ZrO$_2$ TiO$_2$	P-hydroxy Benzoic acid	Batch Continuous	140 50	100
Cu Cu-Co	Ceramic honeycomb	Isopropanol	Pilot RCO	200-400	131
Au	CeO$_2$ Al$_2$O$_3$ Ceramic foams	Isopropanol	Monolith U-shaped glass	100	132
Au	CeO$_2$ Al$_2$O$_3$ TiO$_2$ Fe$_2$O$_3$	Isopropanol	Continuous	40-300	133
(VO)$_2$P$_2$O$_7$	-	Tetrahydrofuran	Micro-reactor	400-435	134
Pt, Cu-Zn, Cu-Mn,	Al$_2$O$_3$	EG	Batch reactor	160-220 15-25	135

Rodriguez et al [147] have studied catalytic wet air oxidation of textile industrial wastewater using copper supported on carbon nano fiber (CNF). They have demonstrated that the use of a Cu/CNF catalyst significantly improves the TOC and colour removal efficiencies and it can be considered as an option for a pre-treatment step in the treatment of these industrial effluents.

Kim et al [118] have studied monometallic Pt/ Al$_2$O$_3$ or bimetallic Pt-Pd/ Al$_2$O$_3$ for catalytic oxidation of reactive dye solutions (Black 5 "B5", Blue 19 "B19", or Red 198 "R198") as a model compound to dye house effluents. They have demonstrated that the bimetallic Pt-Pd/ Al$_2$O$_3$ catalyst showed high activities toward the wet oxidation of reactive dyes (B5, B19, and R198) in the presence of 1% H$_2$ together with excess oxygen.

Abu-Hassan et al [119] have studied wet air oxidation of linear alkyl benzene sulfonate (LAS) on monometallic noble metals Pt/Al$_2$O$_3$, Pd/ Al$_2$O$_3$, Ru/Al$_2$O$_3$ or bimetallic Cu-Zn/Al$_2$O$_3$. LAS are found in the removal from synthetic detergents and surfactants. They have demonstrated that bimetallic Cu-Zn/ Al$_2$O$_3$ was more active than

noble metals (Pt/Al$_2$O$_3$, Pd/ Al$_2$O$_3$, Ru/Al$_2$O$_3$) but bimetallic Cu-Zn/ Al$_2$O$_3$ is less stable than noble metals due to metal leaching with tested solutions.

Pintar et al [113, 114] have studied wet air oxidation of two real effluents from paper plant, the acidic (D0) and alkaline (E1) of kraft bleaching plant on Ru/TiO$_2$, or Ru/ZrO$_2$. The results have shown that the catalysts Ru/TiO$_2$, or Ru/ZrO$_2$. Are considerably active in the TOC removal of both acidic (D0) and alkaline (E1) effluents.

1.12 ENHANCEMENT OF CWAO PERFORMANCE

Optimally, in CWAO, the dissolved organic compounds will be oxidized to carbon dioxide and water but the reality is far from this ideal objective due to economic and environmental reasons. Matthews et al [147] have reported that the performance of CWAO processes can be enhanced by changing the reactor operation mode from continuous mode (plug flow system) to recirculation mode (semi batch system). Several kinetic studies suggested that oxidation reactions of aqueous organic solutions can be occurred by free radical chain mechanism [117]. In CWAO reactions many intermediates of the radical chain autoxidation reactions that formed during the early (rapid) phase of WAO processes (e.g., hydroxyl HO$^\circ$, and alkoxyl RO$^\circ$ radicals) are highly energetic and highly reactive. Hence, if a WAO reactor system is configured appropriately (change from continuous mode to recirculation mode) figure 9 these reactive intermediates might be used to degrade recalcitrant products of partial oxidation. Weinstock as reported by Matthew et al [147] demonstrated that at industrial level, the use of recirculation mode of operation enhanced the performance of WAO of an effluent-free (i.e closed mill) wood-pulp delingnification technology.
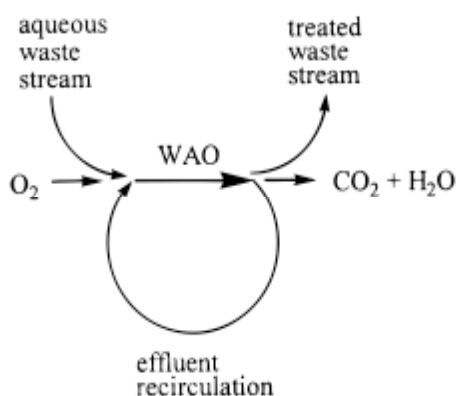
Figure 7: Scheme of recirculation mode for CWAO processes

Three phase trickle-bed reactors have used extensively in CWAO processes in bench scale and industrial application [24] due to the following advantages, fast the gas diffusion through the liquid film to the catalyst surface, little back mixing, easy catalyst separation and simple catalyst regeneration but three phase reactors still have some disadvantage:

- Heat transfer limitations (highly exothermic reactions – oxidation or hydrogenation)
- Mass transfer limitations (catalyst pellet size is too large)
- High pressure drop (catalyst pellet size is too small)

Due to these limitations researchers have motivated for finding other reactor types with new design configurations. Membrane reactor concept has recently proposed as a reactor with new configuration distinguished from conventional three phase reactors. Membrane and membrane reactors will be described in detail in the next section (2.11), membrane reactor investigated in this thesis work is interfacial contactor membrane reactor for wet air oxidation reactions of aqueous liquid phases. CMR operates in a flow through mode with separate feeds. The catalyst is loaded in the membrane wall structure in nanoparticle form with several methods

1.13 MEMRANE AND MEMBRANE REACTORS

1.13.1 MEMBRANE: THE STATE OF ART

A membrane is defined as an intervening phase separating two phases forming an active or passive barrier to the transport of mater [1]. Based on this definition membrane can be found in the three forms of mater, gas, liquid, or solid. The most popular example for membrane in gas phase, is the stratospheric ozone layer around the earth to separate or reflect harmful part of sun rays and the story of ozone layer depletion by CFC compounds also the possibility of global warming from increasing levels of trace atmospheric contaminants [5]. One example of membrane in liquid phase, is supported liquid membrane system containing 2-ethylhexyl phosphoric acid mono 2-ethylhexyle ester for rare earth separation and refining due to high purity objective in the development of functional materials such as super and semi-conductors, this type of membrane liquid allows both extraction and recovery in the single unit [6].

The major popular class of membranes is in the solid phase that may be made from organic or inorganic materials. Inorganic membrane science and technology is relatively a

new field of membrane separation technology which until recently was dominated by the earlier of polymer membranes, currently the subject is undergoing rapid developments and innovation [47].

In recent decades there are several review papers and books related to the subject of membrane and membrane reactors have been published by a number of authors; Burgraaf et al [47] studied the fundamentals of inorganic membrane science and technology. Hsieh [48] studied the general aspects and application of inorganic membranes for separation and reactions. Gryznov [52] have presented the main events in the development of membrane catalysis; also the finding by Frost in the USSR about the hydrogen evolved from Pd film is much more active in hydrogenation than feeded as gas with a hydrogenable substance. Zaman et al [54] have published a very interesting review in various applications of inorganic membrane reactors with particularly emphasis on their application in high temperature gas phase reactions. Tsotsis et al [46] have published a first book completely dedicated to the topic of membrane reactors; different membrane reactors applications to many common classes of catalytic reactions including dehydrogenation; hydrogenation; and partial and total oxidation reactions also the topic of catalytic membrane reactors has discussed in detail.

Leon et al [56] have presented a brief overview of recent developments in inorganic mesoporous membranes; with emphasis on aspects relevant to catalytic membrane processes.

Coronas et al [50] have presented an overview discussion about some of the developments and outstanding opportunities in the field of catalytic reactors based on both inert and catalytic porous ceramic membranes, also inorganic membranes has classified according to their type of material to dense, porous, or composite as shown by table 6

Table 6: Inorganic membrane types

Membrane type	Material
Dense	- Metallic - Solid electrolyte (doped zirconium)
Porous (symmetric or asymmetric) metal oxides (zirconium, titanium; alumina, silica); carbon, glass, zeolite	- Macroporous - Mesoporous - Microporous
Composite	- Glass-metal - Ceramic-metal - Metal-metal

Porous membranes can be further classified based on their pore structure to symmetric and asymmetric. Figure 8 shows pore structure of porous membranes

Symmetric membrane   Asymmetric membranes
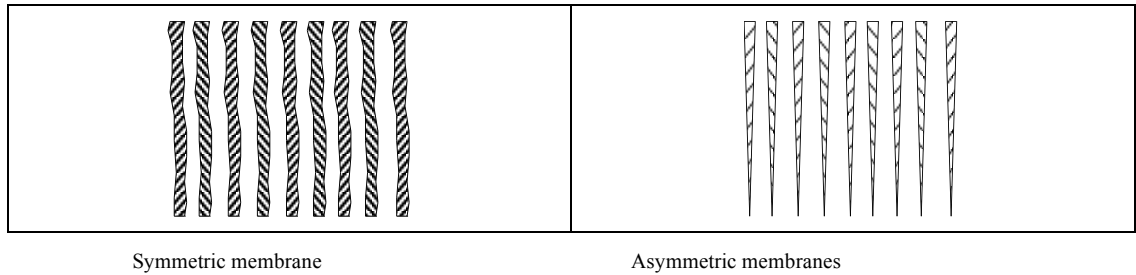
Figure 8 : Pore structures of porous membranes

Classification of membranes based on their geometric shape are shown in figure 9

Plan   *Tube*   *Multichannel*
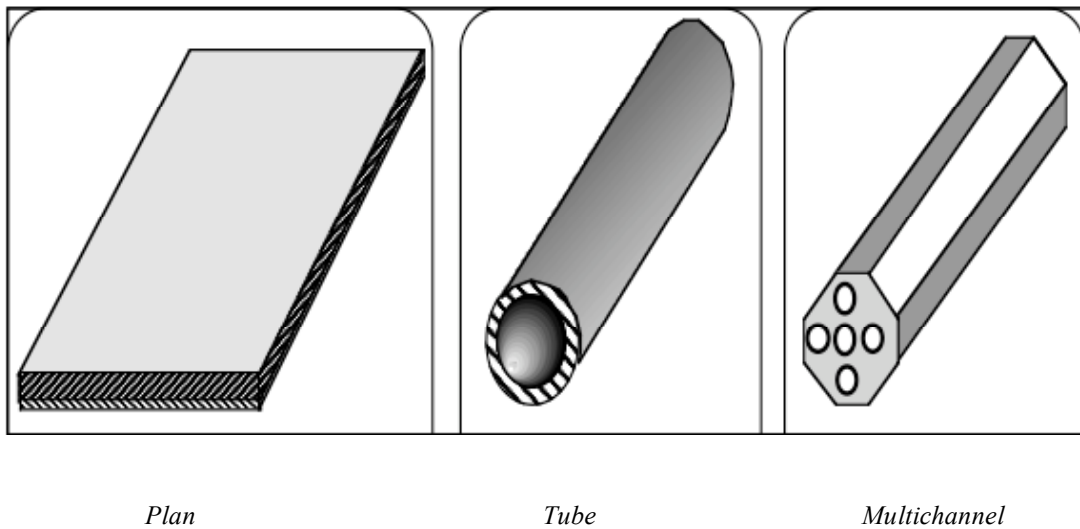
Figure 9 membranes geometric shapes

1.13.2 INORGANIC MEMBRANES:

Inorganic membranes were developed in the 40's for nuclear applications, and essentially for the separation of uranium isotopes by the process of gaseous diffusion applied to UF6. Non-nuclear applications of these membranes started at the beginning of the 80's with MEM- BRALOX produced by CERAVER (now SCT), CARBOSEP produced by SFEC (now TECH- SEP) and CERAFLO produced by Norton (and now SCT) [169]

Organic polymer membranes are established for low temperature applications, especially in membrane bioreactors. Porous organic membranes are usually made of polysulfone, polyacrylonitrile or polypropylene. Dense organic membranes are made of silicone; perfluorpolymers, polyimide or polyamide [40]

Inorganic membranes generally have the advantage of an increased range of applications concerning temperature and chemical stability. High cost and difficult sealing are the most important disadvantage that drawback the development of inorganic membranes [42]. Dense inorganic membranes are either composed of noble metals (Pd, Pt, Ag and alloys or of conductive ceramics (perovskites, modified zirconia). Porous inorganic membranes are made from a variety of materials. Noble metals alloys and stainless steel, ceramics such as aluminium oxides, silicon oxide, titanium oxide, zirconium oxide, zeolite, carbon or diverse glasses [41].

Composite membrane is supposed to combine the permselectivities of dense or microporous membranes with the permeabilities of the macroporous membranes [155].

1.14 INORGANIC MEMBRANES FOR MEMBRANE REACTORS (MR)

Scrutiny of the recent literature concerning the membrane and membrane reactors research, there are different definitions exist for membrane reactors (MR), including or including different border cases. The International Union of Pure and Applied Chemistry (IUPAC) defines a membrane reactor as a device for simultaneously carrying out a reaction and membrane based separation in the same physical enclosure [40].

Julbe et al [55, 155] have presented in first publication an overview and new ideas for porous ceramic membranes for catalytic reactors; and have presented in the second publication the limitations and potentials of oxygen transport dense and porous ceramic membranes for oxidation reactions.

Julbe et al [55] has classified membrane reactors based on either main membrane functions or membrane/catalyst arrangements. There are three types of membrane reactors based on main membrane functions:

i.   Selectively remove the products from the reaction mixture (Extractor) Figure 10

ii.   Control the addition of reactants to the reaction, limits side reactions (Distributor) Figure 11

iii.   Intensify the contact between reactants and catalyst (Contactor)

There are two types of catalytic membrane contactors, interfacial contactors Figure 12 and flow through contactors Figure 13
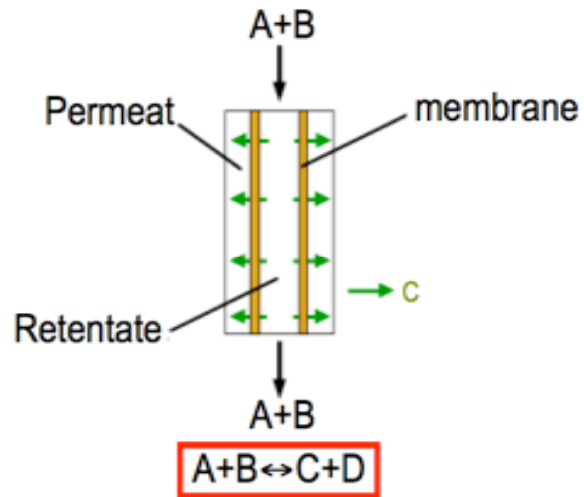
Figure 10 : Extractor membrane reactor [42].
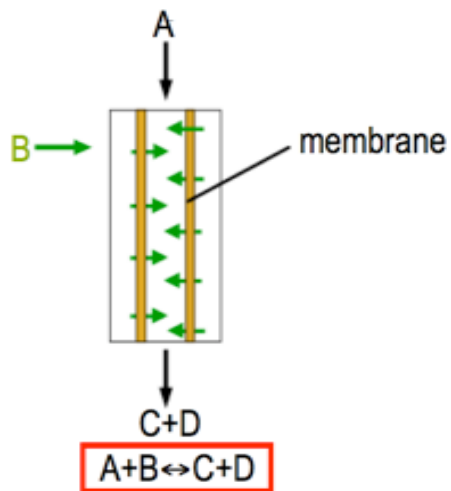
Figure 11 : Distributor membrane reactor [42].

Dittmeyer et al [168] have compared the two types of catalytic membrane contactors: flow through contactors and interfacial contactors for their activity in reduction of nitrites. The activity of flow through contactor is higher than the activity of interfacial contactor for hydrogenation reactions [168].
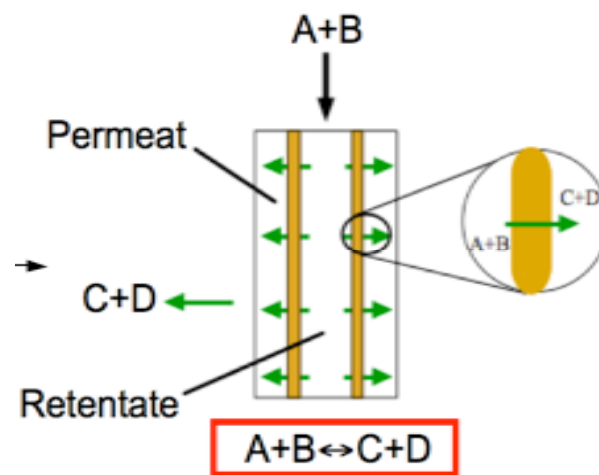
Figure12 : Flow through contactor [42].
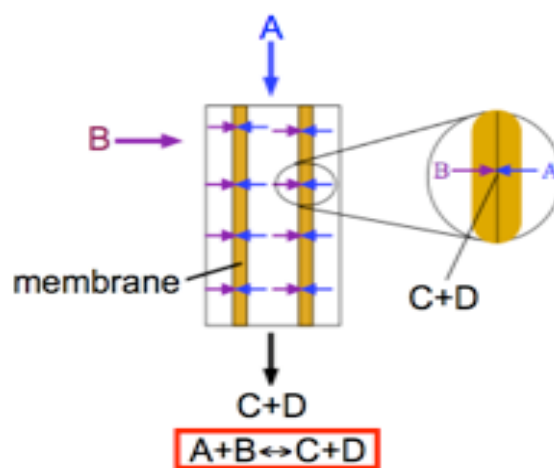
Figure 13 : Interfacial membrane contactor [42].

The different types of membrane reactors configurations can be classified to the relative placement of the two most important elements of this technology: the membrane and the catalyst. Three main configurations can be considered:

- The catalyst is physically separated from the membrane

- The catalyst is dispersed in the membrane

- The membrane is inherently catalytic

The first configuration is often called 'Inert Membrane Reactor' (IMR) by opposition to the two other ones, which are ' Catalytic Membrane Reactors' (CMRs)

Dittmeyer et al [49] has published a very comprehensive review in catalytic membrane layers for gas/liquid reactions. Several aspects in CMRs has discussed in this paper also the targeted benefits of catalytic membrane reactors has splitter into three groups according to scale at which they work:

1. Process level (Eliminating process units and state change):

The benefit would be the reduction in size and complexity of the plant and hence saving on investment. An increased efficiency would additionally result in savings on energy and new materials

2. Reactor level (Optimizing the contact between the phases and the dosing strategy):

The ability of a membrane to transport material can be exploited in a reactor in various ways to improve the efficiency of the combined process compared to the sequential units. The aim of both principles, i.e. catalytic diffuser and forced flow through catalytic membrane, is to optimize the contact between the reactants and the active phase in order to exploit as good as possible its intrinsic catalytic properties.

3. Catalytic level (Influencing catalysis through the chemical nature of the membrane):

The membrane due to its chemical nature supplies one of the reactants in a special form which is more active or selective in the reaction that one wants to catalyse than in it's usual form. An example is a ceramic oxide ion conducting membrane, which can pass oxide ions to a solid catalyst attached to it instead of using molecular oxygen from the reactant gas phase. Another example includes silver membranes, which selectively permeate atomic oxygen or membrane made from Palladium or its alloys that are permeable exclusively to hydrogen in atomic form.

1.15 CATALYST PREPARATION METHODS

Solid catalysts are highly sophisticated products derived from chemicals by means of several different procedures; the choice of a laboratory method for preparing a given catalyst depends on the physical and chemical characteristics desired in the final composition [172]. Heterogeneous catalysts are frequently defined as solids or mixtures of solids, which accelerate chemical reaction without themselves undergoing changes; this definition however is too limited in scope, considering that the properties of catalysts can change significantly with use, with service lives that vary from minutes to years [177].

The aim of the preparation of catalytic materials that can be employed on an industrial scale is to a product with high activity, selectivity, and stability [171]. Several review papers [171, 172, 173, 177] has classified the catalysts with respect to the preparation procedures into three broad categories:

1. Bulk catalysts and supports, bulk catalysts are mainly comprised of active phase substances while the supports are the carrier materials like alumina, silica's, or silicas-aluminas.

2. Impregnated catalysts, impregnated catalysts are usually obtained from performed supports by impregnation with the active phase.

3. Mixed-agglomerated catalysts, the last category of mixed agglomerate catalysts comprise those catalysts obtained by mixing active substances with a powdered support or support precursor and agglomerating the mixture.

The active phase metal (catalyst) can be selected from precious, or transition metals. The active phase metal must be a sufficiently high dispersed form which results in a large specific surface area and consequently in a maximum specific activity. In order to reach this objective the active metal component is usually deposited on the surface of a support, a highly porous and thermo stable materials with a high surface area and suitable mechanical strength) which is able not only to disperse the metal, but also to increase it's thermal stability and hence the catalyst life [171].

The common preparation methods of the dispersed metal catalysts can be classified according to [48, 171, 172, 173, 177] into three main steps:

(i)   Introduction of the metal precursor on the support by impregnation or ion exchange, co-precipitation and deposition precipitation.

(ii)   Drying and calcinations.

(iii)   Reduction.

1.15.1 MONOMETALLIC CATALYST PREPARATION

1.15.1.1 IMPREGNATION METHODS

In impregnation methods the supports are contacted with certain amount of the precursor metal solution, usually salt, dried, calcined and metal reduction. There are two impregnation methods can be distinguished according to the amount of solution used:

i.   Incipient wetness or dry impregnation, in dry impregnation method the volume of the solution containing the precursor doesn't exceed the pore volume of the support. Simply the impregnated solution is sprayed on the support surface which maintained under stirring and has been previously evacuated. This method usually used for costly active component precursor solutions.

ii.   Wet or soaking impregnations, in soaking impregnation method the volume of the solution is in excess wit respect to the pore volume of the support. The system left to age for a certain time, then dried, calcined, and metal reduction.

The concentration of the metal precursor on the support depends on the concentration of parent solution, the pore volume of the support, the type/ or concentration of adsorbing sites exiting in the surface.

Ionic exchange: inorganic oxides such as Al O, SiO, TiO, MgO which are commonly used as support materials, tends to polarize and to be surface charged once suspended in aqueous solution. The charge can be controlled by the pH of the solution. In acidic media, the adsorption surface site (M-OH) is positively charged and will be covered by anions as illustrated by eq (1)

$$M\text{-}OH + H^+ A^- \Leftrightarrow M\text{-}OH_2^+A^- \quad \dots\dots (1)$$

In basic media, the acidic surface site (M-OH) will be negatively charged and covered by cation as shown by eq (2)

$$M\text{-}OH + OH^- \Leftrightarrow M\text{-}O^- + H_2O \quad \dots\dots (2)$$

For each oxide a peculiar pH at which the surface will not be charged will then exist. This pH is called PZC (zero point of charge) or IEPS (Isoelectric point)

1.15.1.2 THE PRECIPITATION METHODS

1. Co-precipitation: in this procedure the solution containing the metal salt and a salt of a compound that will be converted into the support are contacting under   stirring with a base in order to precipitate as hydroxides and /or carbonate. After washing, these can be transformed to oxides by heating.

2. Deposition-precipitation: this procedure is in principles similar to co-precipitation method previously described. It consists in the precipitation of a metal hydroxide carbonate on the particles of a powder support through the reaction of a base with the precursor of metal. The main problem is to allow the precipitation of the metal hydroxide particles inside the porous of the support.

1.16 BIMETALLIC CATALYST PREPARATION

Investigation of membrane catalytic performance for particular model reactions which provide evident that the catalytic behaviour depends on many factor such preparation procedure, the nature of support, the type and the number of active metal phase loaded , which have a great impact on the surface atomic arrangement and the formation of metallic particles (212).

The second metal (when used) usually is a heavy element that plays the role of a promoter. This is a widespread strategy in reaction catalysts preparation, with the promoter being responsible for major improvements in activity, selectivity and durability of the catalysts without having a catalytic activity by itself (204)

Bimetallic nanoparticle have been extensively investigated with great interest because it is possible to improve the catalytic activity, selectivity, and stability as well as to reduce the cost of precious metal such as platinium by combination of two kinds of metals and thier fine structures in the field of catalysis.

A particular advantage on using precious metal catalysts in supported for mis tha the support disperses the metal over a greater surface area and reduces the thermal degredation.

1.16.1 CO-IMPREGNATION

Two or several active components are introduced to the support surface in the single impregnation step

1.16.2: SUCCESSIVE IMPREGNATION

Two or several active components are introduced sequentially. Drying (and often calcinations) takes place between the Impregnations. For the second Impregnation the properties of the surface to take into account are those of the solid obtained after the previous impregnation

1.16.3 THE (LBL) ELECTROLYTE DEPOSITION

The layer-by-layer (LBL) deposition technique, which involves alternating adsorption of complementary materials, has been investigated by many groups for modification of flat surfaces [174]. When charged nanoparticles are utilized as one of the alternating layers, careful selection of adsorption conditions sometimes allows immobilization of well-separated nanoparticles with control over the amount of colloid deposited [175].

Nanomaterials are often used in catalytic applications due to their high surface area to volume ratio [176]. Moreover, metal nanoparticles often have different electronic properties than their bulk metal counterparts, which may lead to enhance catalytic activity. However, due to the high surface energy of small metal nanoparticles, aggregation often occurs to yield larger particles that have decreased catalytic activity. Thus, to prevent aggregation, it is necessary for the metal nanoparticles to be immobilized on metal oxide supports [174] or in polymeric materials [175]. This report focuses on the use of polyelectrolyte multilayer films to encapsulate catalytic metal nanoparticles and form catalytic membrane reactors.

1.17 CATALYST CHARACTERIZATION

Haber et al [173] have presented and reviewed a methods and procedures for catalyst characterization.

1.17.1 CHARACTERIZATION OF SURFACE PROPERTIES BY ADSORPTION METHODS

Adsorption methods may be used to provide information about the total surface area of a catalyst, the surface area of the phase carrying the active sites. The interaction between the

adsorbate and the adsorbent may be chemical (chemisorptions) or physical (physisorption) in nature and ideally should be a surface specific interaction. Physical adsorption is used in the BET method to determine total surface areas of catalysts. Adsorption can be performed in a number of different ways which may involves static and flow or dynamic techniques

1.17.1.1 STATIC METHODS

The static methods are volumetric or gravimetric. The volumetric method involves the use of a vacuum system comprising two sections; a dosing section, which allows the introduction of accurately, measured quantities of the adsorbate, and the sample section, which contains the catalyst. The gravimetric methods may be used to determine adsorption of most molecules, even H2 if proper instruments are used. An advantage of the gravimetric method is that it eliminate the requirement to make dead volume corrections

1.17.1.2 DYNAMIC METHODS

In the single flows technique, a carrier gas containing the molecules to be adsorbed passes continuously over the catalyst. The flow method of determining gas adsorption has the advantages that no vacuum system is required and no dead volume corrections need to make. The method is rapid and easy to use.

Desorption is always an activated process and may conveniently be studied by temperature-programming techniques. Information is obtained in this way on the adsorption kinetics and the energetic of the gas/solid interactions.

1.17.2 CHARACTERIZATION OF THE FINE STRUCTURE OF THE CATALYSTS

Although many techniques are available for the examination of solids not all are appropriate for the study of real catalysts and some require special expertise in the interpretation of the results. Moreover, the nature of the sample may be changed by the application of the techniques. Heterogeneous catalysis being concerned with surfaces, it ids recommended in principle that surface sensitive methods should be used. However, some surface sensitive techniques are only sensitive to the peripheral zones of the particle and cannot probe the internal surfaces of porous materials

-ELECTRON MICROSCOPY

In electron microscopy as in any field of optics the over all contrast is due differential adsorption of photons or particles (amplitude contrast) or diffraction phenomena (phase contrast). The method provides identification of phases and structural information on catalysts, direct images of surfaces and elemental composition and distribution. Routine applications, however, may be hampered by complexities of image interpretation and by constraints on the type and preparation of specimens and on the environment within the microscope.

- Scanning electron microscopy (SEM)

Topographical image in a SEM are formed from back-scattered primary or low energy secondary electrons. The best resolution is about 2-5 nm but many routine studies are satisfied with a lower value and exploit the case of image interpretation and extraordinary depth of field to obtain a comprehensive view of the specimen. With non-crystalline catalysts, SEM is especially useful for examining the distribution and sizes of mesoporous.

- Scanning transmission electron microscopy (STEM)

STEM represents a merger of the concepts of TEM and SEM. Modes of operation and mechanisms of contrast and of imaging are essentially the same but the main advantage of STEM is the ability to carryout microanalysis at very high resolution.

1.18 CATALYTIC MEMBRANE PREPARATION

Catalytic membrane preparation is related and dependent on several types of membrane/catalyst arrangements, which proposed, by Julbe [155]. Among three configurations (the catalyst is physically separated from the membrane, the catalyst is dispersed in the membrane, the membrane is inherently catalytic), we were interested to focus on this type of membrane/catalyst arrangement (the catalyst is dispersed in the membrane). The selection of catalyst placement relative to the membrane surfaces can significantly affect the catalytic membrane reactor performance [48]. Several authors [46, 47, 48] have reported that the critical parameters determining the selection of the catalyst placement are the reaction residence time and the nature of permeating reactants. There are two methods [48] have been

adopted for membrane reactor preparing catalysts, Impregnation and ion exchange. Impregnation method has predominantly used when attaching catalysts to membranes. Wet impregnation method is commonly used for catalysts deposition on their supports, which has been adopted to prepare various catalytic membranes particularly ceramic membranes. Ion exchange method is rarely used in membrane preparation due to low metal loading of active phase metal. In both methods, converting a metal into an active form typically by heat treatment steps that involve calcinations, decompositions, reduction or their combinations activates a catalytic membrane. Dalmon et al [158, 159] have adapted and modified previous two methods into another two methods for membrane preparations conveniently named as:

i. Evaporation-crystallization deposition

ii. Aionic impregnation

The modification that have been by Dalmon et al [158, 159] was mainly in drying step which either by evaporation of the liquid solution contained in membrane pores at atmospheric air in evaporation-crystallization method or by washing the Impregnated membrane by 0.1 N HNO_3 three times before calcinations and reduction steps in case of anionic impregnation.

EVAPORATION-CRYSTALLIZATION METHOD

In Evaporation-Crystallization method, the tubular membranes were soaked vertically under rotating in a precursor solution for overnight period, the upper side of the tubular membrane connected to electrical turner to assure membrane rotating and homogenous. The sample was then kept at room temperature under air and rotated, in order to allow the evaporation and uniform distribution of the precursor solution. The impregnated membranes were then dried in nitrogen flow (60 ml/min) at 100°C for 1h (heating rate of 1°C/min.) and then calcined at 200°C in nitrogen flow (60 ml/min) for two hours (heating rate of 1°C/min.) in order to decompose the Pt precursor, introduced within the membrane wall. The gas flux was then switched to hydrogen for 12h, the platinum species being then reduced to metal particle (149, 150).

ANIONIC IMPREGNATION

In anionic impregnation method tubular membranes were soaked vertically under rotating in a precursor solution for 4h, the Impregnated membranes then washed three times for 20 minutes in 0.1 N HNO3, until the concentration of Pt species in the wash water was negligible. The samples were then dried in nitrogen flow (60 ml/min) at 100°C for 1h (heating rate of 1°C/min.) and then calcined at 200°C in nitrogen flow (60 ml/min) for two

hours (heating rate of 1°C/min.) in order to decompose the Pt precursor, introduced within the membrane wall. The gas flux was then switched to hydrogen for 12h, the platinum species being then reduced to metal particle [149].

The catalytic membrane preparations was done by several investigators [149,151,154, 158], Peureux et al [144] Have prepared catalytic membranes by deposition of the Pt in porous alumina tubes ionic Impregnation

1.19 TUBULAR MEMBRANE STRUCTURES

Several structures of tubular supports have been used in the past. The tubular supports are made of one, three, or four concentric zones, showing an average pore size decreasing from the inner side to external side in the radial direction of the tubular supports. Figure 16 shows SEM Image of 3-layers Pall-Exekia commercial tubular supports
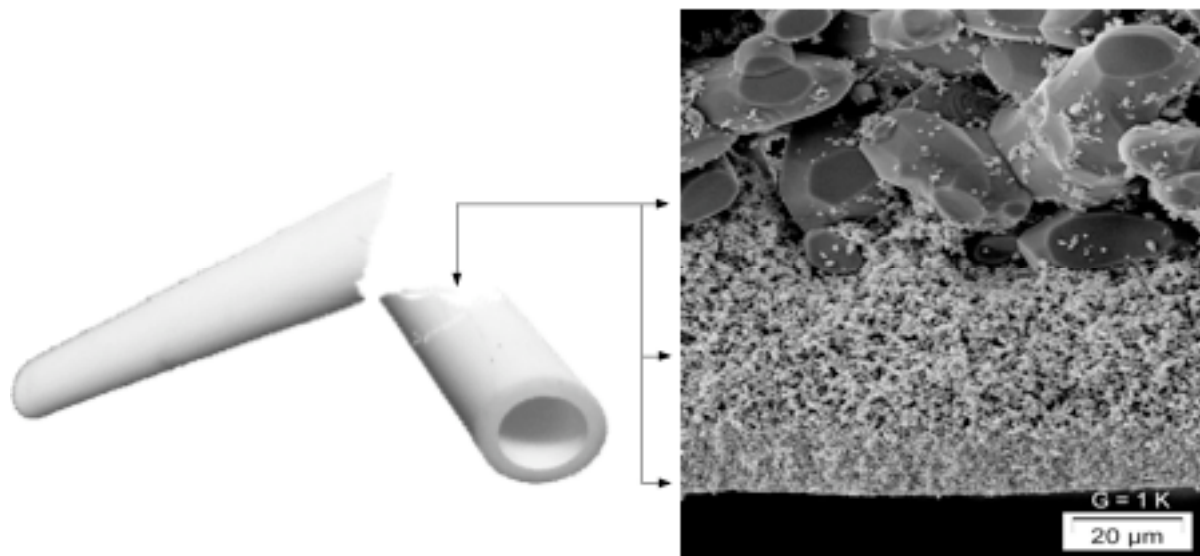
Figure 14: SEM Image of 3-layers Pall-Exekia commercial tubular supports [51].

Table 7 shows some examples of incorporating catalysts into porous ceramic membranes. All metal catalysts have been introduced to a variety of ceramic membranes (e.g. alumina, silica, titania)

Table 7 Incorporated catalysts in ceramic membranes

Catalyst	Membrane material	Precursor solution	Deposition method	Ref
Pd or Pd-Cu	Alumina or titania	Palladium nitrate or copper nitrate	Ionic Impregnation or EC[a]	42
Pd	Porous alumina	Ammonium tetra chloropalladium	Ionic Impregnation	142 143
Pd	Porous alumina	Palladium dichloride	Ionic Impregnation	145
Pt	Porous alumina	Hexachloroplatinic acid	Ionic Impregnation	155
Pt	Alumina	Hexachloroplatinic acid	Ionic Impregnation	158
Pt	Porous alumina	Hexachloroplatinic acid	EC	159
Pd	Alumina	Palladium nitrate	EC	160
Pt	Alumina or titania	Hexachloroplatinic acid	EC	167

- a: EC- Evaporation-crystallization technique

1.20 CWAO ON MEMBRANE REACTORS

Three-phase conventional reactors (Slurry reactors, Trickle-bed reactors, Fixed-bed reactor, Packed-bed reactor), which used in CWAO processes still have some disadvantage because the liquid film covering the solid catalyst pellets increases the resistance to external transfer of the gaseous reactant. This can lead to the formation of so-called preferential flow bath that induces poor contact between the three phases. The presence of uncontrolled areas usually results in the formation of hot spots on the catalyst surface, a problem that must be avoided in the large-scale reactor units [161].

Catalytic membrane reactor (CMR) which has been proposed recently and applied to CWAO of model compound solutions or real effluents by a number of publications [166,167] is a way to improve gas/liquid/solid contact; CMR can be defined as a reactor drawing a special advantage from the synergy of the catalyst and a membrane when implemented in the same device. CMR due to their advantage with respect to conventional three phase reactors, the application of CMR to WAO of aqueous organic solutions is currently being thoroughly investigated and a subject of several published papers [149,151,154, 158]

1.21 CATALYSIS AND MASS TRANSFER IN CMR

Miachon and Dalmon [163] have discussed the catalysis in membrane reactors. They have reported that depending on the application, the environment of the catalysts in the CMR may be quiet different from that exiting in the conventional reactors.

Iojoiu et al. [149] have discussed the performance and stability of CMR interfacial contactor for wet air oxidation of formic acid.

Vospernik et al. [161] have studied mass transfer process in gas-liquid-solid system in membrane contactors; they reported that Wilke-change equation provides a very good estimation for the permeance of various model compounds through the membrane wall. They also have studied liquid-liquid and liquid-gas mass transfer rates in membrane reactors.

Hussain et al. [141] have studied several configurations of tubular ceramic membranes for membrane reactors. They have estimated several heat and mass transfer parameters for multilayer tubular membrane. Mass transfer parameters for every single layer are derived separately by means of dusty gas model in steady state and dynamic modes for combined heat and mass transfer models.

Meixner et al. [140] have studied the characterizations of the transport properties of micro porous layer combined with porous inorganic membrane by Fouling and rejection behaviour for ceramic and polymer-modified ceramic membrane have been studied by Faibish [136]. Surface electrochemical properties of mixed oxide ceramic membranes, pore size change of porous ceramic membranes after modification, and mechanical properties of ceramic membrane supports, and mechanical properties of ceramic membrane support such tensile strength and stress have been discussed in several investigation [137, 138, 139].

1.22 CMR PERFORMANCE

The performance of CMR has tested in hydrogenation reactions as in nitrate removal from drinking water [145], also there are further publications in the literature concerning the use of contactors CMRs in oxidation reactions applied for environmental applications [150, 152, 154, 164, and 166].   Table 8 shows the CWAO in CMR

Iojoiu et al. [150] have prepared tubular ceramic membranes and the membranes were tested for CWAO of aqueous solution of formic acid. The membranes were used are:

1) Inocermic (4 layers) with a mesoporous top layer of CeO_2/ZrO_2 covered with TiO_2

(80 nm)

2) PE (4 layers) with a mesoporous top layer of ZrO_2 (20 nm)

3) PE (3 layers) with a mesoporous top layer of ZrO_2 (50 nm)

Table 8 : CWAO in CMR

Author	Tubular membrane		Polluted	Reactor	T(C)	Ref
	support	catalyst	Model	Type	P(bar)	
Raeder	TAMI-4 layers	Pt	Formic acid	Interfacial CMR	150 10	154
Vospernik	PE-3layers	Pt		Interfacial CMR	25 1	164
Iojoiu	PE-3layers INC-4layers Single tubes	Pt	Formic acid	Interfacial CMR	20 3.6	166
Iojoiu	PE- INC- Multichannel	Pt	Real effluents[a,b,c]	Watercatox pilot unit	68 5	166
Iojoiu	PE-3layers INC-4layers Single tubes	Pt	Formic acid And real effluents	Interfacial CMR And monolith multichannel		167

- a: EOH (Monsanto, Belgium); -b: Refinery waste (MILJOE-Norway), c: Paper industry waste (France)

The metal loading (Pt deposition) by evaporation-crystallization technique using H_2PtCl_6 aqueous solution (preliminary tube drying at 170ºC) + drying in N_2 (60 mL/min) + calcinations at 200ºC (1ºC/min) + reduction with H_2 (60 mL/min) for 6 h

The membranes has Characterized by Gas permeation, mass uptake, quantity of precursor solution adsorbed within the pores during soaking step, SEM (BSE), EPMA, EDS, TOC, pH

The catalytic test of the membranes was done in Watercatox bench setup, the reactor configuration and operating conditions that are outlined as:

-Gas phase fed on shell side and liquid introduced on inner tube (P atm)

-Gas and liquid flow rates: 50 and 7 mL/min (liquid recycled to reservoir). The effect of trans-membrane pressure on the catalytic activity was also studied, Gas TMP shifts G-L interface into the membrane wall (compensation of capillarity pressure), closer to catalytic zone that results in Increase of reaction rate. At room temperature, CMR shows initial activity 3-6 times higher than in batch reactor for wet air oxidation of formic acid, gas permeation results suggest that negligible changes in N_2 permeation values that is means Structures of ceramic membranes not modified by Pt deposition. The mass of catalysts that were loaded in the membranes are 27 and 35 mg Pt, respectively, for IN and PE membranes. In latter membranes, Pt is more localized in the top layer.

Miachon et al. [151] have prepared tubular ceramic membranes and the membranes were tested for CWAO of aqueous solution of formic acid. The Membranes were used are:

-TiO_2 (10 nm) or ZrO_2 (20 nm) mesoporous top layer on a-Al_2O_3 macroporous support (3 layers). Pt metal loading (Catalyst deposition) on the tubular ceramic membrane was done by ionic impregnation, The membranes has Characterized by Titration of deposited Pt, single gas permeation measurements, SEM, TEM, for batch reactor TOC, pH measured continuously. The catalytic test of the membranes was done in Watercatox bench setup, the reactor configuration and operating conditions that are outlined as:

-Liquid and gas pressures kept at 120 and 122 kPa, respectively.

-Gas and liquid flow rates: 40 and 3 mL/min (liquid recycled to reservoir).

-The comparative study between wet oxidation of formic acid in CMR-C and CWAO in batch reactor was done also, the results suggest that the activity of CMR is higher in compared with the activity of batch reactor.

The mass of deposited metal on Membrane is 3 mg of Pt particles (4-5 nm) deposited in mesoporous top layer (Pt loading = 0.27 wt.%) While in Batch reactor: 3 mg Pt on 1.2 g TiO_2 in 300 mL solution, agitation speed is 1200 rpm, gas flow rate = 400 mL/min, Higher performance when the G-L interface is located into the mesoporous catalytic top layer, Gas/liquid solubility in the interface might behave differently than on macroscopic scale, Short-term deactivation by poisoning with intermediate products of formic acid degradation (possible reactivation with H_2 at 200ºC). However, long-term deactivation due to plugging Alumina materials.

1.23 KINETICS OF METAL-BASED CATALYSIS

Kinetics of metal-based catalysis are generally described by empirical power laws if mechanistic information or mechanistic models are not available. There have been several mechanisms presented in the literature [26] that describe the role of various metal-based homogenous or heterogeneous catalysts.

1. Homolytic catalysis: homolytic catalysis involves the promotion of free radical reactions via a homogenous mechanism. The promotion of free radical reactions by a metal-based catalyst involves the introduction of a catalytic cycle through the reduction-oxidation homolytic reactions of hydro peroxides.

2. Coordination catalysis: Coordination catalysis, which can occur via homogenous or heterogeneous mechanism, involves the oxidation of a coordinated substrate by a metal ion. The oxidized form of the metal is subsequently regenerated by reaction of the reduced form with oxygen.

3. Mars-Van Krevelen (MVK) Adsorption model: the (MVK) catalytic reaction mechanism (heterogeneous) is a redox mechanism that involves lattice oxygen. In this reaction mechanism, an oxometal species oxidises the substrate and the reduced form is subsequently reoxidized by oxygen (the redox cycle. The rate determining steps can be oxygen transfer between the catalyst and the substrate to be oxidized (nucleo-philic attack of oxygen vacancies)

4. Eley-Rideal (ER) and Langmuir-Hinshelwood-Hougen-Watson (LHHW) Adsorption Models: The surface catalysis models is the ER system, which is less common in multiphase system, and the more-universal LHHW systems involve the adsorption of one reactant (ER) or all reactants (LHHW). In LHHW kinetics; each reaction step is assumed to be an elemental step and reversible. In ER kinetics, the reaction rate continues to increase as the surface coverage increase; however, in LHHW reactions, the reaction rate goes through a maximum (if reactant covers the complete surface, the rate goes to were, because reactant B cannot adsorb any more).

In the case of catalytic wet air oxidation, many attempts to study reaction mechanisms for WAO of organic compounds have been made. They conclude that the free-radical mechanism is involved in WAO of several organic compounds. Li et al. [189] has proposed a general scheme for CWAO reaction of organic compounds in aqueous phase based on free-radical mechanism.

The free radical reaction mechanism generally considered to be associated WAO of organic compounds in aqueous phase are summarized in the following steps 1 through 6.

– Free radicals in the absence of initiators are formed by the reaction of oxygen with the weakest C-H bonds, as shown in step (3), (4)

$$Rh + O_2 \; \text{---} \; R^* + HO_2{}^* \qquad \text{………………. (3)}$$

$$RH + HO_2{}^* \; \text{---} \; R^* + H_2O_2 \qquad \text{……………… (4)}$$
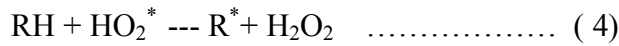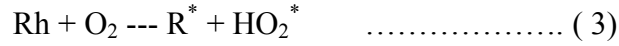
R: denotes organic functional group

-Generation of hydroxyl radical from the decomposition of hydrogen peroxide which interact with the catalyst:

$$H_2O_2 + M \; \text{----} \; 2HO^* \qquad \text{………………. (5)}$$

The term M can be either a homogenous or heterogeneous catalyst.

- The oxidation of organic compounds by hydroxyl radicals as shown in step (6)

$$RH + HO^* \; \text{-----} \; R^* + H_2O \qquad \text{……………… (6)}$$
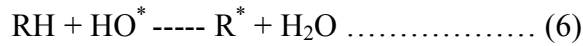
- Reaction between the organic radical R^* and the oxygen to form an organic peroxyradical as shown by step (7)

$$R^* + O_2 \; \text{------} \; ROO^* \qquad \text{…………………… (7)}$$
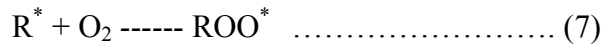
- The organic peroxy radical further abstracts a hydrogen atom from the organic compound as shown by step (8)

$$ROO^* + RH \; \text{---------} \; ROOH + R^* \qquad \text{………….. (8)}$$

Since the organic hydro peroxides formed are relatively unstable, decomposition of such intermediates often leads to molecular breakdown and formation of subsequent intermediate with lower carbon numbers.

Real wastewaters that received as end pipe effluents from several industrial units is a mixture of large number of compounds, so kinetic modelling by developing full mechanistic reactions path ways for such a mixture is impossible. Due to these obstacles, CWAO researchers were motivated to study the kinetics of CWAO reactions by two ways:

i.   Study the kinetics of single model compounds.

ii.   Study the kinetics of real wastewater mixtures by using General Lumped Kinetic Model (GLKM).

1.23.1 KINETICS OF SINGLE MODEL COMPOUNDS

We will present here oxidation reaction mechanisms for some model compounds,these model compounds are, formic acid, oxalic acid, acetic acid, and phenol.

A) FORMIC ACID OXIDATION PATHWAY

The oxidation of formic acid is the final step, resulting in water and carbon dioxide:

$$HCOOH + 0.5O_2 \text{ ---- } H_2O + CO_2 \dots\dots\dots\dots\dots\dots\dots (9)$$

The oxidation of formic acid is also very researched process for is use in Fuel cell [57]. Baldi et al [61] and Margolis et al [68] have performed a CWAO of formic acid on various catalyst types (CuO-ZnO, Pd, or Pt) at different operating conditions. They have reported that formic acid may also undergo thermal decomposition to carbon dioxide and dihydrogen (decarboxylation) or carbon monoxide and water (dehydration)

$$HCOOH \text{ ---- } H_2O + CO \dots\dots\dots\dots\dots\dots\dots. (10)$$

$$HCOOH \text{ ---- } H_2 + CO_2 \dots\dots\dots\dots\dots\dots\dots (11)$$
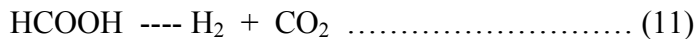
Bjerre et al. (60) have reported that formic acid undergoes oxidative decompostion. The oxidative decomposition of formic acid/ formate performed by the reaction with molecular O_2 is described by the following reactions:

$$HCOOH + 0.5O_2 \text{ ---- } H_2O + CO2 \qquad \dots\dots\dots\dots\dots. (12)$$

$$HCOO^- + 0.5O_2 \text{ ---- } HCO_3^- \qquad \dots\dots\dots\dots\dots\dots (13)$$

B) OXALIC ACID OXIDATION PATHWAY

Formic acid was observed as a major intermediate during oxidation of oxalic acid [82]. An overall reaction pathway for oxalic acid oxidation has been proposed by Shende [86] et al. as shown in eq (15).

$$HOOCCOOH + \frac{1}{2} O_2 \longrightarrow CO_2 + H_2O$$

$$\begin{array}{c} -CO_2 \\ \downarrow \\ HCOOH + 1/2\ O_2 \longrightarrow CO + H_2O \end{array}$$

…………………………….. (14)
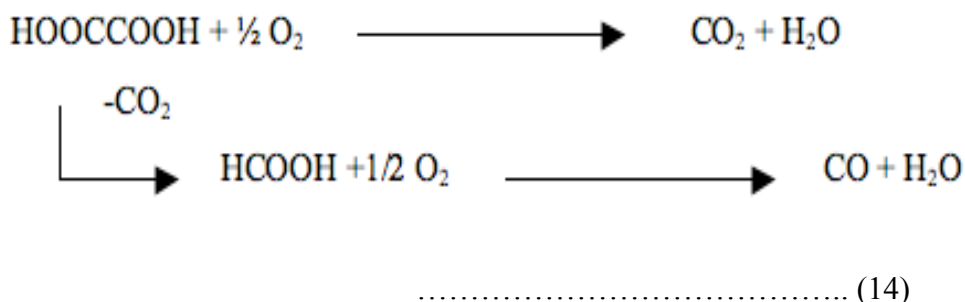
Thus, the decarboxylation and the attack of the C-O group are considered two major reaction routes in the decomposition of oxalic acid.

C) ACETIC ACID OXIDATION PATHWAY

There are a number of previous investigations in the past literature for CWAO of many organic compounds reported that acetic acid is one of the most refractory products of CWAO and its oxidation is the rate determining step for CWAO of many organic compounds.

Duprez et al. [30] have proposed reaction pathway for acetic acid oxidation as shown in figure 16.

The general scheme of the reaction is that the initiation reaction ($CH_3COOH \rightarrow CH_3COO^\bullet + H^\bullet$) occurs necessarily at the catalyst surface or at the metal/support interface [10]. An electron transfer between the substrate and the catalyst can stabilize the radicals. The attack on the a-position of COOH being excluded, four possibilities have been proposed for the propagation reactions: the radical acetate is produced at the surface of the catalyst by attack of CH_3COOH molecule with:

(I)   A hydrogen atom

(II)   A hydroxyl radical OH.

(III)   An oxygen molecule

(IV)   a per hydroxyl radical $HOE^\bullet$.

Reaction (II) with OH- is very rapid. Nevertheless owing to the excess of oxygen in the medium, reaction (III) is most likely to be the dominant one. A $HO_2^\bullet$ radical is then produced which can react further with another molecule of acetic acid (IV). The acetate radical produced by one of the reactions (I-IV) undergoes a decarboxylation. The methyl radical is then oxidized via a peroxyl radical according to the general scheme valid for the free radicals $CH_3COO^\bullet$.
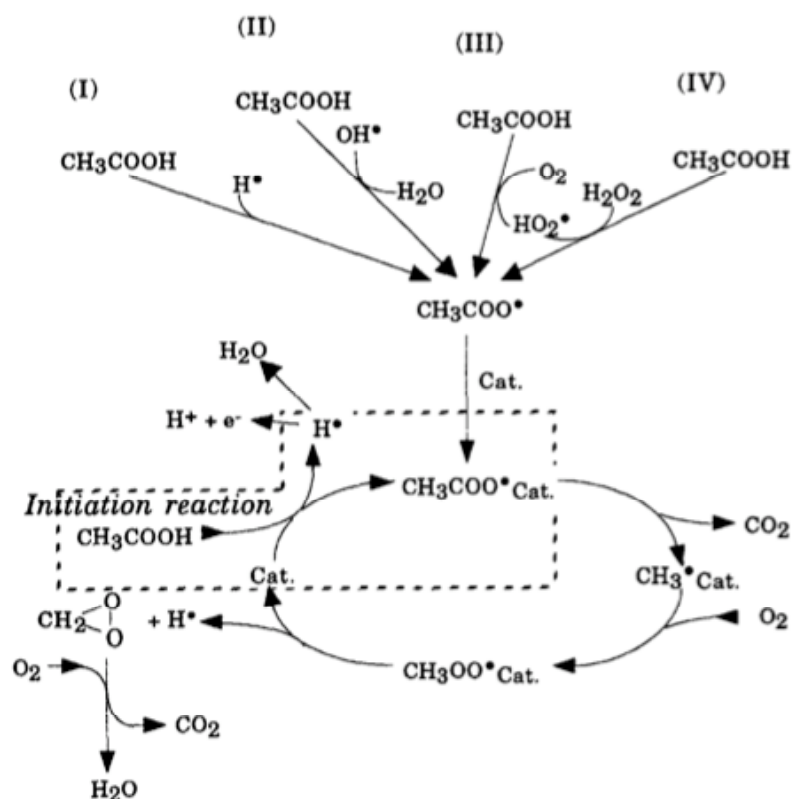
Figure 15: Scheme for acetic acid wet air oxidation

D) PHENOL OXIDATION PATHWAYS

Different reaction pathways have been proposed which lead to different reaction products, the mechanism of the oxidation of phenol is extremely complex and is not yet fully understood. It is generally accepted that reaction products which may be classified into three large categories, i.e., CO_2, carboxylic acids (mainly oxalic, acetic and succinic acids), and quinones-diphenols [108]. Furthermore, the greater part of the reaction products for different types of catalysts (CuO/γ-Al$_2$O$_3$, CuO/Al$_2$O$_3$, CuO-ZnO-CoO, MnO$_2$/CeO$_2$) are CO_2 (mainly), oxalic acid, *p*-benzoquinone, formic acid, acetic acid, succinic acid and catechol [115].

Eftaxias [125], studied the oxidation of phenol over activated carbon catalyst and the proposed reaction path way as shown by figure (14). A group of 20 different possible phenol oxidation products has been tested with standard solution to obtain the intermediate distribution. Among them, six principal intermediates have been identified, i.e. ring compounds namely 4-hydroxybenzoic acid (4-HBA), p-benzoquinone as well as short chain carboxylic acids, such as maleic acid, its isomer fumaric acid, acetic acid and formic acid.
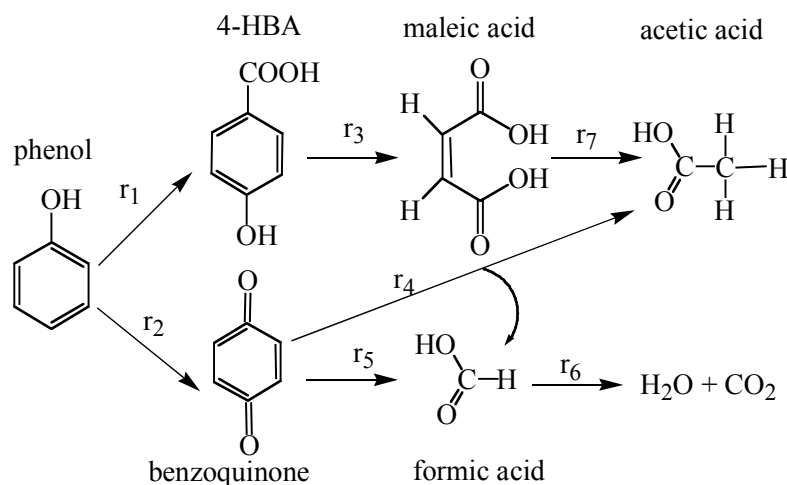
Figure 16: Proposed reaction pathways for phenol oxidation

1.23.2 GENERALIZED LUMPED KINETIC MODEL (GLKM)

Many authors (e.g. Eftaxias et al [193], Pintar et al [179], Cybulski et al. [96], Tawczynski et al. [191]) have used GLKM to analyse kinetic experimental data. The GLKM model of WAO is based on a simplified reaction scheme involving the formation and destruction of rate controlling intermediates. The main authers listed various WAO products such as: analysis of is Short-carboxylic acids, ketones, aldehydes, and alcohols.

Acetic acid is assumed to represent the group of rate controlling intermediates in the GLKM model.

Lets denoted A, B, and C compound groups are exist in the liquid and gases effluents .schematic of the simplified path way is illustrated below:

$$A + O_2 \xrightarrow{\ k_1\ } C$$

$$\searrow k_3 \qquad \uparrow k_2 \qquad \qquad \ldots\ldots\ldots\ldots\ldots\ldots(15)$$

$$B + O_2$$

69
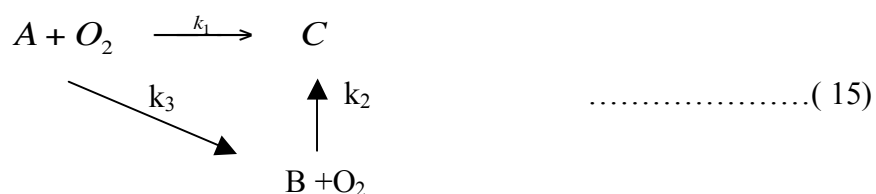
If compound groups A, B and C are expressed in concentration terms, then

[A]: [All initial and intermediate compounds]- [acetic acid]

[B]: [acetic acid]

[C] : [Oxidation end products]

The compound groups A, B, or C may be also expressed in terms of total organic carbon [TOC], or chemical oxygen demand [COD], or total oxygen demand [TOD].

Several studies have been devoted specially for the elucidation of the WAO mechanism of single model compounds such as phenols [32, 93, 95, 105, 111, 117], carboxylic acids [61, 65] , ethylene glycol [135] as model or compounds of real wastewaters [35,211]. Table 9 summarize this bibliographic part devoted to kinetic studies for CWAO.

Table 9 : Reported kinetic studies for CWAO

Catalyst	Model Compound	Kinetic Model	Reaction Order		Activation energy, KJ.mol^{-1}	Ref
			Model compound	Oxygen		
CuO/γ-Al_2O_3	Phenol	PLM[a]	1	0.5	184	93
CuO/Al_2O_3	Phenol	PLM	1	0.5	85	111
CuO/Al_2O_3	Phenol	PLM	-	0.25	84	32
CuO-ZnO-CoO	Phenol	LHHW[b]	1	0.5	137	116
$CuO/ZnO/Al_2O_3$	Phenol	LHHW	1	0.5	139	117
CuO/Al_2O_3	Phenol	PLM	1	0.31	74.5	105
MnO_2/CeO_2	Phenol	LHHW	1	-	65	95
CuO-ZnO	Formic acid	PLM	1	1	146.5	61
Pt/TiO_2	Acetic acid	PLM	-0.5	0.5	96.6	65
Mn-Ce-O	Ethylene glycol	PLM	1	1.09	31.8	135
Ru/TiO_2	IW	PLM	2	0	74.2-96.8	35
$Pd-Pt/Al_2O_3$	IW	PLM	1	-	54.4-50.2	211

a: Power law model –b: Langmuir-Hinshelwood-Hougen-Watson Model, - c: Industrial waste water

GLOSSARY:

COD: Chemical oxygen demand

TOC: Total organic carbon

WAO: Wet air oxidation

CWAO: Catalytic wet air oxidation

CMR: Catalytic membrane reactor

IMR: Inert membrane reactor

TMP: Transmembrane pressure

G-L: Gas-Liquid

AOP: Advanced ooxidation process

ZIMPRO: Zimmerman process

LOPROX: Low pressure oxidation process

WPO: Wet peroxide oxidation

B5: Reactive dye (Black 5) solution

B19: Reactive dye (Blue 19) solution

R198: Reactive dye (Red 198) solution

D0: Acidic effluent of kraft bleaching plant (paper pulp)

E1: Alkaline effluent of kraft bleaching plant (paper pulp)

WTW: Washing Textile wastewater

LAS: Linear alkyle benzene sulfonate

EG: Ethylene glychol

CFC: Chloro flouro carbon compound

 INC: Inocermic company –Germany

PE: Pall-Exkia- France

LBL: Layer by layer metal loading technique

PZC: Zero point of charge

IEPS: Isoelectric point

SEM: Scanning electron microscopy

TEM: Transmision electron microscopy

EDS: Energy dispersive spectroscopy

XRD:X-ray Differaction

BSE: Back scattering electron image

EPMA: Electron probe microanalysis

GLKM: General lumped kinetic model

ER: Eley-Rideal model

LHHW: Langmuir-Hinshelwood-Hougen-Watson model

References

1. Henry. J and G. W. Heinke, Environmental Science and Engineering, 1st edition, Prentice-Hall, New Jersy, 1989.

2. Cheremisinoff. N, HandBook of Water and Wastewater Treatment Technologies, Butterworth-Heinemann, Boston, 1998

3. Watercatox project, http://www.sintef.no/watercatox

4. Costantinides. A, Mostoufi. N, Numerical Methods for Chemical Engineers with MATLAB Applications, 2nd Edition, (2000), Prentice-Hall PTR.

5. Seinfeld. J; The environment and chemical reaction engineering; *Chemical Engineering Science*, 45 (1990) 2045-2055

6. Kojima. T; Nakayama. C; Uemiya. S; Analysis of the mechanism of rare earth metal permeation through the liquid through a liquid membrane with chelating agent in the feed phase; *Can. J. Chem. Eng.* 1994, *72* Feb, 72

7. Smith. J. M, Chemical Engineering Kinetics, 3rd edition (1981), Mc-Graw Hill Book Company

8. Fogler. H. S, Elementary of Chemical Reaction Engineering, 3rd edition (1999), Prentice-Hall International Series

9. Hines. A. L, Maddox. R. N, Mass Transfer Fundamental and Applications, 1st edition (1985), Prentice-Hall International Series

10. Finlayson. B, Non-Linear Analysis in Chemical Engineering, 1st edition (1980), Mc-Graw Hill Book Company

11. Sheintuch. M, Dynamics of catalytic reactions and reactors, *Catal. Today* 36 (1997) 461-471

12. Bird. R. B, Stewart. W. E, Lightfoot. E. N, Transport Phenomena, 1st edition (1960), Wiley International Edition

13. Villadsen. J, Michelsen. M, Solution of differential equation models by polynomial approximation, 1st edition, (1978), Prentice-Hall, INC.

14. Zimmermann. F, New waste-disposal process, *Chem. Eng.* 25 (1958) 117-121

15. Luck .F, A review of industrial wet air oxidation processes, *Catal. Today* 27 (1996) 195-202

16. Donlagic. J, Levec. J, Does the catalytic Wet Oxidation yield products more amenable to biodegradation, Applied Catalysis B: Environmental 17 (1998) L1-L5

17. Suarez-Ojeda. M, Carrera. J, Metacalfe. I, Font. J, Wet air oxidation (WAO) as a precursor to biological treatment: Refractory nature of the WAO intermediates, Chemical engineering journal 144 (2008) 205-212

18. Luck. F, Wet air oxidation: past, present and future, *Catal. Today* 53 (1999) 81-91.

19. Levec. J, A. Pintar, Catalytic oxidation of aqueous solutions of organics. An effective method for removal of toxic pollutants from wastewaters, *Catal. Today* 24 (1995) 51-58.

20. Pintar. A, Catalytic processes for the purification of drinking water and industrial effluents, *Catal. Today* 77 (2003) 461 - 465.

21. Levec. J, A. Pintar, Catalytic wet-air oxidation processes: A review, *Catal. Today* 124 (2007) 172-184.

22. Mishra. V, Mahajani. V, Joshi. J, Review: wet air oxidation. *Ind. Eng. Chem. Res. 34* (1995) 2 - 48

23. Cybulski. A, Catalytic wet air oxidation: Are monolithic Catalyst and Reactors feasible, *Ind. Eng. Chem. Res. 46* (2007) 4007– 4033.

24. Kolaczkowski, S. T.; Plucinski, P.; Beltran, F. J.; Rivas, F. J.; McLurgh, D. B. Wet air oxidation: a review of process technologies and aspects in reactor design. *Chem. Eng. J.* 1999, *73* (2), 143.

25. Eftaxias, A.; Larachi F.; Stu¨ber F. Modelling of trickle bed reactor for the catalytic wet air oxidation of phenol. *Can. J. Chem. Eng.* 2003, *81* (3-4), 784.

26. Bhargava. S. Tradio. J, Prasad. J, Foger. K, Acolekar. D, Grocott. S, wet oxidation and Catalytic wet oxidation, *Ind. Eng. Chem. Res. 45* (2007) 1221– 1258.

27. Imamura, S. Catalytic and Noncatalytic Wet Oxidation. *Ind. Eng. Chem. Res.* 1999, *38* (5), 1743.

28. Besson, M.; Gallezot, P. Deactivation of metal catalysts in liquid-phase organic reactions. *Catal. Today* 2003, *81* (4), 547-559.

29. Imamura, S.; Fukuda, I.; Ishida, S. Wet oxidation catalyzed by ruthenium supported on cerium (IV) oxides. *Ind.Eng.Chem.Res.* 1988, *27*(4), 718-721

30. Duprez, D.; Delanoe F.; Barbier, J., Jr.; Isnard, P.; Blanchard, G. Catalytic oxidation of organic compounds in aqueous media. *Catal. Today* 1996, *29* (1-4), 317-322.

31. Pirkanniemi, K.; Sillanpa a., M. Heterogeneous water phase catalysis as an environmental application: A review. *Chemosphere* 2002, *48* (10), 1047-1060.

32. Pintar A. and J. Levec; Catalytic liquid-phase oxidation of refractory organics in waste water *Chemical Engineering Science*, 47 (1992) 2395-2400

33. Oliviero, L.; Barbier. J, Duprez. D, Review: Wet air oxidation of nitrogen-containing compounds and ammonia in aqueous media, . *Appl. Catal., B 40* 2003, 121-130.

34. Andreozzi. R, V. Caprio, A. Insola, R. Marotta, Advanced oxidation processes (AOP) for water purification and recovery, *Catalysis Today* 53 (1999) 51-59

35. Dudukovic. M, Trends in catalytic reaction engineering, *Catalysis Today* 48 (1999) 5- 15

36. Szpyrkowicz. L, C Juzzolino, S. N. Kaul, S Daniele, M D. De Faveri, Electrochemical oxidation of dyeing baths bearing disperse dyes, *Ind. Eng. Chem. Res.* 39, 2000 , 3241-3248.

37. Adewuyi. Y, Sonochemistry: Environmental Science and Engineering Applications *Ind. Eng. Chem. Res.* 40, 2001 , 4681-4715

38. Grymonpre. D, W. C. Finney, B. R. Locke, Aqueous-phase pulsed streamer corona reactor using suspended activated carbon particles for phenol oxidation: model-data-cmparison, *Chemical Engineering Science*, 54 (1999) 3095-

39. Massa, P.; Ayude, M. A.; Ivorra, F.; Fenoglio, R.; Haure, P. Phenol oxidation in a periodically operated trickle bed reactor. *Catal. Today* 2005, *107-108* (Complete), 630-636.

40. Thomas Westermann; Flow-Through Membrane Microreactor for Intensified Heterogeneous Catalysis, Doctoral Thesis, Berlin Technical University, Germany (2007).

41. Schmidt, A, A Pore flow through membrane Reactor for Selective Hydrogenation Reactions, Doctoral Thesis, Berlin Technical University, Germany (2007).

42. Wehbe. N; Dénitrification de l'eau potable en réacteur catalytique membranaire et photocatalytique, Doctoral Thesis, University Claude Bernard Lyon -1, Lyon, France (2008)

43. Rodriguez, T. M. Etude et Modelisation d'un Reacteur membranaire Applique a des Reactions Triphasiques, Doctoral Thesis, University Claude Bernard Lyon I, Lyon, France (1994).

44. Moreno. V. P, Etude d'un Reacteur membranaire en Catalyse Gaz-Liquid-Solid. Application A l'Oxidation Voie Humide de l'acide Formique, Doctoral Thesis, University Claude Bernard Lyon I, Lyon, France (2001)

45. Eftaxias. A, Catalytic Wet Air Oxidation of Phenol in trickle Bed Reactors. Kinetics and Reactor Modelling, Doctoral Thesis, University Rovira I Virgili, Tarragona, Spain (2002)

46. Sanchez. J, Tsotsis. T, Catalytic membranes and membrane reactors, 1st edition, Wiley-VCH Verlag GmbH, Weinheim, 2002.

47. Burggraaf. A, Cot. L, Fundamentals of inorganic membrane science and technology, 1st edition, Elsevier Science B.V. 1996

48. Hsieh. H, Inorganic membranes for separation and reaction, 1st edition, Elsevier Science B.V. 1996

49. Dittmeyer. R, Svajda. Karel, Reif. M, A review of catalytic membrane layers for gas liquid reactions, *Topics in Catalysis*, 2004, 29, 3-27.

50. Coronas. J, Santamaria. J, Catalytic reactors based on porous membrane, Catal. *Today* 1999, *51*, 377-389.

51. Ismagilov. Z, Monolithic catalyst design, engineering and prospects of application for environmental protection in Russia, React.Kinet.Catal.Lett. Vol. 60, (1997) No. 2, 215-218

52. Gryaznov. V, Membrane catalysis, *Catal. Today,* 1999, *51* , 391-395.

53. Luck. F, Djafer. M, Bourbigot. M, Catalytic wet air oxidation of biosolids in a monolithic reactor, Catal. *Today,* 1995, *24*, 73-78.

54. Zaman. J, Chakma. A, Review: Inorganic membrane reactors, J. of Membrane Sceince, 92 (1994) 1-28

55. Julbe. A, Farrusseng. D, Guizard. C, Review: Porous ceramic membranes for catalytic reactors – overview and new ideas, J. of Membrane Science, 181 (2001) 3-20

56. Van de Water. L, Maschmeyer. T, Mesoporous membranes- a brief overview of recent edevelopments, *Topics in Catalysis* 29 (2004) 67-77.

57. Harmsen. J, Jelemensky. L, Scheffr. P, Kuster. B, Marin. G, kinetic Modelling for wet air oxidation of Formic Acid on a carbon supported platinum catalyst, Applied Catalyses A: General, 165 (1997) 499-509

58. Shende. R, and Mahajani. V, kinetic Modelling of wet oxidation of Formic Acid and acetic acid, Ind. Eng. Chem. Res. 1997, 36, 4809-4814

59. Claudel, B., Nueilati, M., Andrieu., J., Oxidation of Formic Acid in Aqueous Solution by Palladium Catalysts, Applied Catalysis, 11 (1984) 217 – 225.

60. Bjerre. A, Sorensen. E, Thermal Decomposition of Dilute of Formic Acid solutions, Ind. Eng. Chem. Res. 1992, 31, 1574-1577

61. Baldi. G, Goto. S, Chow. C, Smith. J, Catalytic Oxidation of Formic Acid in Water. Interparticle Diffusion in Liquid-Filled Pores, Ind. Eng. Chem. Process. Des. Develop, 13 no. 4 (1974), 447-452

62. Barbier. J, Wet-air oxidation of Acetic acid over Platinum Catalysts supported in Cerium based materials, Influence of Metal and Crystallite size, Journal of Catalysis 251 (2007) 172-181.

63. Look. K, Smith. J, Effectiveness factor for oxidation kinetics, Ind. Eng. Chem. Process. Des. Develop, 17 no. 3 (1978) 368-372

64. Leitenburg de, C.; Goi, D.; Primavera, A.; Trovarelli, A.; Dolcetti, A. Wet oxidation of acetic acid catalyzed by doped ceria. *Appl. Catal, B*, 1996, *11* (1), L29-L35.

65. Barbier Jr., Delano F., Jabouille F., Duprez D.,Blanchard G., and P. Isnard,Total Oxidation of Acetic Acid in Aqueous Solutions over Noble Metal Catalysts, Journal of catalysis 177 (1998) 378–385

66. Pierre. Gallezot, Catalytic Wet-air oxidation of acetic Acid on carbon Supported Ruthenium Catalysts, Journal of Catalysis 168 (1997) 104-109.

67. Hosokawa. S, Kanni. H, Utani. K, Taniguchi. Y, State of ruthenium on CeO_2 and its catalytic activity in the wet oxidation of acetic acid, Applied Catalyses B: Environmental, 45 (2003) 181-187

68. MARGOLIS L. YA, On the Mechanism of Catalytic Oxidation of Hydrocarbons, Journal of catalysis 21, 93-101 (1971)

69. Barbier. J, Characterization of Platinum Catalyst Supported on Ce, Zr, Pr oxides and formation of Carbonate species in Catalytic wet air oxidation of Acetic acid, Catalysis Today 124 (2007) 185-190.

70. Klinghoffer A.A; Cerro R.L. and Abraham M.A; Catalytic wet oxidation of acetic acid using platinum on alumina monolith catalyst. *Catalysis Today*, 1998, 40, 59-71

71. Wang. J, Zhu W, Yang S, He. X, Wei Wang, Catalytic wet air oxidation of acetic acid over different ruthenium catalysts, *Catalysis communication,* 2008, 9, 2163–2167

72. Dukkanci. M, Gunduz. G, Catalytic wet air oxidation of Oxalic acid at atmospheric pressure, Int. J. of Chem. Reactor Eng, 5 (2007) A5

73. Shende. R, and Mahajani. V, kinetics of wet oxidation of Glyoxalic Acid and oxalic acid, Ind. Eng. Chem. Res. 1994, 33, 3125 – 3130

74. Lee; D, Qloyna. F, Efficiency of H2O2 and 02 in Supercritical water oxidation o 2-4 dichlorophenol and acetic acid, Journal of supercritical Fluids 3 (1990) 249-255.

75. Jianli. Y, Savage. P, Kinetics of MnO2-catalyzed Acetic acid oxidation in supercritical water, Ind. Eng. Chem. Res. 33, 2000, 4014 – 4019

76. Krajnc. M, Levec. M, Catalytic oxidation of toxic organics in supercritical water, Applied Catalyses B: Environmental, 3 (1994) L101-L107

77. Thornton. T, Savage. P, Phenol oxidation in Supercritical water, Journal of supercritical Fluids 3 (1990) 240-248.

78. Krajnc. M, Levec. M, The role of catalyst in supercritical water oxidation of Acetic acid, Applied Catalyses B: Environmental, 13 (1994) 93-103

79. Gomes, H. T.; Figueiredo, J. L.; Faria, J. L. Catalytic wet air oxidation of low molecular weight carboxylic acids using a carbon supported platinum catalyst. *Appl. Catal, B,* 2000, *27* (4), L217-L223.

80. Gomes, H. T.; Figueiredo, J. L.; Faria, J. L.; Serp, Ph.; Kalck, Ph. Carbon-supported iridium catalysts in the catalytic wet air oxidation of carboxylic acids: Kinetics and mechanistic interpretation. *J. Mol. Catal, A* 2002, *182-183*, 47-60.

81. Gomes, H. T.; Serp, Ph.; Kalck, Ph.; Figueiredo, J. L.; Faria, J. L. Carbon supported platinum catalysts for catalytic wet air oxidation of refractory carboxylic acids. *Top. Catal.* 2005, *33* (1-2-3-4), 59-68.

82. Shende. R, Levec. J, wet oxidation kinetics of refractory low molecular mass carboxylic acids, Ind. Eng. Chem. Res. 38, 1999, 3830 – 3837.

83. Perkas, N.; Minh, D. P.; Gallezot, P.; Gedanken, A.; Besson, M. Platinum and ruthenium catalysts on mesoporous titanium and zirconium oxides for the catalytic wet air oxidation of model compounds. *Appl. Catal., B* 2005, *59* (1-2), 121-130.

84. Lee, D.-K.; Kim, D.-S. Catalytic wet air oxidation of carboxylic acids at atmospheric pressure. *Catal. Today* 2000, *63* (2-4), 249-255.36

85. Beziat, J.-C.; Besson, M.; Gallezot, P.; Durecu, S. Catalytic Wet Air Oxidation of Carboxylic Acids on TiO2-Supported Ruthenium Catalysts. *J. Catal.* 1999, *182* (1), 129-135.

86. Oliviero, L.; Barbier, J., Jr.; Duprez, D.; Wahyu, H.; Ponton, J. W.; Metcalfe, I. S.; Mantzavinos, D. Wet air oxidation of aqueous solutions of maleic acid over Ru/CeO2 catalysts. *Appl. Catal., B* 2001, *35* (1), 1-12.

87. Pintar, A.; Batista , J.; Tisler, T. Catalytic Wet Air Oxidation oxidation of aqueous solutions formic acid, acetic acid ; phenol in continouse flow trickle-bed reactor over rutheniu, catalysts. *Appl. Catal., B* 2008, *84* , 30-41.

88. Sadana. J, Catalytic Oxidation of maleic acid in aqueuse solutions, Ind. Eng. Chem. Process. Des. Develop, 20 (1981) 576-577

89. Canizares. P, Dominguez. J, Rodrigo. M, Villasenor. J, Rodriguez, Effect of the current intensity in the electrochemical oxidation of aqueous phenol wastes at an activated carbon and steel anode, Ind. Eng. Chem. Res. 38, 1999, 3779 – 3785.

90. LLea. P, Environmental Friendly Electrochemistry – a Solution for a clean oil industry, Petroleum Res. 17 (2005) 1-6.

91. Oliviero, L.; Barbier, J., Jr.; Duprez, D.; Guerrero-Ruiz, A.; Bachiller-Baeza, B.; Rodrıguez-Ramos, I. Catalytic wet air oxidation of phenol and acrylic acid over Ru/C and Ru-CeO2/C catalysts. *Appl. Catal, B* 2000, *25* (4), 267-275.

92. Rivas. F, Kolacakozski. S, Beltran. F, Mclurgh. D, Development of a model for the wet air oxidation of phenol based on a free radical mechanism, *Chem. Eng. Sci. 53 no. 14* (1998), 2575-2586

93. Sadana. A, Katzer. J, Involvement of free radicals in the aqueous-phase catalytic oxidation of phenol over copper oxide, J. of catalysis 35 (1974) 140-152

94. Miguelez. S, Bernal. J, Sanz. E, Ossa. E, Kinetics of wet air oxidation of phenol, *Chem. Eng. Journal. 67* (1997) 115-121

95. Hamoudi. S, Belkacemi. K, Larachi. F, Catalytic oxidation of aqueous phenolic solutions: catalyst deactivation and kinetics, *Chem. Eng. Sci.* (*4* (1999), 3569-3576

96. Minh, D.; Gallezot, P.; Besson, M.; Degradation of olive oil mill effluents by Catalytic Wet Air Oxidation 1. Reactivity of p-coumaric acid over Pt and Ru supported catalysts. *Applied Catalysis B: Environmental 6*3 (2006) 68-75.

97. Minh, D.; Aubert. G, Gallezot, P.; Besson, M.; Degradation of olive oil mill effluents by Catalytic Wet Air Oxidation 2. Oxidation of p-hydroxyphenylacetic acid and p-hydroxybenzoic acid over Pt and Ru supported catalysts. *Applied Catalysis B: Environmental* 73 (2007) 236-246.

98. Pintar A., Bercic. G, Gallezot, P.; Besson, M.; Catalytic wet-air oxidation of industrial effluents: total mineralization of organics and lumped kinetics. *Applied Catalysis B: Environmental* 47 (2004) 143-152.

99. Bernal. J, Miguelez. J, Sanz. E, Ossa. E, Wet air oxidation of oily wastes generated a board ships, kinetics modelling, J. of hazardous materials B67 (1999) 61-73

100. Minh, D.; Gallezot, P.; Besson, M.; Degradation of olive oil mill effluents by Catalytic Wet Air Oxidation 3.Stability of supported ruthenium catalysts during oxidation of model pollutant p-hydroxybenzoic acid in batch and continuous reactors. *Applied Catalysis B: Environmental* 75 (2007) 71-77.

101. Ning Li, Claude Descorme, Michele Besson Catalytic wet air oxidation of aqueous solution of 2-chlorophenol over Ru/zirconia catalysts *Applied Catalysis B: Environmental* 2007, 71, 262–270

102. Ning Li, Claude Descorme, Michele Besson, Application of Ce0.33Zr0.63Pr0.04 supported noble metal catalysts in the Catalytic wet air oxidation of 2-chlorophenol influence of the reaction condition *Applied Catalysis B: Environmental* 2008, 80, 237–247

103. Andrzej Cybulski, Janusz Trawczynski Catalytic wet air oxidation of phenol over platinum and ruthenium catalysts *Applied Catalysis B: Environmental* 2004, 47, 1–24

104. Barbier, J., Jr; Oliviero, L.; Renard, B.; Duprez, D. Catalysts wet air oxidation of ammonia over M/CeO$_2$ catalysts in the treatment nitrogen containing pollutants. *Catal. Today* 2002, *75*, 29-34.

105. A. Eftaxias, J. Font, A. Fortuny, A. Fabregat, F. Stuber Catalytic wet air oxidation of phenol over active carbon catalyst Global kinetic modelling using simulated annealing Applied Catalysis B: Environmental 2006, 67, 12–23.

106. Saracco. G, *Chem. Eng. Sci.* 1995, *50* (17), 2833-2841.

107. Alejandre, A.; Medina, F.; Fortuny, A.; Salagre, P.; Sueiras, J. E. Characterisation of copper catalysts and activity for the oxidation of phenol aqueous solutions. *Appl. Catal, B* 1998, *16* (1) 53-67.

108. Alejandre, A.; Medina, F.; Salagre, P.; Fabregat, A.; Sueiras, J. E. Characterization and activity of copper and nickel catalysts for the oxidation of phenol aqueous solutions. *Appl. Catal., B* 1998, *18* (3-4), 307-315.

109. Alejandre, A.; Medina, F.; Rodriguez, X.; Salagre, P.; Cesteros, Y.; Sueiras, J. E. Cu/Ni/Al layered double hydroxides as precursors of catalysts for the wet air oxidation of phenol aqueous solutions. *Appl. Catal., B* 2001, *30* (1-2), 195-207.

110. Arena, F.; Giovenco, R.; Torre, T.; Venuto, A.; Parmaliana, A. Activity and resistance to leaching of Cu-based catalysts in the wet oxidation of phenol, *Appl. Catal., B* 2003, *45* (1), 51-62.

111. Fortuny, A.; Ferrer, C.; Bengoa, C.; Font, J.; Fabregat, A. Catalytic removal of phenol from aqueous phase using oxygen or air as oxidant. *Catal. Today* 1995, *24* (1-2), 79-83.

112. Fortuny, A.; Font, J.; Fabregat, A. Wet air oxidation of phenol using active carbon as catalyst. *Appl. Catal., B* 1998, *19* (3-4), 165- 173.

113. Alpin. A., water research 38 (2004) 289-300

114. Alpin. A., . *Appl. Catal., B* 30, 1998, 123- 139.

115. Pintar, A.; Levec, J. Catalytic oxidation of organics in aqueous solutions. Kinetics of phenol oxidation *J. Catal.* 1992, *135*, 345-357.

116. Pintar, A.; Levec, J. Catalytic oxidation of aqueous *p*-chlorophenol and *p*-nitrophenol solutions. *Chem. Eng. Sci.* 1994, *49* (24A), 4391-4407.

117. Pintar, A.; Levec, J. Catalytic Liquid-Phase Oxidation of Phenol Aqueous Solutions. A Kinetic Investigation. *Ind. Eng. Chem. Res.* 1994, *33* (12), 3070-3077.

118. Kim. S, Topics in catalysis 33 (2005) 149-154

119. Abu-hassan. M, Topics in catalysis 33 (2005) 141-148

120. Rodriguez. A, J. of supercritical fluids 45 (2008) 120-128

121. Barthholomew. C, Mechanisms of catalyst deactivation, Applied Catalysis A: General 222 (2001) 31- 45

122. Santos, A.; Yustos, P.; Quintanilla, A.; Ruiz, G.; Garcıa-Ochoa, F. Study of the copper leaching in the wet oxidation of phenol with CuO- based catalysts: Causes and effects. *Appl. Catal, B* 2005, *61* (3-4), 323- 333.

123. Manole. C, *Int. J. Chem. React. Eng.* 2007, *5*, A65.

124. Cybulski, A.; Trawczyn´ ski, J. Catalytic wet air oxidation of phenol over platinum and ruthenium catalysts. *Appl. Catal., B* 2004, *47* (1), 1-13.

125. Masende, Z. P. G.; Kuster, B. F. M.; Ptasinski, K. J.; Janssen, F. J. J. G.; Katima, J. H. Y.; Schouten, J. C. Platinum catalysed wet oxidation of phenol in a stirred slurry reactor: The role of oxygen and phenol loads on reaction pathways. *Catal. Today* 2003, *79- 80*, 357-370.

126. Athanasios Eftaxias, Josep Font, Agusti Fortuny, Azael Fabregat, Frank Stuber Kinetics of phenol oxidation in a trickle bed reactor over active carbon catalyst *J Chem Technol Biotechnol* 2005, 80, 677 – 687.

127. Chaliha. S, Bhattacharyya. Usinag Mn(II)-MCM-41 as an enviroment-friendly catalyst to oxidize phenol, 2-chlorophenol, 2-nitrophenol in aqueous solution, Ind. Eng. Chem. Res. 2007, 46, 3863-3870

128. Genlou E; Appl. *Catal, B: 44* (2003) 1-8

129. Barrault J; Appl. *Catal, B: 27* (2000) L225-L230

130. Chritoskova. S, Appl. *Catal, A: 208* (2001) 243-249

131. Lou. J, Huang. S, Treating isopropyl alcohol by a regenerative catalytic oxidizer, *Separation and purification technology 62* (2008) *71-78*

132. Dominguez. M, Sanchez. M, Centeno. M, Montes. M, Odrizola. J, 2-propanol oxidation over gold supported catalysts coated ceramic foams prepared from stainless steel wastes, *Journal of molecular catalysis A: Chemical 227* (2007) *145-154*

133. Liu. S, Yang. S, Complete oxidation of 2-propanol over gold based catalysts supported on metal oxides, Appl. *Catal, A: 334* (2008) 92-99

134. Guliants V, Holmes S; Probing polyfunctional nature of vanadyl pyrophosphate catalysts, oxidation of 16 C_4 molecules, Journal of molecular catalysis A Chemical 175 (2001) 227-239

135. Silva. A, Chem., Eng., Sci., 59 (2004) 5291-5299.

136. Faibish. R, Cohen. Y, Fouling and rejetion behaviour of ceramic and polymer, modified ceramic membranes for ultrafiltration of oil-in-water emulsions and microemulsions Ind. *Eng. Colloids and surfaces A: Physicochemical and engineering aspects 191* (2001) 27 - 40

137. Biesheuvel. P, Verweij, Design of ceramic supports: permeability, tensile strength and stress, Journal *of membrane science*, 156 (1999) 141- 152

138. Mullet M, Fievet. P, Reggiani. J, Pagetti. J, Surface electrochemical properties of mixed oxide ceramic membranes, Zeta-potential and surface charge density, *Journal of membrane science*, 123 (1997) 255- 265

139. Burggraaf. A, Lin. Y, Experimental studies on pores size change of porous ceramic membranes after modification, *Journal of membrane science* 79 (1993) 65- 82

140. Meixner. D, Dyer. P, Characterization of the transport properties of microporous membranes, *Journal of membrane science* 79 (1993) 65- 82

141. Hussain. A, Seidel-Morgenstern. A, Tsotsas. E, Heat and mass transfer in tubular ceramic membranes for membrane reactors, Int. J. of heat and mass transfer 49 (2006) 2239-2253

142. Cini. P, Blaha. S, Harold. M, Preparation and characterization of modified tubular ceramic membranes for use as catalytic supports, *Journal of membrane science*, 55 (1991) 199-225

143. Cini. P and Harlod. M, Experimental study of the Tubular Multiphase Catalyst, AIChE Journal 37, no. 7, (1991), 997 – 1008.

144. Peureux J; Torres M; Mozzanega H; Giroir-Fendler A. and Dalmon J-A; Nitrobenzene liquid-phase hydrogenation in a membrane reactor. *Catalysis Today*, 1995, 25, 409.

145. Daub. K, Emig. G, Chollier. M, Callant. M, Dittmeyer. R, Studies on the use of catalytic membranes for reduction of nitrate in drinking water; *Chem. Eng. Science*, 54 (1999) 2807-2815.

146. Casanave. D; Giroir-Fendler. A, Sanchez. J, Loutaty. R, Dalmon. J, Control of transport properties with a microporous membrane reactor to enhance yields in dehydrogenation reactions, *Catalysis Today*, 25 (1995) 309-314

147. Matthew J. Birchmeier and Charles G. Hill, Jr Carl J. Houtman, Rajai H. Atalla, and Ira A. Weinstock, Enhanced Wet Air Oxidation: Synergistic Rate Acceleration upon Effluent Recirculation Ind. Eng. Chem. Res. 2000, 39, 55-64

148. Casanave. D; Ciavarella. P; Fiaty. K; Dalmon. J, Zeolite membrane reactor for isobutene dehydrogenation: experimental results and theoretical modelling, *Chem. Eng. Science*, 54 (1999) 1577-1582.

149. Iojoiu, E. E.; Miachon, S.; Dalmon, J.-A. Progress in performance and stability of a contactor-type Catalytic Membrane Reactor for wet air oxidation. *Topics in Catal.* 2005, *33* (1-2-3-4), 135-139.

150. Iojoiu, E. E.; Walmsley, J. C.; Ræder, H.; Miachon, S.; Dalmon, J.-A. Catalytic membrane structure influence on the pressure effects in an interfacial contactor catalytic membrane reactor applied to wet air oxidation. *Catal. Today* 2005, *104* (2-4), 329-335.

151. Miachon, S.; Perez, V.; Crehan, G.; Torp, E.; Ræder, H.; Bredesen, R.; Dalmon, J.-A. Comparison of a contactor catalytic membrane reactor with a conventional reactor: Example of wet air oxidation. *Catal. Today* 2003, *82* (1-4), 75-81.

152. Vospernik, M.; Pintar, A.; Levec, J. Application of a catalytic membrane reactor to catalytic wet air oxidation of formic acid. *Chem. Eng. Process*. 2006, *45* (5), 404-414.

153. Berecic. G, Pintar. A, Levec. J, Positioning of reaction zone by coupling results of mass transport and chemical reaction study, Catalysis Today 105 (2005) 589-597.

154. Ræder. H, R. Bredesen, G. Crehan, S. Miachon, J-A. Dalmon, A. Pintar, J. Levec, E.G. Torp, A wet air oxidation process using a catalytic membrane contactor, *Sep. Purif. Technol.* 32 (2003) 349-355.

155. Julbe. A, D. Farrusseng 1, C. Guizard, Limitations and potentials of oxygen transport dense and porous ceramic membranes for oxidation reactions *Catalysis Today 104 (2005) 102–113*

156. Gutierrez. M, P. Pina a, M. Torres, M.A. Cauqui, J. Herguido, Catalytic wet oxidation of phenol using membrane reactors: A comparative study with slurry-type reactors Catalysis Today 149 (2010) 326–333

157. Diaz Taboada. C., A. Pintar, J. Batista, T. Levec, Preparation, characterization and catalytic properties of carbon nanofiber-supported Pt, Pd, Ru monometallic particles in aqueous-phase reactions, Applied Catal. B: Environ. 89 (2009) 375-382.

158. Perez. V, S. Miachon, J-A. Dalmon, R. Bredesen, G. Pettersen, H. Ræder, Ch. Simon, Preparation and characterization of a Pt/ceramic catalytic membrane, Sep. Purif. Technol. 25 (2001) 33-38.

159. Uzio. D, S. Miachon, J-A. Dalmon, Controlled Pt deposition in membrane mesoporous top layers, Catal. Today 82 (2003) 67-74.

160. Vospernik. M, Albin Pintar , Gorazd Ber, Janez Levec, Experimental verification of ceramic membrane potentials for supporting three-phase catalytic reactions, Journal of Membrane Science 223 (2003) 157–169

161. Vospernik. M., A. Pintar, G. Bercic, J. Levec, Mass transfer studies in gas-liquid-solid membrane contactors, Catal. Today 79-80 (2003) 169-179.

162. Iojoiu E., J.C. Walmsey, H. Ræder, R. Bredesen, S. Miachon, J-A. Dalmon, Comparison of different support types for the preparation of nanostructured catalytic membranes, Rev. Adv. Mater. Sci. 5 (2003) 160-165.

163. Miachon. S., J-A. Dalmon, Catalysis in membrane reactors: what about the catalyst? Topics Catal. 29 (2004) 59-65.

164. Vospernik. M., A. Pintar, G. Bercic, J. Levec, J.C. Walmsey, H. Raeder, E.E. Iojoiu, S. Miachon, J-A. Dalmon, Performance of catalytic membrane reactor in multiphase reactions, Chem. Eng. Sci. 59 (2004) 5363-5372.

165. M. Vospernik, A. Pintar, G. Bercic, J. Batista and J. Levec, potentials of ceramic membranes as catalytic three phase reactors,, Chemical Engineering Research and Design, 82(A5): 659–666

166. Iojoiu. E., E. Landrivon, H. Ræder, E.G. Torp, S. Miachon, J-A. Dalmon, The "Watercatox" process: Wet air oxidation of industrial effluents in a catalytic membrane reactor. First report on contactor CMR up scaling to pilot unit, Catal. Today 118 (2006) 246-252. 330

167. Iojoiu. E., S. Miachon, E. Landrivon, J.C. Walmsley, H. Raeder, J.-A. Dalmon, Appl.

Catal. B 69 (2007) 196–206. 1110.

168. Reif. M., R. Dittmeyer, Catalytically active ceramic membranes for gas-liquid reactions: a comparison between catalytic diffuser and forced through flow concept, *CataL. Today* 82 (2003) 3-14.

169. Soria R: Overview on industrial membranes. *Catal Today* 1995, 25:285-290.

170. Dotzauer. M., Abusaloua A., Miachon S., Dalmon J-A, Bruening. L., Wet air oxidation with tubular ceramic membranes modified with polyelectrolyte/Pt nanoparticle films, *Applied Catal. B: Environ.* 91 (2009) 180-188

171. Pinna. F, Supported metal catalysts preparation, Catalysis Today 41 (1998) 129-137.

172. Perego. C, Villa. P, Catalyst preparation methods, Catalysis Today 1997 (1997) 281-305.

173. Haber. J, Block. J, delmon. J, Manual of methods and procedures for catalyst characterization, Pure & Appl. Chem. 67 no. 8-9 (1995) 1257-1306

174. Dotzauer. M. D, Dai. J, Bruening. M, Catalytic Membrane prepared using layer-by layer Adsorption of Polyelectrolyte/Metal Nanoparticle Films in Porous Supports, Nano letters, 6 (2006) 2268-2272

175. Dai. J, Baker. G, Bruening. M, Use of porous membranes modified with Polyelectrolyte multilayer as substrates for protein arrays with low non-specific adsorption, Anal. Chem, 78 (2006) 135-140.

176. Kim. J, Bruening. M, Baker. G, Surface-Initiated Atom Transfer radical polymerisation on Gold at ambient temperature, J. Am. Chem. Soc, 122 (2000)

177. Campanati M., G. Fornasari, A. Vaccari, Fundamentals in the preparation of heterogeneous catalysts, Catalysis Today 77 (2003) 299–314

178. Suarez-Ojeda. M, Metacalfe. I, Font. J, Carrera. J, Calibration of the kinetic model for wet air oxidation (WAO) of substituted phenols: influence of the experimental data on model prediction and practical identifiably, Chem. Eng. Journal, 150 (2009) 328-336

179. Sedmak. G, Hocevar. S, Levec. J, Transient kinetic model of CO oxidation over a nanostructured $Cu_{0.1}Ce_{0.9}O_{2-y}$ catalysts, J. of catalysis 222 (2004) 87-99.

180. Toukoniity. E, Warna. J, Murzin. D, Salmi. T, Modelling of transient kinetics in catalytic three phase reactors: Enantioselective hydrogenation, *Chem. Eng. Science* 65 (2010) 1076-1087

181. Berger. J. R and Kapteijin. F, Coated-Wall Reactor Modelling-Criteria for Neglecting Radial Concentration Gradients. 1. Empty Reactor tubes, Ind. Eng. Chem. Res. 2007, 46, 3863-3870

182. Torres M; Sanchez J; Dalmon J.A; Bernauer B. and Lieto J, Modeling and simulation of a three-phase catalytic membrane reactor for nitrobenzene hydrogenation. *Ind. Eng. Chem. Res*, 33 (1994) 2421-2425

183. Saracco. G and Vito Specchia, Catalytic combustion of propane in a membrane reactor with separates feed of reactants. IV. Transition from the kinetics- to the transport- controlled regime, Chem., Eng., Sci., 55 (2000) 3979-3989

184. Larsoon. M, Henriksson. N, and Andersson. B, Investigation of the kinetics of a deactivating system by Transient experiments. Applied Catalyses A: General, 166 (1998) 9-19

185. Elnashaie S., B. K. Abdallah, S. S. Elshishini, S. Alkhowaiter, M. B. Noureldeen, T. Alsoudani, On the link between intrinsic catalytic reaction kinetics and the development of catalytic processes – Catalytic dehydrogenation of ethyl benzene to styrene, Catalysis Today 64 (2001) 151-162.

186. Lvarez A, P. M.; McLurgh, D.; Plucinski, P. Copper Oxide Mounted on Activated Carbon as Catalyst for Wet Air Oxidation of Aqueous Phenol. 2. Catalyst Stability. *Ind. Eng. Chem. Res*. 2002, *41* (9), 2153-2158.

187. Sabate. J, Anderson. A, Kikkawa. H, Eduards. M, Hill. C, A kinetic study of the photo catalytic degradation of 3-chlorosalicyclic acid over Tio2 membrane catalyst supported on glass, journal of catalysis 127 (1991) 167-177

188. Katz. S, Chemical Reactions catalysed on tube Wall, Chem., Eng., Sci., 10 (1959) 202-211

189. Li. L, Chen. P, Gloyna. E, Generalized Kinetic Model for Wet Oxidation of Organic Compounds, AIChE Journal 37, no. 11, (1991), 1687 – 1697.

190. Weisz. P, and Hicks. J, The behaviour of porous catalyst particles in view of internal mass and heat diffusion effects, Chem., Eng., Sci., 17 (1962) 265-275

191. Mandowara. A, Bhattacharya. P, Membrane Contactor as degasser Operated under vacuum for Ammonia removal form Water: Numerical Simulation of Mass Transfer for Laminar flow Conditions, Computers Chem. Eng 33 (2009) 1123-1131.

192. Keshavarz. P, Dixon. A, Moser. W, Fathikalajahi. J, Mathematical Modelling of gas-liquid membrane contactor using random distribution of fibre, Journal of membrane science, (2008) 98-108.

193. Oyama. S, Hacarlioglu. P, The boundary between simple and complex descriptions of membrane reactors: The transition between 1-D and 2-D analysis, Journal of membrane science, 337 (2009) 188-199.

194. Becker. Y, Dixon. A, Moser. W, Ma. Y, Modelling of Ethyl benzene dehydrogenation in a catalytic Membrane Reactor, Journal of membrane science, 77, (1993) 233-244.

195. Sandelin. F, Oinas. P, Salmi. T, Paloniemi. J, Harrio. H, Dynamic Modelling of Catalytic Liquid-Phase reactions in fixed beds-Kinetics and Catalyst deactivation in the recovery of anthraquinones, Chem., Eng., Sci., 61 (2006) 4528-4539

196. Casanave. D, Fiaty. K, Dalmon. J. A, Computer-aided optimization of catalytic dehydrogenation in packed bed membrane reactor, Computers Chem. Engng 22 (1998) S691-S694.

197. Wouwer. A, Schhiesser. W, Editorial Special Issue on the Method of Lines: dedicated to Keith Miller, Journal of Computational and Applied Mathematics 183 (2005) 241-244

198. Wouwer. A, Saucez. P, Schhiesser. W, Simulation of Distributed Parameter Systems Using a Matlab-Based Method of Lines Tool Box: Chemical Engineering Applications, Ind. Eng. Chem. Res. 43 (2004) 3469-3477.

199. Lee. H, Mathews. C, Braddock. R, Sander. G, Gandola. F, A MATLAB method of Lines template for Transport Equations, Environmental Modelling & Software, 19 (2004) 603-614.

200. Warana. J, Salmi. T, Dynamic Modelling of Catalytic Three Phase Reactors, Computers Chem. Eng 1 (1996) 39-47.

201. Hermann. C, Quicker. P, Dittmeyer. R, Mathematical Simulation of Catalytic Dehydrogenation of Ethyl benzene to Styrene in a Composite Palladium Membrane Reactor, Journal of Membrane science 136 (1997) 161-172

202. Bischoff. K, A note for boundary conditions for flow reactors, Chem. Eng. Sci, 16 (1961) 131-133

203. Goyal, S. K., M. N. Esmail and N. N. Bakhshi, "Application of Orthogonal Collocations to some Transport Phenomena Problems in Co-Axial Cylinders and Spheres", Can. J. Chem. Eng. 65, 833-844 (1987).

204. Deffernez. A, Hermans. S, Devillers. M, Bimetallic Bi-Pt, Ru-Pt and Ru-Pd and tri-metallic catalyst for the selective oxidation of glyoxal into glyoxalic acid in aqueous phase, Applied Catalyses A: General, 282 (2005) 303-313

205. Romanenko. A, Tyschishin. E, Moroz. E, Likholobov. V, Zaikovskii. V, Jhung. S, Park. Y, Influence of ruthenium addition on sintering of carbon supported Palladium, Applied Catalysis A: General 227 (2002) 117- 123

206. Jhung. S, Romanenko. A, Lee. E, Park. Y, Moroz. E, Likholobov. V, Carbon supported Palladium-ruthenium catalyst for hydropurification of terephathalic acid, Applied Catalysis A: General 225 (2002) 131- 139.

207. Micheaud. C, Marécot. P, Guérin. M, Barbier. J, Preparation of alumina supported Palladium-Platinum catalysts by surface redox reactions. Activity for complete hydrocarbon oxidation, Applied Catalysis A: General 171 (1998) 229- 239

208. Rosset. J, Cadrot. A, Aires. F, Renouprez. A, Mélinon. P, Perez. A, Pellarin. M, Vialle. J, Broyer. M, Study of bimetallic Pd-Pt clusters in both free and supported phases, J. Chem. Phys. 102 (21), 1 june 1995

209. Kim. S, Park. H, Lee. D, Pd-Pt /Al$_2$O$_3$ bimetallic catalysts for the advanced oxidation of reactive dye solutions, Catalysis Today 87 (2003) 51-57.

210. Breen. J, Burch. R, Griffin. K, Hardacre. C, Hayes. M, Huang. X, O'Brien. S, Bimetallic effects in the liquid phase hydrogenation of 2-butanone, Journal of Catalysis 236 (2005) 270-281. (Pt – Ru – Rh)

211. Zhang. Q, Chuang. K, Kinetics of wet oxidation of black liquor over a Pt-Pd-Ce/ alumina catalyst, Journal of Catalysis 17 (1998) 322-332. (Pt – Pd – Ce)

212. Kim. T, Kobyashi. K, Nagai. M, Preparation and characterization of Platinum-ruthenium bimetallic nanoparticles using Reverse Microemulsiomns for fuel cell catalyst, J. Oleo. Sci. 56 (10) (2007) 553-562.

213. Batista. J, Pintar. A, Gomilsek. J, Kodre. A, Bornette. F, On the structural characteristics of γ-alumina-supported Pd-Cu bimetallic catalysts, Applied Catalysis A: General 217 (2001) 55- 68.

214. Fortuny A., C. Bengoa. J. Font, A. Fabregat, bimetallic catalysts for continous catalytic wet air oxidation of phenol, Journal of Hazardos Materials B 64 (1999) 181-193.

215. Ponec. V, Alloy catalysts the concept, Applied Catalysis A: General 222 (2001) 31- 45.

2 EXPERIMENTAL METHODS

2.1 Ceramic membranes

The ceramic membrane supports used in this work, provided by either Pall-Exekia (Bazet, France) or Inocermic, (Germany), all membranes have tubular geometry (OD 10mm, ID 7mm) with a total The ceramic membrane supports used in this work, provided by either Pall-Exekia (Bazet, France) or Inocermic, (Germany). All membranes have tubular geometry (OD 10mm, ID 7mm) with a total length of 250mm. They consisted of three or four concentric layers showing an average pore size decreasing from external to internal side of the tubular membrane. The final mesoporous top layer, located in the inner side of the ceramic membranes as shown in figure 17. Both ends of the tubular membranes (ca. 1.5 cm in each side) have been covered with enamel or glaze, which assure tight sealing and prevent gas by-pass. For membrane supports that provided by Pall-Exekia, the top layer was made from TiO_2 or ZrO_2 (thickness, 3-6 μm, mean pore size, 20-50 nm) while the subsequent layers were made of α-Al_2O_3 coated with TiO_2.

For membrane that provided by Inocermic (Germany), the membrane top layer was made from CeO_2 -doped ZrO_2 (thickness, 8 μm, mean pore size, 30, 80, or 100 nm) while the subsequent layers were made of TiO_2.

Tables 10 and 11 show the main characteristics of the Pall-Exekia and Inocermic supports.
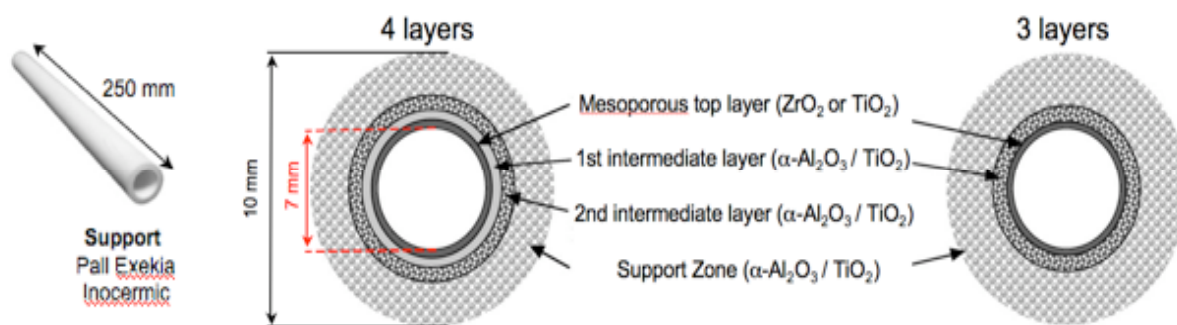
Figure 17 Schematic cross-section of the membrane showing the three or four-layers structure

Table 10 main characteristics of Pall-Exekia supports

Support Supplier	Number of layers	Layer	Material	Mean pore size (nm) / Thickness (μm)
PALL -EXEKIA	4	1 (top layer)	ZrO_2	20/3
		2	α-Al_2O_3 (TiO_2)	200/20
		3	α-Al_2O_3 (TiO_2)	800/30
		4	α-Al_2O_3 (TiO_2)	1200/1500
PALL	3	1 (top layer)	ZrO_2	50/6
		2	α-Al_2O_3 (TiO_2)	800/15
		3	α-Al_2O_3 (TiO_2)	1200/1500

Table 11 main characteristics of Ino-cermic supports

Supplier	Number of layers	Layer	Material	Mean pore size (nm) /
INO-CERMIC	4	1 (top layer)	(CeO_2 / ZrO_2) or TiO_2	80/8
		2	TiO_2	250/20
		3	TiO_2	800/30
		4	TiO_2	1200/1500
INO-CERMIC	3	1 (top layer)	TiO_2 (CeO_2/ZrO_2)	100/8
		2	TiO_2	800/30
		3	TiO_2	5000/1500

2.2 CATALYTIC MEMBRANE PREPARATION:

Active phase deposition: The common preparation methods of the dispersed metal catalysts requires a combination of different unit operations (7) or several steps, which can be described as: (i) introduction of the metal precursor on the support by impregnation or ion exchange, co-precipitation and deposition precipitation, (ii) drying and calcinations, and (iii) reduction.

Precursor solutions: Different solutions have been used as an active phase metal precursors solutions are shown in Tables 12 and 13.

Table 12 Precursor solutions used for membranes preparations

Name	Precursor formula	Delivered by	Active phase metal
Cuppric nitrate trihydrate	$Cu (NO_3)_2.3H_2O$	Fluka	26.1% Cu
Zinc nitrate	$Zn (NO_3)_2$	Fluka	33.8% Zn
Zinc chloride	$ZnCl_2$	Aldrich	14.8% Zn
Nickel chloride hexahydrate	$NiCl_2.6H_2O$	Fluka	24.6% Ni
Nickel nitrate hexa hydrate	$Ni (NO_3)_2.6H_2O$	Fluka	20.1% Ni
Iron (III) nitrate nona hydrate	$Fe(NO_3)_3.9H_2O$	Sigma Aldrich	13.8% Fe
Cobalt (II) nitrate hexahydrate	$Co(NO_3)_2.6H_2O$	Sigma Aldrich	20,0% Co

Table 13 Precursor solutions used for membranes preparations

Name	Precursor formula	Delivered by	Active phase metal
Hydrogen hexa chloro platinate (IV) hydrate	H_2PtCl_6	Aldrich	39.8% Pt
Tetra amine platinum (II) chloride hydrate	$Pt(NH_3)_4 Cl_3$	Aldrich	65.0% Pt
Tetra amine platinum (II) nitrate	$Pt (NH_3)_4 (NO_3)_2$	Aldrich	49.1% Pt
Palladium (II)chloride anhydrous	$PdCl_2$	Fluka	59.8% Pd
Palladium (II) nitrate dihydrate	$Pd(NO_3)_2.2H_2O$	Fluka	40.0% Pd
Rruthenium (III) nitrosylnitrate	$Ru(NO)(NO_3)_3$	Alfa Aesar	1.5% Ru
Ruthenium (III) chloride anhydrous	$RuCl_3$	Fluka	45-55% Ru

2.2.1 Membrane Preparation Protocol

1- Primary drying of membrane

The support was dried over night in oven at 120°C in order to remove any condensed water content inside the membrane pores also to know the mass of membrane before catalyst deposition due to estimation of the active phase metal (catalyst) after wards.

2- Membrane impregnation

The support was soaked in a metal precursor solution for 12 hrs, the same method was used in case of the impregnation of bimetallic or trimetallic catalysts (co-impregnation with a mixture of two or three precursor solutions), which prepared based on already selected atomic ratio of active phase metals. The support (see fig. 18b) was placed vertically in eprouvette that has filled with a precursor solution at a level longer than the support length. The upper part of the support was fixed to mechanical stirrer, which revolved on 60 rev/min, to assure more homogenous distribution of the precursor solution on the support porous media.

(a)   (b)

Figure 18 (a) Membrane primary drying   (b) Impregnation

3- Membrane washing or drying

In case of anionic impregnation, the membrane was washed by nitric acid solution (0.1 N) under a magnetic agitation for 20 min. The washing process was repeated three times in order to wash the excess active phase metal and residuals. It has been to conserve part of the washing solutions after each three washing processes for ICP analysis in order to quantify the amount of metal present in the washing solution. In case of eva poration recrystallization, the membrane was dried in air at ambient temperature in horizontal position under rotation with electric motor (60 rev/min) for 12 hrs to evaporate the solvent from the exterior of the tubular membrane. Complete drying of the membrane will be attained

in next preparation step, by drying under nitrogen flow at 100 °C for 2hrs.

4- Membrane reduction and activation

First, the membrane was dried at 100°C under nitrogen flow (60ml/min) for 2hrs in calcinations / reduction bench setup as shown in figure 19b, then the metal loaded in membrane was reduced under hydrogen flow (60 ml/min) at 250°C for 8hrs. Then the hydrogen flow, replaced by nitrogen flow in order temperature decreasing step which considered as the last step in membrane thermal treatment program.
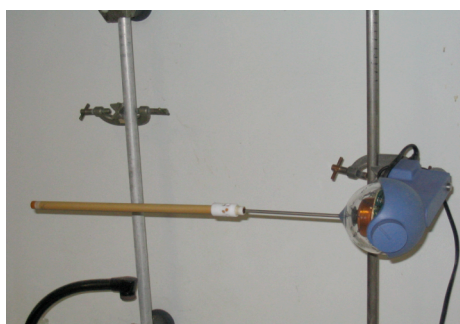
Figure 19 (a) Membrane evaporation   Fig 19 (b) Membrane calination and reduction

Applying temperature – time program as shown in figure 20, performed thermal treatment program.
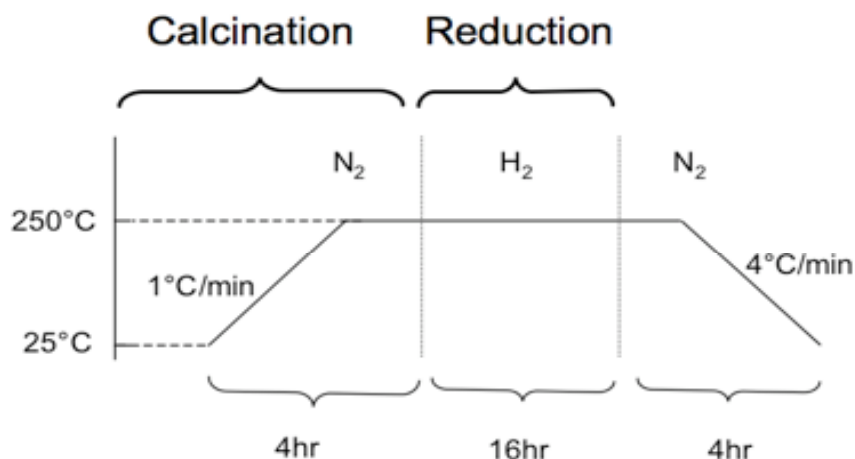
Figure 20 - Temperature-time profile used for catalytic membrane activation

2.2.2 Monometallic membranes preparation

Monometallic catalytic membranes with different types of active phase metals, (Pt, Pd, Ru, or Cu), were prepared by either evaporation-crystallisation method, anionic impregnation or layer-by layer electrolyte deposition.

Monometallic catalytic membranes with different types of active phase metals, (Pt, Pd, Ru, or Cu), were prepared by soaking impregnation and evaporation-crystallisation method. Before impregnation, all the membranes were dried in air at 120°C for 12 hrs, the membrane were then soaked overnight, in a vertical position, with an active phase precursor solution. A mechanical stirrer (60 rpm) has been used in order to assure a more homogenous contact of the precursor solution with a membrane support. In order to allow the solvent evaporation and uniform distribution of the precursor solution, the membranes were then kept in horizontal position at room temperature under air and rotated (60 rpm). The impregnated membranes have then been dried in nitrogen flow (60 ml/min) at 120°C for 1h (heating rate of 1°C/min.) and calcined at 200°C in nitrogen flow (60 ml/min) for 12 hours (heating rate of 1°C/min.)

The gas flux was then switched to hydrogen for 8 hrs at 200°C, in order to decompose the metal precursor. Metal species introduced within the membrane wall being then reduced to metal nanoparticle.

a- Evaporation-crystallization method

The support was rotated vertically in a precursor solution (impregnation step) for 15 hrs, then removed and dried at room temperature in horizontal position under rotation (60 rpm) under air in order to allow the evaporation and uniform distribution of the precursor solution (evaporation step) for 24 hrs.

The impregnated membranes were then dried in nitrogen flow (60 ml/min) at 100°C for 1h (heating rate of 1°C/min.) and then calcined at 200°C in nitrogen flow (60 ml/min) for two hours (heating rate of 1°C/min.) in order to decompose the Pt precursor introduced within the membrane wall. The gas flux was then switched to hydrogen for 12h, the metal species being then reduced to metal particle [1, 2].

b- Anionic impregnation method

The support was rotated vertically in a precursor solution (impregnation step) for 15 hrs, then removed and washed three times for 20 minutes in 0.1 N HNO_3, until the concentration of Pt species in the water was negligible (washing step).

The washed membranes were then dried in nitrogen flow (60 ml/min) at 100°C for 1h (heating rate of 1°C/min.) and then calcined at 200°C in nitrogen flow (60 ml/min) for two hours (heating rate of 1°C/min.) in order to decompose the Pt precursor, introduced within the membrane wall. The gas flux was then switched to hydrogen for 12h, the metal species being then reduced to metal particle [2].

c- Layer-by layer (LBL) electrolyte deposition

In this type of metal deposition, three different modified methods were used. These methods use a polyelectrolyte multilayer film. Each layer was deposited by passing a polyelectrolyte or metal nanoparticle solution through the membrane pores by using a pump to the feed solution. Flow occurred from the inside of the membrane to the outside [3].

- LBL-1 Ex situ nanoparticle formation (PAA/PAH/Pt-NP)

Briefly, 250 mL of PAA (polyacyclic acid) solution (0.002 M, 5000 Mw, 0.1 M NaCl, pH = 4.5) was passed through the membrane pores at approximately 25 mL/min. This was followed by passing water for 30 minutes, passing 250 mL of PAH (Polallylamine) solution (0.002 M, 17000 Mw, 0.1 M NaCl, pH = 5.5), and rinsing with water again for 30 minutes. Deposition of the metal nanoparticles was achieved by passing the desired amount of nanoparticle solution through the membrane and then rinsing with water for 30 minutes, To form Pt or Pd nanoparticles, a solution of 0.1 M $NaBH_4$ is passed through the membrane to reduce the Pt or Pd salt to nanoparticles [6].

- LBL-2 In situ nanoparticle formation (PAA/PEI/Pt(0))

In a slight modification to method LBL-1, LBL-2 incorporates a PEI-Pt complex in the deposition procedure rather than using preformed Pt nanoparticles. Briefly, loading involoving sequential deposition of PAA (0.002 M, 0.1 M Nacl, pH adjusted to 4.5) and PEI (0.002 M, 0.0004 M K_2PtCl_4, pH adjusted to 9). To form Pt nanoparticles, a solution of 0.1 M $NaBH_4$ is passed through the membrane to reduce the Pt to metal nanoparticles [3, 6].

- LBL-3 In situ nanoparticle formation (Pt(0)/PEI)

LBL-3 also utilizes sodium borohydride to reduce the Pt precusor to Pt nanoparticle after the polyelectrolyte film is deposited. In this method, the membrane first dipped in a solution of hexachloroplatinic acid (0.1 g_{Pt}/L) for 20 hrs with mild stirring. After rinsing away excess Pt solution, PEI (0.002 M, 0.1 M NaCl, pH adjusted to 9) was deposited. A second $PtCl^{2-}$/PEI bilayer was also deposited before reducing the Pt with $NaBH_4$ [6] .

2.2.3 Bimetallic membranes

Bimetallic catalytic membranes with different combination of active phase metals (Pt with either Pd, or Ru with Pd, or Cu with either Pd or Ni, or Ni with Zn, Fe with Co), all bimetallic membranes were prepared by soaking co-impregnation and evaporation-crystallisation method. Soaking co-impregnation is the soaking of a membrane support in a

solution mixture of two active phase metals precursors. The concentration of the active phase metals was prepared based on constant atomic ratio. Before impregnation, all the membrane were dried in air at 120°C for 12 hrs, the membrane were then soaked overnight, in a vertical position, with an active phase precursor solution. A mechanical stirrer (60 rpm) has been used in order to assure a more homogenous contact of the precursor solution with a membrane.

In order to allow the solvent evaporation and uniform distribution of the precursor solution, the membranes were then kept in horizontal position at room temperature under air and rotated (60 rpm). The impregnated membranes have then been dried in nitrogen flow (60 ml/min) at 120°C for 1h (heating rate of 1°C/min.) and calcined at 200°C in nitrogen flow (60 ml/min) for 12 hours (heating rate of 1°C/min). The gas flux was then switched to hydrogen for 8 hrs at 250°C, in order to decompose the metals. Metals species introduced within the membrane wall being then reduced to metal nanoparticles

2.3 Membranes characterization

2.3.1 Bubble point pressure determination

Bubble point pressure test of the membrane support is the gas-liquid displacement experiment using ethanol as liquid agent and nitrogen as gas. Ceramic membranes used in this thesis work were made of hydrophilic oxide materials, so any liquids that came in contact with tested membranes was quickly drawn into pores by capillary forces. Theoretical value of the capillary pressure for tested membrane can be well estimated by means of Laplace's equation [5]:

$$\Delta p = 2.\gamma.\cos\theta / R_p \quad \ldots\ldots\ldots\ldots (16)$$

Where,

R_p: is the radius of pores in membrane (nm)

γ: The liquid surface tension in (N/m)

θ: is the contact angle,

$\theta = 0$, for completely wetting fluid, water contacting ceramic membrane can be assumed to fulfil this condition [5]

Δp: the capillary pressure in (Pa)

The importance of gas-liquid displacement experiment (bubble point pressure) test is due to ability to estimate the maximum transmembrane pressure difference in the investigated

reaction system. During the operation of a gas-liquid membrane reactor, the diffusion of the gas phase into the liquid phase should be avoided because gas bubbles covers the membrane top layer surface and reduce the catalytic activity of the membrane.

2.3.2 Bubble point test protocol

The first bubble point pressure test is used as the criteria for the hydrodynamic performance of the tubular ceramic membranes. The bubble point pressure to nitrogen gas under ethanol was measured on the membrane before metal deposition, in order to check for the first bubble of gas penetrated.

- Membrane wetting

Two different pre-treatment wetting procedures of membranes by ethanol were used, either normal wetting, or vacuum wetting.

- Normal wetting

The membrane was dried in oven at 120°C over night (14 hrs), and then let membrane cool down to room temperature inside glass keeper to prevent from humidity. Then membrane was wetted in ethanol by slowly dipping it in small layer of ethanol as shown in figure 21. The ethanol level is equal to mid-thickness of membrane wall for 15min.Then membrane was rolled in forward and back ward directions several times. The membrane is immersed in ethanol for 12 hrs, and then bubble point test was done for each individual support under ethanol.
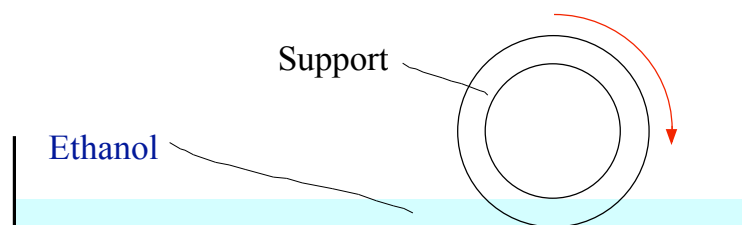
Figure 21   Normal wetting appartus for membrane [4]
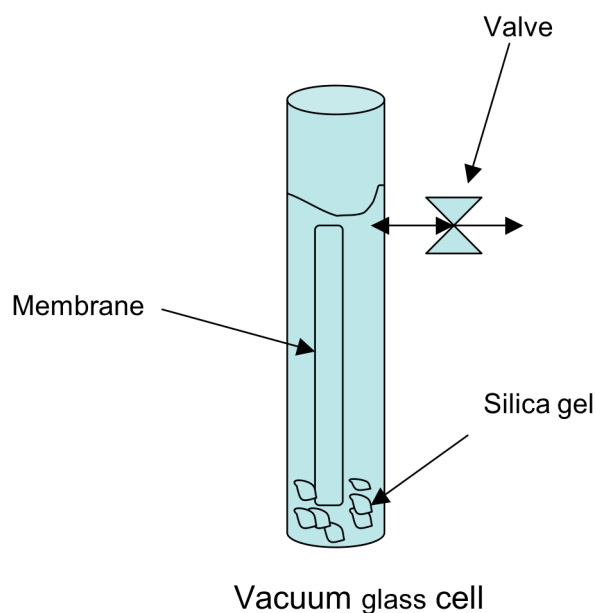
Figure 22 vacuum glass cells

Vacuum wetting

The membrane was dried in oven at 120°C for 14 hrs and then let membrane cool down to room temperature inside the vacuum glass cell that contains dried silica gel as shown in figure 22. Then membrane was mounted in a vacuum metal cylinder to start evacuation for 10 mn periods by using a vacuum pump. The vacuum metal cylinder has two valves in both sides as shown in figure 23. The valve between the vacuum metal cylinder and the vacuum pump was closed before stopping the pump. The other valve (on the left, fig. 23) is already closed before start evacuation, disconnect the vacuum metal cylinder from vacuum pump line, then one side of vacuum metal cylinder was immersed in ethanol, the valve that situated beside the ethanol pan was opened to start wetting by ethanol, the other side of vacuum metal cylinder already connected to transparent plastic tube to verify complete wetting by looking liquid ethanol flow through vacuum wetting process, then let membrane immersed for 1hr, then bubble point test was done for each individual support under ethanol.
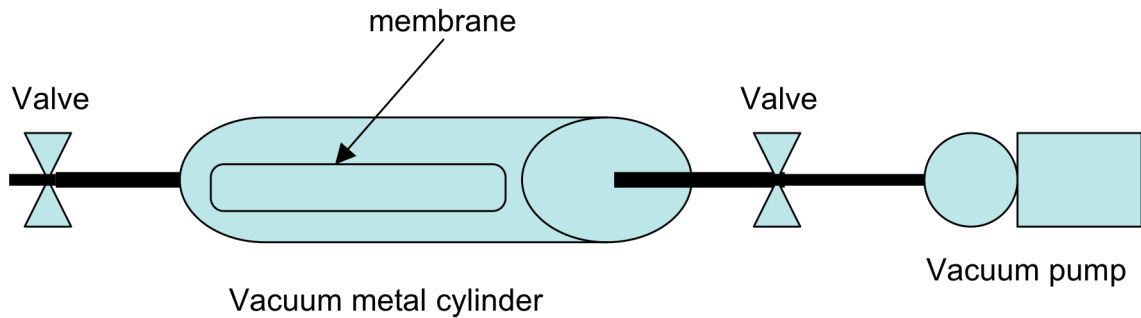
Figure 23 Vacuum wetting setup

2.3.3 Bubloscopy meter test

A bubbloscopy meter (Figure 24) was used for bubble-point pressure test. In this test, gas pressure was gradually increased in inner compartment from 0 bar to the value of bubble point pressure.
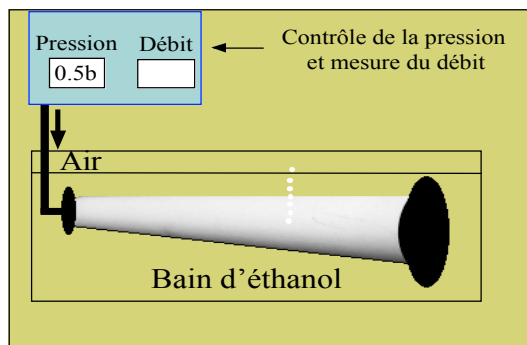
Figure 24 Bubble point test setup [4]

2.3.4 Gas permeation measurements

Gas permeability is a measure of permeation flux that flows through the membrane wall under internal flux at constant pressure [4]. Gas permeation can be considered as a measure of the intrinsic membrane quality along with the transport properties for applied fluid without any forward hypothesis about the form, the type of pores and the flow regime of the fluid in porous media. This measurement characterizes the global mass transfer resistance of the membrane. The permeation of a gas is defined by IUPAC [5] as the gas flux per unit force. Experimentally the permeation can be calculated by the equation:

$$\prod_i = \frac{Q_i^{trans}}{A * \Delta P_i} \qquad (17)$$

Where

$\prod_i$: Gas permeation of component i in (mol. m^{-2} s^{-1}.Pa^{-1})

Q_i^{trans} : Transmembrane molar flow of component I in (mol/s)

A : Surface area of membrane in (m^2)

ΔP_i : Transmembrane pressure of component I (Pa).

Permeation can be considered as quality criteria to membrane hydrodynamic behaviour [4] of:

$\prod_I = 0.0$

Q_i^{trans} : no flow for all pore size (very low porosity)

$\prod_i = \infty$,

Q_i^{trans} : very high flow for zero pore size (very high porosity)

2.3.4.1 Gas permeation test protocol

Nitrogen was used as a permeation gas to evaluate the permeation behaviour of the composite ceramic membranes. Nitrogen permeability was measured at room temperature. The experimental system used in gas permeation measurements shown in figure 25. The tubular membrane was installed in the reactor module with a graphite seal. The gas was introduced in the tube side and the flux permeating the membrane wall was measured by a simple bubble flow meter. To sweep gas from both sides of the reactor, module was introduced separately to the upstream and the downstream sides to a pressure difference-measuring device. The permeated gas flow rate was measured while setting a constant pressure difference across the membrane and varying the pressure in the inner compartment of the reactor.
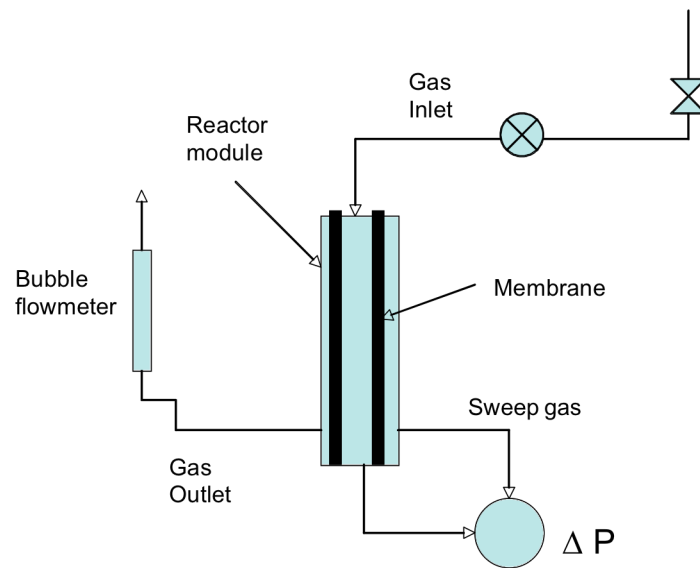
Figure 25 - Gas permeation measurement system

2.3.4 Measurement of the membrane specific area

Specific surface area of the membrane represents the total surface area per unit mass of a membrane material. The general principle of solid catalyst surface area measurements is based on physical adsorption and capillary condensation to obtain information about the surface area and porosity of porous materials. Physical adsorption phenomena are occurred due to very low Van der Wall forces between nitrogen adsorbed molecule and membrane solid material (in powder form).

This information (adsorbed gas volume) is sufficient to determine specific surface area of solid material either by Brunauer-Emmet Teller (BET) method. S_{BET} can be calculated from the relation:

$$S_{BET} = \frac{V_m N S}{V_M m_S} \quad (m^2/g) \qquad (18)$$

Where:

• **Vm** : adsorbed gas volume in (cm3),

• **N** : Avogadro's number $= 6.023 \ 10^{23}$ molecules

• **S** : surface covered by one adsorbed molecule

S = 16.2 10^{-20} m2/molecule in case of nitrogen

• **VM** : molar volume of nitrogen in (cm3)

• **mS** : mass of solid material (g)

Surface area measurements (BET method) and pore size distribution (Barret-Joyer-Halenda (BJH) method) for the membranes material (in powder) were performed based on a liquid nitrogen adsorption-desorption (Isotherm) in micrometrics apparatus TRISTAR 3000.

- Sample preparation

The primary objective is to evacuate the powder sample from any water molecules, CO_2 or any condensed gases on the sample surface. In fact the sample was degassed under vacuum at 250°C for 1hr.

- Refrigeration

The sample contained in an evacuated sample tube was cooled to -196 °C. Then, the sample is exposed to analysis gas at a series precisely controlled pressures. With each incremental pressure increase, the number of gas molecules adsorbed on the surface increases.

- Injection of adsorbent

Nitrogen gas was used as adsorbed gas. The surface are filled first, then the free surface becomes completely covered, and finally the larger pores are filled by capillary condensation. The process may be continuing to the point of bulk condensation of the analysis gas. Then, the desorption process may begin in which pressure systematically is reduced resulting in liberation of the adsorbed molecules. As with adsorption process, the changing quantity of gas on the solid surface at each decreasing equilibrium pressure is quantified. These two sets of data describe the adsorption and desorption isotherms. Analysis of the shape of the isotherms yields information about the surface and internal pore characteristic of material. The final result of sample specific surface area is the average value between the areas obtained from adsorption and desorption processes.

2.3.5 Surface structure and topography

   1-X-ray diffraction (XRD)

X-ray diffraction is one of the characterization techniques to catalytic membrane material. Mineral phases of micro and polycrystalline of active phase metal or solid supports can determine by using x-ray diffraction. This technique permit to know diversity of crystalline phases for a given solid material in powder form and to determine the crystal size of any

material in the range of 3 – 100 nm. Average dimensions of crystallite size can be calculated by the following equation:

$$d(hkl) = \frac{K\lambda.C}{\sqrt{\beta^2 - b^2}.\cos\theta_{hkl}} \qquad (19)$$

where:

d(hkl) : average dimensions of crystallites

K : Scherrer constant, depending on utilized peak profile, reflection and form of external crystallite faces.

Let k=1 (5), for all reflection that correspond to spherical form

λ: wave length of X-ray

θ **(hkl)** : Bragg angle

β : angular mid-height width of diffracted rays (in degree).

b : Instrumental width (in degree)

C : conversion factor from degree to radian = 57.3

XRD spectra of powder scratched from the top layer of the membrane gave information on the deposited metal crystallite size.

In case of platinum containing membrane, platinum crystallite size was obtained on the (111) Pt peaks, situated at $2\theta=39.7°$ after careful calculations, due to close TiO_2 peak at 39.2°.

The sample was irradiated by x-rays of copper tube, a monochromatic placed in front of selected detector wave length of CuKa rays, λ= 1.542A°. The diffractogram was registered in the domain angle 2θ, in the range of 5° to 80°

2-Electron microscopy analysis

- Scanning electron microscopy (SEM)

Topographical image in a SEM are formed from back-scattered primary or low energy secondary electrons. The best resolution is about 2-5 nm but many routine studies are satisfied with a lower value and exploit the case of image interpretation and extraordinary depth of field to obtain a comprehensive view of the specimen. With non-crystalline catalysts,

SEM is especially useful for examining the distribution and sizes of mesoporous materials. Some of active phase metals that deposited on membrane have been characterized either after metal deposition directly before any catalytic test or after several catalytic tests. The characterization have been done using MEB JSM 5800LV (JEOL), analysis system has coupled the energy dispersion spectrometry with diode Si-Li (PGT), use 0.3 -30 kv, resolution 3.5 nm at WD8mn and 30kv. The distribution profile of loading metal has been studied along the membrane thickness.

In order to determine cross-sectional composition of a membrane wall, scanning electron microscopy (SEM) in back scattering electron (BSE) mode, was carried out in JEOL *5800* scanning electron microscope equipped with oxford instruments for part of crushed membranes.

2.4 Elemental chemical analysis

The objective of elemental chemical analysis is to determine the total quantity of active phase metal deposited on the membrane and to verify the nature of a catalyst deposition process on the membrane, also to check for the catalyst leaching in the membrane reactor effluents.

- Inductively coupled plasma mass spectrometry (ICP-MS)

The ICP analysis is based on the plasma phenomena that discovered in atomic physics, the main unit in ICP-MS analyser, is the ICP ion source that operates at 7000°K. A plasma or gas consisting of ions, electrons and neutral particles, is formed from argon gas, which is then utilized to atomize and ionize the elements in the sample matrix. These resulting ions are then passed through a series of apertures into a high vacuum mass analyser where the isotopes of the elements are identified by their mass to charge ratio. The intensity of the specific peak in the mass spectrum is proportional to the amount of the elemental isotope from the original sample.

2.4 .1- ICP for precursor solutions

An elemental analysis has been realized for active metal precursor solution before and after impregnation of the membrane. The objective of this analysis is an attempt to know the nature of the catalyst deposition process on membrane surface. Catalyst deposition process can be occurred either physically by pores filling or chemically by adsorption on membrane support by ionic exchange. If the case of pure chemically process, the amount of active phase metal deposited on the membrane can be estimated by mass difference and confirmed by the

concentration difference of metals in solution before and after impregnation.

2.4 .2- ICP for membrane material

ICP analysis was done for membrane materials in powder form. The membrane in powder form was dissolved in attack acid (HF, water aqua regia) and the dissolved solution was analysed.

2.4 .3- ICP for metal leaching

The model compound solution effluents that received after catalytic oxidation test in membrane reactor were analysed by ICP to check for metal leaching

2.5 ESTIMATION OF THE AMOUNT OF DEPOSITED METAL

The estimation of the amount of metal deposited within the wall of the membrane was based on one hand on the mass uptake during the deposition and on the other hand on the quantity of precursor solution which was absorbed within the pores during the soaking step. The chemical analysis by ICP (Inductive Coupled Plasma) of the impregnation solution was also carried out, before and after catalyst deposition, in order to estimate the amount of deposited metal after deposition and calcinations steps. In fact, the membrane was weighed before and after each treatment step, the mass weighing of the membrane permit to estimate the mass of deposited catalyst

2.6 Membrane reactor setup and catalytic test

The performances of the catalytic membranes were tested in WATERCATOX bench setup (figure 26). The tubular ceramic membrane was mounted in a membrane reactor using a tight seal separating the liquid and gas feeds. To minimize the diffusion resistance within the membrane structure, the gas phase was supplied from the outer (shell) side, while the liquid phase containing the dissolved reactant (model compound solutions) was fed through the membrane channel. The catalyst was deposited primarily on the inner tubular membrane surface. The liquid phase was maintained close to atmospheric pressure. The gas overpressure was monitored and carefully controlled using a pressure difference gauge connected to an electronic regulator, acting in the gas feed through the mass flow controller ($50ml_{N2}$/min). The membrane reactor operated in continuous

liquid flow mode (close to 5-7 ml/min). The gas overpressure steady state was reached using nitrogen, before switching to air to start the oxidation. The same initial concentrations (0.11 mol/l) were used, for all model compound solutions to obtain the same carbon content. All experiments were carried out at room temperature (22-24°C).

Figure 26 Membrane reactor setup

1. Mass flows controller (Model 5850 E series-Max flow rate (50ml$_{N2}$/min)-Company Brooks instrument B.V (Holland).

2. Gas-liquid contactor (Tubular catalyst membrane + Module).

3. Liquid Pump (Power (0.12 hp-Impeller velocity (2790 rpm)-Company (Simplatorll Ltd) (England).

4. Magnetic mixer and heater. 5. Solution of model compound tank. 6. Pressure difference regulator.

7. Pressure difference (sensor)-Type Keller PR-23/ 8666.1-Pressure range 0 - 5 bar

8. Vent gas line to extractor. 9. Liquid Effluent tank (sampling).

10. Gas pressure sensor (Keller type PR-23/ 8666.1.-Pressure range 0 - 5 bar

11. Liquid pressure sensor.-Keller type AAA-21-10.- Pressure range 0 - 5 bar

12. Pump rgulator.-Power (1 hp)-Frequency (50~60 Hz)- Company (Industrial control equipment) (England).

13. Gas needle valve
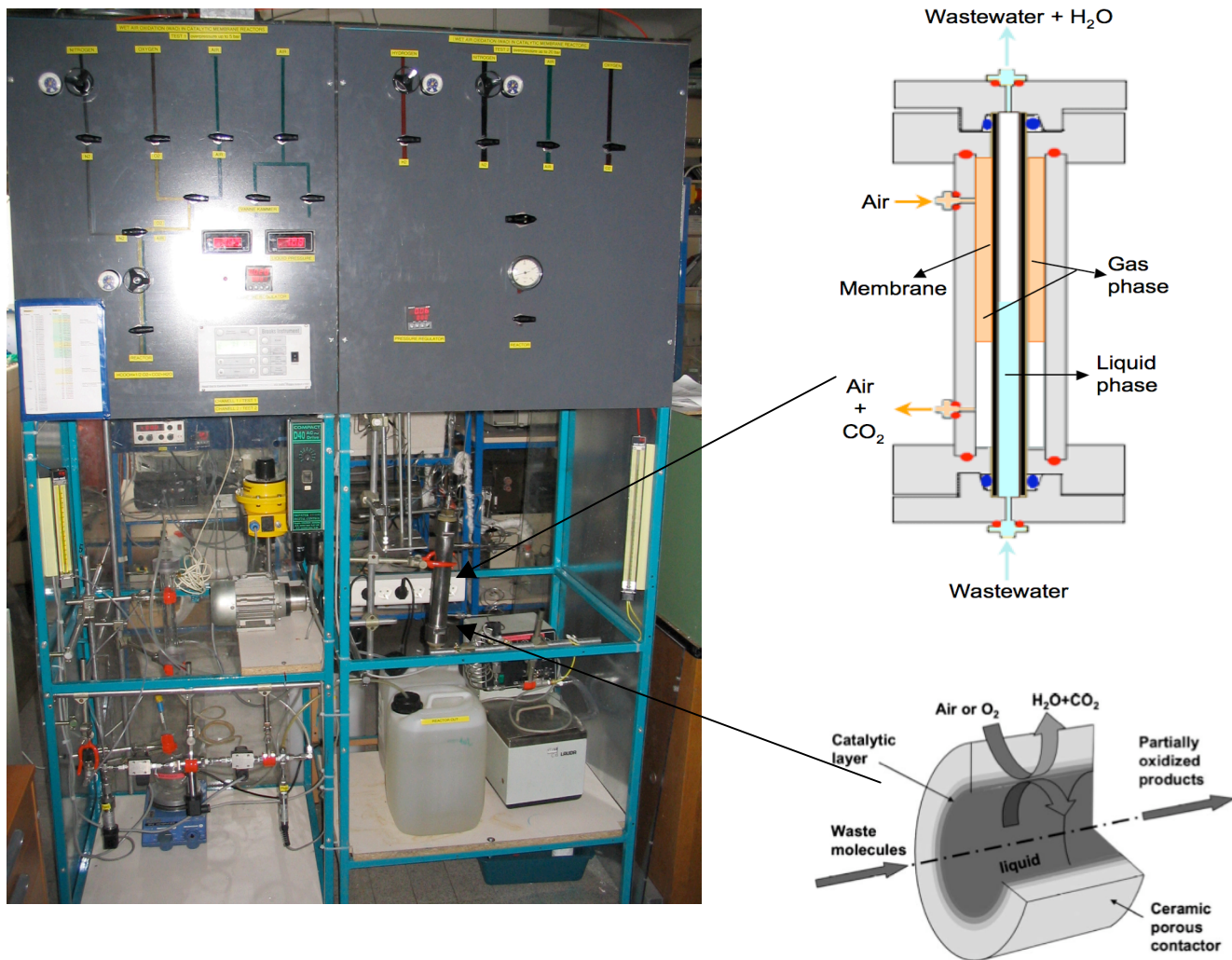
Figure 27- Experimental setup for catalytic test

2. 7 Chemical Analysis of membrane reactor effluents

Samples of membrane reactor effluents were analysed by either Shimadzu 5050A Total Organic Carbon analyser (TOC) or High pressure Liquid Chromatography (HPLC) for acids or phenols.

Due to HPLC laboratory regulations, it is used to analyse low molecular weight carboxylic acids in one HPLC (conveniently named HPLC for acids) and to analyse high

molecular weight carboxylic acids and phenol compounds in other HPLC (conveniently named HPLC for phenols). The technical specifications of both HPLC are given below:

1. HPLC for acids: (Varian Prostar with auto sampler model 410). An UV spectrophotometer at λ=210 was employed as the detector (type of the detector PDA 330- four channels), pump 230, mobile phase H_2O with H_2SO_4, flow rate of the mobile phase was set to be 0.7 ml/min.

2. HPLC for phenol compounds: (Varian Prostar with auto sampler model 410). An UV spectrophotometer at λ=222 was employed as the detector (type of the detector PDA 330- one channel), pump 230, mobile phase H_2O with H_3PO_4, flow rate of the mobile phase was set to be 0.7 ml/min.

2.7.1 Identification of the compounds during HPLC analysis

Single compounds were quantitatively identified by analysing pure samples of the expected partial oxidation products. In tables 14 and 15 the approximate retention times of all compounds analyzed are given.

Table 14 - Retention times of some carboxylic acids during the HPLC analysis

Carboxylic acids	Retention time (min)	λ(UV wave length)
Formic acid	11.32	210
Acetic acid	12.51	210
Maliec acid	14.98	222
Oxalic acid	11.45	222
Acrylic acid	2.11	222

Table 15 - Retention times of some phenols during the HPLC analysis

Phenols	Retention time (min)	λ (UV wave length)
Hydroquinone	1.9	222
Catechol	3.38	222
1-4 Benzoquinone	3.18	222
Phenol	6.6	222

Only some of these compounds were identified in the sample solutions. Calibration curves were established for each model compound solution, detected using standard solution

that cover the composition range of the tested model compounds. An example of HPLC Chromatograph for phenol solution is shown in figure 28
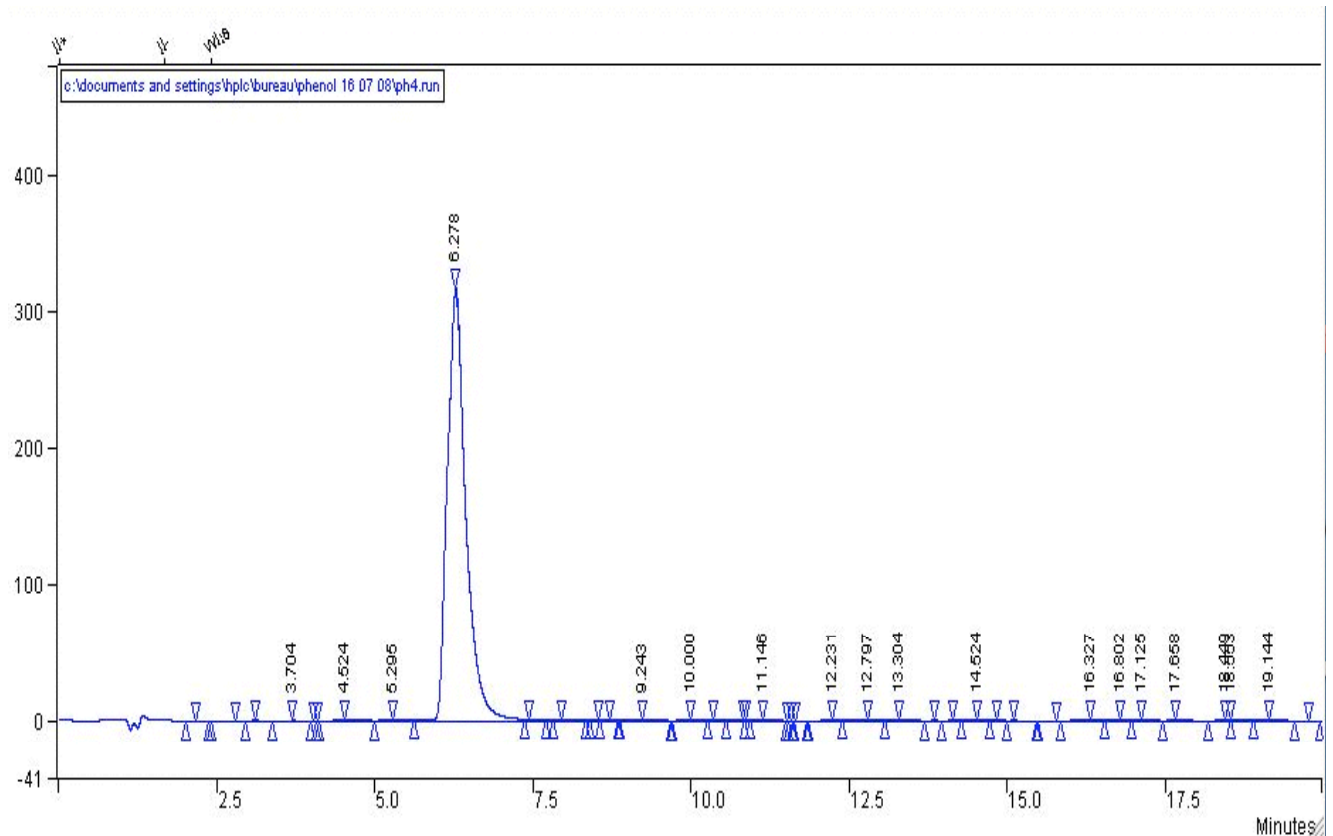
Figure 28 Chromatograph for phenol solution

References

1. Uzio D., S. Miachon, J-A. Dalmon, Controlled Pt deposition in membrane mesoporous top layers, Catal. Today 82 (2003) 67-74.

2. Perez V., S. Miachon, J-A. Dalmon, R. Bredesen, G. Pettersen, H. Ræder, Ch. Simon, Preparation and characterization of a Pt/ceramic catalytic membrane, Sep. Purif. Technol. 25 (2001) 33-38.

3. Dotzauer. M., Abusaloua A., Miachon S., Dalmon J-A, Bruening. L., Wet air oxidation with tubular ceramic membranes modified with polyelectrolyte/Pt nanoparticle films, Applied Catal. B: Environ. **91** (2009) 180-188

4. Wehbe N, Dénitrification de l'eau potable en réacteur catalytique membranaire et photocatalytique, thèse de doctorat de l'Université Claude Bernard Lyon 1, octobre **2008**

5. Alshebani. A, Développement de membranes céramiques pour la séparation des gaz. Fibres creuses et composites mésoporeux de nouvelle génération, thèse de doctorat de l'Université Claude Bernard Lyon 1, décembre **2008**

6. Dotzauer. D, Dai. J, Bruening. M, Catalytic Membrane prepared using layer-by layer Adsorption of Polyelectrolyte/Metal Nanoparticle Films in Porous Supports, Nano letters, 6 (2006) 2268-2272

7. Perego. C, Villa. P, Catalyst preparation methods, Catalysis Today 1997 (1997) 281-305.

3 RESULTS

Some parts of this chapter included publications devoted to this thesis work.

3-1 Preparation and characterisation of catalytic membranes

3-2 Effect of deposition method on the membrane catalytic activity

(Applied Catalysis B: Environmental 91 (2009) 180-188)

3-3 Effect of wetting method on the membrane catalytic activity.

(Catalysis Today xxx (2010) xxx-xxx) article in press.

3-4 Bimetallic catalysts for wet air oxidation of model compound solutions in

membrane reactors   (To be submitted in applied environmental B)

3.1 Preparation and characterisation of catalytic membranes

3.1.1 Commercial support characteristics

Several supports were provided either by Pall-Exekia-France or Inocermic-Germany with different kind of oxide (alumina, titania, or zirconia, top layer pore size and number of layers. Table 16 and 17 show the main characteristics of the Pall-Exekia and Ino-cermic supports.

Tableau 16 - Main characteristic of Pall-Exekia supports

Support Supplier	Number of layers	Layer	Material	Mean pore size (nm) / Thickness (μm)
PALL -EXEKIA	4	1 (top layer)	ZrO_2	20/3
		2	α-Al_2O_3 (TiO_2)	200/20
		3	α-Al_2O_3 (TiO_2)	800/30
		4	α-Al_2O_3 (TiO_2)	1200/1500
PALL	3	1 (top layer)	ZrO_2	50/6
		2	α-Al_2O_3 (TiO_2)	800/15
		3	α-Al_2O_3 (TiO_2)	1200/1500

Table 17 - Main characteristics of Ino-cermic supports

Supplier	Number of layers	Layer	Material	Mean pore size (nm) / Thickness
INO-CERMIC	4	1 (top layer)	(CeO_2 / ZrO_2) or TiO_2	80/8
		2	TiO_2	250/20
		3	TiO_2	800/30
		4	TiO_2	1200/1500
INO-CERMIC	3	1 (top layer)	TiO_2 (CeO_2/ZrO_2)	100/8
		2	TiO_2	800/30
		3	TiO_2	5000/1500

To illustrate the successive layers of this kind of inorganic material, the figure 29 shows cross-sectional SEM-BSE image - 3 layers of 25cm ceramic membrane AAB-022 and AAB-024 (Inocermic-Germany – table 17)

(a)   (b)
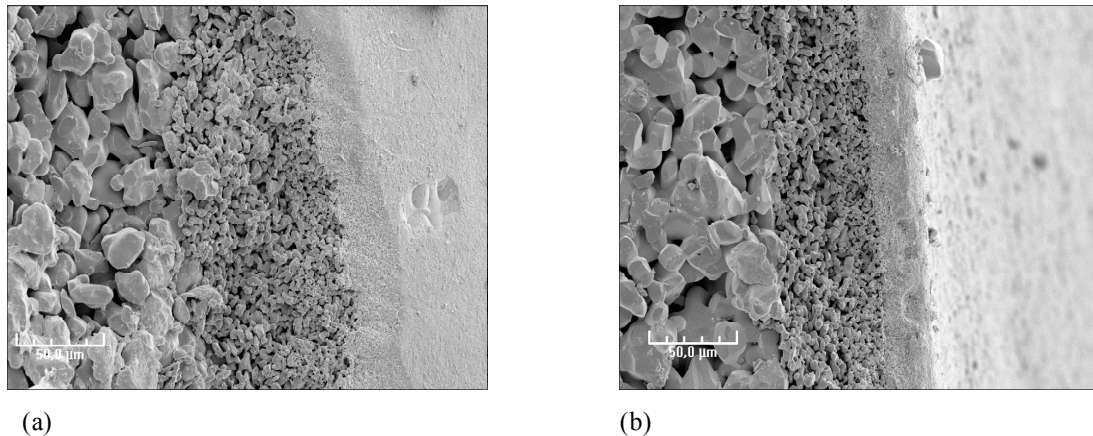
Figure 29 – Cross sectional SEM-BSE image inocermic Germany (a) AAB-022 (b) AAB-024

3.1.2 Bubble point pressure

The bubble point pressure to nitrogen gas under ethanol was measured on the bare tubes (supports) before metals deposition, in order to check for the first bubble of gas penetrated.

The bubble point pressure measurement were made by two ways of membrane wetting by ethanol as a pre-treatment step before the experimental test, either normal wetting or vacuum wetting like it is described in the experimental part (see page 97 and 99). Results of bubble point pressure for several Inocermic supports are shown in the table 18.

Table 18 - Bubble point results for Inocermic supports (Normal wetting/ Vacuum wetting)

Supports INOCERMIC	Number of layers	Normal wetting Bubble Pressure (bar)	Vacuum wetting Bubble Pressure (bar)
AAB001- INC	3	0.40	0.64
AAB008 - INC	4	0.53	1.4
AAB019- INC	4	1.54	2.3
AAB023- INC	4	0.32	1.2
AAB024- INC	4	0.72	0.47

In table 18, the results show that the hydrodynamic behaviour for all membranes is improved by vacuum wetting in ethanol as a pre-treatment step before bubble point test, in compared with normal wetting in ethanol except for membrane AAB024. In this case the result is different and may be due to incomplete vacuum wetting. For Pall-Exekia supports, results of hydrodynamic performance (bubble point pressure) are given in the figure 30.
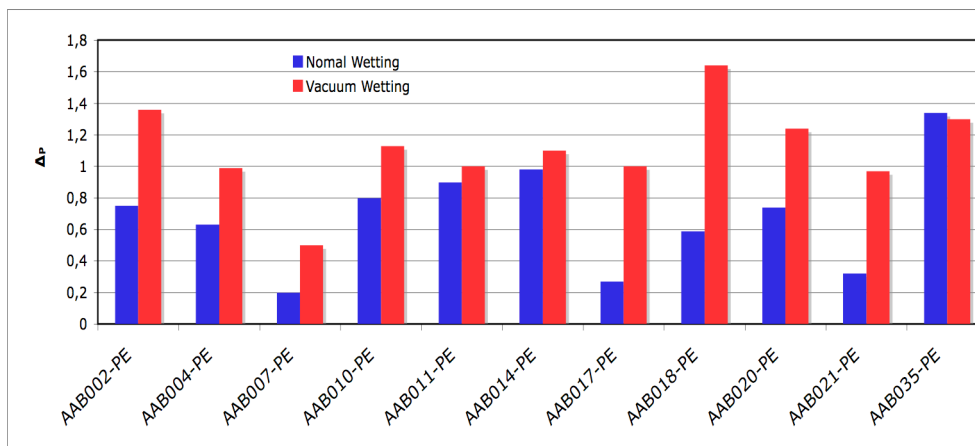
Figure 30 - Bubble pressure for Pall-Exekia supports

As can be seen in figure 30, vacuum wetting improves the hydrodynamic performance (bubble pressure) for all membranes, but more particularly for membranes that already have bubble pressure near to 1.0 in normal wetting conditions. To conclude, the vacuum wetting must be used to compare the different supports and more particularly before catalytic measurement.

3.1.3 Nitrogen permeance

The permeance to nitrogen was measured for several membranes (fig. 31) in order to estimate the quality of the top layer for each commercial support.
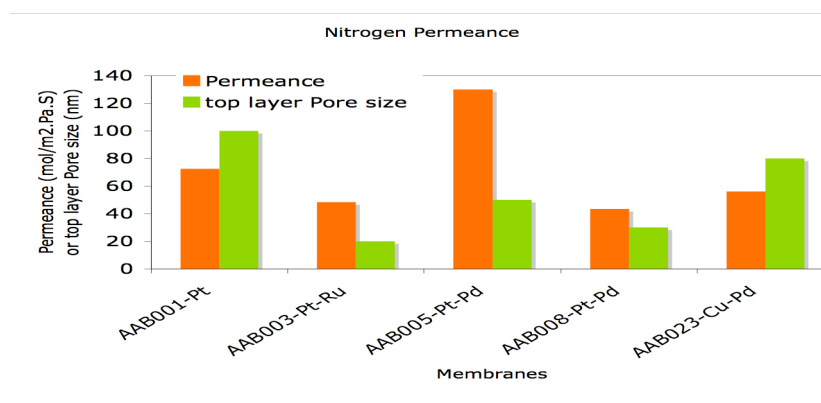
Figure 31 – Distribution of the nitrogen permeance and their top layer pore size.

The results show that the presence of the catalytic species did not change the permeance. Estimation of nitrogen permeance has been studied by Iojou et al (1). With these kinds of supports, they have reported that the nitrogen permeances were in the range of 30-40 mol/m^2/Pa/s and that the presence of the catalytic species did not change the values. Our results show that the nitrogen permeance measured in our experimental conditions varied from 35 to 70 mol/m^2/Pa/s except for bimetallic membrane AAB-005-Pt-Pd. For this membrane the nitrogen permeance present a higher value.

3.1.4 Determination of surface area

Table 19 shows surface area, pore size, and pore volume per gram of membrane material. Low surface areas have been obtained for all membrane, in the range of 1 m^2/g, in consistency with obtained surface areas for the same membrane materials in some previous studies. Determination of internal surface area of membrane porous media has studied in a number of publications [2,3]. Due to the composite multilayer structure of tubular ceramic membranes and usually the active phase metal catalyst is located in the membrane top layer, the determination of the specific internal surface area of membrane porous media is different in compared with other supports of solid materials with approximately regular sizes of porous media. Cini et al (4) have studied the determination of BET surface area for composite tubular membrane. They concluded that the BET surface area is a linear function of the ratio of the top layer film mass to the total tubular membrane mass. They have reported that the overall internal surface area in the range from 1 m^2/g for membrane supports (macro porous α-Al$_2$O$_3$) to 13 m^2/g for membrane after metal loading (macro porous α-Al$_2$O$_3$ + Micro porous γ-Al$_2$O$_3$)

Table 19 - Surface areas, pore size, and pore volume per gram of membrane material

Membrane	Supplier /layers	Pore size (nm)	Pore volume (cm^3/g)	BET Surface area (m^2/g)	BJH Surface area (m^2/g)
AAB022-	INC-3	43.34 - 47.26	0.0067	0.5672	0.622
AAB024-	INC-4	71.46 - 79.33	0.019	0.6720	1.05
AAB036	PE-3	75.12 - 81.68	0.007	0.2864	0.3754

Vospernik et al (5) have studied the determination of BET surface area for composite tubular membranes. Nitrogen adsorption-desorption (BET) and mercury penetration technique are used for measuring the surface area. They have reported that the overall internal surface area is very low for membrane contactor is 0.12 m^2/g, low pore volume 0.1 ml/g (mercury penetration technique) and 0.3 m^2/g (Nitrogen adsorption-desorption BET).

3.2 Estimation of the amount of deposited metal

The estimation of the amount of deposited metal within the wall of the membrane was based on one hand on the mass uptake during the deposition and on the other hand on the quantity of precursor solution which was absorbed within the pores during the impregnation step. Chemical analysis by ICP (Inductive Coupled Plasma) of the impregnated solutions is carried out before and after impregnation in order to estimate the theoretical mass (the amount of deposited active phase metals). The mass uptake of the membrane was also carefully controlled, after sufficient drying, in order to avoid water condensation in the mesoporous structure. The estimation of the amount of deposited metal based on mass uptake by precisely measuring the membrane mass after drying before metal deposition process and directly after metal reduction step. The results obtained through these methods for catalytic membranes are shown in Tables 20, 21, 22 and 23.

In tables 20 and 22 for monometallic membranes, the measured mass uptake is in fairly good agreement with the theoretical mass uptake, which calculated from the amount of impregnation solution contained in the porous volume of the tubes. For other some membranes, the measured mass uptake is higher than that expected from calculations. This difference may arise from residual materials originating from the metal salt precursor where the temperature of calcinations and reduction may be too low temperature to fully burn the residual material trapped in the membrane pores.

In tables 21 and 23 for bimetallic membranes, the measured mass uptake are in good agreement with the theoretical mass uptake but for some samples in fairly good agreement with the theoretical mass uptake. This difference may arise from using average concentrations of precursor solutions where most solution concentrations almost constant before and after impregnation even some solutions or may arise from residual materials originating from the metal salt precursor where the temperature of calcinations and reduction may be low temperature to fully burn the residual material trapped in the membrane pores, or also due to use the same apparent pore volume for bimetallic catalytic membranes.

Table 20 Measured amount of deposited metal for monometallic membranes.

Membrane/ Company	Pore volume (ml)	Conc. Of active phase (g/L)	Metal Precursor	Deposition method	Theoretical Mass (mg)
AAB 001-IN	4.5	10.0 – Pt	H_2PtCl_6	Evap.	45- Pt
AAB 002-PE	3.4	10.0 – Pt	H_2PtCl_6	Evap.	34- Pt
AAB 007-PE	3.0	10.0 – Pt	H_2PtCl_6	Evap.	30- Pt
AAB 011-PE	2.5	3.4 – Cu	$Cu (No3)2$	Evap.	8.5- Cu
AAB 018-PE	3.1	3.0 – Pd	$PdCl_2$	Evap.	9,3- Pd
AAB 019-IN	3.2	3.0 – Cu	$Cu (No3)2$	Evap.	10- Cu
AAB 021-PE	3.1	3.0 – Ru	$Ru(NO)(NO_3)_3$	Evap.	9.3- Ru
AAB 022-IN	4.2	5.0 – Pt	$Cl_3Pt(NH_3)_4$	Evap.	21- Pt
AAB 025-PE	4.0	0.15 – Pt	$Pt ((NH_3)_4) (NO_3)_2$	Evap.	0.6- Pt
AAB 030-PE	3.5	0.15 – Pt	$Pt ((NH_3)_4) (NO_3)_2$	Evap.	0.53- Pt
AAB 032-PE	4.1	0.15 – Pt	$Pt ((NH_3)_4) (NO_3)_2$	AI.	0.615
AAB 033-PE	3.6	0.15 – Pt	$Pt ((NH_3)_4) (NO_3)_2$	AI.	0.54

Table 21: Theoretical amount of deposited metal for bi and trimetallic membrane.

Membrane/ Company	Pore volume (ml)	Conc. Of active phases (g/L)	Metal precursor	Deposition method	Theoretical mass (mg)
AAB 003-IN	2.5	10.0 Pt - 3.0 Ru	H_2PtCl_6 + Ru $(NO)(NO_3)_3$	Co-impregnation. Evap.	33.0
AAB 004-PE	2.6	10.0 Pt - 5.0 Ru	H_2PtCl_6 + $Ru(NO)(NO_3)_3$	Co-impregnation. Evap.	39.0
AAB 005-PE	3.6	6.0 Pt - 3.0 Pd	$H_2PtCl_6 + PdCl_2$	Co-impregnation. Evap.	33.0
AAB 006-PE	3.7	2.2 Pt - 1.6 Ru	$H_2PtCl_6 + RuCl_3$	Co-impregnation. Evap.	21.0
AAB 008-IN	3.0	6.0 Pt - 3.0 Pd	$H_2PtCl_6 + PdCl_2$	Co-impregnation. Evap.	27.0
AAB 010-PE	2.5	2.0 Cu -1.0 Pd	Cu $(No3)2$ + $Pd(No3)2$	Co-impregnation. Evap.	7.5
AAB 014-PE	3.6	0.5 Pd - 1.5 Ru	$Pd(No3)2$ + $Ru(NO)(NO_3)_3$	Co-impregnation. Evap.	7.0
AAB 017-PE	3.7	4.0 Zn - 2.0 Ni	$ZnCl2 + NiCl2$	Co-impregnation. Evap.	21.0
AAB 020-PE	2.2	6.0 Pt - 3.0 Pd - 0.5 Ru	Pt $((NH_3)_4)$ $(NO_3)_2$+ $Pd(No3)2$ + Ru $(NO)(NO_3)_3$	Co-impregnation. (Pt-Pd), Succesive impregnation Ru Evap.	21.0
AAB 023-IN	4.0	2.0 Cu - 1.0 Pd	Cu $(No3)2$ +$Pd(No3)2$	Co-impregnation. Evap.	12,0
AAB 024-IN	2.5	7.5 Cu - 1.5 Ni	Cu $(No3)2 + Ni(No3)2$	Co-impregnation. Evap.	22.0
AAB 035-PE	3.8	1.6 Fe – 1.6 Co	$Fe(NO_3)_3 + Co(NO_3)_2$	Co-impregnation. Evap.	12.16

Table 22 Measured amount of deposited metal for monometallic membranes

Membrane	Deposited Metal	Mass after drying (no metal loaded) (g)	Mass after Reduction (g)	Measured Mass uptake (mg)
AAB 001	Pt	34,7414	34,8301	88,7
AAB 002	Pt	27,5072	27,5555	48,3
AAB 007	Pt	30.4895	30.5325	30
AAB 018	Pd	28,2176	28,2262	8,6
AAB 019	Cu	35,0601	35,0696	9,5
AAB 021	Ru	27,8102	27,8194	9.2
AAB 022	Pt	35.0490	35.0684	19.4
AAB 025	Pt	31.5983	31.6007	2.4
AAB 030	Pt	31.5042	31.5061	1.9
AAB 032	Pt	31.7808	31.7837	2.9
AAB 033	Pt	30.6800	30.6835	3.5

Table 23 measured amount of deposited metal for bi and trimetallic membranes

Membrane	Deposited Metal	Mass after drying (no metal loaded) (g)	Mass after Reduction (g)	Measured mass uptake (mg)
AAB 003	Pt-Ru	27,063	27,0863	23,3
AAB 004	Pt-Ru	30,935	30,9694	34,4
AAB 005	Pt-Pd	30,4518	30,4838	32,0
AAB 006	Pt-Ru	31,791	31,8065	15,5
AAB 008	Pt-Pd	32,212	32,2367	24,7
AAB 010	Cu-Pd	32,0166	32,0216	5,0
AAB 014	Pd-Ru	31,9367	31,9438	7,1
AAB 017	Zn-Ni	30.6311	30.6749	43.8
AAB 020	Pt-Pd-Ru	28.1189	28.1295	10.6
AAB 023	Cu-Pd	37.3476	37.3732	25.6
AAB 024	Cu-Ni	33.2833	33.3204	37.1
AAB 035	Fe-Co	30.6897	30.7081	18.4

.

3.3 Electron Microscopy analysis

3.3.1 EDS analysis

1- monometallic membrane

The monometallic (Pt) Inocermic membrane (AAB-001-Pt) was characterized by Scanning electron microscopy. The results of the Pt EDS- radial analysis of scanning electron microscopy are given in figure 32. The line scan mode gives some examples of the distribution of platinum through the membrane wall. EDS results suggested that low loading of active phase metal in Figure 31 Pt Electron microscopy (SEM) in energy dispersive spectroscopy (EDS) mode.
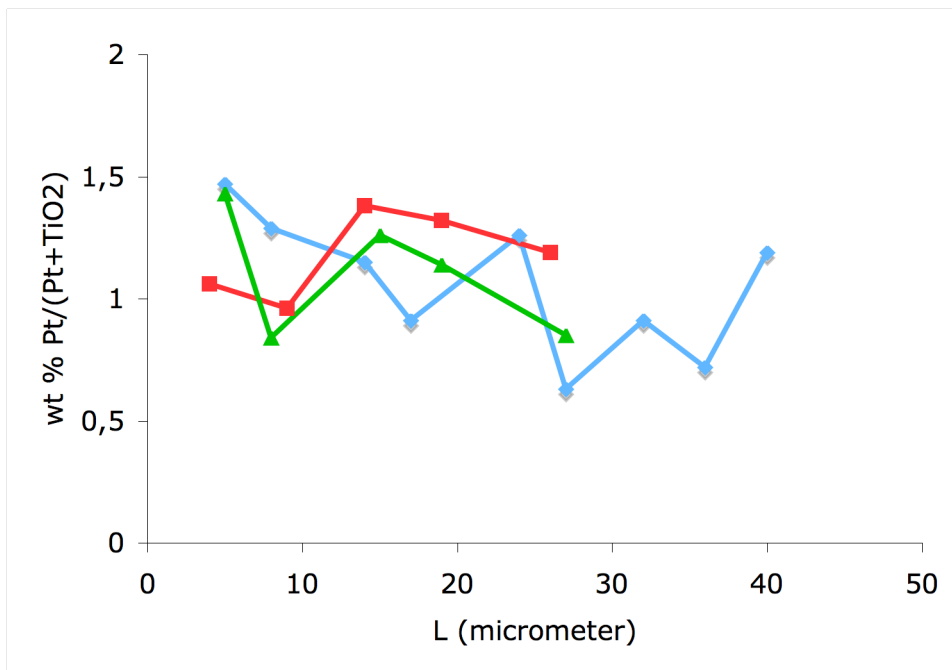
Figure 32 EDS analysis for Inocermic membrane (three layers) (The different lines corresponding to different position of EDS analysis)

Membrane top layer is in the range of 1-1.5 wt%. These results are expected due to originally low loading of metal catalyst by this method of membrane metal loading technique. The SEM characterization of the monometallic membrane AAB022-Pt has been done in energy dispersive spectroscopy (EDS) mode. EDS was performed with the electron beam scanning in the rectangular region that is indicated approximately in each top layer. Theelectron beam current and counting times were the same for each analysis. Figure 33 shows the EDS spectra of a section of catalytic membrane tube.
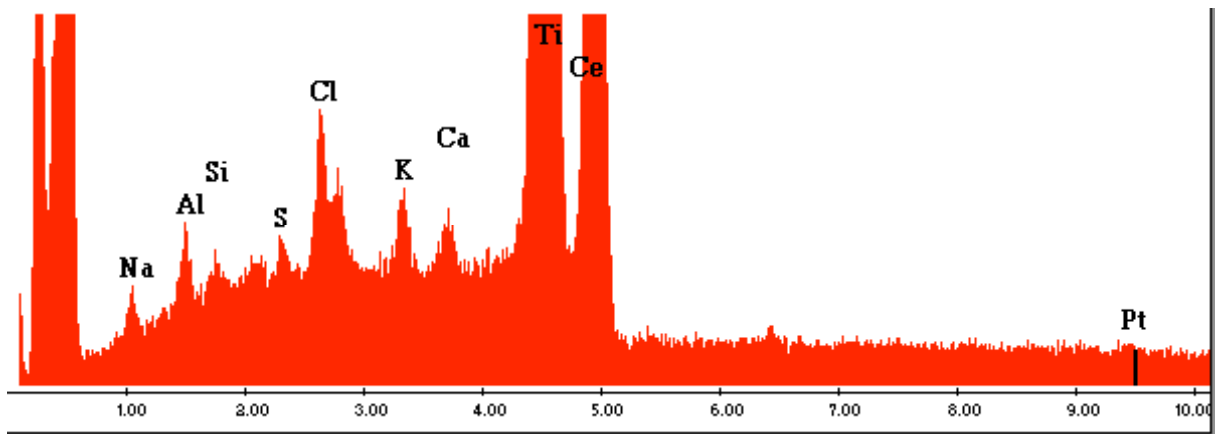
Figure 33 EDS spectra of a section of catalytic membrane tube.

In figure 33 EDS spectra shows the general composition of metals in the mesoporous top layer

3.3.2 X-Ray Diffraction (XRD) analysis

XRD analysis on membrane material in (powder form) was performed. Figure 34 shows XRD spectrum of membrane material showing the Pt-peak at $2\theta = 39.7°$ and TiO_2 peak at $2\theta = 39.2°$. XRD spectra gave information on the deposited platinum crystallite size. This was obtained on the (111) Pt peak.
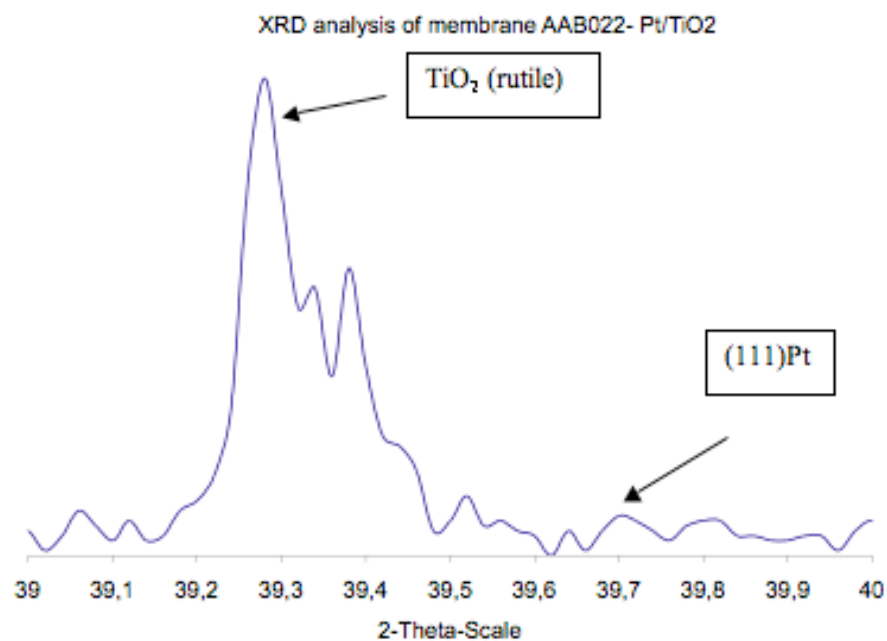
Figure 34 XRD spectrum membrane powder,

3.2.4 SEM (EPMA) -(BSE) analysis

1- bimetallic membranes

Two samples of bimetallic membranes were characterized by electron probe micro-analysis (EPMA) and Back Scattered electron (BSE) imaging in scanning electron microscopy (SEM) JSM 5800 LV. SEM analysis system coupled energy dispersive spectrometry (EDS) with a diode Si-Li (PGT). The samples for (EPMA) analysis were prepared by standard metallographic procedures, mounting in resin, grinding in silicon carbide paper, followed by final polish using diamond paste. The samples were coated in a thin layer of carbon to eliminate charging. EPMA elementary maps were performed at two magnification scales with an accelerating voltage of 15kv and fixed step sizes, normalized metal levels were measured for each sample. It should be pointed out that the back-scattered images were recorded using a small probe size to show accurate detail of the microstructure. For EPMA mapping, a much higher probe current was used, to generate a strong analytical signal. As a result the apparent top layer thickness is greater in the maps than in the back-scattered images, due to a corresponding loss of spatial resolution. EPMA analysis was performed to map the distribution of active phase metals within the membrane top layer. Figure 35 shows an example of this analysis performed on bimetallic membrane AAB024-Cu-Ni after metal deposition. BSE images show the top, and the beginning of the intermediate layer. The presence of bimetallic catalyst Cu-Ni in membrane AAB024-Cu-Ni was shown in elemental cartography map (fig. 35) for major three metals in the top layer (Cu-Ni-Ti). In this case, Cu is seen in more and larger distribution spots than Ni in top layer. This is in agreement with ICP analysis, which suggested that, the Ni element was detected in reactor effluent outlet due to metal leaching with tested phenol solution. Cu was also detected in reactor effluent outlet but in rather low concentrations in comparison with Ni element. The course clustering of metal particles within the top layer was observed may be due to metal loading technique for bimetallic membrane (coimpregnation). Figure 36 shows the analysis results for a second bimetallic sample membrane AAB008-Pt-Pd after metal deposition.

AAB-A-024-01_6-CARTO1-X2200

Ti

Ni

Cu

Zr

Ce

Ti-Ni-Cu
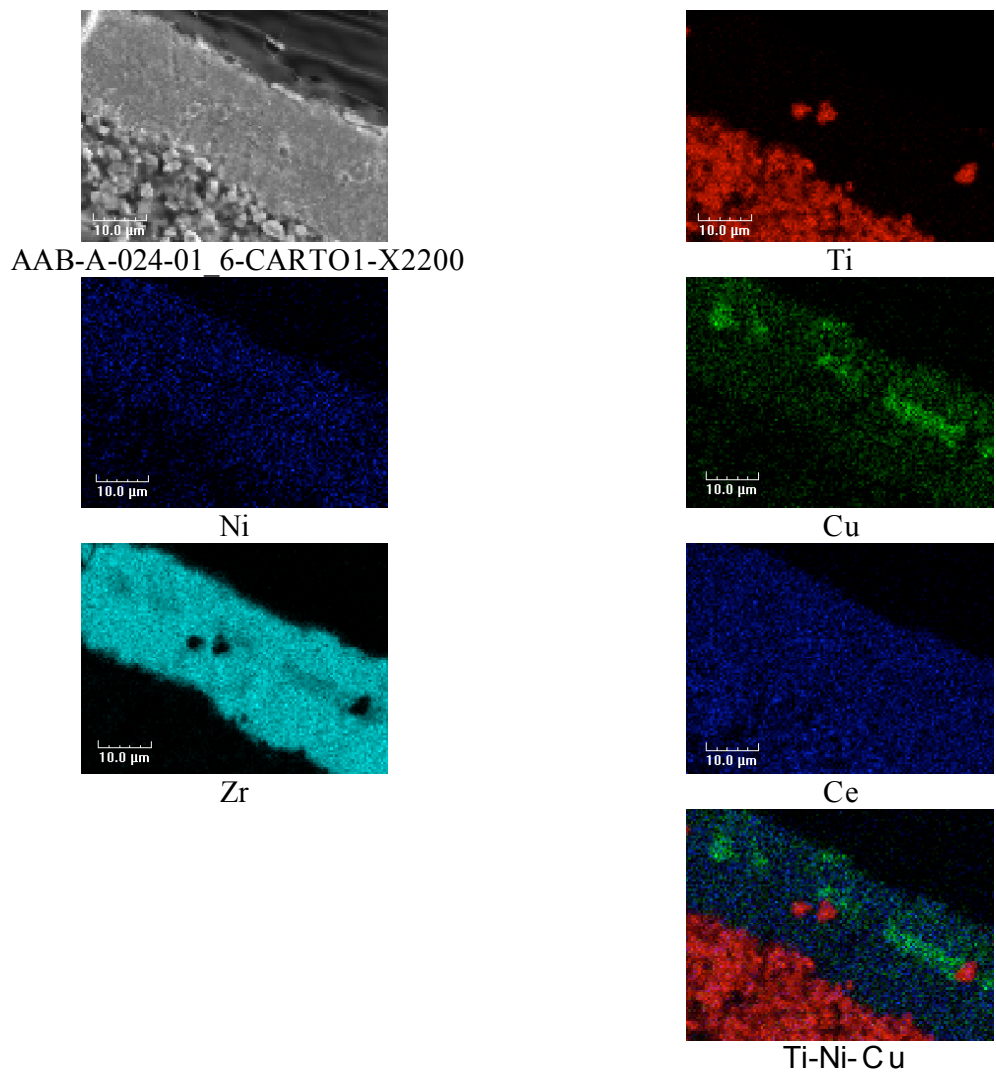
Figure 35 BSE images and EPMA Ti, Ni, and Cu maps of the membrane after active phase metal deposition (SEM-BSE images (first left) and EPMA-WDS cartography (right) of the last layers of the catalytic membrane)

AAB-A-008-03_carto1-x2200.tif

Ti

Zr

Pd

Ce

Pt

Ti-Pd-Pt
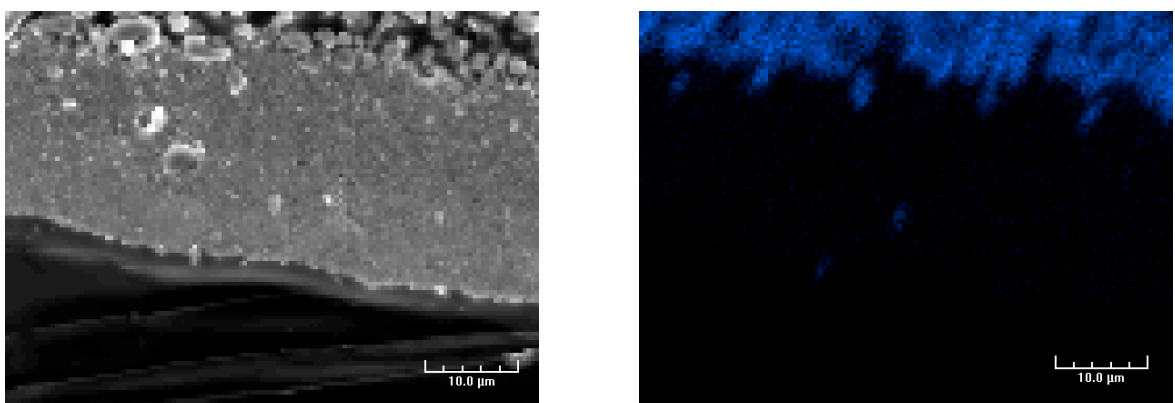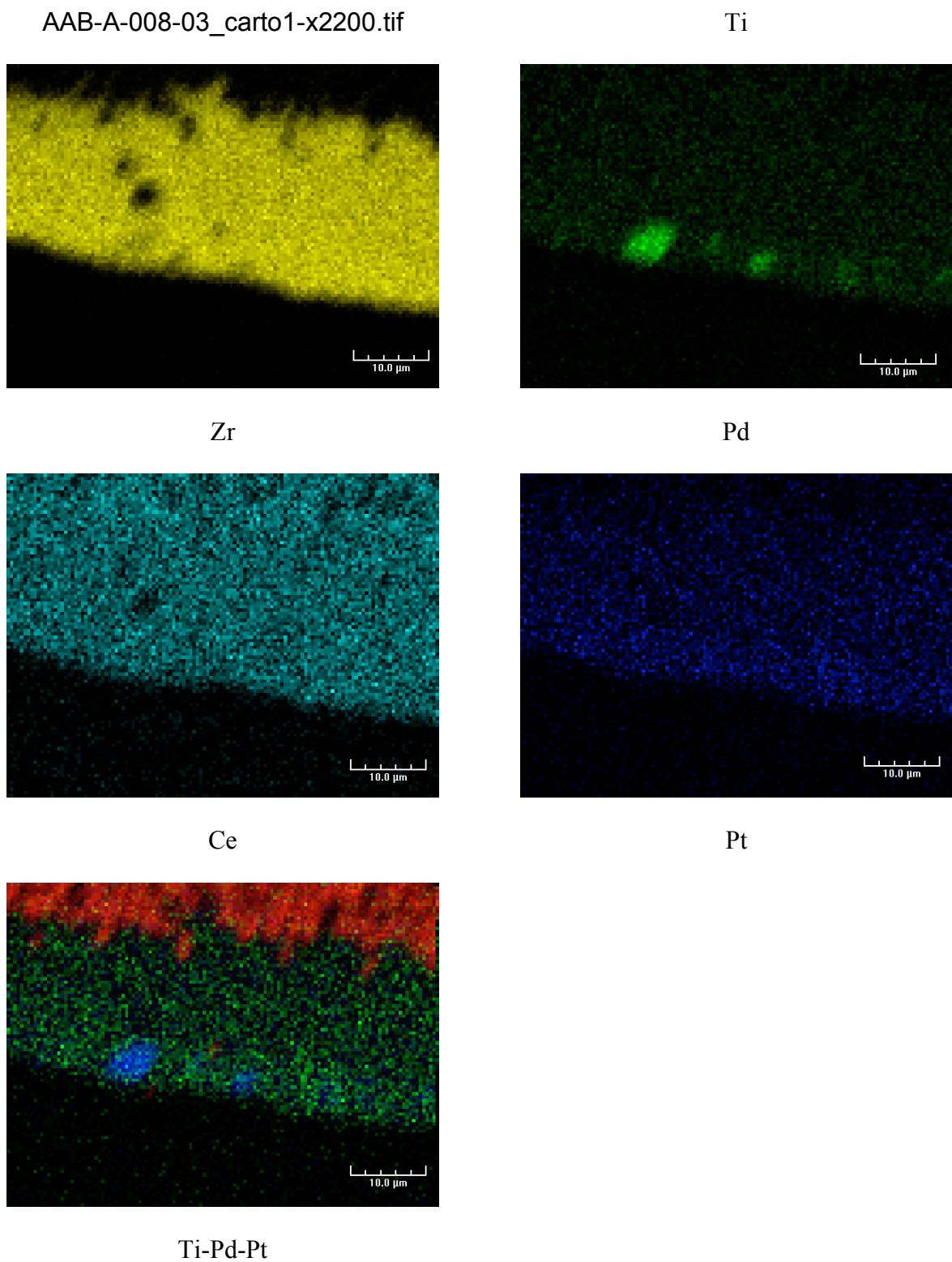
Figure 36 shows BSE images and EPMA Pt and Zr maps of the membrane after active phase metal deposition (SEM-BSE images (first left) and EPMA-WDS cartography (right) of the last layers of the catalytic membrane.

In figure 35, BSE images show the top and the beginning of the intermediate layer, On the contrary, Pt is more localized in the rather thin top layer. The presence of bimetallic catalyst Pt-Pd in membrane AAB008-Pt-Pd was shown in elemental cartography map (fig.36) for major three metals in the top layer (Pt-Pd-Ti)

References:

1. Vospernik M., A. Pintar, G. Bercic, J. Levec, J.C. Walmsey, H. Raeder, E.E. Iojoiu, S. Miachon, J-A. Dalmon, Performance of catalytic membrane reactor in multiphase reactions, Chem. Eng. Sci. 59 (2004) 5363-5372.

2. Perez V., S. Miachon, J-A. Dalmon, R. Bredesen, G. Pettersen, H. Ræder, Ch. Simon, Preparation and characterization of a Pt/ceramic catalytic membrane, Sep. Purif. Technol. 25 (2001) 33-38.

3. Uzio D., S. Miachon, J-A. Dalmon, Controlled Pt deposition in membrane mesoporous top layers, Catal. Today 82 (2003) 67-74.

4. Cini. P, Blaha. S, Harold. M, Preparation and characterization of modified tubular ceramic membranes for use as catalytic supports, Journal of membrane science, 55 (**1991**) 199-225

5. Vospernik M, Albin Pintar, Gorazd Ber, Janez Levec, Experimental verification of ceramic membrane potentials for supporting three-phase catalytic reactions, Journal of Membrane Science 223 (2003) 157–169 M.

6.Vospernik M, A. Pintar, G. Bercic, J. Levec, Mass transfer studies in gas-liquid-solid membrane contactors, Catal. Today 79-80 (2003) 169-179.

3-2   Effect of deposition method on the membrane catalytic activity

(Applied Catalysis B: Environmental 91 (2009) 180-188)

Wet air oxidation with tubular ceramic membranes modified with polyelectrolyte/ Pt nanoparticle films

David M. Dotzauer [a], Ali Abusaloua[b], Sylvain Miachon[b], Jean-Alain Dalmon[b], Merlin L. Bruening b*

a: Department of Chemistry, Michigan State University, East Lansing, MI 48824, United States

b: Institut de Recherches sur la Catalyse et l'Environnement de Lyon, UMR 5256 CNRS/Université´ Claude Bernard Lyon 1, 69626 Villeurbanne, France

A B S T R A C T

Gas–liquid reactions with membrane-supported catalysts often use the interfacial contactor configuration in which the reaction occurs at the gas–liquid-catalyst interface within the membrane. Thus, control over the catalyst location in the membrane is crucial for making efficient use of expensive materials such as noble metal nanoparticles. Layer-by-layer (LBL) adsorption of polyelectrolyte/metal nanoparticle films in tubular ceramic membranes allows deposition of the catalytic nanoparticles only near the interior of the tube

where the gas–liquid interface is typically located. In wet air oxidation of formic acid, tubular membranes modified by LBL deposition of polyelectrolyte/Pt nanoparticle films show 2 to 3 times higher specific activities than similar membranes modified by traditional methods such as anionic impregnation/reduction and evaporation/recrystallization/reduction. In acetic acid and phenol oxidations, the LBL method gives order of magnitude increases in specific activity relative to the traditional membrane modification methods. The enhanced activity with LBL-modified membranes is likely due to the controlled deposition of the Pt in the catalytic inner layer of the tubes, as only the LBL method gives tubular membranes that show higher activity than pulverized membranes in stirred tank reactors.

_E-mail address: bruening@chemistry.msu.edu (M.L. Bruening).

Introduction

Wet air oxidation is an important process in which hazardous organic pollutants react with oxygen to give more benign compounds, ideally H_2O and CO_2 [1–3]. This technique is attractive for processing wastewater pollutants that are too dilute to be treated by incineration [4,5] and too concentrated to be treated by biological methods [6–9]. Traditional wet air oxidation of organic and inorganic substrates often requires high temperature and pressure (150–350 8C, 20–200 bar air) [10,11], but the use of catalysts such as Pt, Ru, or other precious metals immobilized on inorganic powders allows much milder reaction conditions (room temperature, 1–5 bar air) [12–14]. However, implementation of catalytic wet air oxidation in conventional stirred tank reactors requires a catalyst recovery step, and reaction rates are often limited by diffusion of oxygen and/or the liquid phase compounds to the catalyst surface.

Porous membranes are an attractive alternative to powders as catalyst supports because the high internal surface area of the membrane affords a high loading of the active catalyst material, and there is no need to separate the catalyst from the reaction mixture. Thus, reactions can run continuously. Furthermore, catalytic membranes operated as gas–liquid contactors enhance the accessibility of the reactants to the metal catalyst [15]. The two most common membrane configurations for gas–liquid reactions are flow-through and interfacial contactors. Flow-through contactors, where all reactants flow through the membrane in a single solution, are advantageous because when the membrane pores are sufficiently small, reactions will not be limited by the rate of mass transport to the catalyst [16]. Furthermore, by controlling the flow rate and, hence, the residence time of a substrate within the membrane, side reactions may be minimized to give high selectivity for a particular product [17–21]. Unfortunately, in gas–liquid reactions with flow-through contactors the low solubility of the gaseous reactant in the liquid phase often limits the extent of reaction [16]. A similar problem occurs in fixed-bed reactors. In interfacial contactors, the walls of a catalytic membrane serve as the interface between gas and liquid phases (Fig. 1) to allow rapid transport of gas to the solid–liquid-catalyst interface and provide a high catalytic activity [22]. Recent work by Pera-Titus et al. also suggests that the enhanced catalytic activity in

interfacial contactors may be due to increased gas solubility in the confined pores of the membrane [23]. However, if pore sizes are larger than 10 nm, this effect is not observed.

A number of studies in the Watercatox project examined the use of tubular catalytic membranes as interfacial contactor reactors for wet air oxidation of model and industrial effluents at the laboratory and pilot scale [24–29]. These studies showed that the interfacial contactor configuration leads to increased activity when compared to a conventional stirred tank reactor, and that the high activity stems from the ability to control the location of the gas–liquid interface within the membrane (Fig. 1).
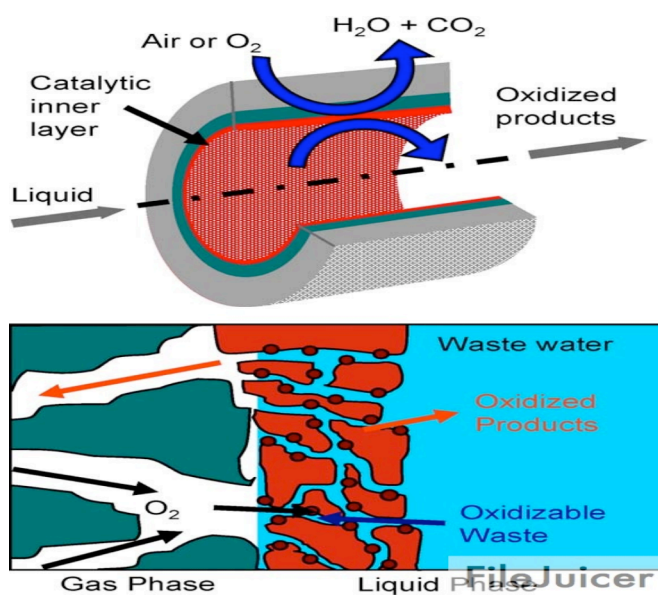
Fig. 1. Schematic diagram showing the interfacial contactor configuration in a tubular membrane and its application to wet air oxidation.

In the interfacial contactors thus far employed for wet air oxidation, catalytic noble metal particles were formed in the membrane by evaporation/recrystallization/reduction and anion impregnation/ reduction methods [30,31], but other strategies for particle deposition may provide even higher catalytic activities. Among the many methods for incorporating precious metal catalysts in porous materials [32–37], layer-by-layer (LBL) adsorption of polyelectrolyte/metal nanoparticle films is attractive because it offers fine control over nanoparticle size and composition and can be applied to a variety of membrane materials [38]. LBL adsorption of

complementary materials has been investigated by many groups for modification of flat surfaces [39–41], and when charged nanoparticles are utilized as one of the alternating layers, careful selection of adsorption conditions sometimes allows immobilization of well- separated nanoparticles with control over the amount of material [42,43]. One requirement of any technique used for catalyst deposition in interfacial contactors is that the precious metal catalysts are highly concentrated in the membrane region where the gas/liquid interface occurs. Because LBL nanoparticle adsorption in membranes is very rapid, limiting the amount of nanoparticle-containing solution passed through the membrane can readily control the depth to which deposited nanoparticles penetrate the membrane. Hence it is a simple

matter to localize catalyst deposition in the inner layer of a tubular membrane. This research examines wet air oxidation of formic acid, acetic acid, and phenol using tubular ceramic membrane modified with Pt nanoparticles by LBL deposition. Results from these membranes are compared with data from membranes modified by conven-

tional techniques used in the Watercatox project. The LBL- modified membranes have especially high specific activities (activities normalized to Pt content) in the oxidation of these model compounds.

Experimental methods

Anodisc aluminum oxide membranes (25 mm disks with 0.2 or 0.1 mm diameter pore sizes, Whatman), tubular ceramic mem- branes (Pall Exekia) and 100 mesh aluminum oxide (Aldrich) were modified with catalytic nanoparticles using the LBL technique. The tubular membranes (25 cm long, 7 mm inner diameter, 10 mm outer diameter) consisted of three layers: a TiO_2-covered alumina support layer with 12 mm-diameter pores, a TiO_2-covered alumina intermediate layer with 0.8 mm-diameter pores, and a ZrO_2 inner layer with 50 nm-diameter pores. Hexachloroplatinic acid, potas- sium tetrachloroplatinate (II), mercaptosuccinic acid, sodium citrate, sodium borohydride, poly(acrylic acid) (PAA, Mw = 5000), (poly-allylamine hydrochloride) (PAH, Mw = 17,000), and branched poly(ethylenimine) (PEI, Mw = 25,000) were obtained from Aldrich.

2.1. Modification of aluminum oxide powder

LBL modification of the alumina powder involved: (1) stirring 2.5 g of alumina powder in 20 mL of PAA solution (0.02 M PAA, 0.5 M NaCl, pH adjusted to 4.5 with 1 M NaOH) for 10 min; (2) stirring the PAA-modified powder in 20 mL of PAH solution (0.02 M PAH, 0.5 M NaCl, pH

adjusted to 5.0 with 0.1 M HCl) for 10 min; and (3) stirring the PAA/PAH-coated powder in 20 mL of a metal nanoparticle solution for 10 min. (Polymer concentrations are given with respect to the repeating unit.) After each of the above steps, the liquid was decanted, and the alumina powder was washed three times with 20 mL of deionized water. Pt nanoparticles were prepared with thiol or citrate stabilizing agents. To synthesize the thiol-stabilized particles, under vigorous stirring 5 mL of 0.0676 M NaBH4 was added to an aqueous solution containing 10 mL of 3.38 mM H2PtCl6   6H2O and 1 mL of 0.0237 M mercaptosuccinic acid (MSA) [44]. The resulting MSA stabilized Pt solution was diluted by a factor of 4 priors to use in LBL adsorption.

To prepare the citrate-stabilized particles, 30 mL of a 1 wt% aqueous sodium citrate solution was added to 255 mL of a refluxing solution of 0.3 mM H2PtCl6   6H2O under vigorous stirring. The solution was refluxed for 4 h to allow completion of the reaction [45]. The resulting Pt nanoparticle solution was used directly for deposition on the alumina powder. Alumina powder (2.5 g) was also modified by the anionic impregnation technique by stirring the powder in a 0.1 g/L solution of H2PtCl6 for 2 h, washing three times with 20 mL of deionized water, reducing the Pt ions to nanoparticles by adding 20 mL of 0.1 M NaBH4 and stirring for 10 min, and rinsing three more times with 20 mL of deionized water. The Pt content of modified alumina powder samples was determined by dissolving the Pt with aqua regia and analyzing the solutions with atomic absorption spectro- scopy (AAS). The amounts of Pt in the three catalysts were 0.82, 0.56, and 0.44 mg Pt per g powder for anionic impregnation, MSA- stabilized, and citrate-stabilized samples, respectively.

2.2. Membrane modification

LBL modification of disk-shaped alumina membranes was described previously for membranes containing polyelectrolyte/ Au nanoparticle films [46]. Briefly, deposition of each layer involved passing the polyelectrolyte or nanoparticle solution through the membrane using a peristaltic pump located at the permeate side of the membrane. For these membranes, the films consisted of an initial PAA layer followed by a PAH/metal nanoparticle bilayer. The as-prepared Pt nanoparticle solutions were diluted by a factor of 4 prior to deposition in the alumina membranes. As described in detail below, tubular ceramic membranes were modified by several variations of the LBL method as well as by the evaporation/crystallization/reduction and anionic impregnation/reduction techniques. During LBL modification, polyelectrolyte and metal nanoparticle solutions were deposited by flowing from the inside of the membrane to the outside

as shown in Fig. 2.
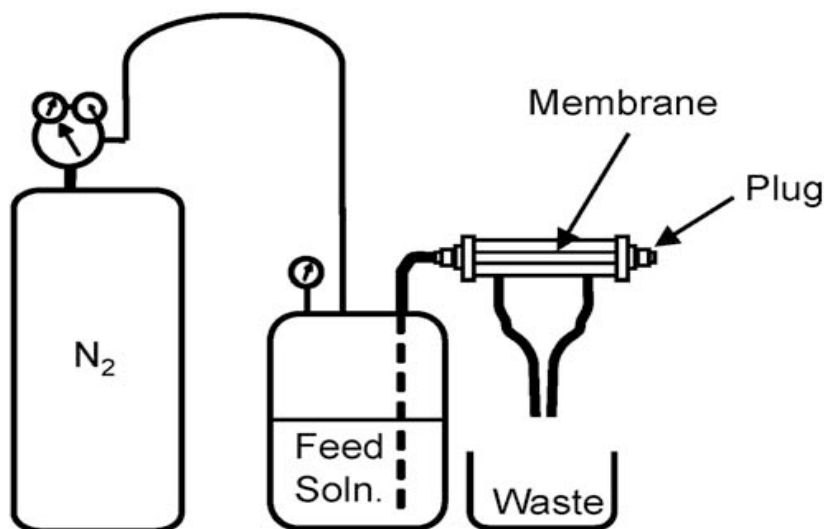
Fig. 2. Schematic diagram of the apparatus used for depositing polyelectrolyte/ metal nanoparticle films in tubular ceramic membranes. The pressurized solution flows through the membrane pores in an inside-out configuration.

2.2.1. Method 1—LBL with ex situ nanoparticle formation [PAA/PAH/Pt-NP]1

For tubular membranes, the modification procedure included sequential flow through the membrane of 250 mL of PAA solution (0.002 M PAA, 0.1 M NaCl, pH adjusted to 4.5), 500 mL of water, 250 mL of PAH solution (0.002 M PAH, 0.1 M NaCl, pH adjusted to 5), 500 mL of water, 1000 mL of a citrate-stabilized Pt nanoparticle solution prepared by diluting 25 mL of as-prepared colloid solution with 975 mL of water, and 500 mL of water. The flow rate of the solutions through the membrane was between 20 and 25 mL/min and was maintained by applying a pressure between 0.2 and 0.5 bar. Fig. 3-1 shows a general scheme of this procedure.

2.2.2. Method 2—LBL with in situ nanoparticle formation [PAA/PEI-Pt (0)]1

In a slight modification to previous procedures for modifying alumina powder with polyelectrolyte/Pd nanoparticle films [47], method 2 incorporated a PEI–Pt complex in the deposition procedure rather than preformed Pt nanoparticles. Briefly mod- ification included sequential flow through the membrane of 250 mL of PAA solution (0.002 M PAA, 0.1 M NaCl, pH adjusted to 4.5), 500 mL of water, and 250 mL of PEI solution that contained Pt(II) (0.002 M PEI, 0.0004 M K_2PtCl_4, pH adjusted to 9). To form Pt nanoparticles, 250 mL of 0.1 M $NaBH_4$ was passed through the membrane to reduce the Pt salt (Fig. 3-2), and the membrane was rinsed by the passage of 500 mL of water.

2.2.3. Method 3—LBL with in situ nanoparticle formation [Pt (0)/PEI]2

Similar to a previous method for modifying alumina powder [48], the membrane was first immersed in a solution of chloroplatinic acid (0.1 g Pt/L) for 20 h so that the inside and outside of the tube were in contact with solution. After putting the membrane in the holder, 500 mL of water was passed through the membrane pores to remove excess Pt solution. PEI was deposited by flowing 250 mL of solution (0.002 M, 0.1 M NaCl, pH adjusted to 9) through the membrane, which was subsequently rinsed by passage of 500 mL of water. A second PtCl62 /PEI bilayer was deposited similarly before reducing the Pt with NaBH4 in the same manner as in method 2 (Fig. 3-3).
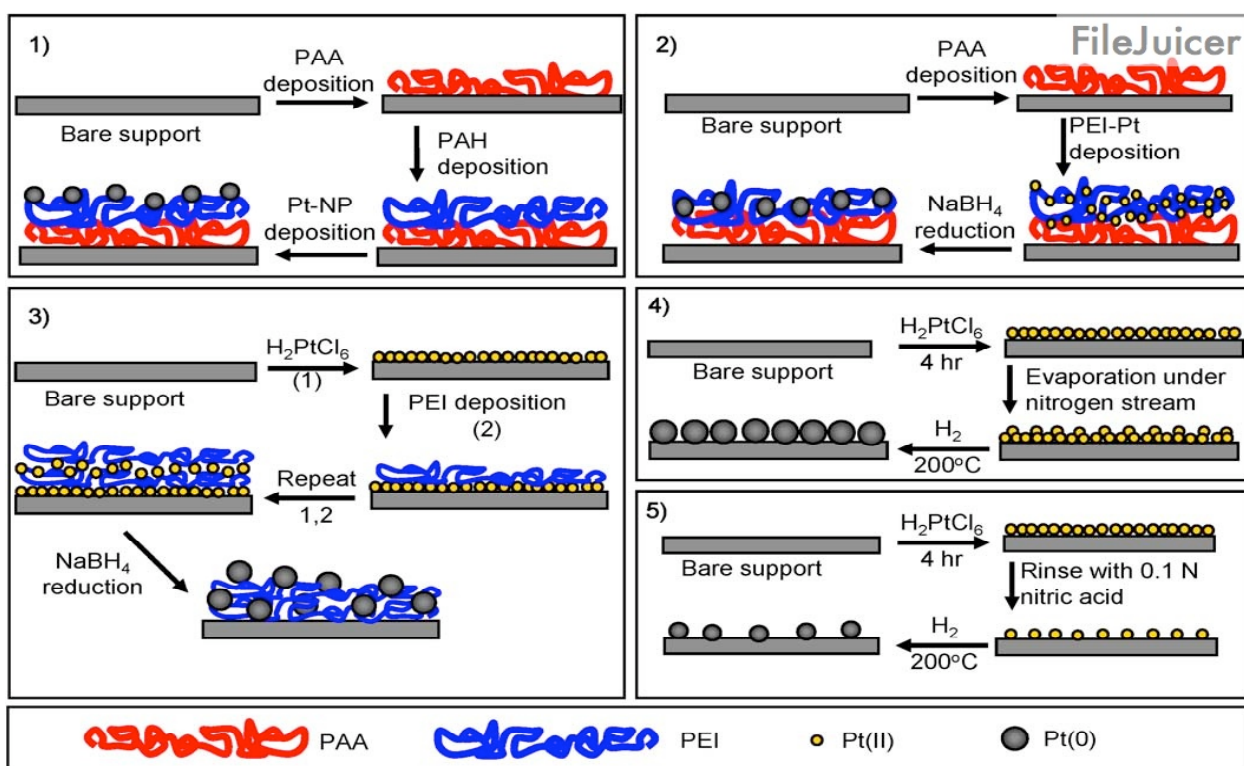
Fig. 3. Schematic diagram of modification of membrane pore surfaces using (1) layer-by-layer deposition of PAA/PAH/Pt-nanoparticle films, (2) layer-by-layer deposition of PAA/PEI–Pt (II) films followed by reduction, (3) layer-by-layer deposition of [Pt(II)/PEI]2 films followed by reduction, (4) evaporation/recrystallization of H2PtCl6 followed by reduction, and (5) anionic impregnation with H2PtCl6 followed by reduction.

2.2.4. Method 4—evaporation/recrystallization with reduction by hydrogen at 200 C

The technique of evaporation/recrystallization was similar to a previously reported procedure in the Watercatox project [30]. Briefly, the membrane was immersed in a 0.1 g/L chloroplatinic acid solution for 4 h, removed from the solution, and allowed to dry at room temperature. Evaporation of the solvent led to concentration of the Pt precursor on the surface of the membrane with more of the Pt located in the inner layer. Reduction of the Pt was performed by placing the membrane under flowing H2 at 200 8C (Fig. 3-4).

2.2.5. Method 5—anionic impregnation with reduction by hydrogen at 200 C

The anionic impregnation technique was also performed in a manner similar to previous Watercatox research [30]. In this case, the support was immersed in a 0.1 g/L chloroplatinic acid solution for 4 h and then rinsed by flowing a 0.1 N nitric acid solution through the pores to remove any unbound Pt species from the membrane. After rinsing with water and then drying under flowing nitrogen at 100 8C, the Pt was reduced under flowing hydrogen at 200 8C (Fig. 3-5).

2.3. Characterization

Nanoparticle solutions were characterized by transmission electron microscopy (TEM) to determine the approximate size and shape of the nanoparticles, and TEM was also used to demonstrate the deposition of nanoparticle-containing films in disk-shaped porous alumina membranes. Prior to imaging, the membrane was ground into a powder with a mortar and pestle and dispersed in water using a vortex mixer. A drop of the resulting solution was then placed onto a carbon-coated copper grid and dried before analysis. The Pt content of the disk-shaped membranes was determined by completely leaching the metal with aqua regia (3 parts HCl, 1 part HNO3) and analyzing the leachate by flame AAS. For tubular membranes, the amount of deposited Pt was estimated by AAS analysis of the deposition solutions beforeand after passing them through the membrane. These values were verified by grinding the membranes into powder with a mortar and pestle, dissolving the Pt in aqua regia, and analyzing the solution by AAS.

2.4. Catalytic reactions

Formic acid, acetic acid, and phenol were employed as substrates for oxidation reactions. Initial experiments were performed with powder catalysts to see if the nanoparticle stabilizer or deposition technique affected the nanoparticle activity. In these reactions, oxygen was continuously bubbled into 50 mL of a vigorously stirred solution containing catalyst and 5 g/L of

formic acid. Samples of the reaction mixture were collected after several time intervals and analyzed by ion chromatography (Dionex LC20, Ionpac AS16 column) to determine the amount of formic acid that remained in solution. Similar experiments were also performed with powders prepared by grinding tubular membranes. Continuously bubbling oxygen into a formic acid solution and then passing that solution through a nanoparticle- modified membrane at a given flux carried out reactions performed with disk-shaped membranes. Samples of the membrane effluent were analyzed by ion chromatography to determine the extent of formic acid oxidation. For interfacial contactor reactions, the modified tubular membranes were mounted in a gas tight module that allows the flow of liquid through the lumen of the tube and countercurrent gas flow on the shell side of the tube (Fig. 4). The liquid flow rate was typically between 7 and 10 mL/min, and the gas overpressure was set to values between 0.2 and 4 bar. The gas flow rate was maintained at 50 mL/min with a mass flow controller. Air was used as the oxidant in all of the interfacial contactor reactions, which were carried out at 20 or 60 8C by controlling the temperature of the feed solution. The starting concentrations of formic acid, acetic acid, and phenol were 5 g/L (0.108 M), 3.25 g/L (0.054 M), and 1.7 g/L (0.018 M), respectively, and correspond to carbon contents of approximately 1.3 g/L in each case. For the interfacial contactor reactions, the conversion of each substrate was monitored using total organic carbon (Shimadzu TOC 5050A) and/or HPLC (Varian Prostar with UV–vis detection) analysis. The uncertainty in the calculated specific activities was <10% for formic acid oxidation experiments and <20% for acetic acid and phenol oxidation experiments.
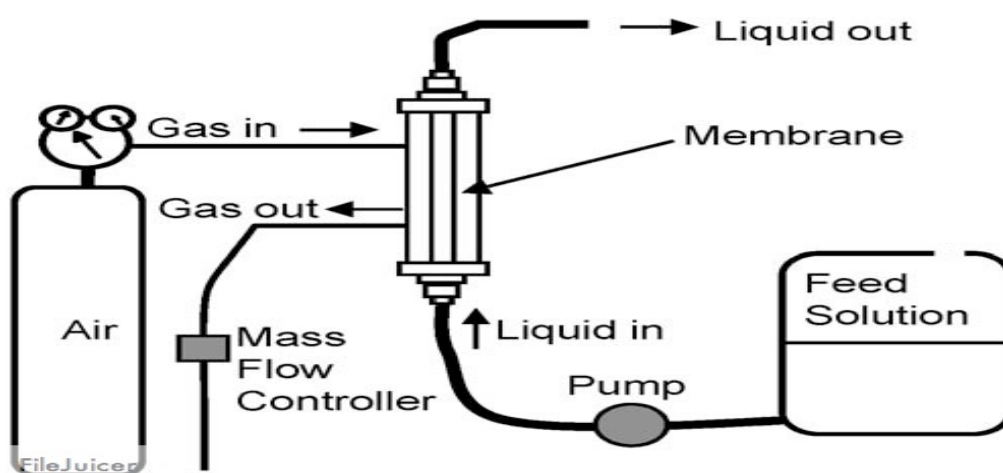
Fig. 4. Schematic diagram of the wet air oxidation apparatus that employs tubular catalytic membranes as interfacial contactors.

3. Results and discussion

3.1. Membrane characterization

TEM images of nanoparticles and membrane samples were collected to determine the size and shape of the Pt nanoparticles and to see if these particles are effectively deposited in the membranes. The images and size distributions of MSA- and citrate- stabilized Pt nanoparticles in Fig. 5 show that the average particle diameters are 2.6 and 3.2 nm, respectively. Fig. 6 presents TEM images of the citrate-stabilized Pt nanoparticles immobilized in a disk-shaped alumina membrane by method 1 (Fig. 3). These images show that LBL deposition yields a high density of nanoparticles within the pores of the membrane and that there is minimal particle aggregation, which should lead to accessible nanoparticles with a high catalytic surface area.
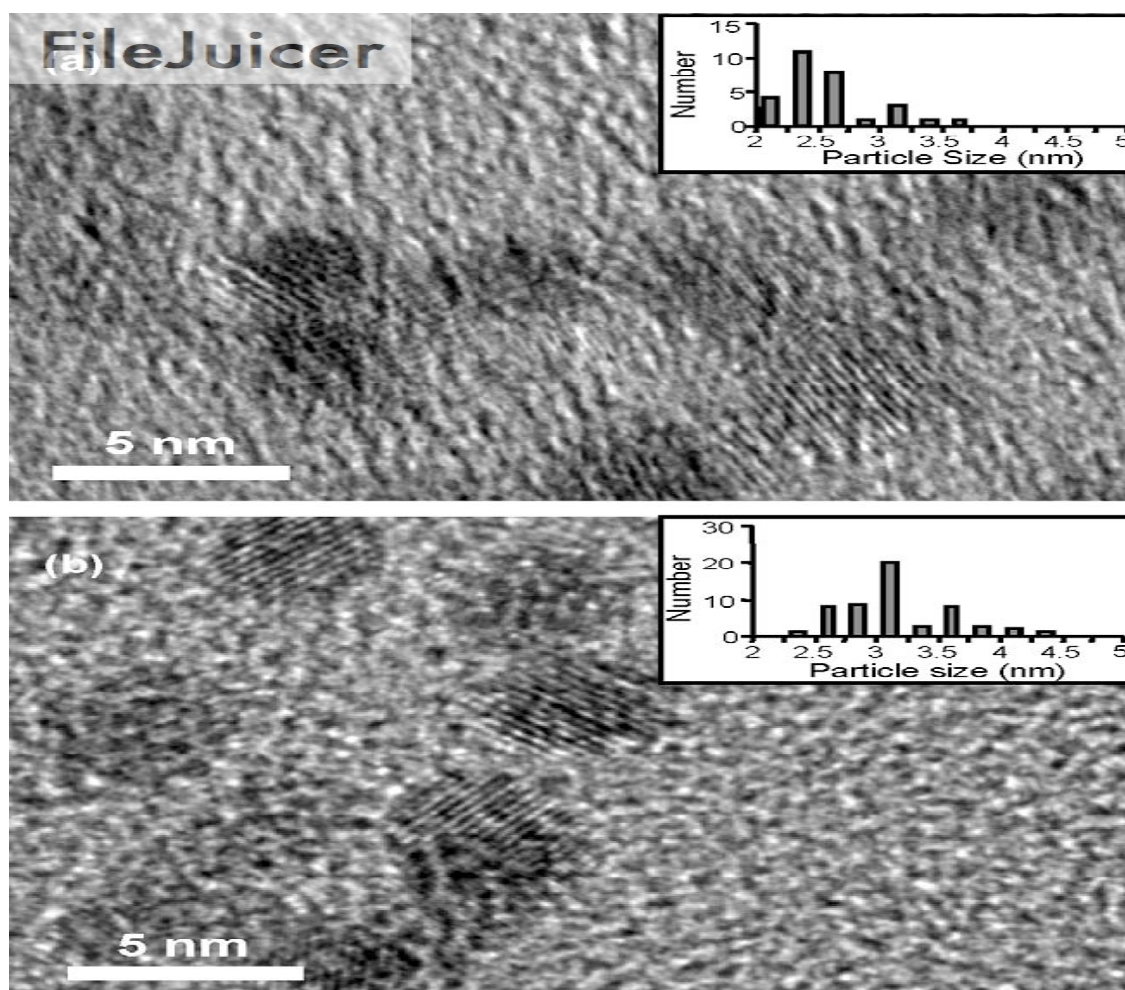
Fig. 5 The average particle diameters are 2.6 and 3.2 nm
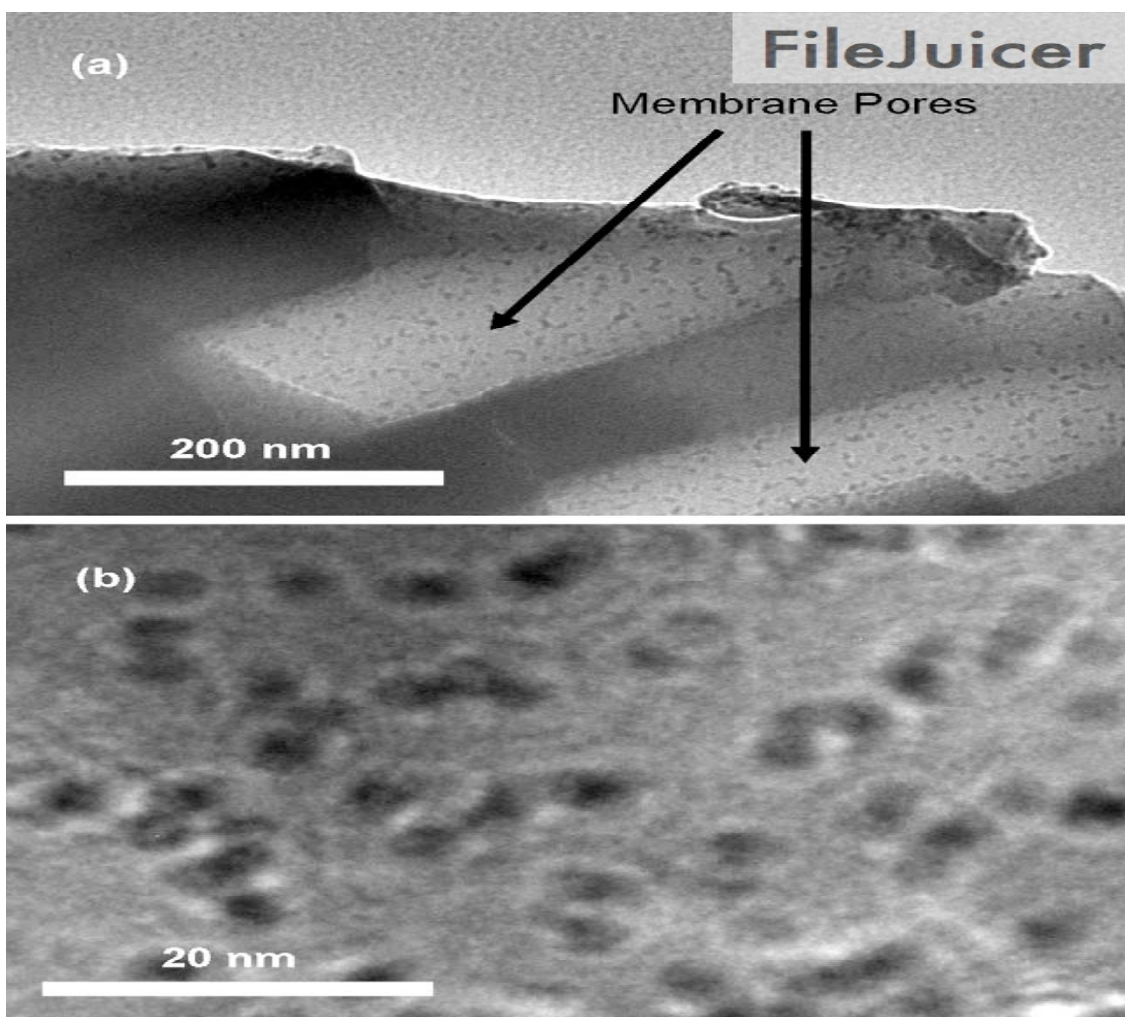
Fig. 6 TEM images of the citrate-stabilized Pt nanoparticles immobilized in a disk-shaped alumina membrane by method 1

The amount of Pt in each of the tubular membranes was determined by chemical analysis of precursor Pt solutions before and after passing them through the membrane. These values were later confirmed by dissolving the immobilized Pt in aqua regia and analyzing these solutions by AAS. Table 1 shows that the two methods for determining the amount of immobilized Pt are in good agreement for all membranes except those prepared by method 5. The difference in the two values for method 5 is likely due to some Pt being washed away in the nitric acid rinsing step during the membrane modification. This Pt loss is not accounted for in the initial mass balance. For all membranes, the Pt content is 200–1000 mg of Pt per m2 (1–5 mg of Pt per membrane), based on the area calculated from the inner tube diameter, and the relatively similar Pt loading among the different membranes facilitates comparison of their catalytic activities.

3.2. Wet air oxidation catalyzed by Pt nanoparticles on alumina powder

To examine the effect of the stabilizing agent on the activity of Pt nanoparticles, alumina powder was modified with a PAA/PAH bilayer and either citrate- or MSA-stabilized Pt nanoparticles to prepare heterogeneous catalysts. In wet air oxidation of formic acid with these materials, the catalyst modified with citrate-stabilized Pt nanoparticles exhibits an activity of 1.3 ∓0.2 mmol/(s gPt) whereas the catalyst containing MSA-stabilized Pt nanoparticles has an activity data suggest that the polyelectrolyte multilayer does not inhibit the activity of the Pt nanoparticles of 0.7 ∓ 0.1 mmol/(s gPt). The average nanoparticle size is similar for both types of particles, so differences in surface area should not account for the difference in activity. In fact, of the two types of nanoparticles, MSA-stabilized particles show slightly smaller diameters (higher surface area per mass) in TEM images (Fig. 5). The most likely explanation for the difference between the two types of nanoparticles is that the thiol stabilizers bind more tightly than citrate to the surface of the nanoparticle, and this stronger binding limits the number of active sites for catalysis. Previous studies of catalysis by thiol-stabilized metal nanoparticles also reported low reaction rates [49,50]. Alumina powder modified by impregnation of $PtCl_6^{2-}$ and subsequent reduction of Pt (IV) to Pt nanoparticles shows an activity of 1.0∓ 0.1 mmol/(s gPt), which is again lower than that of the catalyst containing citrate- stabilized nanoparticles. Thus, LBL deposition with citrate-stabilized nanoparticles provides catalysts with comparable or better activities than traditional methods of catalyst preparation. Furthermore, these

3.3. Oxidation of formic acid in disk-shaped membranes

In initial studies of membrane-based oxidation, solutions sparged with O2 were passed through an alumina membrane coated with a PAA/PAH/Pt nanoparticle film. Fig. 7 shows the results of these studies. At initial formic acid concentrations <2 mM, nearly all of the formic acid is oxidized to CO_2 and water

Table 1 Pt contents in tubular membranes.

Modification method	Pt loading (mg Pt/m)	
	Mass balance[b]	Membrane powder[c]
1	220∓40	220∓20
2	220∓20	200∓20
3	910∓90	830∓80
4	470∓60	480∓40
5	690∓90	400∓40

a Based on an internal membrane surface area of 0.00506 m2 (internal tube diameter of 7 mm, active length of 230 mm). b Determined by chemical analysis of precursor solutions before and after deposition.
c Determi
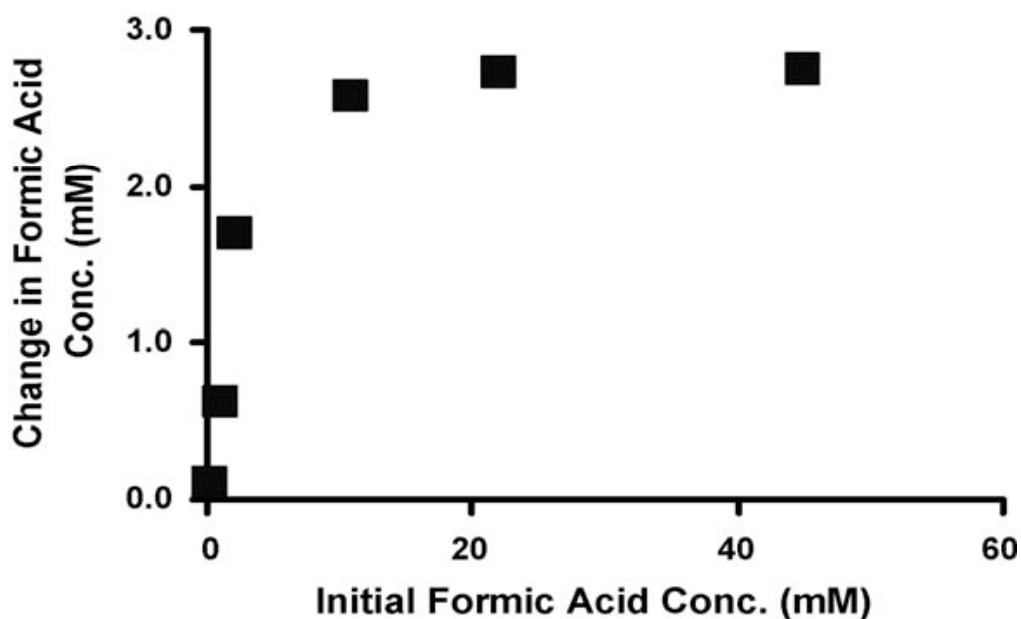
Fig. 7. Change in formic acid concentration in membrane-catalyzed oxidation with several initial formic acid concentrations. (The membrane acted as a flow-through contactor.) Solutions were sparged with O2, and the flux through the disk-shaped porous alumina membrane modified with citrate-stabilized Pt nanoparticles (method 1) was 0.023 mL/(cm2 s).

ned by chemical analysis of aqua regia solutions used to remove Pt from ground membrane sample
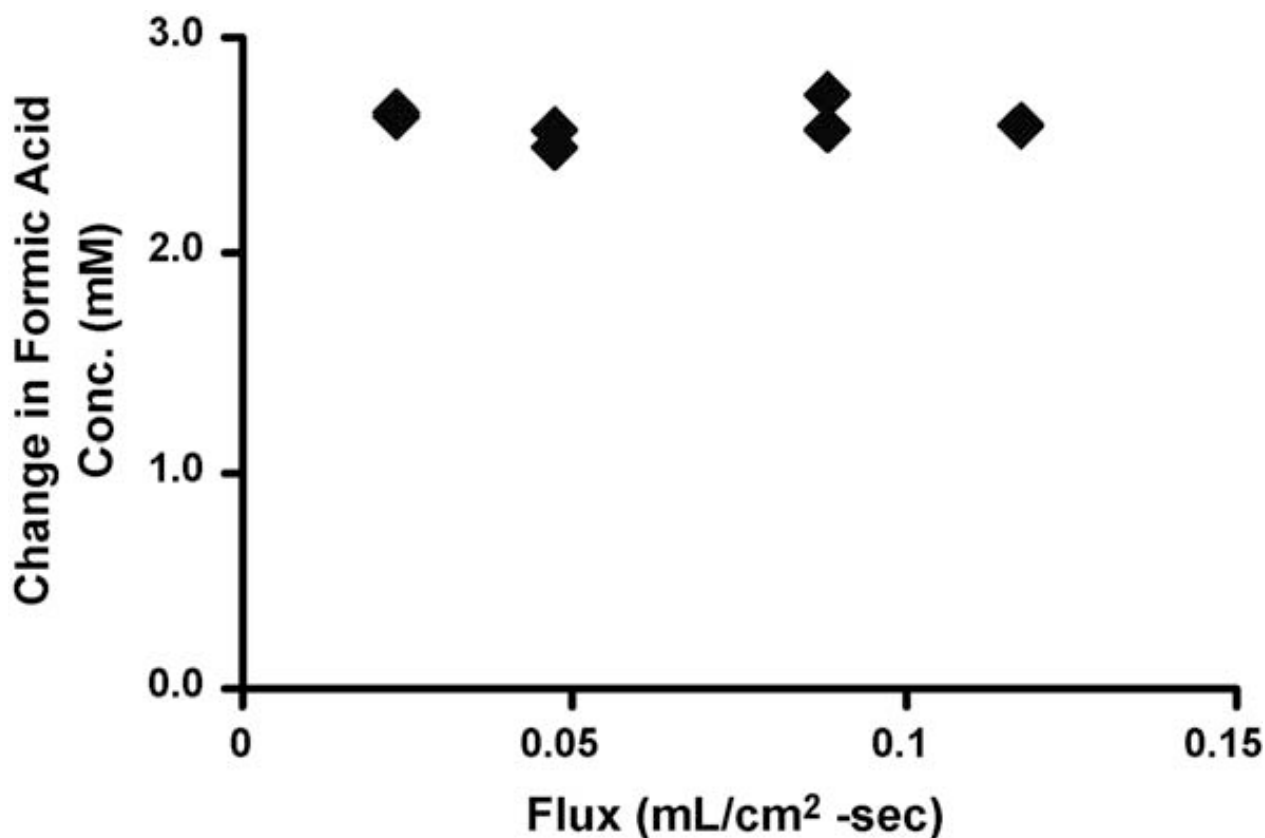
Fig. 8. Change in formic acid concentration during membrane-catalyzed oxidation as a function of flux through a nanoparticle-modified disk-shaped alumina membrane (method 1). (The membrane acted as a flow-through contactor.) The initial solution concentration was 10.8 mM and solutions were sparged with O2 before passing through the membrane.

during passage through the membrane because at these concentrations, formic acid is the limiting reactant. However, at formic acid concentrations >10 mM, the amount of oxidation is essentially independent of initial formic acid concentration because O2 is the limiting reagent. The solubility of O2 in water at 1 atm of O2 is roughly 1.25 mM [51], which would correspond to a concentration of 2.5 mM formic acid that could be oxidized. This is similar to the maximum change in formic acid concentration seen in Fig. 7. For oxygen-sparged solutions containing 10.8 mM formic acid, increasing the solution flux through the membrane did not significantly affect decreases in formic acid concentration (Fig. 8). This again suggests that the reaction is limited by the amount of O2 in the solution because if the reaction were kinetically limited, we would expect smaller declines in the formic acid concentration at higher flow rates to lower residence times in the membrane. In most fast gas–liquid reactions with flow-through contactors, the solubility of the gas in solution will limit the reaction rate unless high gas pressures are employed. For this reason, tubular interfacial contactors are often more attractive than flow-through contactors for membrane-catalyzed gas–liquid reactions such as wet air oxidation.

3.4. Wet air oxidation with tubular membranes

This section compares the catalytic activities of five types of tubular interfacial contactor membranes (Fig. 3) in sequential studies of the oxidation of formic acid, acetic acid, and phenol. Experiments were performed on at least two membranes modified by each method. Because catalyst deactivation often occurs during phenol oxidation [52], membranes were again tested in the oxidation of formic acid after experiments with phenol to see if catalyst deactivation occurred.

3.4.1. Formic acid oxidation

Initially, formic acid oxidation was examined at 1, 2, 3, 4, and 4.3 bar of air overpressure to determine the effect of overpressure on reaction rates (Fig. 9). High air overpressures increase the solubility of O_2 in the solution, but more importantly, they control the location of the gas–liquid interface. The highest activity in formic acid oxidation occurs at 4 or 4.3 bar of overpressure because the gas–liquid interface is closest to the inner layer of the tube where most of the catalyst is located. However, in some cases much of the air begins to come through the defects in the membrane at an overpressure of 4.3 bars. As a result, the catalytic activity sometimes starts to decrease at 4.3 bars because the gas/ liquid interface is no longer well maintained in the catalytic layer of the membrane. This is consistent with previous

149

results [28]. Membranes prepared by methods 1 and 2 exhibit similar rates of formic acid
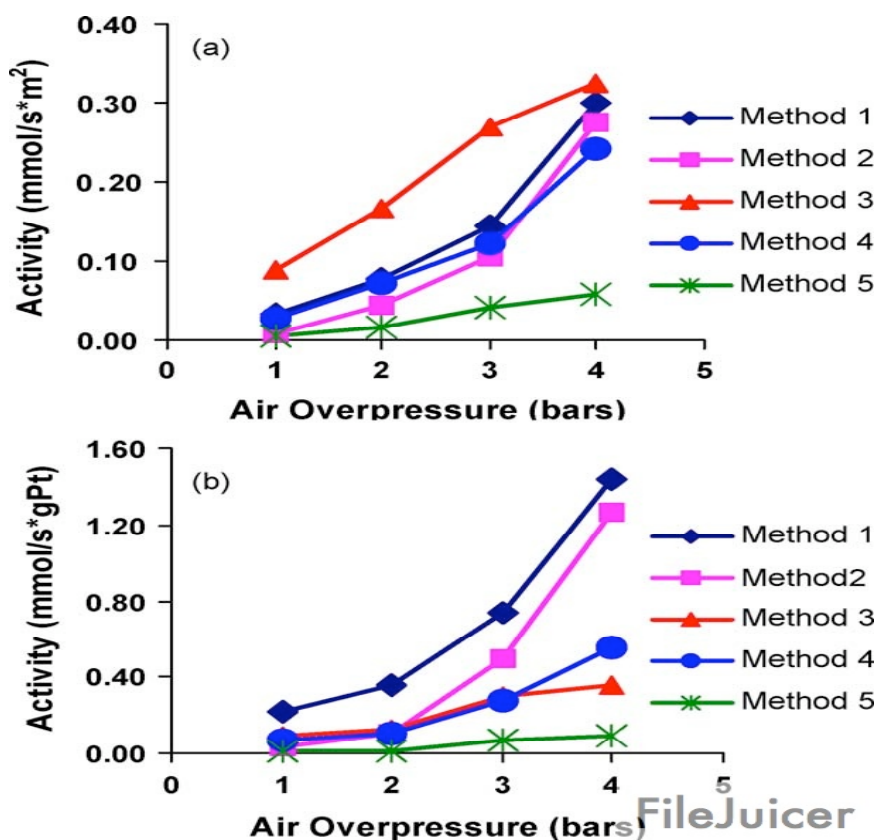
oxidation and similar specific activities (Fig. 9).

Fig. 9. Normalized rate of formic acid oxidation vs. air overpressure for Pt- containing membranes prepared by the methods shown in Fig. 3. (The membrane served as an interfacial contactor.) Normalization was performed with respect to (a) the area of the internal wall of the membrane and (b) the amount of Pt in the membrane.

Membranes prepared by method 3 show a similarly high reaction rate (Fig. 9a), but because the platinum content of these membranes is higher than that of all other membranes (Table 1), their specific activity at overpressures >3 bar is lower than for membranes prepared by methods 1 and 2 (Fig. 9b). This is not surprising because in method 3, the initial Pt deposition occurs throughout the membrane, not just in the surface layer. Only the Pt that is near the gas–liquid interface is efficiently used for formic acid oxidation. In Fig. 9a, the relatively high oxidation rates at low overpressures for the membranes prepared by method 3 likely occur because at low overpressures the gas–liquid interface is deeper in the tube wall, where these particular membranes still have significant amounts of Pt. Membranes prepared by method 4 show a high rate of formic acid oxidation (Fig. 9a) but a lower activity per gram of Pt (Fig. 9b) than methods 1 and 2. This suggests that method 4 deposits the platinum deeper into the

membrane than methods 1 and 2, and therefore the specific activity with method 4 membranes is low at the higher air overpressures because all of the platinum is not being used effectively. On the other hand, the membranes prepared by method 5 exhibit a much lower activity than those prepared by the other four methods. This is expected because PtCl62 does not bind well to the surface of ZrO2 and is easily removed during the nitric acid rinsing step. Therefore, the Pt is mostly bound to regions that are not washed well with nitric acid. Since these regions most likely appear away from the gas–liquid interface, the method 5 membranes should have relatively low activity. When comparing the LBL-modified membranes (methods 1–3) with membranes described in the literature, the rate per membrane area is only 1/3 to 1/2 as high as published values [29]. On the other hand, the rate is 5-fold higher than published values when normalizing to Pt content. The specific activity is also 50% higher than previous values obtained with ''low-loading'' membranes, which had Pt contents similar to the membranes prepared in this study [29].

3.4.2. Acetic acid oxidation

Similar to results with formic acid, the rate of acetic acid oxidation at room temperature is highest at 4 or 4.3 bar (Fig. 10). The oxidation rate was determined by TOC analysis and thus tells how much of the acetic acid is completely oxidized to CO_2 and H_2O but does not account for any partial conversion to formic acid. Fig. 10a shows that membranes prepared by methods 1 and 2 have a much higher activity for room temperature acetic acid oxidation than membranes prepared by the other 3 methods. The membranes prepared by method 3 show a small specific activity, but membranes prepared by methods 4 and 5 exhibits essentially no detectable activity for acetic acid oxidation at room tempera- ture. At 60 8C, membranes prepared by methods 1–4 exhibit higher activity than at room temperature, as expected. In the case of membranes prepared by methods 1 and 2, on going from room temperature to 60 8C, the activity increases by about 60% and 90%, respectively. In contrast, the activities of membranes prepared by methods 3 and 4 increases by factors of 9 and 10, respectively. Even with this large increase in activity, however, the membranes prepared by methods 3 and 4 still have a lower activity at 60 8C than the membranes prepared by the first two methods. The membranes prepared by method 5 show low activity even at the higher temperature.

3.4.3. Phenol oxidation

In phenol oxidation, samples were collected at 1, 3, and 4 bar overpressures and subsequently analyzed by both TOC and HPLC. In TOC analysis, catalytic activities are determined from

the difference in carbon content between the inlet and outlet solutions, whereas in HPLC analysis, catalytic activities are determined from the decrease in phenol concentration. Similar to previous experiments involving oxidation of formic acid and acetic acid, the highest activity occurs at air overpressures of 4 bar. Tables 2 and 3 show that, again, the highest activity occurs with membranes prepared by methods 1 and 2, and that membranes prepared by method 5 show little or no activity for the oxidation of phenol. Membranes prepared by methods 3 and 4 exhibit more than 4-fold lower specific activities than membranes prepared by the first two methods, even at higher temperature. Oxidation experiments performed at 60 8C result in higher activities (two times higher or more) than experiments performed at room temperature. We would expect to achieve even higher activities with temperatures in excess of 150 8C [14,52], but these high temperatures are not compatible with the experimental apparatus (Fig. 4) used in this study. Furthermore, these high temperatures may also lead to film deformation and possible sintering of the catalyst. Future studies need to explore the stability of polyelec- trolyte/metal nanoparticle films at temperatures at or above 150 °C.

The catalytic activities determined from HPLC are generally higher than those from TOC because TOC analysis only shows how much of the sample is transformed to CO_2 or insoluble species, whereas HPLC shows how much phenol is oxidized to any product. The higher activities seen with HPLC suggest that some phenol is oxidized to smaller organic compounds, and not completely to CO_2. Because the conversion in phenol oxidation is low (<10%), the quantities of these other compounds in the analyzed samples are below detectable levels in HPLC. As a result, the identity and amount of each byproduct in the reaction were not determined. The activities determined by TOC analysis and HPLC are generally in better agreement at 60 8C than at room temperature, suggesting that more of the phenol is converted to CO_2 and H_2O at higher temperatures.
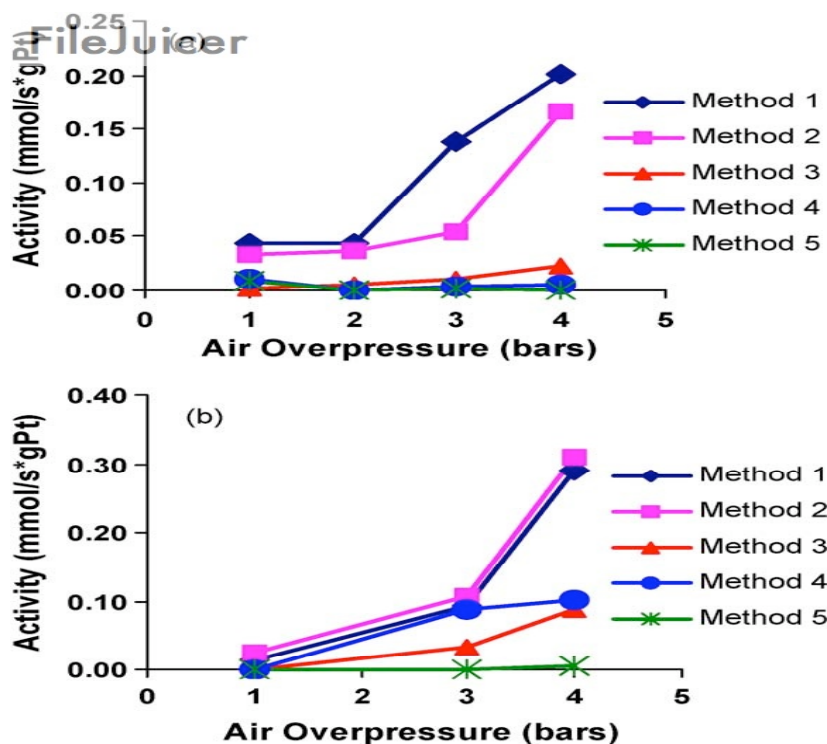
Fig. 10. Normalized rates of membrane-catalyzed acetic acid oxidation vs. air overpressure for different membrane types at (a) room temperature and (b) 60 8C. (The membrane served as an interfacial contactor.) Oxidation rates were normalized to the amount of Pt in the membrane.

Table 2 Catalytic activities of several tubular membranes in phenol oxidation at room temperature with 4 bar air overpressure.

Preparation method	Activity[a] mmol/(s gPt)[a]	mmol/(s gPt)[b]
1	0.064	0.13
2	0.050	0.11
3	0.006	0.015
4	0.000	0.000
5	0.003	0.012

a Determined by TOC analysis. , b Determined from HPLC analysis.

After phenol oxidation, the various membranes were again used to catalyze formic acid oxidation at room temperature to determine if the oxidation of refractory compounds like

phenol causes catalyst deactivation. While a decrease in activity for formic acid oxidation could be due to poisoning or other effects such as nanoparticle leaching or aggregation, a constant activity may suggest that the extent of catalyst deactivation is minimal. However, if formic acid oxidation is simply limited by O2 solubility, then catalyst deactivation would not be observed by this method. In nearly all cases, there was no decrease in formic acid oxidation rates after using the membranes for phenol oxidation. However, one of the membranes prepared by method 4 showed a 40% activity decrease in formic acid oxidation after the membrane was used for phenol oxidation. The decreased activity may have been due to leaching of Pt for that specific membrane or to poisoning of the catalyst during phenol oxidation. With that exception, each membrane maintained a constant activity for formic acid oxidation.

3.4.4. Conventional reactions with pulverized tubular membranes

To show that the interfacial contactor configuration is advantageous for these reactions, each type of membrane was also ground into a powder that was used as a heterogeneous catalyst in a conventional stirred tank reaction. In these reactions, a solution containing 0.108 M formic acid was continuously bubbled with oxygen while stirring rapidly. Pure oxygen was used as the oxidant instead of air to provide as much oxygen to the reaction as possible. The results in Table 4 show that all five types of membranes in the powder form have similar activities when normalized to the amount of Pt in the catalyst. However, the activities of different membranes operated as interfacial con- tactors vary significantly with the method of modification. In the case of methods 1 and 2, membranes operated as interfacial contactors at 4 bar overpressure show activities that are 2.5 times higher than those of membrane powders used as heterogeneous catalysts. Conversely, membranes prepared by methods 3 and 4 exhibit little difference in activity between interfacial contactors and powder catalysts, and the membrane prepared by method 5 shows higher activity in the conventional reaction. These results demonstrate that the interfacial contactor configuration can be quite valuable for gas–liquid reactions, but to take full advantage of this configuration, the catalyst must be localized in the inner layer of the membrane.

4. Conclusions

The overall objective of this study was to compare the catalytic activity of membranes prepared using LBL deposition methods with the activity of membranes prepared by the traditional methods of evaporation / recrystallization / reduction and anionic impregnation / reduction. Although the rate of formic acid oxidation with LBL-modified membranes was 1/3

to 1/2 lower than previous results when normalized to membrane surface area, the rate when normalized to Pt content improved 5-fold. In this study, the Pt content for all membranes studied was less than 5 mg of Pt per membrane. Membranes prepared by LBL methods 1 and 2 exhibited the highest activity when normalized to the Pt content inside the membranes, most likely because of strong localization of the Pt in the inner layer of the tubular membrane. Conversely, the other three methods deposit Pt on the entire surface of the membrane, which means that any Pt that gets deposited on the support layer or intermediate layer is most likely not being utilized when performing oxidation at higher air overpressures. The biggest limitation to the methods involving LBL deposition is the low loading of Pt. Since the support is quite expensive, the cost of Pt is not as much of a concern as in other systems; however, Pt cost cannot be disregarded. In the future, low loading with the LBL method can be overcome by optimizing the LBL deposition procedure or by depositing multiple layers. Further studies should also include examination of catalytic activity in continuous experiments over longer periods of time to learn more about the catalyst stability. (Experiments in this study were typically performed only for a few hours.) LBL modification is quite versatile and could also be applied to polymeric hollow fiber supports, which are much less expensive than the traditional ceramic supports. This should result in a more cost-effective system for gas–liquid reactions as long as the polymer membrane is sufficiently stable.

Table 3 Catalytic activities of several tubular membranes in phenol oxidation with a feed temperature of 60 °C with 4 bar air overpressure.

Preparation method	Activity	
	mmol /(s gPt)[a]	mmol/(s gPt)[b]
1	0.15	0.21
2	0.11	0.21
3	0.026	0.035
4	0.027	0.025
5	0.003	0.000

a : Determined by TOC analysis. b: Determined from HPLC analysis.

Table 4 Catalytic activities in formic acid oxidation for tubular membranes used as interfacial contactors and as powders in conventional stirred tank reactors.

Modification method	Activity (mmol/s gPt)	
	Interfacial contactor[a]	Conventional reactor[b]
1	1.5 0.3	0.6 0.05
2	1.3 0.2	0.5 0.03
3	0.5 0.1	0.7 0.1
4	0.7 0.2	0.5 0.03
5	0.1 0.03	0.5 0.1

a   Activity at air overpressure = 4 bar., b Pure O2 was sparged into the reaction mixture.

References

[1] V.S. Mishra, V.V. Mahajani, J.B. Joshi, Ind. Eng. Chem. Res. 34 (1995) 2–48.

[2] F.J. Zimmerman, Chem. Eng. 65 (1958) 117–120.

[3] F. Luck, Catal. Today 53 (1999) 81–91.

[4] E. Guibelin, Water Sci. Technol. 49 (2004) 209–216.

[5] B.J. Kim, S. Qi, R.S. Shanley, Water Environ. Res. 66 (1994) 440–455.

[6] P. Adriaens, T.M. Vogel, in: L.Y. Young, C.E. Cerniglia (Eds.), Microbial Transformation and Degradation of Toxic Organic Chemicals, Wiley, New York, 1995 , pp. 435–486.

[7] C.A. Fewson, Trends Biotechnol. 6 (1988) 148–153.

[8] Y.I. Matatov-Meytal, M. Sheintuch, Ind. Eng. Chem. Res. 37 (1998) 309–326.

[9] M. Jeworski, E. Heinzle, Biotechnol. Annu. Rev. 6 (2000) 163–196.

[10] H. Debellefontaine, J.N. Foussard, Waste Manage. (Oxford) 20 (2000) 15–25.

[11] F. Luck, Catal. Today 27 (1996) 195–202.

[12] J. Levec, A. Pintar, Catal. Today 124 (2007) 172–184.

[13] D. Pham Minh, P. Gallezot, S. Azabou, S. Sayadi, M. Besson, Appl. Catal. B 84 (2008) 749–757.

[14] A. Pintar, J. Batista, T. Tisler, Appl. Catal. B 84 (2008) 30–41.

[15] A. Julbe, D. Farrusseng, C. Guizard, J. Membr. Sci. 181 (2001) 3–20.

[16] R. Dittmeyer, K. Svajda, M. Reif, Top. Catal. 29 (2004) 3–27.

[17] G. Bengtson, D. Fritsch, Desalination 200 (2006) 666–667.

[18] H. Purnama, P. Kurr, A. Schmidt, R. Schoma¨ cker, I. Voigt, A. Wolf, R. Warsitz, AlChE J. 52 (2006) 2805–2811.

[19] A. Schmidt, R. Haidar, R. Schoma¨ cker, Catal. Today 104 (2005) 305–312.

[20] A. Schmidt, R. Schoma¨ cker, J. Mol. Catal. A: Chem. 271 (2007) 192–199.

[21] C. Lange, S. Storck, B. Tesche, W.F. Maier, J. Catal. 175 (1998) 280–293.

[22] M. Reif, R. Dittmeyer, Catal. Today 82 (2003) 3–14.

[23] M. Pera-Titus, S. Miachon, J.-A. Dalmon, AlChE J. 55 (2009) 434–441.

[24] S. Miachon, V. Perez, G. Crehan, E. Torp, H. Raeder, R. Bredesen, J.A. Dalmon, Catal. Today 82 (2003) 75–81.

[25] H. Raeder, R. Bredesen, G. Crehan, S. Miachon, J.-A. Dalmon, A. Pintar, J. Levec, E.G. Torp, Sep. Purif. Technol. 32 (2003) 349–355.

[26] E.E. Iojoiu, S. Miachon, E. Landrivon, J.C. Walmsley, H. Raeder, J.-A. Dalmon, Appl. Catal. B 69 (2007) 196–206.

[27] E.E. Iojoiu, E. Landrivon, H. Raeder, E.G. Torp, S. Miachon, J.-A. Dalmon, Catal. Today 118 (2006) 246–252.

[28] E.E. Iojoiu, J.C. Walmsley, H. Raeder, S. Miachon, J.-A. Dalmon, Catal. Today 104 (2005) 329–335.

[29] E.E. Iojoiu, S. Miachon, J.-A. Dalmon, Top. Catal. 33 (2005) 135–139.

[30] D. Uzio, S. Miachon, J.-A. Dalmon, Catal. Today 82 (2003) 67–74.

[31] V. Perez, S. Miachon, J.-A. Dalmon, R. Bredesen, G. Pettersen, H. Raeder, C. Simon, Sep. Purif. Technol. 25 (2001) 33–38.

[32] P. Braunstein, H.-P. Kormann, W. Meyer-Zaika, R. Pugin, G. Schmid, Chem. Eur. J. 6 (2000) 4637–4646.

[33] K. Daub, V.K. Wunder, R. Dittmeyer, Catal. Today 67 (2001) 257–272.

[34] C. Perego, P. Villa, Catal. Today 34 (1997) 281–305.

[35] G. Centi, R. Dittmeyer, S. Perathoner, M. Reif, Catal. Today 79–80 (2003) 139–149.

[36] L. Gro¨ schel, R. Haidar, A. Beyer, H. Coelfen, B. Frank, R. Schoma¨ cker, Ind. Eng. Chem. Res. 44 (2005) 9064–9070.

[37] J. Xu, A. Dozier, D. Bhattacharyya, J. Nanopart. Res. 7 (2005) 449–467.

[38] D.M. Dotzauer, J. Dai, L. Sun, M.L. Bruening, Nano Lett. 6 (2006) 2268–2272.

[39] J. Schmitt, G. Decher, W.J. Dressick, S.L. Brandow, R.E. Geer, R. Shashidhar, J.M. Calvert, Adv. Mater. 9 (1997) 61–65.

[40] T.C. Wang, M.F. Rubner, R.E. Cohen, Chem. Mater. 15 (2003) 299–304.

[41] J. Dai, M.L. Bruening, Nano Lett. 2 (2002) 497–501.

[42] D. Lee, M.F. Rubner, R.E. Cohen, Nano Lett. 6 (2006) 2305–2312.

[43] J.W. Ostrander, A.A. Mamedov, N.A. Kotov, J. Am. Chem. Soc. 123 (2001) 1101–1110.

[44] S. Chen, K. Kimura, J. Phys. Chem. B 105 (2001) 5397–5403.

[45] P.A. Brugger, P. Cuendet, M. Graetzel, J. Am. Chem. Soc. 103 (1981) 2923–2927.

[46] D.M. Dotzauer, S. Bhattacharjee, Y. Wen, M.L. Bruening, Langmuir 25 (2009) 1865–1871.

[47] S. Bhattacharjee, M.L. Bruening, Langmuir 24 (2008) 2916–2920.

[48] S. Kidambi, M.L. Bruening, Chem. Mater. 17 (2005) 301–307.

[49] S.E. Eklund, D.E. Cliffel, Langmuir 20 (2004) 6012–6018.

[50] J. Alvarez, J. Liu, E. Roman, A.E. Kaifer, Chem. Commun. (2000) 1151–1152.

[51] F.D. Wilde (Ed.), Field Measurements: U.S. Geological Survey Techniques of Water-Resources Investigations, book 9, chap. A6, accessed from http://www.ubs.water.usgs.gov/twri9A/on2/6/2009.

[52] S. Nousir, S. Keav, Barbier Jr., M. Bensitel, R. Brahmi, D. Duprez, Appl. Catal. B 84 (2008) 723–731.

3-3 Effect of preteatment wetting method on the membrane catalytic activity.

(Catalysis Today xxx (2010) xxx-xxx) article in press.
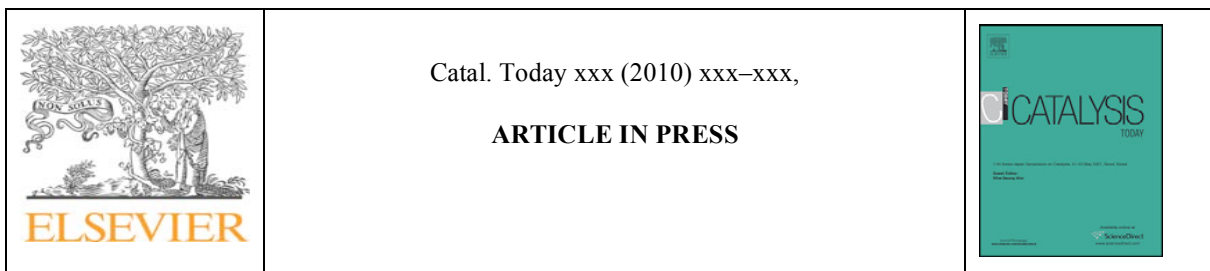
High-performance catalytic wet air oxidation (CWAO) of organic acids and phenol in interfacial catalytic membrane contactors under optimized wetting conditions

M. Alame[a], A. Abusaloua[a], M. Pera-Titus[a], N. Guilhaume[a], K. Fiaty[b], A. Giroir-Fendler[a]

a : Université de Lyon, Institut de Recherches sur la Catalyse et l'Environnement de Lyon (IRCELYON), UMR 5256 CNRS – Université Lyon 1, 2, Av. A. Einstein, 69626 Villeurbanne Cedex, France

b : Laboratoire d'Automatique et de Génie des Procédés(LAGEP), UMR 5007 CNRS, CPE Lyon, Bât308G, Université de Lyon, 43 Bddu11novembre1918, 69622 Villeurbanne Cedex, France

abstract

This paper is intended to evaluate the effect of membrane wetting on the performance of interfacial catalytic membrane contactors applied to the wet air oxidation of organic pollutants. To this aim, two wetting methods (i.e. by capillarity at ambient pressure and under dynamic vacuum) have been used prior to the oxidation tests. A series of monometallic and bi/trimetallic catalytic membranes have been prepared and tested using both wetting methods for the oxidation of formic, acetic and oxalic acids as model pollutants. In these experiments, the solution with the target pollutant was pumped along the contactor on the catalytic layer side, while air or pure oxygen was pumped along the other side.

The gas/liquid interface was located within the membrane wall by means of a transmembrane pressure compensating capillary forces. In all cases, higher catalytic activities have been obtained after wetting the membranes under dynamic vacuum. On the basis of the coarse-grained nature of the membranes, wetting under vacuum might help removing air blocked in larger sized pores and cavities, allowing there fore a more accurate

control of the position of the confined gas–liquid interface by the transmembrane pressure. Using optimized wetting conditions, we show promising results on the application of interfacial catalytic membrane contactors to the oxidation of phenol at room temperature and air over pressures in the range 1–4bar.

1. Introduction

Wet air oxidation (WAO), earlier developed by Zimmerman during the1950s [1], constitutes an attractive technology for the treatment of industrial effluents containing low to intermediate concentrations of refractory and toxic compounds for which incineration or biological remediation are in efficient and / or costly.

Thermal WAO usually takes place at high temperatures 473–623K) and pressures (2–15MPaair, O2orO3), the residence times of the liquid phase ranging from 15 to 120 min, and with typical chemical oxygen demand (COD) removal about 75–90% [2].The high-energy demands combined with strong corrosion are detrimental for a wide spread industrial application of thermal WAO.

The efficiency of WAO can be improved by the use of heterogeneous catalysts. Nevertheless, the main shortcoming of catalytic wet air oxidation (CWAO) is ascribed to the diffusion of the gaseous reactant to the catalyst surface, as well as catalyst recovery and leaching phenomena [3]. In order to improve the gas/liquid/solid contact in CWAO, the development of innovative catalytic reactors is desired. The use of catalytic membrane reactors (CMRs), coupling a catalyst and a membrane in the same unit, could be an option. Among the different types of CMRs described in the literature (i.e. extractors, distributors and contactors [4]), the application considered here corresponds to a contactor-type CMR (CMR-C). Within this family, CMR-Cs operated in interfacial mode seem the most appropriate for conducting CWAO processes applied to environmental issues. In this mode, the gas and liquid reactants are introduced separately from the opposite sides of the membrane. The gas/liquid interface is then located within the membrane wall [5]. This configuration favours three-phase contact, leading to abetter accessibility of the reactants to the catalyst zone and in its turn to enhanced conversion rates at relatively mild temperature and pressure conditions [6–8]. Contrary to what is usually observed in other 3-phase reactors (e.g. slurry stirrers and trickle-beds), the gaseous reactant may not be kinetically limiting. This might be attributed not only to lower gas diffusion constraints when conveniently operated [9–12], but also to increased gas solubility in nanoconfined liquids in the vicinity of catalyst nanoparticles, as we have advanced in recent studies [13,14]. Moreover the catalyst being part of the reactor, its

recovery does not require any separation step from the liquid medium. This paper pursues the research activities carried out by our group in the last years in the context of the 'WaterCatox' European project, aimed at the development of catalytic membrane contactors for the WAO of toxic but diluted wastewaters [15–17]. The 'WaterCatox' process is based on multi-layered tubular porous ceramic membranes (usually made of alumina, titania, alumina coated with titania, ziconia or ceria depending on the application [9,18–20]) containing the catalyst nanoparticles in the mesoporous top layer, acting as an interfacial gas/ liquid contactor (seeFig. 1).
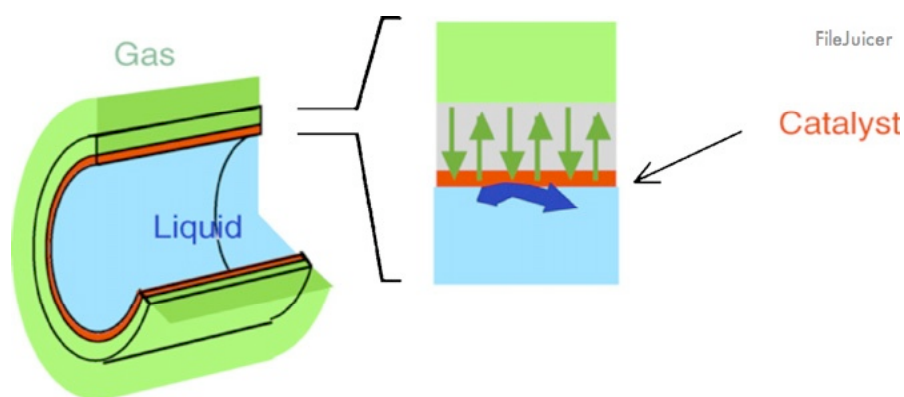
Fig.1. Scheme of a gas–liquid interfacial membrane contactor.

The catalyst is usually dispersed in the mesoporous layer by ionic impregnation or evaporation-crystallization using a convenient precursor (e.g. hexachloroplatinic acid in the case of Pt deposition) [21,22], or by layer-by-layer deposition methods [23], and further activated by reduction under H_2 flow at 473K. Using these methods, Pt nanoparticles up to 1.5 nm in size can be synthesized with loadings in the contactor up to 1.5 wt.% for mean pore sizes lying in the range 5–20 nm [9]. The position of the gas–liquid interface with in the membrane thickness plays a relevant role on the catalytic performance of inter-facial membrane contactors, as has been reported in several studies [24–26]. Higher reaction rates can be achieved by locating this interface as close as possible to the catalytic zone by increasing the transmembrane pressure. This poses obvious problems related to the quality of the supports (need of high bubble points) and wetting taking into account their asymmetric porous structure and coarse grained nature. The first part of this paper is therefore devoted to assess for the specific role of wetting on the CWAO performance of catalytic membranes using formic, acetic and oxalic acids as model pollutants. To this end two different kinds of

wetting protocols have been considered: (1) wetting by capillarity (standard wetting) and (2) wetting "under vacuum" where the solution is forced through the porous volume by the action of primary vacuum. The second part of the paper focuses on the potentials of catalytic membranes under optimized wetting conditions for the CWAO of priority pollutants, with special insight into phenol degradation. A series of mono-and bi/trimetallic catalytic membranes have been prepared relying on noble metals and supports that have already proven their efficiency in the CWAO of carboxylic acids and aromatics [27–31].

2. Experimental

2.1. Materials

The membranes used in this study (o.d.10 mm, i.d.7 mm, length 25 cm) consisted of tubes made of three or four concentric layers (see Fig.2), showing an average pore size decreasing from the outside to the internal surface of the tubes. The top layer was located on top of the inner membrane surface. Both ends of the tubes (ca. 1.5 cm on each side) were enamelled to achieve proper sealing, defining an internal active surface of ca. 50 cm2. The membrane supports were provided by Pall-Exekia (France) and Inocermic (Germany). In the former case, the supports where made of   -Al2O3 covered by TiO2 with a top layer or TiO2 or ZrO2 (thickness, 3–6 m; mean pore size, 20 –50nm), while in the second case they were
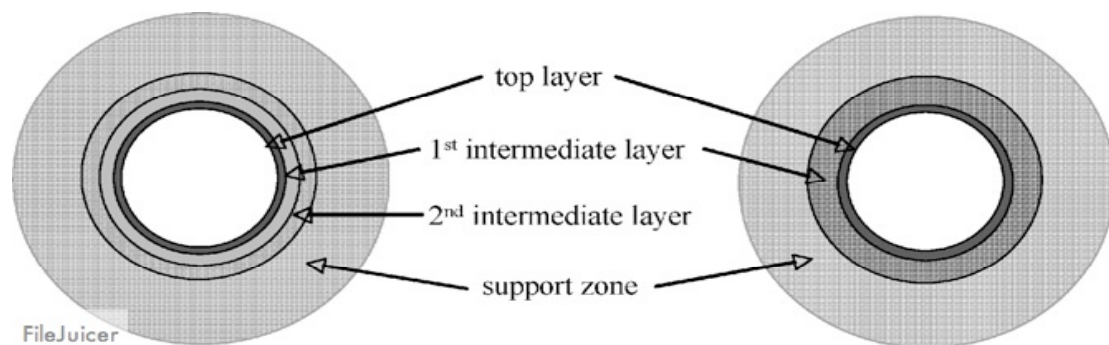
madeofTiO2withaCeO2-dopped ZrO2 top layer (thickness, 8 m; mean pore size, 80 – 100nm). Further details on these membrane supports can be found else where [19,21].

Fig.2. Schematic cross-section of the membrane supports used in this study showing the three-layered (right) and four-layered (left) structure.

The metallic precursors used in the preparation of the catalytic membranes, all supplied by Sigma–Aldrich or Strem, were: (Pt) H2PtCl6 (39.8%Pt), PtCl2(NH3)2 (65.0%Pt) and [Pt(NH3)4](NO3)2 (49.1%Pt); (Pd) PdCl2 (59.8%Pd) and Pd(NO3)2 ·2H2O(40.0% Pd); (Ru) RuCl3 (45–55%Ru) and Ru(NO)(NO3)3 (1.5%Ru); (Cu) Cu(NO3)2 ·3H2O(26.1%Cu); (Zn)

ZnCl2 (14.8%Zn) and Zn(NO3)2 (33.8%Zn);(Ni)NiCl2 ·6H2O(24.6%Ni) and Ni(NO3)2·6H2O (20.1% Ni); (Fe)Fe(NO3)3 ·9H2O (13.8%Fe); and (Co) Co(NO3)2·6H2O(20.0% Co). Formic acid (98–100%, Riedel-de-Haen), acetic acid (99.7%, Sigma–Aldrich), oxalic acid (>99%, Fluka) and phenol (99%, Carlo Erba) were used as model pollutants treated during the catalytic tests. The gases (N2, O2 and air), purity >Air Liquid supplied 99.999%.

2.2. Catalytic membrane preparation

The mono-and bi/trimetallic catalytic membranes were pre- pared using convenient precursors either by impregnation or by evaporation-crystallization following the experimental protocols presented in previous studies [20–22]. The metals were chosen on the basis of reported catalytic activities for the oxidation of either organic acids or phenol. The estimation of the amount of metal deposited within the membrane porosity was based both on weight uptake after deposition and on the amount of precursor solution adsorbed during the soaking step. The results obtained using both methods for monometallic membranes were found to be in good agreement, lying in the range 35–1000 g/ cm2.

2.3. Wetting methods

Prior to the catalyst deposition, the quality of the supports was assessed by gas–liquid displacement (bubble point test) using ethanol as liquid phase and N2 as gas. According to Laplace law, the pressure of the first bubble allows the determination of the largest passing-through pore of the support. The bubble point of the membrane will condition the maximum transmembrane pressure (i.e. gas over pressure) to be applied in the catalytic experiments.
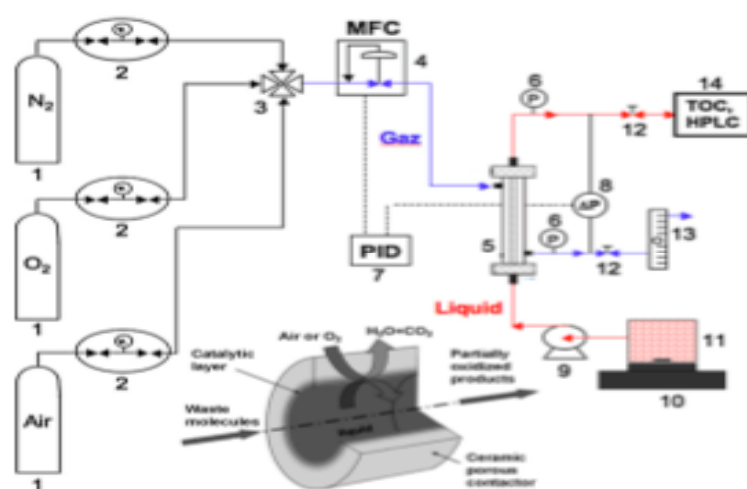
Fig.3. Schematic drawing of amembrane reactor system. Nomenclature: (1) gas cylinder, (2)gas regulator, (3)multi-port valve, (4)mass-flow controller (50mL(STP)/min), (5) membrane module, (6)pressure gauge, (7) temperature regulator(PID), (8) differential pressure gauge, (9) liquid pump, (10) magnetic stirrer and heater, (11) solution reservoir, (12)regulationvalve, (13) bubble meter, (14)TOC and HPLC analyzers.

Consequently, high bubble points, approaching as much as possible to the maximum theoretical value predicted by Laplace law for the top layers (in practice >1.0 bar for pure ethanol), are necessary to avoid the formation of bubbles in the liquid side during operation. Note that, in all cases, the bubble point pressure is much lower than the pressure difference that would be expected for a50-nm pore size top layer (about 58bar). As a consequence, the gas/liquid interface cannot be localized in the mesoporous top layer during operation. However, our aim will be to locate the gas / liquid interface as close as possible to the top layer.

Before the gas–liquid displacement tests, the porous tubes were wetted in pure ethanol to fill the porosity with the liquid. Two different wetting methods were used: (1) normal wetting by capillarity and (2) wetting under dynamic vacuum (here in after referred to as vacuum wetting). The first wetting method consists of a direct ethanol impregnation of the support pores at ambient pressure by capillarity, in a similar way described by ASTM316-86 standard procedure [32]. In the second one, the membranes were placed vertically in a two-ends module and the topside up to a vacuum pressure of about 20 mbar evacuated the gas phase. Ethanol was then introduced in the bottom side of the module and pumped until complete filling of the module.

2.4. CMR setup and CWAO tests

The tubular membranes were mounted in a membrane reactor module using gas-tight o-rings separating the liquid and gas feeds. The gas phase was fed into the shell side, while the liquid phase was introduced into the lumen tube side at atmospheric pressure (seeFig.3).The air overpressure (0–5bar) was monitored and controlled using a differential pressure gauge connected to an electronic regulator, acting on the gas feed through a mass-flow controller (50mL(STP)/min). Pure nitrogen was used to stabilize the transmembrane pressure before switching to air to start the oxidation. The membrane reactor was operated in continuous liquid flow mode at a flow rate in the range 4–5mL/min. The performance of the catalytic membranes was first evaluated in the CWAO of aqueous solutions of formic, acetic and oxalic acids operating at an initial concentration of 5, 6.5 and10 g/L, respectively. Some of the membranes were also tested in the oxidation of a phenol aqueous solution at an initial concentration of 1.7g/L. All the experiments were carried out at room temperature (20–25∘C) and in excess of oxygen. The conversion of the organic compounds was monitored using a Shimadzu TOC5050A total organic carbon analyser and by high-performance liquid chromatography (HPLC, Varian Prostar, UV detector). The reaction rate was expressed as

converted moles of reactant per unit time related to the geometric membrane area, i.e. molm−2s−1, as the membrane area is th e cost-limiting factor of the process. The conversion data were accurate to ±1%.

3. Results

3.1. Effect of membrane wetting on first bubble points

Table 1 lists the main results on the first bubble points in ethanol obtained using both wetting methods (i.e. normal wetting and wetting under vacuum) for the collection of catalytic membranes prepared in this study. As can be seen, wetting plays a key role in the measured bubble points. The bubble points measured after normal wetting show an increasing trend with the wetting time, approaching after 24 h the values obtained using vacuum wetting. At shorter times, however, the difference between both wetting methods is remarkable, the bubble points measured after 1-h normal wetting showing a reduction up to 80% (sample14) compared to the values obtained using wetting under vacuum. The bubble points measured in ethanol using vacuum wetting for the membranes listed in Table 1 show values lying in the range 0.5–4.4bar. These values translate into a range of maximum admissible overpressures of 1.5–14 bar during operation in aqueous solutions (the surface tensions of water and ethanol at 25◦C are 7 2and 22 mN / m,). These pressure limits have been taken explicitly into account for each membrane when carrying out the catalytic tests.

3.2. Effect of membrane wetting on the catalytic activity

Among the membranes listed inTable 1, two of them (i.e. membranes3-Pt/PE and 4-Pd/IN) were chosen to assess for the influence of the wetting method on their catalytic performance.

Activity of these membranes in the CWAO of formic, acetic and Oxalic acids under air has been compared after both normal (2h) And vacuum wetting methods. The results are presented in Table2 and Figs.4 and 5. It is note worthy that despite the low bubble point value of membrane 3-Pt (0.5 bar), the catalytic results indicate that large defects in the membrane donot exert much influence on its catalytic performance. As a matter of fact, no bubbles were observed in the liquid side of the modules during operation for over pressures up to 3 bars. This result is consistent with the extremely low increase observed for the gas flow for pressures higher than the bubble point

Table1 Bubble point pressure (liquid, ethanol; gas, N2) for normal wetting and wetting under dynamic vacuum and main characteristics of catalytic membranes prepared in this study (Dp, TL: mean pore size of the top layer).

Membr.	Metal/supplier		Wetting in EtOH				
	(layers)	(Dp, TL)	Normal				Vacuum
			1h	6h	12h	24h	1h
1	Pt/INC(3)	100a	0.59	-	0.64	0.8	0.8
2	Pt/PE(4)	20a	–	–	1.36	1.7	1.8
3	Pt/PE(3)	50a	–	0.2	–	0.4	0.5
4	Pd/PE(3)	50a	–	0.59	1.64	1.7	1.7
5	Ru/PE(3)	50a	0.25	0.32	1.24	1.5	1.6
6	Cu/PE(3)	50a	–	0.9	1	1.1	1.1
7	Cu/INC(4)	80c	–	1.54	2.3	2	3.7
8	Pt–Pd/INC(4)	80c	–	0.53	1.4	1.7	1.9
9	Pt–Ru/PE(4)	20a	–	–	0.5	4.4	4.4
10	Pt–Ru/PE(3)	50a	0.65	–	0.99	1.2	1.3
11	Pt–Pd–Ru/PE(3)	50a	–	0.74	0.97	1.1	1.2
12	Pd–Ru/PE(3)	50a	–	0.98	1.1	1.2	1.3
13	Cu–Pd/PE(3)	50a	0.28	0.8	1.13	0.9	1.1
14	Cu–Pd/INC(4)	30b	–	0.32	1.2	2.7	1.6
15	Cu–Ni/INC(4)	80c	0.38	0.72	0.47	0.5	0.5
16	Zn–Ni/PE(3)	50a	–	0.27	1	1.1	1.1
17	Fe–Co/PE(3)	50a	0.4	1.34	–	1.3	1.3
18	INC(4)	5b	–	–	–	3.2	3.1

Supports: (PE) PallExekia; (INC) Inocermic. a : ZrO2, b : TiO2, c : CeO2-dopedZrO2.

In the gas–liquid displacement tests (not shown). The catalytic results show that, under Pt and Pd catalysis, the oxidation of oxalic acid is easier than that of formic and acetic acids.

The activity of membrane3-Pt in the oxidation of oxalic acid is 5 times higher than that of acetic acid and 3 times higher than the activity of formic acid. In all cases, complete mineralization was achieved. As can be inferred from Table2, for over pressures $\geq$ 2 bar and, what ever the acid is considered, the conversions and reaction rates achieved in the CWAO of formic, acetic and oxalic acids are remarkably higher (by4–11times) when subjecting the membranes to vacuum wetting prior to the catalytic tests than in the case of normal wetting (see Fig. 5 in the case of acetic acid oxidation). Moreover, the use of pure oxygen instead of air in the CWAO of formic acid under vacuum wetting allows an increase about twice of the catalytic activity of membrane 3-Pt (see Fig. 6).

3.3. Influence of metal loading on the catalytic membrane performance

Fig. 7 shows the evolution of the reaction rate with the gas overpressure in the CWAO of formic acid at room temperature for three catalytic membranes (termed A–C) loaded, respectively, with 37, 50 and 620 g/cm2 of Pt. As can be deduced from Fig. 7, beyond a minimum value, a large increase of the metal loading doesn't apparently promote the membrane activity. For the sake of comparison, please note the similar reaction rates obtained for membranes B and C in formic acid oxidation at 3-bar air overpressure (169 molm−2s−1vs.150 molm−2s−1). For this reason, the reaction rate was calculated as a function of m2 of area of the inner side of tube and not as function of amount of catalyst deposited.

3.4. Phenol oxidation

Three catalytic membranes (4-Pd, 15-Cu-Ni, 17-Fe-Co), all subjected to both normal and vacuum wetting before the catalytic tests, were tested in the room temperature CWAO of phenol. Although a Cu-based membrane (6-Cu) has also been tested for phenol oxidation, the results reveal the absence of long-term stability due to Cu leaching in the presence of phenol solutions. In the former three membranes, the catalytic activity of the membranes is promoted when using vacuum wetting.
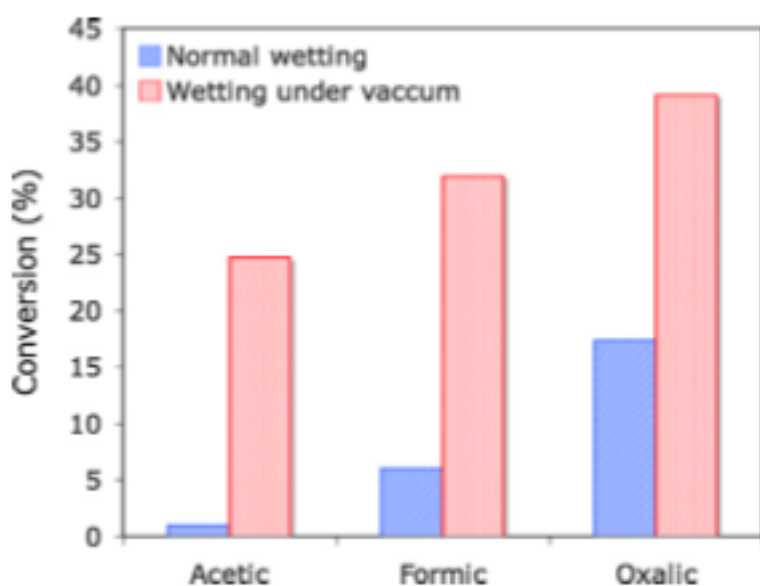
Fig.4. Influence of support wetting on the room temperature CWAO performance of formic, acetic and oxalic acids under air for membrane3-Pt.

Table2 Summary of CWAO results of formic, acetic and oxalic acids under air for membranes 3 (Pt) and 4 (Pd) listed in Table1as a function of the wetting method.

Model acids	Membr.	Normal wetting/wetting under vacuum				
		Conversion, % (reaction rate, $\times 10^{-3}$ mmol m^{-2} s^{-1})^a				
		0.2 bar	1 bar	2 bar	3 bar	4 bar
Formic	3-Pt	1 (20)/2 (40)	4 (74)/8 (146)	6 (108)/11 (197)	7 (121)/32 (588)	–
	4-Pd	3 (60)/7 (144)	4 (78)/8 (164)	4 (71)/9 (170)	2 (40)/14 (282)	4 (85)/26 (523)
Acetic	3-Pt	1 (4)/1 (6)	2 (8)/15 (63)	2 (6)/24 (98)	2 (9)/25 (103)	–
	4-Pd	2 (40)/1 (30)	3 (70)/4 (87)	3 (90)/12 (265)	4 (108)/16 (349)	4 (114)/22 (472)
Oxalic	3-Pt	6 (236)/9 (316)	12 (461)/25 (887)	13 (473)/36 (1253)	18 (633)/38 (1336)	–
	4-Pd	2 (80)/6 (201)	4 (151)/14 (498)	10 (357)/26 (899)	15 (525)/39 (1339)	20 (678)/40 (1398)

Reaction rates computed using the internal membrane surface area.

The effect of wetting is more Remarkable at higher overpressures, the reaction rate at 4-bar air overpressure showing an increase up to 50%. Among the three membranes tested, membranes 4-Pd and 17-Fe–Co provide the highest activities in phenol oxidation, the phenol conversion and reaction rate reaching values up to 30% and 200 molm−2s−1.
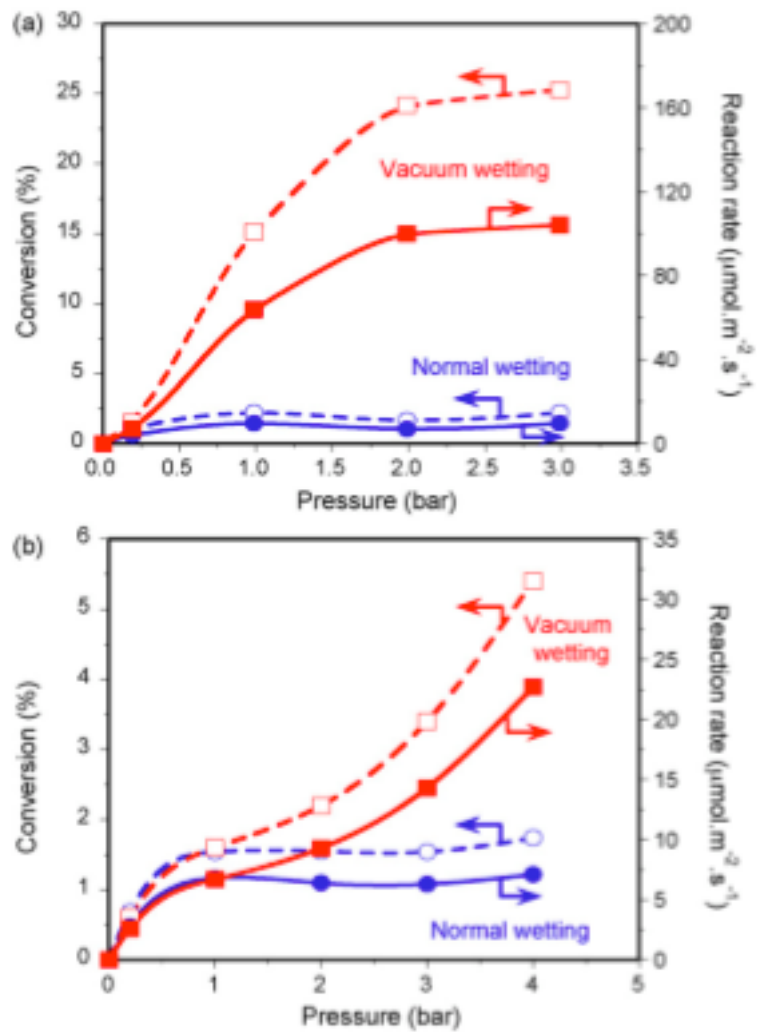
Fig.5. Evolution of the conversion and reaction rate as a function of gas overpressure in the room temperature CWAO of acetic acid under air subjected to normal (2h) and vacuum wetting. On top, membrane3-Pt;onbottom, membrane6-Cu.
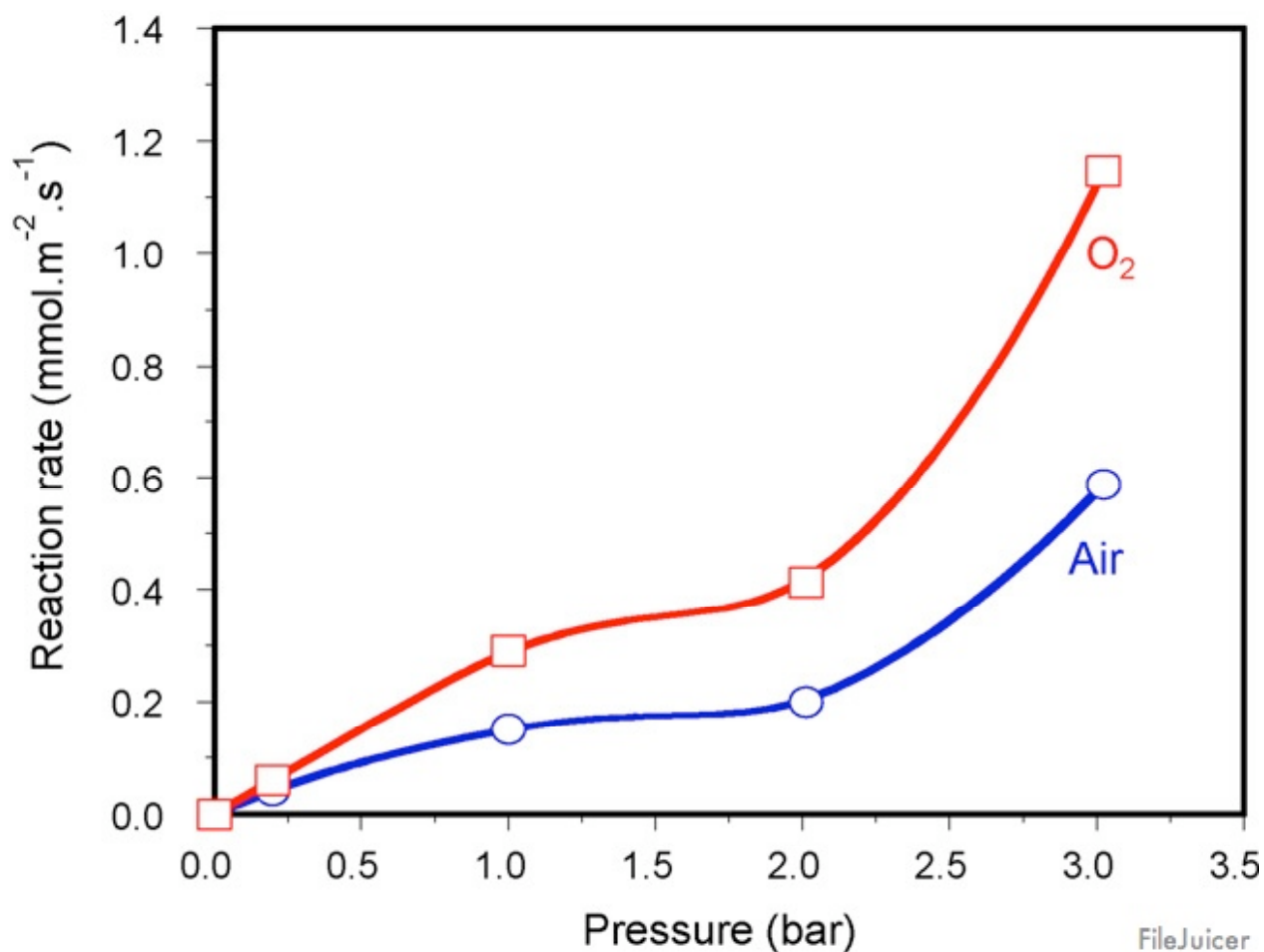
Fig. 6. Reaction rate as a function of gas over pressure in the room temperature CWAO of formic acid under air and pure oxygen for membrane 3-Pt subjected to vacuum wetting.

However, membrane 15-Cu–Ni provides the highest TOC reduction, being practically coincident with the phenol conversion measured by HPLC. Fig. 8 shows the TOC reduction performance of membrane15-Cu–Ni subjected to both normal and vacuum wetting protocols in the room temperature CWAO of phenol. In this case, using vacuum wetting and extremely mild oxidation conditions (room temperature and 4-bar air overpressure), the TOC reduction for this membrane reaches a value ca. 10%. The intermediates formed (not analyzed in detail) are enriched in a variety of small-chain organic acids.

4. Discussion

4.1. Gas/liquid/catalyst triple contact in catalytic membranes as a function of membrane

wetting

As has been stated above, the position of the confined gas/liquid interface near the catalytic zone in the membrane wall plays a crucial role on the final performance of interfacial CMR-Cs. Due to the multi-layered structure of the membranes, the position of the gas/liquid interface is expected to depend strongly on the
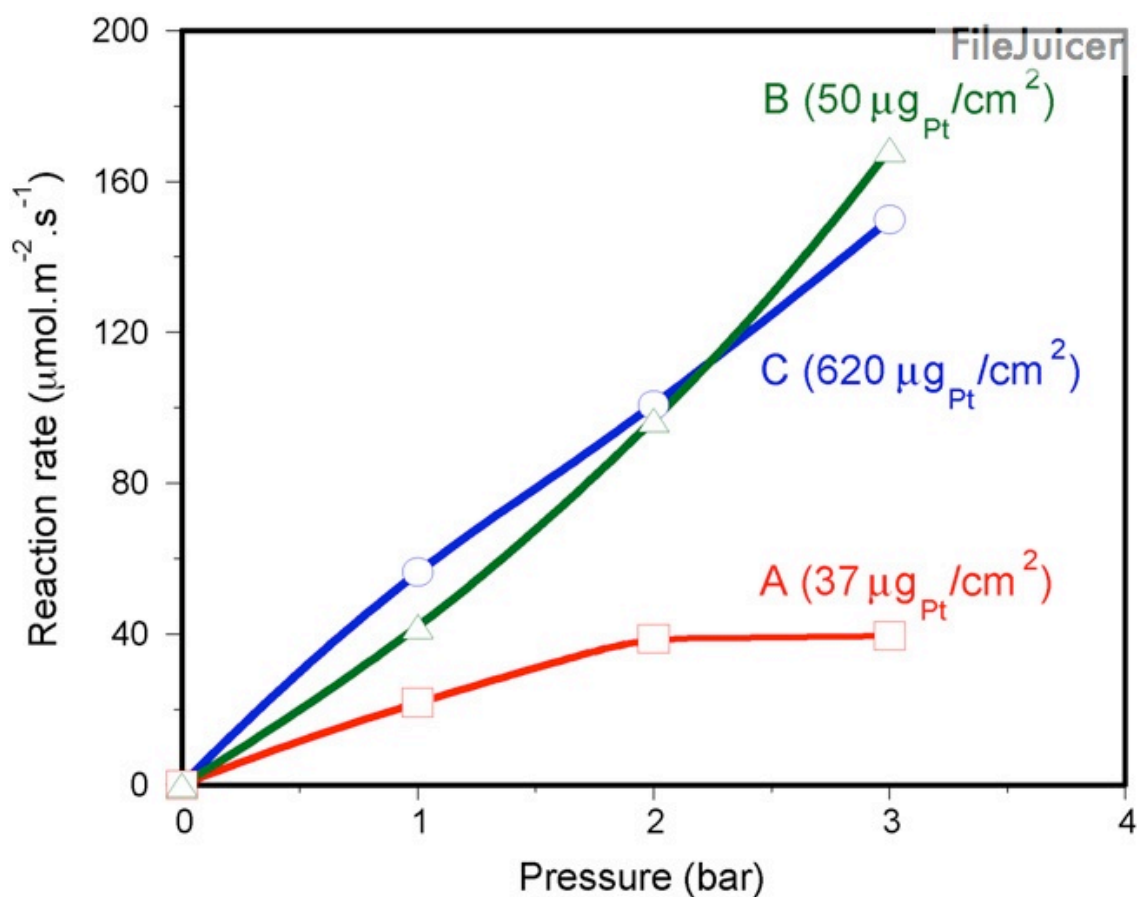
Fig.7. Evolution of the reaction rate as a function of gas over pressure in the room-

Temperature CWAO of formic acid under air using three different Pt-impregnated

Catalytic membranes (three-layered supports, top layer50-nmZrO2) subjected to

Vacuum wetting: (A) 37 gPt/cm3, (B) 50 gPt/cm3 and (C) 620 gPt/cm3   .
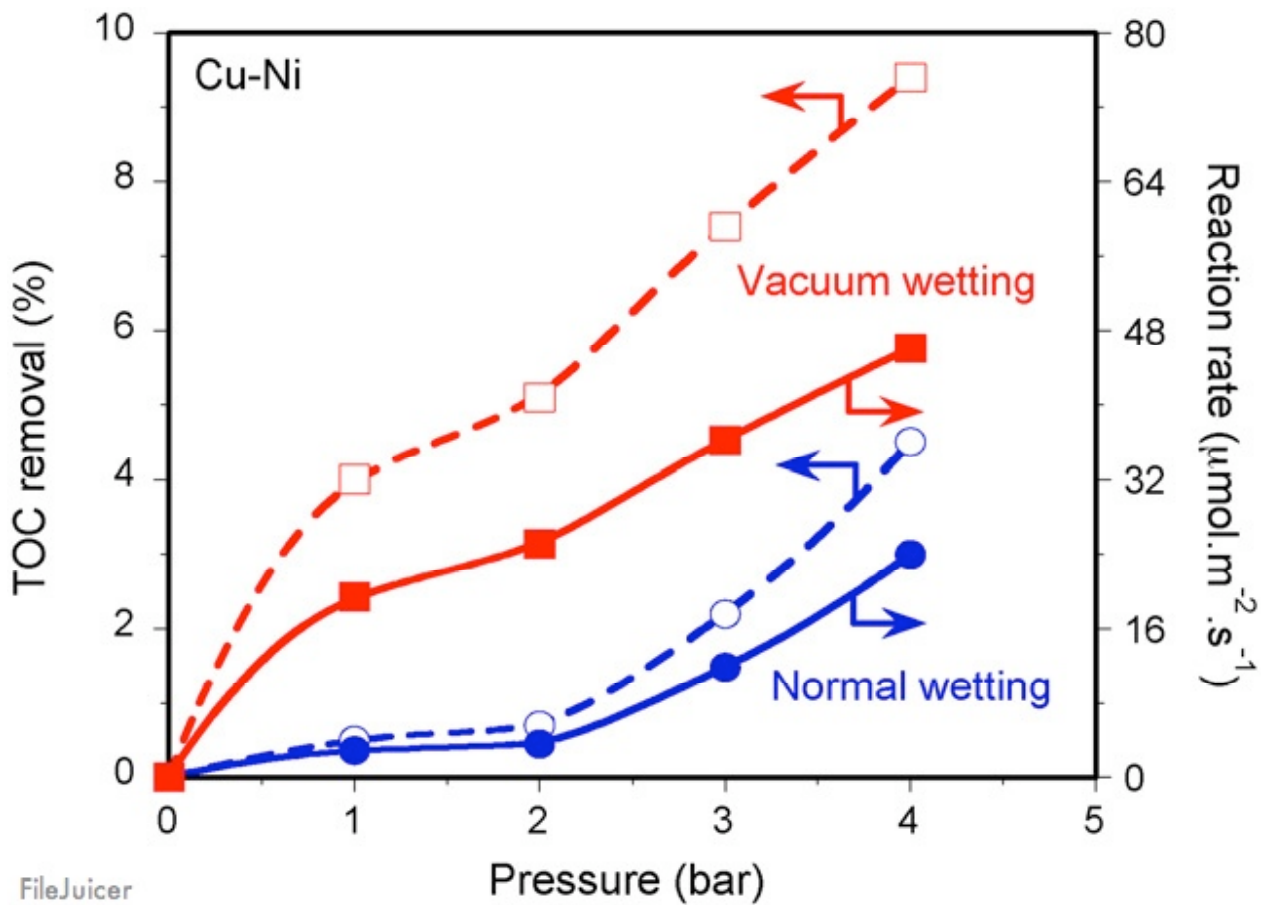
Fig. 8. Evolution of the TOC removal and reaction rate (TOC basis) as a function of gas overpressure in the room temperature CWAO of phenol under air normal (2h) and vacuum wetting for membrane 15-Cu–Ni.

Wetting protocol. As a matter of fact, wetting a membrane at ambient pressure relying on capillary forces (normal wetting) is only expected to provide effective liquid impregnation in the case of large pores (>0.1 m), as in the case of MF membranes.

In contrast, in the case of membranes showing smaller sized pores (<0.1 m) as in the case of the membranes used in this study, this 'normal' wetting protocol seems un suitable. This explains why, in addition to the high pressures involved, gas–liquid displacement is not recommended for the determination of pore size distributions in UF and NF membranes (pore size of top layer <50nm), and only used as a primary intregrity test. In this case, Hg porosimetry is preferred on the basis of the better wetting capacity of Hg [33]. Vacuum wetting allows overcoming the inherent shortcomings ascribed to normal wetting by

removing the air stored in the membrane pores. This forces the liquid to penetrate to the membrane porosity, favouring the 3-phase gas/liquid/catalyst contact in the catalytic experiments. Using vacuum wetting, the catalytic activity is enhanced by a factor of 3–16 in the air-assisted CWAO of aqueous solutions of formic, acetic and oxalic acids at room temperature (see Figs. 4and5). In the case of using oxygen instead of air, under vacuum wetting, the catalytic activity can be promoted by a factor of 2(see Fig. 6).

It is also note worthy that the use of vacuum wetting instead of wetting by capillary has also potential benefits in the synthesis (MFI) and MCM-type membranes, as we have put forward in two recent studies [34,35]. In both cases, the use of static or dynamic vacuum wetting helps improving the penetration of the precursor solution in to the porous network, allowing the synthesis of nanocomposite crystallites rather than thin films on top of asupport.

4.2. Catalyst dispersion in membrane porosity

The experiments performed in the catalytic oxidation of aqueous solutions of formic acid depicted in Fig. 7 reflect that only a small part of the deposited metal (Pt in this case) is active in the reaction. This observations consistent with the conclusions addressed by Vospernik et al. [12] from their experimental and simulation studies on Pt-catalyzed acetic acid oxidation in interfacial membrane contactors. The fact that only a part of the catalyst is active is justified by the catalytic membrane protocols used in the preparation of these membranes (impregnation and evaporation-crystallization), leading to partial metal concentration in the membrane top layer [21]. Un like these classical techniques for catalyst deposition, higher accuracy in the localization of the catalyst in the mesoporous top layer can be achieved through the use of layer-by-layer deposition methods from a suspension of catalyst nanoparticles. The proof of concept of this technique has been recently demonstrated by Bruening and co-workers [23], the membranes showing promis- ing results in the CWAO oxidation of aqueous solutions of formic acid and phenol at mild temperature and pressure conditions. In addition to the benefits of the layer-by-layer technique in terms of catalyst economy, it is worth mentioning that this technique allows the definition of the reaction rate related to the mass of active metal, i.e. mol/(gcats), as the catalyst is well-localized. This allows in its turn a more direct comparison with other reactor configurations.

4.3. Prospects in aromatics oxidation

The results plotted in Fig. 8 indicate that, although the application of interfacial membrane contactors to phenol oxidation is still in an early stage, the results obtained here on Cu–Ni membranes are promising for a prospective application of interfacial CMR-Cs to the CWAO of aromatic compounds under mild temperatures and pressures. As in the case of oxidation of carboxylic acids, the use of proper membrane wetting seems imperative to optimize the capacity of these reactors in the oxidation of aromatics. Moreover, the fact that, using appropriate catalysts, these reactors also show good oxidation performance for acetic and oxalic acids (see

Figs. 4 and 5), usually found as end-of-chain intermediates in the degradation pathway of aromatics, is also outstanding. Our results are especially promising for acetic acid oxidation, usually refractory to CWAO due to catalyst deactivation by the formation of carbonates (see for instance Ref. [36]). The results presented in this study open up interesting perspectives in the conception of multimetallic membrane systems (preferentially bimetallic, based on Pt/Pd and Ru, see for instance Refs. [37–40]) Under optimized catalyst deposition conditions and liquid wetting, for the simultaneous concerted oxidation of aromatics and (intermediate) acids in the same membrane unit.

5. Final remarks

We have shown in this paper that membrane wetting plays a crucial role on the performance of catalytic membrane contactors. Liquid impregnation in the membrane porosity not only affects

The maximum admissible gas overpressures in the contactor to limit bubble formation in the liquid phase, but also conditions the gas/liquid/catalyst contact in the membrane wall and how this contact is governed by gas over pressure. On the basis of the coarse- grained nature of the membranes, vacuum wetting might help removing air blocked in smaller sized pores and cavities, allowing therefore a more accurate control of the position of the confined gas–liquid interface by means of the transmembrane pressure. In all cases, as a consequence, normal wetting lacks of reproducibility. Using optimized metal deposition protocols and wetting conditions, interfacial membrane contactors appear as promising candidates for the oxidation of aromatics at mild temperature and pressure conditions.

Acknowledgements

References

[1] F.J. Zimmermann, Chem. Eng. 25(1958) 117.

[2] F. Luck, Catal. Today 27 (1999) 81.

[3] J. Levec, A. Pintar, Catal. Today 124 (2007) 172.

[4] S. Miachon, J.-A. Dalmon, Top. Catal. 29(2004) 59.

[5] H. Ræder, R. Bredesen, G. Crehan, S. Miachon, J.-A. Dalmon, A. Pintar, J. Levec, E.G. Torp, Sep. Purif. Technol. 32 (2003) 349.

[6] A. Gabelman, S.-T. Hwang, J. Membr. Sci. 159 (1999) 61.

[7] M. Reif, R. Dittmeyer, Catal. Today 82 (2003) 3.

[8] S. Miachon, V. Perez, G. Crehan, E. Torp, H. Ræder, R. Bredesen, J.-A. Dalmon, Catal. Today82(2003)75.

[9] J.Peureux,M.Torres,H.Mozzanega,A.Giroir-Fedler,J.-A.Dalmon,Catal.Today 25(1995)409.

[10] R. Dittmeyer, V. Höllein, K. Daub, J. Mol. Catal. A173(2001)135.

[11] S.Miachon,V.Perez,G.Crehan,E.G.Torp,H.Ræeder,R.Bredesen,J.-A.Dalmon, Catal. Today82(2003)75.

[12] M. Vospernik, A. Pintar, J. Levec, Chem. Eng. Process45(2006)404.

[13] S. Miachon, V.V. Syakaev, A. Rakhmatullin, M. Pera-Titus, S. Caldarelli, J.-A. Dalmon, ChemPhysChem9(2008)78.

[14] M. Pera-Titus, S. Miachon, J.-A. Dalmon, AIChEJ. 55(2009)434.

[15] R. Bredesen, H. Ræder, J.-A. Dalmon, S. Miachon, PatentEP1368278(Europe), 2001.

[16] E.E. Iojoiu, E. Landrivon, H. Ræder, E.G. Torp, S. Miachon, J.-A. Dalmon, Catal. Today118(2006)246.

[17] Watercatoxproject, http://www.sintef.no/watercatox.

[18] E.E. Iojoiu, J.C. Walmsey, H. Ræder, R. Bredesen, S. Miachon, J.-A. Dalmon, Rev. Adv. Mater. Sci. 5(2003)160.

[19] E.E. Iojoiu, S. Miachon, J.-A. Dalmon, Top. Catal. 33(2005)135.

[20] E.E. Iojoiu, J.C. Walmsey, H. Ræder, S. Miachon, J.-A. Dalmon, Catal. Today104 (2005)329.

[21] D. Uzio, S. Miachon, J.-A. Dalmon, Catal. Today82(2003)67.

[22] V. Perez, S. Miachon, J.-A. Dalmon, R. Bredesen, G. Pettersen, H. Ræder, Ch.

Simon, Sep. Purif. Technol. 25(2001)33.

[23] D.M. Dotzauer, A. Abusaloua, S. Miachon, J.-A. Dalmon, M.L. Bruening, Appl. Catal. B:Environ. 91(2009)180.

[24] M. Vospernik, A. Pintar, G. Bercic, J. Levec, Catal. Today79–80(2003)169.

[25] G. Bercic, A. Pintar, J. Levec, Catal. Today105(2005)589.

[26] M. Vospernik, A. Pintar, G. Bercic, J. Levec, J.C. Walmsey, H. Ræder, E.E. Iojoiu, S. Miachon, J.-A. Dalmon, Chem. Eng. Sci. 59(2004)5363.

[27] P. Gallezot, N. Laurain, P. Isnard, Appl. Catal. B:Environ. 9(1996)L1.

[28] N. Perkas, D. PhamMinh, P. Gallezot, A. Gedanken, M. Besson, Appl. Catal. B: Environ. 59(2005)121.

[29] A.Quintanilla,J.A.Casas,J.A.Zazo,A.F.Mohedano,J.J.Rodriguez,Appl.Catal.B: Environ. 62(2006)115.

[30] J. Mikulova, J. BarbierJr., S. Rossignol, D. Mesnard, D. Duprez, C. Kapperstein, J. Catal. 251(2007)172.

[31] C. DiazTaboada, A. Pintar, J. Batista, T. Levec, Appl. Catal. B:Environ. 89(2009) 375.

[32] ASTMStandardF316-03,Standardtestmethodsforporesizecharacteristicsof membranefiltersbybubblepointandmeanflowporetest,ASTMInternational, WestConshohocken, PA, 2003, www.astm.org.

[33] K.Scott,HandbookofIndustrialMembranes,1sted.,ElsevierSciencePublishers Ltd., 1995.

[34] Y. Li, M. Pera-Titus, G. Xiong, W. Yang, E. Landrivon, S. Miachon, J.-A. Dalmon, J. Membr. Sci. 325(2008)973.

[35] B. Hamad, A. Alshebani, M. Pera-Titus, M. Torres, B. Albela, L. Bonneviot, S. Miachon, J.-A. Dalmon, Micropor. Mesopor. Mater. 115(2008)40.

[36] J. Mikulova, S. Rossignol, J. BarbierJr., D. Duprez, C. Kapperstein, Catal. Today 124(2007)185.

[37] L. Oliviero, J. BarbierJr., D. Duprez, H. Wahyu, J.W. Ponton, I.S. Metcalfe, D. Mantzavinos, Appl. Catal. B:Environ. 35(2001)1.

[38] N. Li, C. Descorme, M. Besson, Appl. Catal. B:Environ. 76(2007)92.

[39] P. Massa, F. Ivorra, P. Haure, F. MedinaCabello, R. Fenoglio, Catal. Commun. 8 (2007)424.

[40] A. Pintar, J. Batista, T. Tisler, Appl. Catal. B:Environ. 84(2008)30.

3- 4 Effect of catalyst nature on the membrane catalytic activity.

(to be submitted to Applied Catalysis: B Enviromental *) article in preparation.*

3-4 Bimetallic catalysts for wet air oxidation of model compound solutions in membrane reactors

A. Abusaloua[a], E. Iojoiu[c], K. Fiaty[b], A. Giroir-Fendler*[a]

[1]*Institut de Recherches sur la Catalyse et l'Environnement de Lyon (IRCELYON), UMR 5256 CNRS - Université Claude Bernard Lyon 1,*
2, av. A. Einstein, 69626 Villeurbanne cedex, France

[2] *Laboratoire d'Automatique et de Génie des Procédés (LAGEP), Université de Lyon, 43 Bd du 11 novembre 1918, 69622 Villeurbanne, France*

c: Volvo Power train France (Performance & After treatment),

1 Avenue Henri Germain, 69800 Saint-Priest, France

Abstract

Several aqueous model compound solutions with short chain carboxylic acids, such as formic, acetic, oxalic acids, and phenol were oxidized in a catalytic membrane reactor using tubular ceramic membranes supported by different combinations of monometallic and bimetallic of active phase metal catalysts. Monometallic (Pt, Ru, and Pd), bimetallic (Pt-Ru, Pt-Pd, and Pd-Ru) and trimetallic (Pt-Pd-Ru) membranes were used to oxidize aqueous acid solutions of formic acid, acetic acid or oxalic acid. One monometallic membrane of transition metal (Cu); two monometallic membranes of noble metals (Pt, Pd); one bimetallic membrane (Cu-Pd), several combinations of bimetallic membranes of transition metals (Fe-Co, Cu-Ni, and Zn-Ni) were used to oxidize aqueous solutions of phenol. Oxidation reactions were carried out in catalytic membrane reactors (CMRs) at room temperatures (22-24 °C) and at different gas overpressures ranged from 0.2 to 4bars.

.

Introduction

In an era of increasing economical and environmental strain, conducting chemical transformation with high yield and selectivity in a benign medium is more than ever the priority. Also, growing concern about the environment is making it necessary to develop techniques to treat wastewaters containing compounds that are toxic to aquatic life. In this context, for few decades ago, a number of studies have been devoted to evaluating the economic and environmental feasibility of treatment techniques for the destruction of organic materials in wastewater [1-6, 25]. Wet air oxidation (WAO) process for treating industrial waste in order to meet discharge standards is becoming increasingly popular among environmental engineers. Catalytic wet air oxidation is the further development of wet air

oxidation process using a homogenous [1] or heterogeneous [2-8] catalyst that allows process operation under less severe reaction conditions but being limited by the diffusion of the gas reactant down to the solid catalyst, as well as in catalyst recovery and leaching phenomena. Catalytic wet air oxidation (CWAO) has been demonstrated to be an efficient technology for treating a variety of dilute aqueous streams, the nature of catalyst being crucial for achieving good performances [25].

1.1 Catalyst deactivation in CWAO

The stability and possible catalyst deactivation has a significant impact on the cost of CWAO processes [47]. Catalyst stability is therefore a crucial aspect of many investigations CWAO research area. Catalyst deactivations can occur by several mechanisms as reported by Bartholomew [48]. Hamoudi et al. [49] reported the deactivation due to formation of heavy polymers through in CWAO of aqueous phenol over MnO_2/CeO_2. Santos et al. [50] reported catalyst deactivation due to copper leaching in CWAO of phenol aqueous solution. Barbier et al. [51] have reported that the degradation of acetic acid is decreased due to formation of carbonate species on the catalyst surface, the formation of carbonates being depended on how the support (titanium, zirconium, or ceria) can prevent the formation of carbonates. The authors suggested that when ceria or ceria doped zirconium supports are used, the formation of carbonates is less due to the unique stability of an elevated oxygen transport capacity coupled with the ability to shift easily between reduced and oxidizes states (i.e. Ce^{+3} - Ce^{+4}). Besson et al. [52] have presented a detailed description about deactivation of metal catalysts in CWAO of liquid phase organic reactions. Several research groups have focused their work to develop new catalyst preparation techniques to avoid catalyst deactivation phenomena by metal sintering or aggregation in supported metal catalysis systems. Bimetallic catalysts have been investigated with great interest due to their potential to improve the catalytic activity, selectivity, and stability as well as to reduce the cost of precious metal [26]. Bimetallic catalyst preparation technique that has been presented in several publications [38, 40, 44, 53] is one option to avoid metal sintering or aggregation. Sinfelt is the first one who has introduced the term "bimetallic" [45]. Alloys can form a continuous series of solid solutions (monophasic alloys) or segregate under the critical temperature into two phases (biphasic alloys). Elements of a very limited solubility can still form the "surface alloys". There are a number of studies oriented toward characterization and morphology analysis of bimetallic catalysts. Rousset et al [38] have studied and characterized Pt-Pd bimetallic catalyst clusters in both free and supported phases. They observed a sequential evaporation of Pd atoms in the mixed clusters due to a palladium segregation process. This tendency has been also observed

on supported particles by using high-resolution TEM and EDX analysis. Batista et al [43] have studied bimetallic (Pd-Cu) catalysts with different Pd: Cu atomic ratio (2:1,1:1,1:2) that was prepared by successive impregnation, the bimetallic material being characterized by XRD, EDX, TEM, and EXAFS analysis. It is found that both surface compositions and bulk structure of the bimetallic particles varied with the Pd: Cu atomic ratio, while the size of particles did not change significantly. Pd: Cu with 2:1 atomic ratio exhibited the highest selectivity in a liquid-phase nitrate reduction. Kim et al [42] have studied Pt-Ru bimetallic catalysts prepared by reverse micro emulsions for fuel cell catalysts. The prepared bimetallic Pt-Ru particles have a high electrochemically active surface area and stability. The bimetallic Pt-Ru catalyst prepared by this method has higher activity for reformat gas oxidation. Romanenko et al [35] have studied the influence of ruthenium in addition of sintering of carbon-supported palladium. It was shown that the introduction of ruthenium in the composition of palladium catalysts results in the increase of their sintering stability. Jhung et al [36] have studied bimetallic Pd-Ru supported on activated carbon for hydropurfiction of terphathalic acid. Breen et al [40] have studied Pt-Ru bimetallic catalysts supported on activated carbon for liquid phase hydrogenation of 2-butanone at 30°C and 3 bar. The activity of this bimetallic catalyst was higher than of the sum of the monometallic Pt or Ru catalysts.

1.2 Bimetallic catalysts for WAO

Many research efforts have been recently focused on the use of bimetallic catalysts for CWAO reactions in order to improve catalytic activity of supported metal catalysts. The use of bimetallic catalysts could improve the activity by reducing metal sintering that occurs during preparation or reaction. Fortuny et al [44] have explored the ability of bimetallic (Cu-Co, Co-Fe, Cu-Mn, Cu-Zn) catalysts supported on alumina for WAO of aqueous phenol solutions at 140° C and 9 bars in packed bed reactor operating in trickle flow regime. Lifetime tests were conducted for 8 days, severe deactivation being detected during first two days followed by a constant activity. The catalyst deactivation is related to the dissolution of the metal oxides from the catalyst surface due to the acidic reaction condition. Michaud et al [37] have studied bimetallic catalysts (Pd-Pt) supported on alumina using co impregnation for complete hydrocarbon oxidation. Deffernez [34] has studied several types of bimetallic catalysts (Bi-Pt, Ru-Pd, Pt-Ru) supported on active carbon for the selective oxidation of glyoxal into glyoxalic acid in aqueous phase. Kim et al [39] have studied the bimetallic catalysts (Pd-Pt) supported on alumina for oxidation of real effluents from textile plants (reactive dye solutions) in presence of 1% H_2. Zhang et al [41] have studied the bimetallic catalysts (Pd-Pt) supported on alumina for wet air oxidation of real effluents from paper and pulp mill plants (black liquor). Barbier et al [46] have studied bimetallic Pd-Ru catalyst supported on alumina or ceria /alumina for WAO of aniline or ammonia at 150-250 °C and 20 bar. The greatest interest of CWAO compared to the classical biological one is that the selectivity toward molecular nitrogen is much higher (90%).

Catalytic Membrane Reactors (CMR) was recently suggested [9,10] as a possible alternative to conventional reactors employed in CWAO. According to the suggested classification of the membrane reactors [21], the interfacial contactor mode would be the most adequate for conducting CWAO processes [11]. When operating the CMR as an interfacial contactor, the membrane provides a well-defined contact region between the gas and liquid phases flowing on the opposite sides of the membrane, and serves as a support for the catalytic active phase deposited on its internal structure [12]. The potentials of catalytic membrane reactors are studied in order to gain the productivity of hydrogenation reactions [13,14] or oxidation reactions [15,16].

Previous work in our group was focused on the loading of tubular membranes with a platinum via evaporation-crystallization and anionic impregnation techniques [9, 11] and the subsequent use of these membranes for wet air oxidation of model compound solutions (formic acid) at the laboratory scale [28, 29,30, 31] and some real effluents at pilot scale [32, 33] . In these studies, the positive effect of high trans-membrane pressure (TMP) on the performance of catalytic membrane reactor has been already demonstrated. It was also shown that external and or/ internal mass-transfer resistance considerably influence the membrane reactor performance, the diffusion path of gaseous reactant (i.e., the position of gas liquid interface within the membrane wall) being the most important parameter concerning the optimization of this reactor type for a commercial application [31]. Scrutiny of the past literature reveals that a large number of previous investigations of catalytic wet air oxidation CWAO processes employed simulated wastewaters, which consisted of a single organic compound. Information on catalytic oxidation of the multi-component mixture of organic pollutants is very limited. The real wastes are very rich in component diversity, and therefore quite difficult to be characterized completely. Optimal model systems should be defined in order to reduce complexity, either by mimicking upstream effluents with a mixture of few representative components, or by studying the individual components one by one. Short chain carboxylic acids proved to be good model systems for wet air oxidation applications [19,20].

To investigate further applications of catalytic membrane reactors for CWAO of organic pollutants in the wastewater, the oxidation of formic acid, oxalic acid, acetic acid and phenol was conducted in catalytic membrane reactors. In the present work, the first part was devoted to study wet air oxidation of several model compound solutions (formic acid, acetic acid, oxalic acid, and phenol) in catalytic membrane reactor by using monometallic (Pt, Pd, Ru, and Cu), bimetallic (Pt-Ru, Pd-Ru, and Pt-Pd, Fe-Co, Cu-Ni, Zn-Ni, Cu-Pd) and tri-

metallic (Pt- Ru -Pd) catalytic membranes with a special insight into bimetallic catalytic membrane performance, the active phase metals being selected on the basis of reported catalytic activity for the oxidation of either short chain carboxylic acids or phenol. The second part of this work was devoted to investigate the catalytic membrane stability for leaching of active phase metals supported in tubular ceramic membrane with special insight into the root causes of catalyst deactivation an reactivation.

2. Experimental

2.1 Ceramic membranes

The ceramic membrane supports used in this work have been provided by Pall-Exekia (France) or Inocermic (Germany). All these membranes have tubular geometry (10mm external diameter, 7mm internal one) with a total length 250mm, being consisted from three or four concentric layers showing an average pore size decreasing from external to internal side of the tubular membrane. The final mesoporous top layer, is located in the inner side of the ceramic membranes as shown in figure 1. Both ends of the tubular membranes (ca. 1.5 cm in each side) have been covered with enamel or glaze in order to ensure tight sealing and prevent gas by-pass.

For the membrane provided by Pall-Exekia, the top layer was made from TiO_2 or ZrO_2 (thickness of3-6 μm, mean pore size between 20 and 50 nm) while the subsequent layers were made of α-Al_2O_3 coated with TiO_2. For the membranes provided by Inocermic (Germany), the membrane top layer was made from CeO_2 -doped ZrO_2 (thickness of 8 μm, mean pore size of 30, 80, or 100 nm) while the subsequent layers were made of TiO_2.
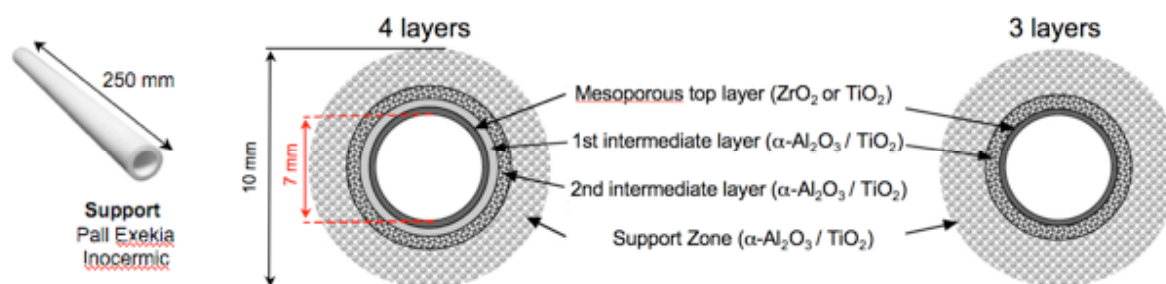
Fig. 1. Schematic cross-section of the membrane showing the three-layer and four-layer structure

2.2 Catalytic membrane preparation

The catalytic layer for each membrane was loaded by soaking impregnation and evaporation- crystallization technique [12, 22, 23] using active phase precursor solutions. The impregnated membranes are shown in (Table 1). The metallic precursors used in the preparation of the catalytic membranes, all supplied by Sigma-Aldrich or Strem, were: H_2PtCl_6 (39.8% Pt), $Pt\ Cl_2\ (NH_3)_2$ (65.0% Pt), $[Pt\ (NH_3)_4](NO_3)_2$ (49.1% Pt), $PdCl_2$ (59.8% Pd), $Pd(NO_3)_2 \cdot 2H_2O$ (40.0% Pd); (Ru) $RuCl_3$ (45-55% Ru), $Ru(NO)(NO_3)_3$ (1.5% Ru), $Cu(NO_3)_2 \cdot 3H_2O$ (26.1% Cu), $ZnCl_2$ (14.8% Zn), $Zn(NO_3)_2$ (33.8% Zn), $NiCl_2 \cdot 6H_2O$ (24.6% Ni), $Ni(NO_3)_2 \cdot 6H_2O$ (20.1% Ni); $Fe(NO_3)_3 \cdot 9H_2O$ (13.8% Fe), $Co(NO_3)_2 \cdot 6H_2O$ (20,0% Co). Formic acid (98-100%, Riedel-de-Haen), acetic acid (99.7%, Sigma-Aldrich), oxalic acid (>99%, Fluka) and phenol (99%, Carlo Erba) were used as model pollutants treated during the catalytic tests. The gases (N_2, O_2 and air) were supplied by Air Liquid with a purity >99.99%.

2.2.1 Monometallic membranes preparation:

Monometallic catalytic membranes with different types of active phase metals, (Pt, Pd, Ru, or Cu), were prepared by soaking impregnation and evaporation-crystallisation method. Before impregnation, all the membrane were dried in air at 120°C for 12 hrs, the membrane were then soaked overnight, in a vertical position, with an active phase precursor solution. A mechanical stirrer (60 rpm) has been used in order to ensure a homogenous contact of the precursor solution with the membrane support. In order to allow the solvent evaporation and uniform distribution of the precursor solution, the membranes were then kept in horizontal position at room temperature under air and rotated (60 rpm). The impregnated membranes have then been dried in nitrogen flow (60 ml/min) at 120°C for 1h (heating rate of 1°C/min.) and calcined at 200°C in nitrogen flow (60 ml/min) for 12 hours (heating rate of 1°C/min.)

The gas flux was then switched to hydrogen for 8 hrs at 200°C, in order to decompose the metal precursor, the metal species introduced within the membrane wall being then reduced to metal nanoparticle (14, 15).

Table 1. Monometallic prepared membranes

Membrane/ Company	Deposited metal
AAB 002-PE	Pt
AAB 018-PE	Pd
AAB 019-INC	Cu
AAB 021-PE	Ru

2 Bimetallic membranes:

Bimetallic catalytic membranes with different combination of active phase metals (Pt with either Pd, or Ru with Pd, or Cu with either Pd or Ni, or Ni with Zn, Fe with Co), all bimetallic membranes were prepared by soaking coimpregnation Evaporation-crystallization method. Soaking co impregnation is the soaking of a membrane support in a solution mixture of two active phase metals precursors; the concentration of the active phase metals was prepared based on fixed atomic ratio. Before impregnation, all the membrane were dried in air at 120°C for 12 hrs, the membrane were then soaked overnight, in a vertical position, with an active phase precursor solution. A mechanical stirrer (60 rpm) has been used in order to assure a more homogenous contact of the precursor solution with a membrane support. In order to allow the solvent evaporation and uniform distribution of the precursor solution, the membranes were then kept in horizontal position at room temperature under air and rotated (60 rpm). The impregnated membranes have then been dried in nitrogen flow (60 ml/min) at 120°C for 1h (heating rate of 1°C/min.) and calcined at 200°C in nitrogen flow (60 ml/min) for 12 hours (heating rate of 1°C/min.) The gas flux was then switched to hydrogen for 8 hrs at 250°C, in order to decompose the metals precursor, metals species introduced within the membrane wall being then reduced to metals nanoparticles (14, 15).

Table 2. Bimetallic & Trimetallic Prepared membranes

Membrane/ Company	Deposited Metals	Atomic ratio (ICP)
AAB 003-PE	Pt-Ru	3Pt: 1Ru
AAB 005-PE	Pt-Pd	2Pt: 1Pd
AAB 014-PE	Ru-Pd	3Ru: 1Pd
AAB 017-PE	Zn-Ni	2Zn: 1Ni
AAB 020-PE	Pt-Pd-Ru	12Pt: 6Pd:1Ru
AAB 023-INC	Cu-Pd	2Cu: 1Pd
AAB 024-INC	Cu-Ni	5Cu: 1Ni
AAB 035-PE	Fe-Co	1Fe: 1Co

2.3 Membranes characterization:

BET (Bruhaur-Emmet-Teller), surface area measurements were performed based on a liquid nitrogen adsoption-desorption (Isotherm) in micrometrics apparatus TRISTAR 3000.

Inducted Coupled Plasma (ICP) analysis was used to check for metal leaching in membrane reactor outlet effluent or check for the concentration of active phase metals in precursor solutions

Membrane reactor Setup and catalytic test

The catalytic performance of prepared membranes were tested in WATERCATOX bench setup which is described in detail elsewhere (24), only a brief description will be given here. The tubular ceramic membrane was mounted in a membrane reactor using a tight seal separating the liquid and gas feeds. To minimize the diffusion resistance within the membrane structure, the gas phase was supplied from the outer (shell) side, while the liquid phase containing the dissolved reactant (model compound solutions) was fed through the membrane channel. The catalyst was deposited primarily on to the membrane filtration top layer (inner tubular membrane surface). The liquid phase was maintained close to atmospheric pressure. The gas overpressure was monitored and carefully controlled using a pressure difference gauge connected to an electronic regulator, acting in the gas feed through the mass flow controller ($50ml_{N2}$/min). The membrane reactor operated in continuous liquid flow mode (close to 5-7 ml/min). The gas overpressure steady state was reached using nitrogen, before switching to air to start the oxidation. The same initial concentrations (0.11 mol/l) were used, for all model compound solutions to obtain the same carbon content. All experiments were carried out at room temperature (22-24°C).

The conversion of organic acid compounds was monitored using a Shimadzu TOC 5050A total organic carbon analyser and/or HPLC analyzer. Residual concentrations of each particular model compound solutions in the reactor effluent were determined by TOC (total organic carbon-shemadzu-5050) analyzer or a HPLC (high performance liquid chromatography), (Varian Prostar with auto sampler model 410), An UV spectrophotometer at λ=220 was employed as the detector (type of the detector PDA 330), pump 230, mobile phase H_2O with H_2SO_4, flow rate of the mobile phase was set to be 0.7 ml/min.

Results and Discussion:

Characterizations:

1. *Determination of specific surface area*:

The standard method for measuring catalyst specific surface areas is based on physical adsorption of a gas on a solid surface. If nitrogen is the adsorbed gas, the amount of nitrogen usually adsorbed at equilibrium at normal boiling point 77 °K (-195.8 °C) is measured over a range of nitrogen pressures below 1 atom. As seen in Table 1, Low BET surface area was obtained, less than 1 m^2/g.

Table 1 BET surface area of different membranes

Membrane	Supplier /layers	BET Surface area (m^2/g)
AAB022-	INC-3	0.5672
AAB024-	INC-4	0.6720
AAB036	PE-3	0.2864

Vospernik et al (28) studied the determination of BET surface area for composite tubular membranes. Nitrogen adsorption-desorption (BET) and mercury penetration techniques were used for measuring the surface area. They reported that the overall internal surface area was very low for membrane contactors, 0.12 m^2/g, with low pore volume 0.1 ml/g (mercury penetration technique) and 0.3 m^2/g (Nitrogen adsorption-desorption BET)

Catalytic membrane reactor performance:

1- Monometallic membranes:

In the oxidation experiments of all membranes with sort chain carboxylic acids, samples were taken at 1.0, 2.0, 3.0, and 4.0 bars to see the effect of TMP on over all activity. In this study, several membranes were used in a different experiments looking at the oxidation of formic, oxalic, acetic acid and phenol. After performing each oxidation experiment with the membrane, they were washed by pure water in dead-end flow mode to clean membrane pores from any condensates, then dried over night at 140°C. The results obtained during the catalytic oxidation of these short chain carboxylic acids over monometallic Pt, Pd, and Ru, membranes are shown in figures 3, 4 and 5.
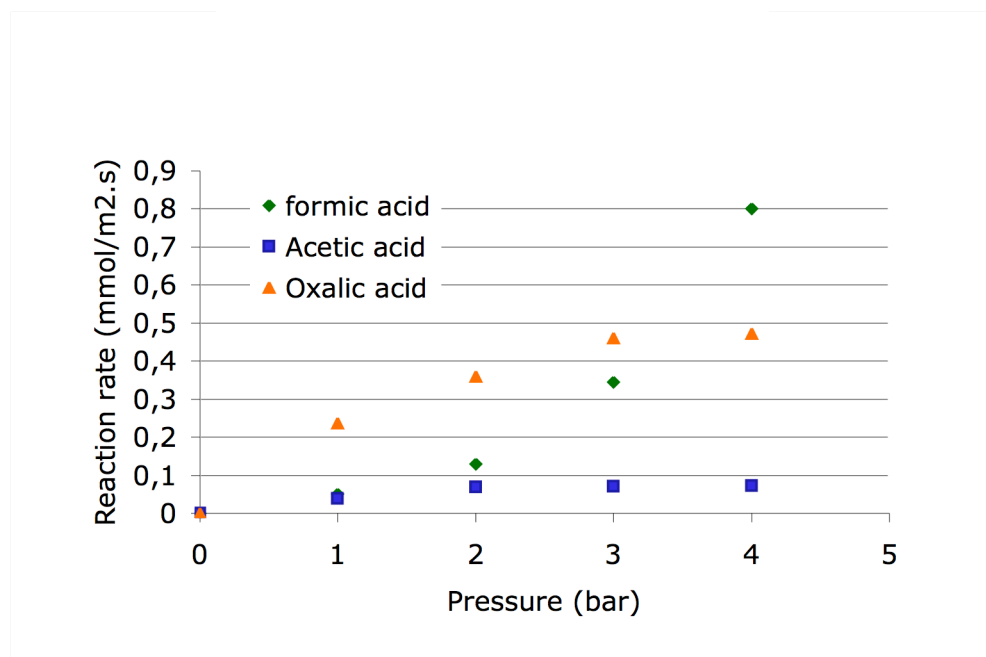
Figure 3. Oxidation reaction rates of different low chain carboxylic acids on Pt-membrane

As can be seen in figure 3, Pt-membrane has different activities in the oxidation reaction rate of acetic acid, formic acid, and oxalic acid. The oxidation rate of oxalic acid on Pt/membrane, increases as the pressure increases, up to 3 bars, then the activity trend like a plateau.
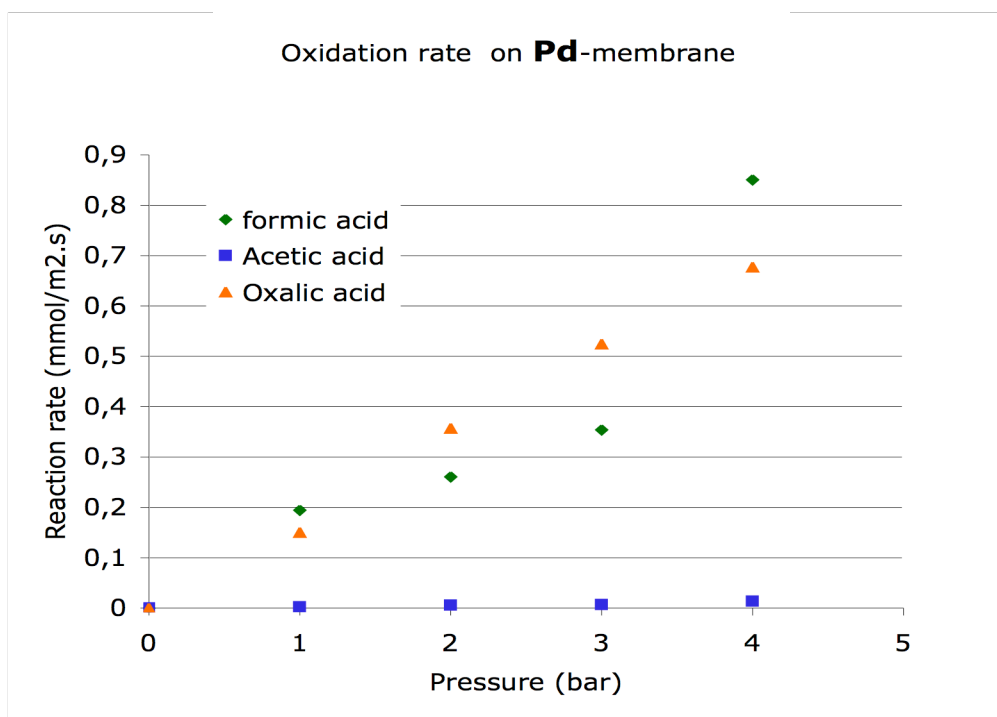
Figure 4. Oxidation reaction rates of different low chain carboxylic acids on Pd-membrane

The oxidation rate of acetic acid, which almost constant after 2 bars, also the lowest activity on Pt membrane was obtained by acetic acid due to calicitrat behaviour of acetic acid. The oxidation rate of formic acid, is rather sharply increases, when the pressure changes from 3 bars to 4 bars, in keeping with the theoretical consideration where the gas-liquid interface moves from one layer to another layer after 3.6 bars, toward the more active zone (top layer).

Figure 4 shows the oxidation rates of oxalic, formic, and acetic acids on Pd-membrane. As can be seen in figure 4, Pd-membrane has higher activity to oxidize oxalic acid than Pt-membrane, but Pd-membrane has lower activity to oxidize acetic acid than Pt-membrane. The oxidation rate of formic acid is almost the same in Pd-membrane and Pt-membrane.
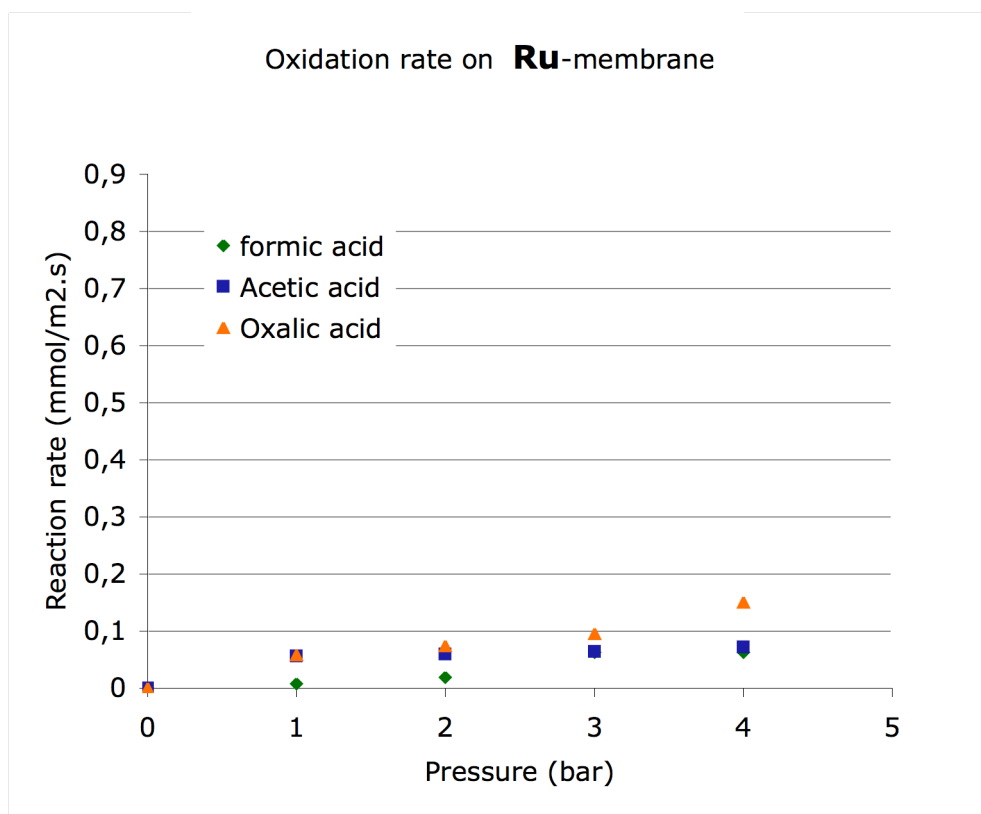
Figure 5. Oxidation reaction rates of different low chain carboxylic acids on Ru-membrane

Figure 5 shows the oxidation rates of oxalic, formic, and acetic acids on Ru-membrane. As can be seen in Ru-membrane has almost the same activity for all acids, which rather low in compared with the activity of Pt-membrane and Pd-membrane.

It is noteworthy that despite the active phase metal loaded in catalytic membrane, oxalic acid is easier to oxidize than formic acid or acetic acid, while acetic acid is the more calcitrat, but when compared our results for acetic acid to that already reported in the

literature, interfacial catalytic membrane reactor is well established an active reaction zone for liquid, gas reactants over the solid catalyst by reducing the mass transfer resistances between phases.

2- Bimetallic or trimetallic membranes:

-Phenol oxidation:

In the oxidation experiments of all membranes with phenol, samples were taken at 1.0, 2.0, 3.0, and 4.0 bars to see the effect of TMP on over all activity. Several bimetallic membranes were used in a different experiments looking at the oxidation of formic, and phenol. After performing each oxidation experiment with the membrane, they were washed by pure water in dead-end flow mode to clean membrane pores from any condensates, then dried over night at 140°C. According to previous work by Iojoiu et al (35), Pt-membrane has a rapid deactivation when used as the catalyst to phenol oxidation, bimetallic transition metals was used for phenol oxidation. The results obtained during the catalytic oxidation of phenol over bimetallic Zn-Ni, Cu-Ni, and Fe-Co membranes are shown in figure 6.
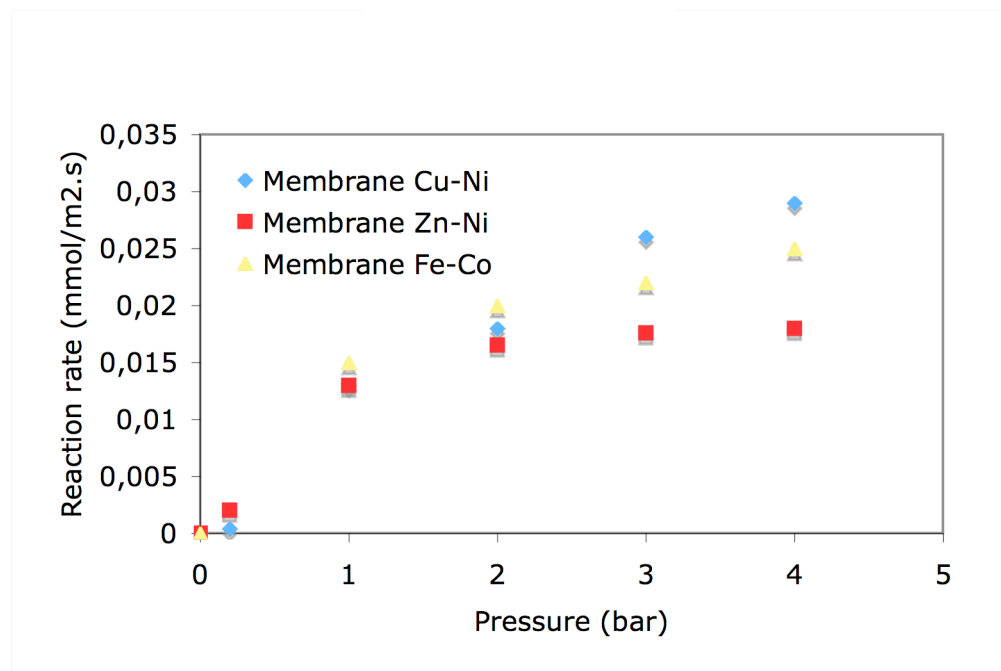
Figure 6. Comparison between phenol oxidation reaction rates on different bimetallic membranes

As seen in figure 6, Cu-Ni bimetallic membrane has a highest activity, Fe-Co bimetallic membrane had activity lower than Cu- Ni bimetallic membrane, and while the Zn-Ni bimetallic membrane had a lowest activity.

-Formic acid:

Bimetallic membranes Pt-Pd, Pt-Ru, and Pd-Ru were tested for formic acid to look for improving the catalytic activity. Figure 7 shows the comparison between oxidation rates of formic acid on different bimetallic membranes.
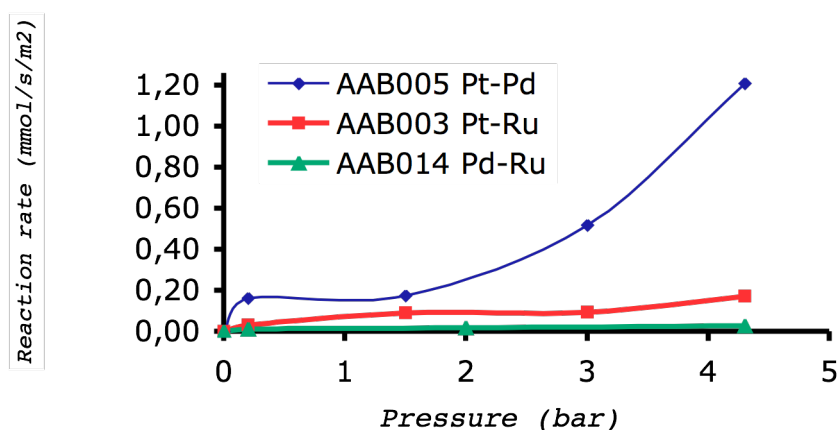
Figure 7- Oxidation reaction rate of formic acid on different bimetallic catalyst

As seen in figure 7, Pt-Pd bimetallic membrane had a highest activity, Pt-Ru bimetallic membrane had a significantly lower activity than Pt-Pd, while the Pd-Ru had a lowest activity, the lowest activity that obtained by Pd-Ru membrane is expected because Pd-Ru catalyst usually used for hydrogenation reactions as reported in the literature (37). The effect of another metal addition in the catalytic activity of formic was studied on all possible combination of Pt, Pd, and Ru. Figure 8 shows the effect of another metal addition on the catalytic activity

.
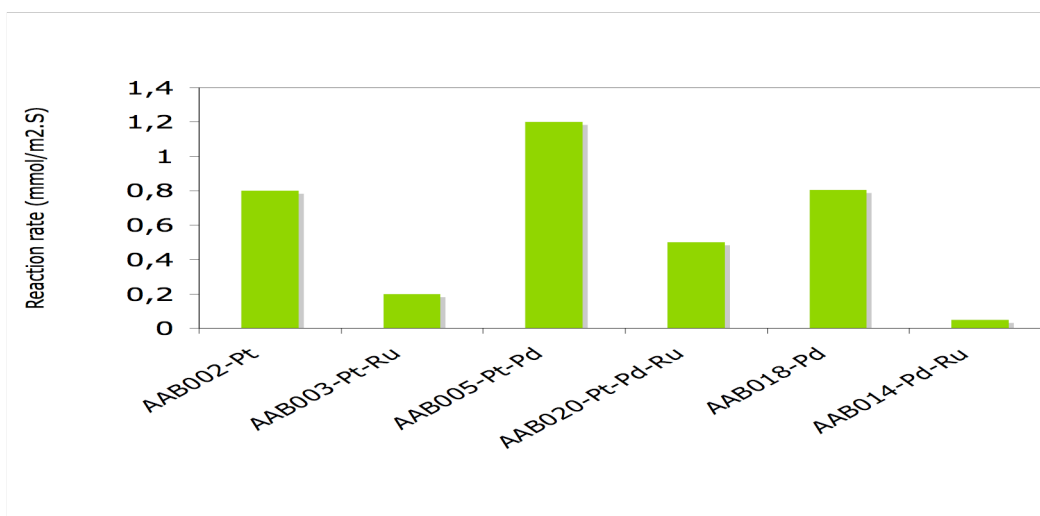
Figures 8 Catalytic activity of formic acid on mono.bi or trimetallic membranes

When looking at the results of these experiments, we see that Pt or Pd membrane activities were decreased by the addition of Ru. Pt membrane activity was increased the addition of Pd, while the activity of Pt-Pd membrane was decreased by the addition of Ru. So to conclude, with platinum and palladium bimetallic system, a synergic effect can be obtained to increase the catalytic performance of the CWAO membrane reactor.

Catalyst deactivation:

Leaching of the active phase metals has been assayed during the experiments under different reaction conditions and different model compound solutions. Due to continuous mode of operation for membrane reactor used, the catalyst leaching has been studied as a function of time on stream. Different model compound solutions have been tested on a number of monometallic or bimetallic catalysts in membrane reactors. Mass rate of metal leaching of several tests have been calculated from the liquid flow rate and a metal concentration in effluent solutions, by using the following equation:

$$F_{Xions} = QL * C_{Xions}$$

Where

F_{Xions}: mass flow rate of metal leaching in (mg metal/min)

QL: Volumetric flow rate effluent solution in (L/min)

C_{Xions}: Concentration of metal leaching in effluent solutions in (mg/L)

The results are shown on the figures 9, 10 and 11 for noble metal leaching with acids.
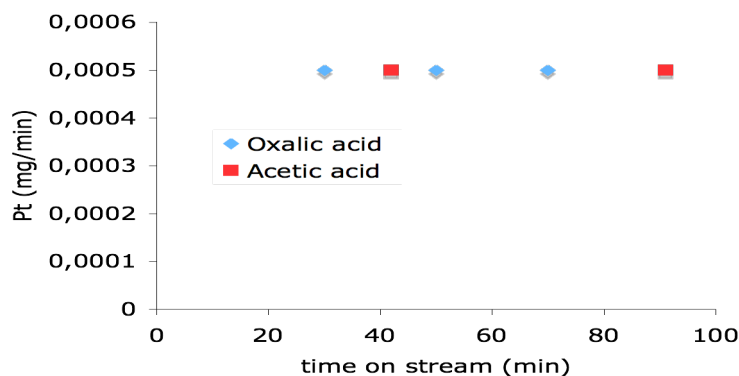
Figure 9 - Metal leaching of Pt-membrane with acids

As shown in figure 9, Pt leaching in the same rate with oxalic acid and acetic acid, but it can be taken into account at the time scale of experiment (typically 300min)
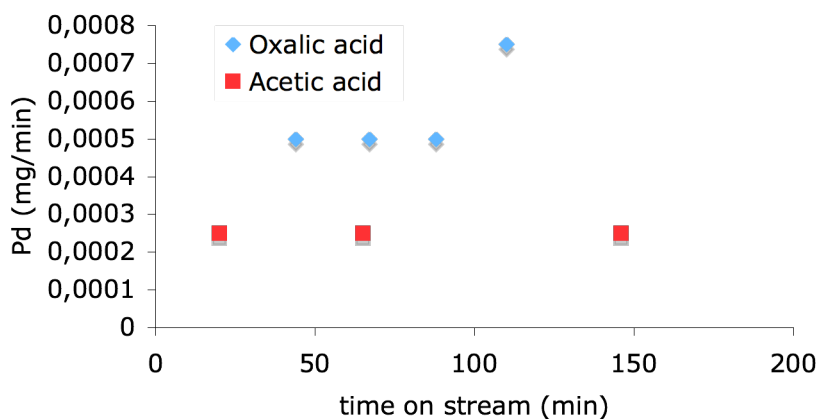
Figure 10 Metal leaching of Pd-membrane with acids

As shown in figure 10, Pd leaching rate is higher with oxalic acid than acetic acid
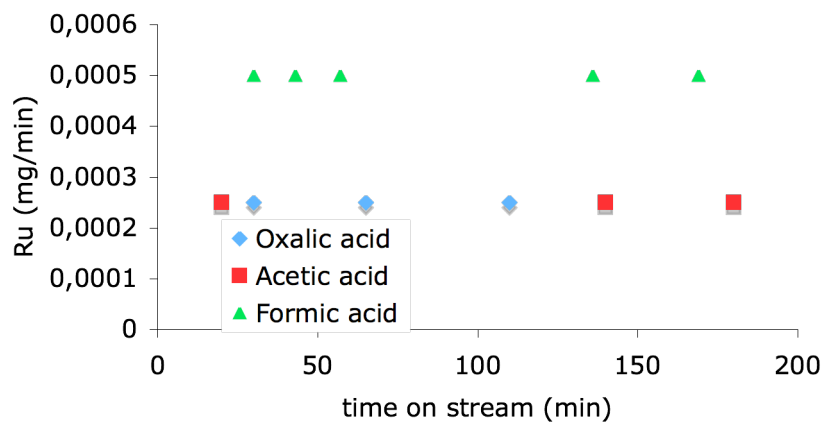
Figure 11 Metal leaching of Ru-membrane with acids

As shown in figure 11, Ru leaching in the same rate with oxalic acid and acetic acid, but it is higher with formic acid.

For bimetallic system exempt of noble metal, the results are shown on the figure 12, 13 and 14 for metal leaching with phenol.

Leaching on Zn-Ni membrane with phenol
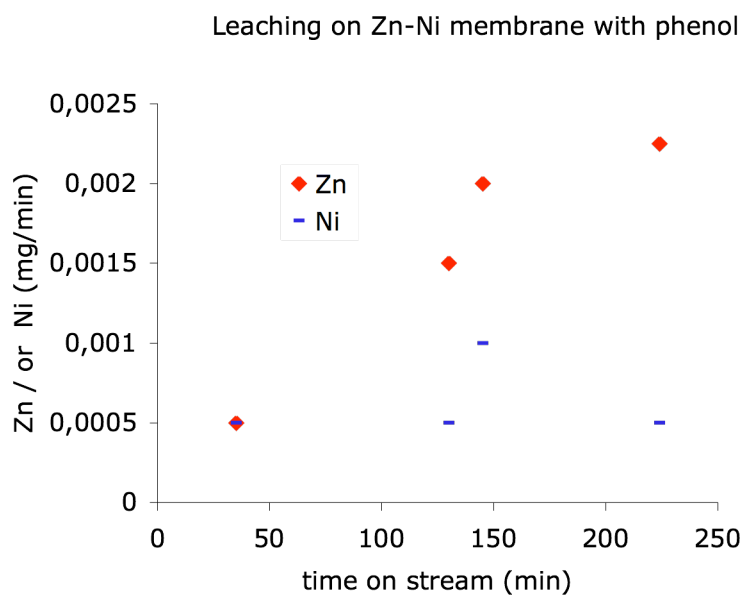
Figure 12 metal leaching of bimetallic Zn-Ni membrane leaching with phenol

Zn leaching rate is higher than nickel leaching rate, especially at higher time on streams.
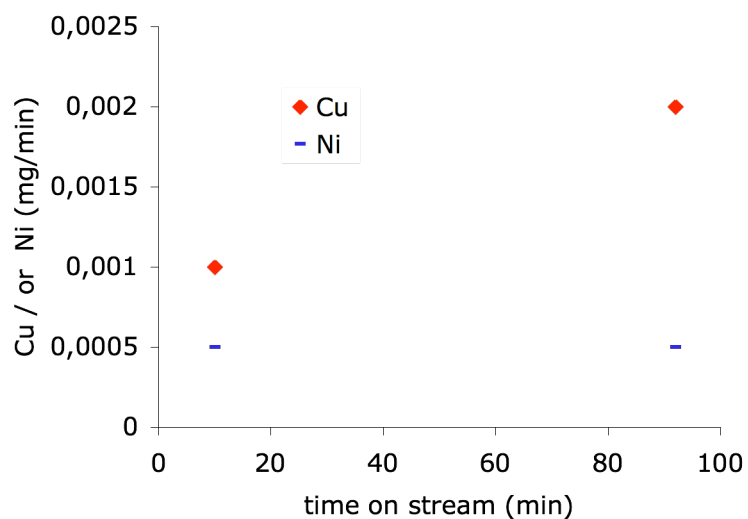
Figure 13 Metal leaching of bimetallic Cu-Ni membrane leaching with p
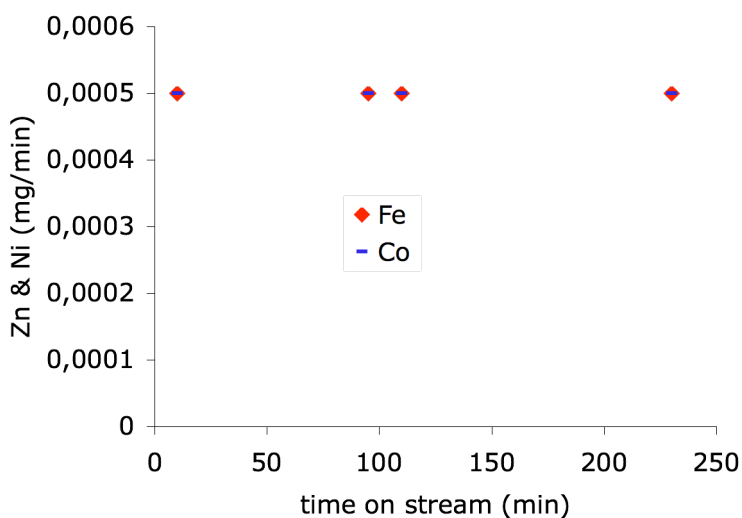
Figure 14 Metal leaching of bimetallic Fe-Co membrane with phenol

At all tos, there is noticeable metal leaching of monometallic or bimetallic transition metal catalysts (Cu, Ni, Zn) with phenol model compound solution, there is no metal leaching of phenol solutions with bimetallic Fe-Co and Cu-Pd but Fe-Co have higher activity for phenol oxidation

Carbonaceous deposit:

Previous studies of WAO with (Pt, Pd, and Ru) catalysts reveal a certain tendency to deactivation by poisoning of the catalyst with carbonaceous deposits formed during the oxidation [37]. Carbonaceous deposit has been noticed during the experiments of acetic acid oxidation with monometallic Pt membrane due to severe deactivation of the catalyst after one run of oxidation experiment in progress towards modifying the pore surface for hydrophobic or selective adsorption processes.

 Conclusion:

At all tos, there is no noticeable metal leaching of all model compound solutions (formic acid, acetic acid, oxalic acid and phenol) with monometallic or bimetallic noble metal

catalysts (Pt, Pd, and Ru). At all tos, there is noticeable metal leaching of monometallic or bimetallic transition metal catalysts (Cu, Ni, Zn) with phenol model compound solution, there is no metal leaching of phenol solutions with bimetallic Fe-Co and Cu-Pd but Fe-Co have higher activity for phenol oxidation.

The treatment of catalytic membrane deactivations that applied in this work can be divided into two ways, the first way in primary stages of membrane preparations before catalytic test by trying to prepare bimetallic catalysts, which recently proved as one way to avoid rapid catalyst deactivation, the second way after catalytic test, and the deactivation has occurred as in oxidation of acetic acid on Pt containing membrane where the formation of carbonaceous species has been observed.

The carbonaceous species that formed due to acetic acid oxidation reaction on Pt containing membrane was treated by soaking the membrane in bleach water (2.6 % liquid chlorine) for a period of 4-6 hrs. The residual washing solution is dark but after a period of time, the black species that already suspended in the residual washing solution start to settle down in the bottom of the beaker up to precipitated completely. The membrane then has washed by pure water in dead end flow mode, and then the membrane has dried under nitrogen at 100°C for 4-6 hrs and reactivated under Hydrogen at 200°C for 4hrs.

References
[1] F. Luck, Catal. Today 53 (1999) 81.
[2] F. Luck, Catal. Today 27 (1996) 195.
[3] D. Duprez, F. Delanoe, J.J. Barbier, P. Isnard, G. Blanchard, Catal. Today 29 (1996) 317.
[4] Y.I. Matatov-Meytal, M. Scheituch, Ind. Eng., Chem. Res. 37 (1998) 309.

[5] S. Imamora, Ind. Eng. Chem. Res. 38 (1999) 1743

[6] J. C. Beziat, M. Besson, P. Gallezot, S. Durecu, J. of Catal. 182 (1999) 129.
[7] A. Pintar, Catal. Today 77 (2003) 451.
[8] F. Larachi, Top. Catal. 33 (2005) 109.
[9] E.E. Iojoiu, J.C. Walmsley, H. Ræder, S. Miachon, J.-A. Dalmon, Catal. Today 104 (2005) 329.
[10] E.E. Iojoiu, S. Miachon, E. Landrivon, J.C. Walmsley, H. Ræder, E.G. Torp, J.-A. Dalmon, Appl. Catal. B 69 (2007) 196.
[11] V. Perez, S. Miachon, J. -A. Dalmon, R. Bredesen Sep. Purif. Technol. 25 (2001) 33.
[12] S. Miachon, V. Perez, G. Crehan, E. Torp, H. Ræder, R. Bredesen, J. A. Dalmon, Catal. Today (2003) 75.
[13] P. Cini, M. P. Harold, AIChE J. 37 (1991) 997.
[14] O. M. Ilinitch, F. P. Cuperus, L. V. Nosova, E. N. Gribov, Catal. Today 56 (2000) 137.
[15] M. Vospernik, A. Pintar, G. Bercic, J. Batista, J. Levec, Chem. Eng. Res. And Des. 82 A5 (2004) 659.
[16] R. Bredesen, H. Ræder, S. Miachon, J. -A. Dalmon, Patent EPI368278 (Europe), 2 May 2001.
[17] R. Dittmeyer, S. Perathoner, M. Rief, Top. Catal. 29 (2004) 3.
[18] Watercatox project, http://www.sintef.no/watercatox.
[19] V. S. Mishra, V. V. Mahajani, J. B. Joshi, Ind. Eng. Chem. Res. 34 (1995) 2.
[20] E.E. Iojoiu, S. Miachon, E. Landrivon, J.C. Walmsley, H. Ræder, E.G. Torp, J.-A. Dalmon, Appl. Catal. B 27 (2000) L217.
[21] V. Perez, S. Miachon, J. -A. Dalmon, R. Bredesen Sep. Purif. Technol. 25 (2001) 33.
[22] E.E. Iojoiu, S. Miachon, J.-A. Dalmon, Top. Catal. 33 (2005) 135
[23] D. Uzio, S. Miachon, J.-A. Dalmon, Catal. Today 82 (2003) 67.

[24] M. Vospernik, A. Pintar, G. Bercic, J. Batista, J. Levec, J. of Memb. Sci. 203 (2003) 157-169.

[25] Mishra, V. S., Mahajani, V. V., Joshi, J. B., Ind. Eng. Chem. Res. 34 (1995) 2-48.

[26] Kim, T., Kobayashi, K., Nagai, M., J. Oleo Sci. 56. (10) (2007) 553-562.

[27] E.E. Iojoiu, J.C. Walmsley, H. Ræder, S. Miachon, J. A. Dalmon, Catal. Today 104 (2005) 329.

[28] V. Perez, S. Miachon, J.-A. Dalmon, R. Bredesen Sep. Purif. Technol. 25 (2001) 33.

[29] S. Miachon, V. Perez, G. Crehan, E. Torp, H. Ræder, R. Bredesen, J. A. Dalmon, Catal. Today (2003) 75.

[30] M. Vospernik, A. Pintar, G. Bercic, J. Batista, J. Levec, J. of Memb. Sci. 203 (2003) 157-169.

[31] M. Vospernik, A. Pintar, G. Bercic, J. Batista, J. Levec, J.C. Walmsley, H. Ræder, E.E. Iojoiu,

   S. Miachon, J. A. Dalmon, Chem. Eng Sci. 59 (2004) 5363-5372.

[32] E.E. Iojoiu, E. Landrivon, H. Ræder, E.G. Torp, S. Miachon, J. A. Dalmon, Catal. Today (2006) 196.

[33] E.E. Iojoiu, S. Miachon, E. Landrivon, J.C. Walmsley, H. Ræder, E.G. Torp, J. A. Dalmon, Appl. Catal.
   B 69 (2007) 196.

[34] Deffernez. A, Hermans. S, Devillers. M, Applied Catalyses A: General, 282 (2005) 303-313

[35] Romanenko. A, Tyschishin. E, Moroz. E, Likholobov. V, Zaikovskii. V, Jhung. S, Park. Y, Applied Catalysis A: General 227 (2002) 117- 123

[36] Jhung. S, Romanenko. A, Lee. E, Park. Y, Moroz. E, Likholobov. V, Applied Catalysis A: General 225 (2002) 131- 139.

[37] Micheaud. C, Marécot. P, Guérin. M, Barbier. J, , Applied Catalysis A: General 171 (1998) 229- 239

[38] Rosset. J, Cadrot. A, Aires. F, Renouprez. A, Mélinon. P, Perez. A, Pellarin. M, Vialle. J, Broyer. M, Study of bimetallic Pd-Pt clusters in both free and supported phases, J. Chem. Phys. 102 (21), 1 june 1995

[39] Kim. S, Park. H, Lee. D, Catalysis Today 87 (2003) 51-57.

[40] Breen. J, Burch. R, Griffin. K, Hardacre. C, Hayes. M, Huang. X, O'Brien. S, Journal of Catalysis 236 (2005) 270-281.

[41] Zhang. Q, Chuang. K, Journal of Catalysis 17 (1998) 322-332.

[42] Kim. T, Kobyashi. K, Nagai. M, J. Oleo. Sci. 56 (10) (2007) 553-562.

[43] Batista. J, Pintar. A, Gomilsek. J, Kodre. A, Bornette. F, Applied Catalysis A: General 217 (2001) 55- 68.

[44] A. Fortuny, C. Bengoa. J. Font, A. Fabregat, B 64 (1999) 181-193.

[45] Ponec. V, Alloy catalysts the concept, Applied Catalysis A: General 222 (2001) 31- 45.

[46] Barbier, J., Jr; Oliviero, L.; Renard, B.; Duprez, D. *Catal. Today* **2002**, *75*, 29-34.

[47] Bhargava. S. Tradio. J, Prasad. J, Foger. K, Acolekar. D, Grocott. S, *Ind. Eng. Chem. Res. 45* (**2007**) 1221–1258.

[48] Barthholomew. C, Applied Catalysis A: General 222 (2001) 31- 45

[49] Hamoudi. S, Belkacemi. K, Larachi. F, *Chem. Eng. Sci.* (*4* (**1999**), 3569-3576

[50] Santos, A.; Yustos, P.; Quintanilla, A.; Ruiz, G.; Garcıa-Ochoa, F, *Appl. Catal, B* **2005**, *61* (3-4), 323- 333.

[51] Barbier. J, Journal of Catalysis 251 (2007) 172-181.

[52] Besson, M, Gallezot, P. *Catal. Today* **2003**, *81* (4), 547-559.

[53] Perego. C, Villa. P, Catalysis Today 1997 (1997) 281-305

4   MODELLING OF CATALYTIC MEMBRANE REACTOR

MODELLING OF CATALYTIC MEMBRANE REACTOR

4.1 Overview in membrane reactor modelling and kinetics law in catalytic membrane reactor (CMR)

Reactor engineering in the current practice requires more and more hydrodynamic and kinetic modelling of different reactor types and different reaction systems [1].

Computational modelling is now generally accepted as essential procedures for the dynamic analysis of the chemical processes

There has been a significant amount of modelling work done with membrane reactors in gas phase applications [2, 3, 4, and 5].

Models of three-phase catalytic membrane reactor (CMR) have already been developed in several previous studies of Cini et al [6], Torres et al. [7], Vospernik et al [8] Becker et al [9], and Warna et al [22].

The model of system we study was obtained by coupling the catalytic reaction kinetics and membrane reactor hydrodynamics. Under particular considerations by optimizing the operating conditions and the catalytic test time as a function of the whole catalytic test time period to obtain low conversions where the membrane reactor can be considered as a differential reactor to conducting the kinetic studies from kinetic rate equation and hydrodynamics parameters

Catalytic membrane reactor (CMR), that combine separation and reaction in the single unit, are widely studied by chemical engineers, and catalyst and material and scientists because of their potential in either selectivity or conversion enhancement for several chemical reactions. CMR is a special type from coated wall reactor or empty reactor tubes, Catalytic membrane contactor have often been recommended to eliminate mass transfer resistance due to their good hydrodynamics and transport characteristics.

There are some restrictions in the analysis of kinetic data obtained from systems employing heterogeneous catalysts is that of elucidating the influence of diffusion and mass transfer processes on the observed reaction rate, in other words, to optimize the process (reactor operating conditions and reaction kinetics) to ward kinetically dominant regime.

It is important to develop kinetics and reactor models for wet air oxidation in a membrane reactor based on the new kinetics models on the catalytic ceramic membranes and a comprehensive numerical model. Recently, due to increase of the wide spread applications of membrane reactors, several analyses of kinetic data that obtained from reaction kinetics conducted in membrane reactors have been reported (32).The primary efforts that has been made in conducting kinetic studies in reactor types that totally different from batch reactors made by Katz (23) in 1959. They have studied chemical reactions catalysed in tube wall reactors (the catalyst was located on the walls of tubular reactor). Also they have presented procedures for mathematically transforming an observed axial profile of cross-section average reactant concentration vs. the wall concentration at which the reaction is proceeding.

Weisz et al (24) have studied the behaviour of porous catalyst particles in view of internal mass and heat diffusion effects. They have presented the criteria for assessment of the reaction processes is kinetically dominant or diffusionally dominant for several reaction systems case studies. This paper can be considered as one of the most important papers in assessment of reaction systems is in kinetically controlling regime or in diffusion controlling regime.

Berger et al (1) have studied the catalysed wall reactors (CWR) with special insight to empty reactor tubes (ERT) type, which can be considered as special case to membrane reactors. They have recommended to Study reaction kinetics in the laboratory reactor itself which will be used for particular studying applications,. For studying and developing such reactors properly, it is very important to characterize on activity and selectivity in order to characterize the rector performance. However, in most cases, it is hardly possible to characterize catalytically coating outside the CWR, e.g., by crushing the tube in small pieces and testing these in a conventional reactor. Such a treatment may cause irreversible changes to the catalyst properties. Therefore, the characterization of the catalyst is, by preference, performed in the configuration in which it is prepared.

Cini et al (6) have studied the kinetics of ethyl benzene hydrogenation in tubular supported ceramic membrane; they have reported that the tubular-supported catalyst could operate without transport limitations at lower temperatures. This invites the possibility of exploiting the data for intrinsic kinetic analysis of multi-phase reactions.

Sabate et al (25) have conducted a kinetic study on Tio2 membrane supported on glass for the degradation of 3 Chlorosalicyclic acids. They have tested LHHW model to fit the obtained data by verifying the effect of mass transfer process in the observed reaction rates.

Saracco et al (4) have applied the concept of transition from the kinetics- to the transport-controlled regime to extract the kinetic parameters for catalytic combustion of propane in a membrane reactor with separate feed of reactants.

Larsoon et al (26) have applied a transient approach to a system deactivating due to the coke formation, in order to determine the kinetics for the main reaction. By separating the deactivation from the main reaction kinetics, it was possible to obtain kinetic parameters.

Elnashaie et al (27) have presented a procedure for linking kinetic modelling of catalytic reactions to reactor modelling for different configurations and they have applied these procedures to catalytic dehydrogenation of ethyl benzene to styrene from laboratory data to industrial units.

Baldi et al (28) have studied formic acid oxidation in a CSTR flow reactor over a commercial Cu-O-Zn-O catalyst. They have tested simple power law model to fit the experimental data. Rate measurements and data analysis suggest that the reaction to be first order with respect to both dissolved oxygen and formic acid concentration.

Claudel et al (29) have studied formic acid oxidation in fixed bed reactor over palladium catalysts. They have tested LHHW model to fit the experimental data. Good agreement is obtained between LHHW model and experimental data.

Harmsen et al (30) have studied the oxidation of formic acid on carbon supported platinum catalyst in a continuous flow stirred slurry reactor. They have tested simple power law model to fit the experimental data. The parameter estimation of the reaction rate variables suggest that the reaction is first order with respect to formic acid concentration and half order with respect to dissolved oxygen concentration

In our case we choose to study the catalytic wet air oxidation (CWAO) of formic acid in CMR.

4.2 Development of reactor model:

Many of chemical engineering processes are distributed parameter systems, i.e., systems of which state variables depend on several independent variables (such as time and space) and which are described by sets of nonlinear partial differential equations (PDEs). Under experimental conditions used in this work, fick's law is sufficient to describe the diffusion. The general continuity equation that represents the mass balances equation is given by:

$$\frac{\partial C_i}{\partial t} + \nabla.J_i - R_i^v = 0 \tag{20}$$

Where,

C_i: is the local concentration of component i

J_i: total flux of component i

R_i^y: Algebraic rate of generation of component i due chemical reaction

For the description of our catalytic membrane reactor model with separate feed reactants, we will consider four zones as depicted in figure 36: liquid side, membrane, support, and gas side.

The resolution of the mathematical model in general form is very complicated, we will consider fundamental hypothesis based on our experiment physical situations in order to simplify the model.
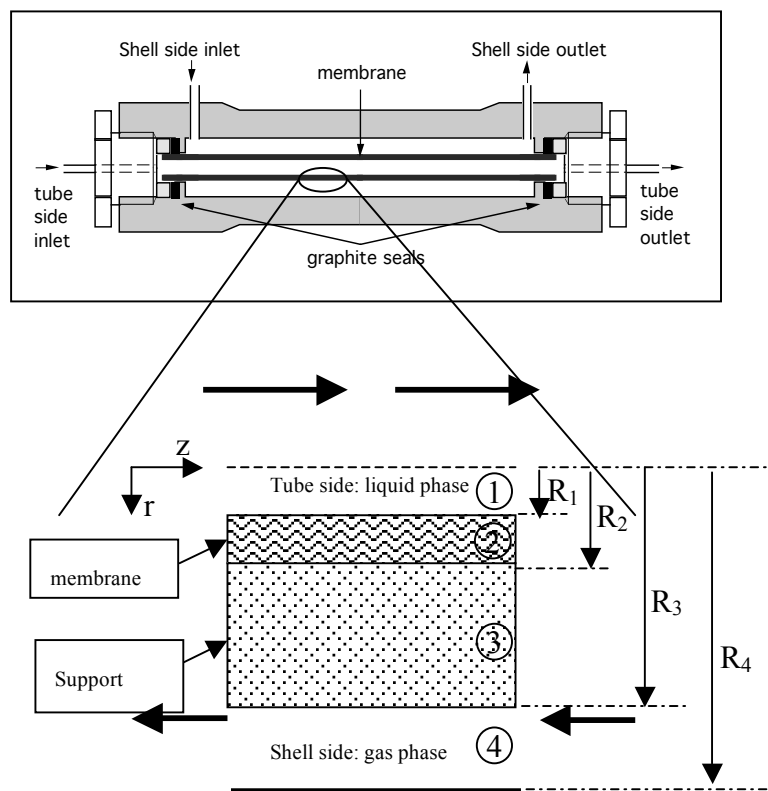
Figure 37 the axial cross-section of membrane reactor system

The following assumptions are made

. an irreversible reaction taken place within the porous membrane

$$CHOOH + 1/2\ O_2 \xrightarrow{\text{Pt/ceramic membrane}} CO_2 + H_2O$$
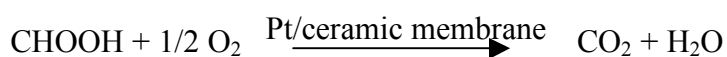
. isothermal conditions.

. constant physical properties

. membrane porous filled with liquid by capillarity

. Henry's law is applied in gas-liquid interface inside the membrane wall

. uniform porosity and tortuosity

. the chemical reaction occurs only on the membrane wall

Figure 37 shows the concentration profiles for formic acid and oxygen through the porous membrane.
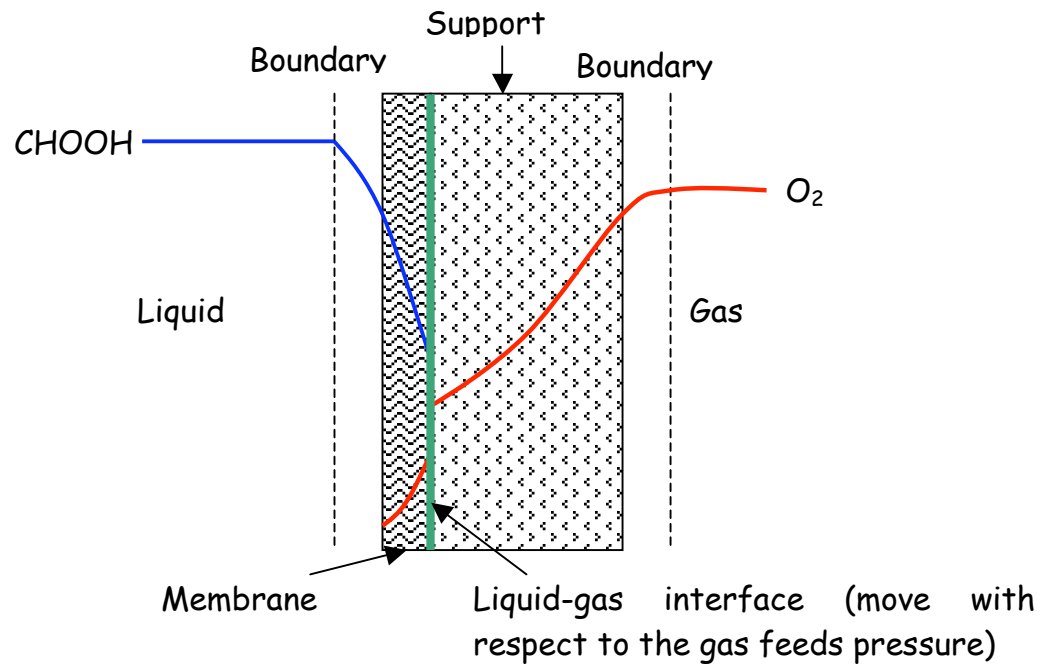
Figure 38: Concentration profiles for formic acid and oxygen through the porous membrane.

Taking into account the previous assumptions, the non-steady state differential equations obtained from mass balances for the reactants inside our system are:

• *in liquid side:*

$$\frac{\partial C_A^{(1)}}{\partial t} = D_A^{(1)} \frac{\partial^2 C_A^{(1)}}{\partial z^2} - u_1 \frac{\partial C_A^{(1)}}{\partial z} + \frac{2}{R_1} D_{e,A}^{(2)} \frac{\partial C_A^{(2)}}{\partial r}\bigg|_{r=R_1^+} \tag{21}$$

• *in membrane:*

The mass balance equation for formic acid (A) and oxygen (B) are:

$$\frac{\partial C_i^{(2)}}{\partial t} = D_{e,i}^{(2)} \left(\frac{\partial^2 C_i^{(2)}}{\partial r^2} + \frac{1}{r} \frac{\partial C_i^{(2)}}{\partial r} \right) + R_i^v \quad \text{with } i = A, B \tag{22}$$

• *in support:*

Only oxygen flows through this layer, its equation is:

$$\frac{\partial P_B^{(3)}}{\partial t} = D_{e,B}^{(3)} \left(\frac{\partial^2 P_B^{(3)}}{\partial r^2} + \frac{1}{r} \frac{\partial P_B^{(3)}}{\partial r} \right) \tag{23}$$

• in gas side:

The gas is fed in counter current configuration. Therefore the mass balance of oxygen is:

$$\frac{\partial P_B^{(4)}}{\partial t} = u_4 \frac{\partial P_B^{(4)}}{\partial z} - D_B^{(4)} \frac{\partial^2 P_B^{(4)}}{\partial z^2} - \frac{2R_3}{R_4^2 - R_3^2} D_{e,B}^{(3)} \frac{\partial P_B^{(3)}}{\partial r}\bigg|_{r=R_3^-} \tag{24}$$

All the previous equations are subjects to the following initial and boundary conditions:

• at t = 0,

$$C_A^{(1)} = C_{A0}, \ P_B^{(4)} = P_{B0}, \ C_i^{(2)} = 0 \ \text{for i = A, B and} \ P_B^{(3)} = 0 \tag{25}$$

• at z = 0,

$$u_1 C_{A0}\big|_{z=0^-} = u_1 C_A - D_A^{(1)} \frac{\partial C_A^{(1)}}{\partial z}\bigg|_{z=0^+} \tag{26}$$

$$\frac{\partial P_B^{(4)}}{\partial z}\bigg|_{z=0} = 0 \tag{27}$$

• at z = L,

$$\frac{\partial C_A^{(1)}}{\partial z}\bigg|_{z=L} = 0 \tag{28}$$

$$u_4 P_{B0}\big|_{z=L^+} = u_4 P_B^{(4)} - D_B^{(4)} \frac{\partial P_B^{(4)}}{\partial z}\bigg|_{z=L^-} \tag{29}$$

• at r = R₁ (liquid-membrane interface):

$$k_A \left(C_A^{(1)} - C_A^{(2)}\big|_{r=R_1} \right) = -D_{e,A}^{(2)} \frac{\partial C_A^{(2)}}{\partial r}\bigg|_{r=R_1} \tag{30}$$

• at r = R₂ (liquid-gas or membrane-support interface):

$$\left. \frac{\partial C_A^{(2)}}{\partial r} \right|_{r=R_2} = 0 \tag{31}$$

$$\left. C_B^{(2)} \right|_{r=R_2^-} = C_B^{(2)*} \tag{32}$$

$$\left. D_{e,B}^{(3)} \frac{\partial P_B^{(3)}}{\partial r} \right|_{r=R_2^+} = \left. D_{e,B}^{(2)} \frac{\partial C_B^{(2)}}{\partial r} \right|_{r=R_1^-} \tag{33}$$

• at r = R_3 support-gas interface:

$$\left. -D_{e,B}^{(3)} \frac{\partial P_B^{(3)}}{\partial r} \right|_{r=R_3} = k_B \left(\left. P_B^{(3)} \right|_{r=R_3} - P_B^{(4)} \right) \tag{34}$$

The system of partial differential equations (21)-(24) with their initial and boundary conditions (25) through (34) were rearranged by introducing the following dimensionless variables:

$$\theta_A^{(1)} = \frac{C_A^{(1)}}{C_{A0}}, \ \theta_A^{(2)} = \frac{C_A^{(2)}}{C_{A0}}, \ \theta_B^{(2)} = \frac{C_B^{(2)}}{C_{B0}}, \ \psi_B^{(3)} = \frac{P_B^{(3)}}{P_{B0}}, \ \psi_B^{(4)} = \frac{P_B^{(4)}}{P_{B0}} \tag{35}$$

$$\xi = \frac{z}{L}, \ r_m = \frac{r-R_1}{R_2-R_1}, \ r_s = \frac{r-R_2}{R_3-R_2} \tag{36}$$

$$\tau = \frac{t}{t_0}, \ \ t_0 = \frac{e_m^2}{D_{e,A}^{(2)}}, \tag{37}$$

Writing the equations in dimensionless form brings the previous equations in the form below for uses:

• *in liquid side:*

$$\frac{\partial \theta_A^{(1)}}{\partial \tau} = -\frac{u_1 t_0}{L} \left(-\frac{D_A^{(1)}}{u_1 L} \frac{\partial^2 \theta_A^{(1)}}{\partial \xi^2} + \frac{\partial \theta_A^{(1)}}{\partial \xi} - \frac{2}{R_1} \frac{D_{e,A}^{(2)} L}{u_1 e_m} \left. \frac{\partial \theta_A^{(2)}}{\partial r_m} \right|_{r_m=0} \right) \tag{38}$$

• in membrane:

$$\frac{\partial \theta_i^{(2)}}{\partial \tau} = \frac{D_{e,i}^{(2)} t_0}{e_m^2} \left(\frac{\partial^2 \theta_i^{(2)}}{\partial r_m^2} + \frac{e_m}{R_1 + e_m r_m} \frac{\partial \theta_i^{(2)}}{\partial r_m} \right) + R_i^v \frac{t_0}{C_{i0}} \qquad \text{with i =A, B} \tag{39}$$

210

• in support:

$$\frac{\partial \Psi_B^{(3)}}{\partial \tau} = \frac{D_{e,B}^{(3)} t_0}{e_s^2} \left(\frac{\partial^2 \psi_B^{(3)}}{\partial r_s^2} + \frac{e_s}{R_2 + e_s r_s} \frac{\partial \psi_B^{(3)}}{\partial r_s} \right) \tag{40}$$

• in gas side:

$$\frac{\partial \psi_B^{(4)}}{\partial \tau} = \frac{u_4 t_0}{L} \left(\frac{\partial \psi_B^{(4)}}{\partial \xi} - \frac{D_B^{(4)}}{u_4 L} \frac{\partial^2 \psi_B^{(4)}}{\partial \xi^2} - \frac{2R_3}{R_4^2 - R_3^2} \frac{D_{e,B}^{(3)} L}{u_4 e_s} \frac{\partial \psi_B^{(3)}}{\partial r_s} \Big|_{r_s = 1} \right) \tag{41}$$

All the previous equations are subjects to the following initial and boundary conditions:

• at $\tau = 0$,
$$\theta_A^{(1)} = 1, \; \psi_B^{(4)} = 1, \; \theta_i^{(2)} = 0 \text{ for i = A, B and } \psi_B^{(3)} = 0 \tag{42}$$

• at $\xi = 0$,
$$1 = \theta_A^{(1)} - \frac{D_A^{(1)}}{u_1 L} \frac{\partial \theta_A^{(1)}}{\partial \xi} \Big|_{\xi = 0^+} \tag{43}$$

$$\frac{\partial \psi_B^{(4)}}{\partial \xi} \Big|_{\xi = 0} = 0 \tag{44}$$

• at $\xi = 1$,
$$\frac{\partial \theta_A^{(1)}}{\partial \xi} \Big|_{\xi = 1} = 0 \tag{45}$$

$$1 = \theta_B^{(4)} - \frac{D_B^{(4)}}{u_4 L} \frac{\partial \theta_B^{(4)}}{\partial \xi} \Big|_{\xi = 1} \tag{46}$$

• at $r_m = 1$ (liquid-membrane interface):
$$\left(\theta_A^{(1)} - \theta_A^{(2)} \Big|_{r_m = 0} \right) = -\frac{D_{e,A}^{(2)}}{k_A e_m} \frac{\partial \theta_A^{(2)}}{\partial r_m} \Big|_{r_m = 0} \tag{47}$$

• at $r_m = 0$ (liquid-gas or membrane-support interface):

$$\left. \frac{\partial \theta_A^{(2)}}{\partial r_m} \right|_{r_m = 1} = 0 \tag{48}$$

$$\left. \theta_B^{(2)} \right|_{r_m = 1^-} = \frac{C_B^{(2)*}}{P_{B0}} \tag{49}$$

$$\left. \frac{\partial \psi_B^{(3)}}{\partial r_s} \right|_{r_s = 0} = \frac{D_{e,B}^{(2)}}{D_{e,B}^{(3)}} \frac{e_s}{e_m} \frac{C_{B0}}{P_{B0}} \left. \frac{\partial \theta_B^{(2)}}{\partial r_m} \right|_{r_{sm} = 1} \tag{50}$$

• at $r_s = 1$ support-gas interface:

$$-\frac{D_{e,B}^{(3)}}{k_B e_s} \left. \frac{\partial \psi_B^{(3)}}{\partial r_s} \right|_{r_s = 1} = \left(\left. \psi_B^{(3)} \right|_{r = R_3} - \psi_B^{(4)} \right) \tag{51}$$

4.3 Correlation used for simulation

● *Estimation of diffusion coefficients in the liquid:*

   - For oxygen

The diffusion coefficient of oxygen was estimated by employing the well known Wilke-Chang correlation (Vospernik et al [6]):

$$D_B = \frac{7.4 \times 10^{-8} (\phi_B M_B)^{0.5} T}{\eta_B V_A^{0.6}} \tag{52}$$

   -For formic acid

The estimation of the diffusion coefficient of formic acid Is obtained from the Hayduk-Minhas equation (Vospernik et al [6]) was employed:

$$D_A = 1.25 \times 10^{-8} (V_A^{-0.19} - 0.292) T^{1.52} \eta_B^{\xi} \tag{53}$$

$$\xi = \left(\frac{9.58}{V_A} \right) - 1.12 \tag{54}$$

   The molar volume is obtained from Tyn and Calus relation (Vospernik et al [6])

$$V_A = 0.285 V_C^{1.048} \tag{55}$$

If the critical volume V_c is not available it can be evaluated using Schroeder rule (Reid and Prausnitz [33]).

●*Estimation of mass transfer coefficients:*

Mass transfer coefficient in liquid and gas sides were estimated from the Sherwood number Sh by using the Lévèque correlation defined for laminar flow in the cylindrical tubes (Viegas et al [34])

$$Sh = 1.62 \, Re^{1/3} \, Sc^{1/3} \left(\frac{d}{L} \right)^{1/3} \tag{56}$$

Where d and L are respectively the diameter and the length of the tube. For laminar flow in the shell side the tube hydraulic diameter d_h is used instead of d. The Reynolds number Re, the Schmidt number and the Sherwood number are defined as followed:

$$Re = \frac{u \rho d}{\mu} \tag{57}$$

$$Sc = \frac{\mu}{\rho D} \tag{58}$$

$$Sh = \frac{kL}{D} \tag{59}$$

Where D is the component diffusivity, ρ and u are respectively the fluid density and average velocity

●*Estimation of dissolved oxygen:*

The equilibrium concentration $C_B^{(2)*}$ of dissolved oxygen in the liquid phase was calculated at any oxygen partial pressure P_o (in this case the liquid-gas interface) and total pressure P, using a correlation proposed by Benson et al [35]:

$$C_o^* = \frac{\rho P_o}{k_o M} \left(1 - \theta_o P \right) \tag{60}$$

where M and ρ are respectively a gram molecular mass and density of pure water, k_o, θ_o and ρ are given by:

$$ln\,k_o = \left(3.71814 + \frac{5596.17}{T} - \frac{1049668}{T^2}\right) \tag{61}$$

$$ln\,\rho = \left(-0.589581 + \frac{326.785}{T} - \frac{45284.1}{T^2}\right) \tag{62}$$

$$\theta_o = \left(0.000975 - 1.426*10^{-5}t - 6.436*10^{-8}t^2\right) \tag{63}$$

where T is in Kelvin , ρ in g.cm^{-3}, k_o in atm and 0<t<40°C .

4.4 Kinetic law

The simple process design engineer friendly model in any heterogeneous reaction is power law model which a macroscopic view (Gunal et al [36]). This form is suitable for them because the catalyst activity is proportional to the weight of the catalyst and expressed this in term of weight would be more process design engineer rather than expressing the kinetic as turn over frequency. Therefore the rate of formic acid oxidation on catalysed membrane can be expressed as:

$$-R_A = kC_A^m C_B^n \tag{64}$$

Where C_A and C_B are respectively the concentration of formic acid and oxygen in the liquid phase in the membrane, m and n are the orders of the reaction with respect to formic acid and oxygen. Their values are obtained using non-linear regression.

The microscopic view is described by a series of adsorption, surface reaction and desorption and kinetic rate is expressed after assuming the rate-controlling step in the proposed mechanism. One of the well known useful model frequently used is the Langmuir-Hinshelwood one.

Rate equation from Proposed Mechanism of formic acid oxidation

Wet air oxidation of aqueous formic acid on Pt-membrane can be illustrated by the redox mechanism. The rate derived from the proposed mechanism is therefore compared to the experimental data for agreement. Suppose that the reaction occurs by the following series of elementary steps:

$$\text{a. } \frac{1}{2}O_2 + X \Leftrightarrow O.X \tag{65}$$

$$\text{b. } O.X + HCOOH_{aq} \rightarrow HCOOH.O + X \tag{66}$$

214

$$\text{c.} \quad HCOOH.O \xrightarrow{K_3} \text{int } ermediate + O_2 \xrightarrow{fast} CO_2 + H_2O \qquad (67)$$
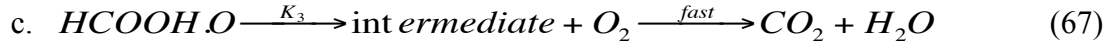
Where:

X: refers to a reduced catalyst site.

O_2 : refers to Oxygen

O.X: refers to activated complex

HCOOH: refers to formic acid

HCOOH.O: refers to activated complex

CO_2 : refers to carbon dioxide

H_2O : refers to water

In this scheme, the previous steps considered are:

1. Reversible adsorption of oxygen by a dissociative mechanism forming an oxidizing site on the catalyst surface.
2. Reaction of this oxidizing site with formic acid from the liquid phase to form the complex HCOOH.O

3. Decomposition of HCOOH.O into intermediate products followed by further reaction with more oxygen to give CO_2 and H_2O. This step is assumed to be intrinsically fast with respect to steps a- and b-.

Assume that the stationary state hypothesis can be applied to complexes O.X and CHOOH.X (Levenspiel [16] , Smith et al [17] and Fogler [18]), the rate equations can be expressed as:

for $C_{O.X}$,

$$-r_{C_{O.X}^*} = 0 = k_1 C_{O_2}^{0.5} C_X^* - k_1' C_{O.X}^* - k_2 C_{O.X}^* C_{HCOOH} \qquad (68)$$

and for $C^*_{CHOOH.X}$

$$-r_{C_{CHOOH.O}^*} = 0 = k_2 C_{O.X}^* C_{HCOOH} - k_3 C_{CHOOH.O}^* \qquad (69)$$

Equations (68) and (69) may be solved for activated complexes O.X and HCOOH.X to yield.

$$C_{O.X}^* = -\frac{k_1 C_{O_2}^{0.5} C_X^*}{k_1' + k_2 C_{CHOOH}} \qquad (70)$$

$$C^*_{CHOOH.O} = \frac{k_1 k_2 C^{0.5}_{O_2} C_{CHOOH} C^*_X}{k_3 (k_1^{\cdot} + k_2 C_{CHOOH})} \tag{71}$$

and therefore

$$r_{CHOOH} = -\frac{(k_1 k_2 C^*_X) C^{0.5}_{O_2} C_{CHOOH}}{k_1^{'} + k_2 C_{CHOOH}} \tag{72}$$

For low concentrations of oxygen and formic acid in these dilute aqueous solutions, the fraction of surface coverage by the X.O activated complex could be low. Then, C_X^* in equation (51) would be nearly constant, therefore the consumption rate of formic acid will be:

$$-r_{CHOOH} = \frac{k C^{0.5}_{O_2} C_{CHOOH}}{k_1^{\cdot} + k_2 C_{CHOOH}} \tag{73}$$

Then, equation (51) was inserted in membrane reactor model, in general form as follows:

$$-R_A = \frac{k C_A C^{0.5}_B}{k_1^{\cdot} + k_2 C_A} \text{ or } R_A = -\frac{k^{'} C^{0.5}_B C_A}{1 + k^{''} C_A} \tag{74}$$

The kinetic parameters were estimated from an objective function based on the comparison between reactor outlet acid formic concentrations, which are measured experimentally and predicted by the membrane reactor model.

4.5 Numerical simulation

The dimensionless set of partial differential equations with the adequate kinetic laws was solved numerically by the method of lines: the PDEs were converted to ODEs by discretization of the spatial derivatives with finite difference after taking into account the relevant boundary conditions in it dimensionless form. Also this method named as the quasi-finite difference method because it only descritizes space derivative by finite difference

The method of line (MOL) is probably the most widely used approach to the solution of the evolutionary PDEs [10, 11, and 12]. Due to the functionality of MATLAB for the solution of differential equation, and the MATLAB library host several ODE solvers which are designed to implement the method of lines. This most popular method for solving evolutionary PDEs proceeds in two basic steps (in the following, it is assumed that space and time are two independent variables under consideration) [13, and 14]:

    (i)   Spatial derivatives are approximated using finite difference, -element, or –volume methods.

(ii) The resulting of semi discrete (discrete in space and continuous in time) equations is integrated in time.

Direction of integration

t > 0					
t = 0	j-2	j-1	j	j+1	j+2
$\theta(0)$	$\dfrac{d\theta_{j-2}}{d\tau}$	$\dfrac{d\theta_{j-1}}{d\tau}$	$\dfrac{d\theta_{j}}{d\tau}$	$\dfrac{d\theta_{j+1}}{d\tau}$	$\dfrac{d\theta_{j+21}}{d\tau}$
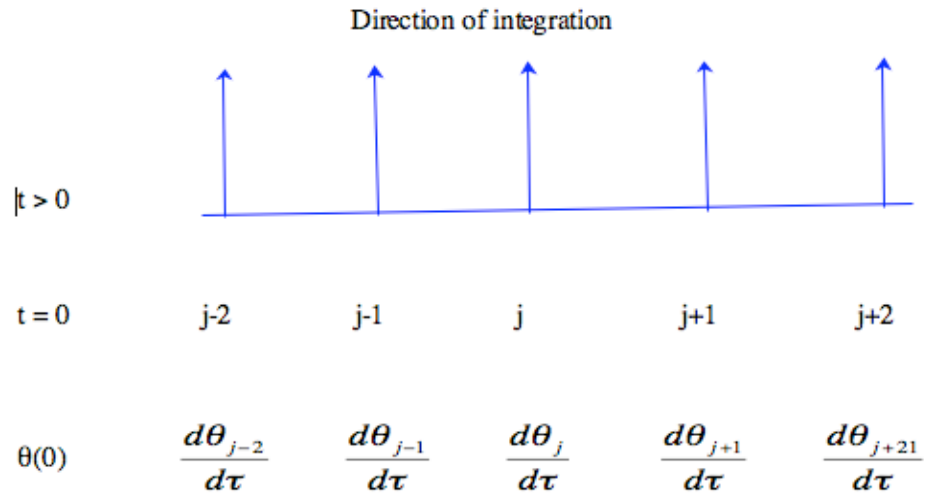
For the finite difference method, we used the following approximation:

- first derivative:

$$\frac{\partial \theta}{\partial x} = \frac{(\theta_j - \theta_{j-1})}{\Delta x} \qquad (75)$$

- second derivative

$$\frac{\partial^2 \theta}{\partial x^2} = \frac{(\theta_{j+1} - 2\theta_j + \theta_{j-1})}{\Delta x^2} \qquad (76)$$

The complete set of model equations after discretization is presented in appendix (A).

The simulation algorithm was written in MATLAB codes to solve the non-homogenous parabolic partial differentials equations obtained from the mass balances. Figure 38 shows the flow chart of reactor model simulation algorithm

217
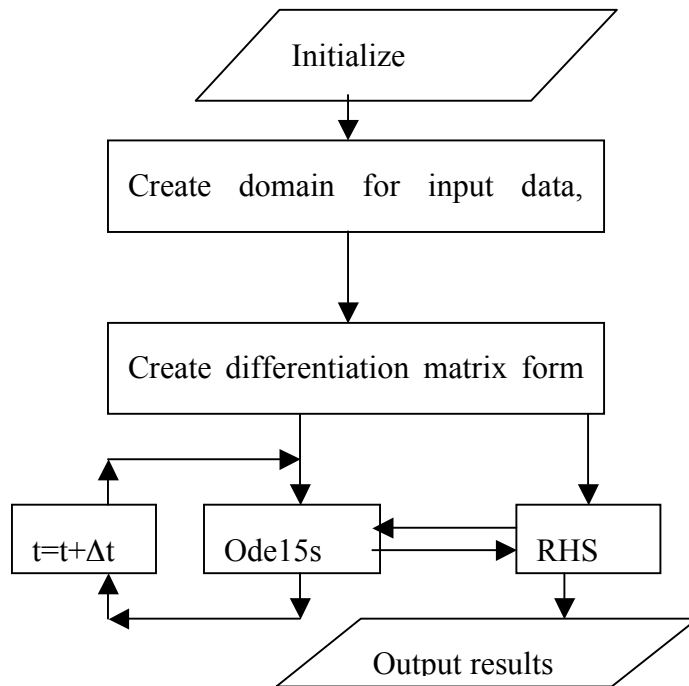
Figure 39 : Flow chart of reactor model simulation algorithm

The initialization step defines the essential parameters for the model " initialize" routine will define initial concentrations for both reactants, physical properties for both reactants, catalytic membrane reactor dimensions, catalyst properties, initial kinetic parameters. Also, the code will initialize the function required to estimate mass transfer parameters. A separate function has been constructed from the right hand side (RHS) of all equations in the model that already discretized in spatial domain. The RHS of model equations in matrix form then passed to (ode15s) solver that available in the MATLAB with required time domain. All available information was passed from ode15s solver to RHS function to approximate all derivatives. The derivative vector is then returned to the ode15s solver to calculate the concentrations in the next step. In general ode15s from a MATLAB library is used as the ode solver in flow chart, which is based on fourth and fifth order of Runge-Kutta formulae with special trend to treat sparse matrices, which usually obtained from reaction-diffusion problems. The last step "output routine" will provide graphical representations of the numerical output. The functionality of the graphics package in MATLAB is large and well suited to obtaining information in the output.

The complete MATLAB codes for solving model equations can be found in appendix (B).

4.6 Parameter estimation in the kinetics law

Commonly the conducting of kinetic studies has been performed either in batch reactors for homogenous reactions or in differential flow reactors for heterogeneous reactions [18].

In batch reactor experiments, concentration, pressure, and/or volume are usually measured and recorded at different times during the course of the reaction. Data are collected from batch reactors during unsteady state operation; where as measurements on the differential reactors are made during steady-state operation. In experiments with differential reactor, the product concentration is usually monitored for different feed conditions [21].

The kinetics of the oxidation reactions can be expressed using simple pseudo homogenous model or more complex model based on Langmuir-Hinshelwood mechanism as previously mentioned.

In the modelling of CWAO reaction kinetics, simple power law model was proposed and tested and so is the extended Langmuir-Hinshelwood which has been implemented. Previous studies in CWAO kinetics with simple power law kinetics suggested that, a first order for the oxidized component, while the oxygen are mostly being close to 0.5. However, the application of simple power law kinetics occasionally leads to reaction orders that lack of physical meaning (e.g. negative) due ignoring the effect of adsorption into the catalyst surface. Thus the development of detailed kinetic modelling, using Langmuir-Hinshelwood expressions or more advanced equations should be considered as a priority item in future research work in the field of CWAO [31]. These kinetic parameters were determined by fitting the rate expression to available experimental data that can be obtained either from batch, CSTR, or plug flow reactors. The main restriction of the reactor operation is to carryout the reaction in kinetic controlling regime rather than diffusion controlling regime. The experimental kinetic data can then be related to the reaction rate by means of differential or integral methods.

In differential methods, the concentration-time derivatives expressions are evaluated from experimental kinetic data and subsequently the reaction rate r is transformed by linearization techniques to estimate the kinetic parameters. One advantage of the differential methods is that they don't need to define priori initial guess values for the kinetic parameters.

In integral methods an adequate rate equation is proposed, then the rate equation is fitted by numerical integration solution. Recently, due to the continuous improvements in

computational power, integral methods coupled with nonlinear parameter estimation have replaced the differential methods.

Regression analysis is the application of mathematical and statistical methods for the analysis of the experimental data and the fitting of the mathematical models to these data by the estimation of the unknown parameters of the models. Most mathematical models encountered in engineering and sciences are nonlinear in the parameters. Attempts in linear zing the models, by rearranging the equations and regrouping the variables, were common practice in the pre-computer era, where graph paper and the straightedge were the tools for fitting models to experimental data. Such primitive techniques have been replaced by the implementation of linear and non-linear regression methods on the computer.

The optimization of parameter estimation by nonlinear regression have been widely employed in gradient-based methods, among these methods, the Levendberg-Marquardt algorithm is most popular algorithm that used in computer implementation [10].

$$SSR = \sum \left(C_{\exp} - C_{calc} \right)^2 \tag{77}$$

where SSR: (sum of square residuals).

$C_{\exp}$: experimental outlet concentration of formic acid

C_{calc}: theoretical (calculated) outlet concentration of formic acid

The least square nonlinear regression function (LSQNONLIN) for parameter estimation that available in the MATLAB was used to minimize the following objective function:

The essential process for parameter estimation by nonlinear regression, using the functionality and matrix based capabilities of MATLAB. The conception steps and corresponding subroutines with information pathways for the computer-based implementation are shown in figure39.
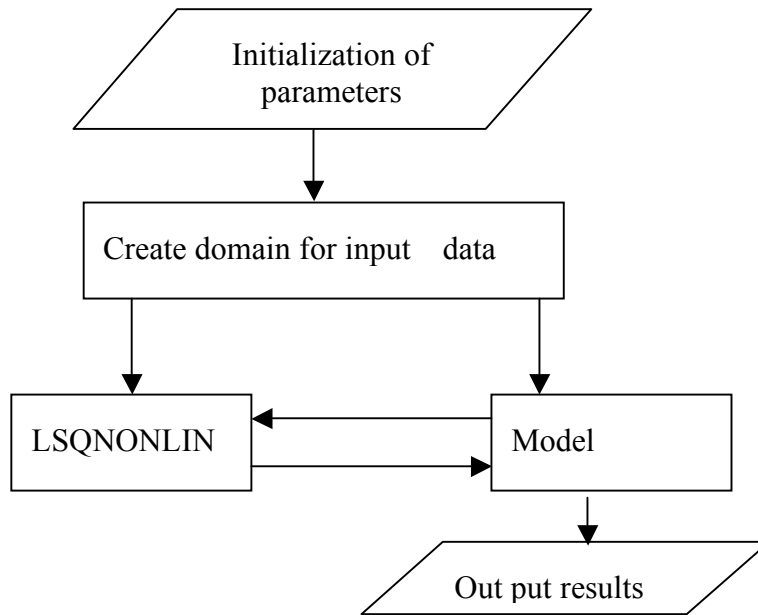
Figure 40: MATLAB flow chart for parameter estimation

The initialization step defines the essential parameters for the model, initial guess values of estimated parameters, then passed to LSQNONLIN function in matlab library. A separate function has been constructed to our kinetic models, kinetic model with estimated parameters then linked to lsqnonlin function in matlab library. The last step, output routine will provide a graphical representation of the numerical output. The complete MATLAB codes for solving model equations can be found in appendix (C).

4.7 Model validation

Effect of reactants concentration on observed reaction rate:

-Formic acid. A series of experiment was conducted in which the only independent variable was the initial concentration of formic acid, the temperature, TMP transmembrane pressure, fluid flow rates, and a total volume of reacting solution were all held constant. The purpose of these experiments was to determine the dependence of the reaction rate on the concentration of formic acid.

-Dissolved oxygen. In order to evaluate the effects of dissolved oxygen in the rate of oxidation reaction of formic acid, a series of experiments was performed in which transmembrane pressure was varied. Since the solubility of these gases obey Henrys law, these variations have the effect of varying both the gas phase partial pressure of oxygen and the concentration of oxygen dissolved in the aqueous phase. It should be noted that no

degradation was observed when pure N_2 was used as the feed gas. Data obtained in these experiments were used to test pseudo homogenous power law model and mechanistic Langmuir-Hinshelwood

The rate expressions considered in the analysis of the kinetic data are summarized in table 24. The membrane characteristics are summarised in table 25.

Table 24: Models considered for kinetic study

Model number	Model form	Effective parameters
1	$kC_{O_2}^n C_{CHOOH}^m$	k, m, and n
2	$\dfrac{k' C_{O_2}^{0.5} C_{CHOOH}}{1 + k'' C_{CHOOH}}$	k', and k''

C_{CHOOH}: Formic acid concentration C_{O2}: Oxygen concentration

Table 25: Membrane characteristics used in kinetic study

Inner diameter		7mm	
Outside diameter		10 mm	
Active length		230 mm	
Membrane porosity		0.4	
Membrane tortuosity		2.5	
Support porosity		0.26	
Support tortuosity		1.5	
Layer	Material	Mean pore size (nm) / Thickness (μm)	
1 (top layer)	TiO_2 (CeO_2/ZrO_2)	100/8	
2	TiO_2	800/30	
3	TiO_2	5000/1500	

- Effect of liquid flow rate on the reaction rate:

The effect of liquid flow rate on the reaction rate of formic acid was studied in three layers Pt-membrane. Results are shown in figure 40
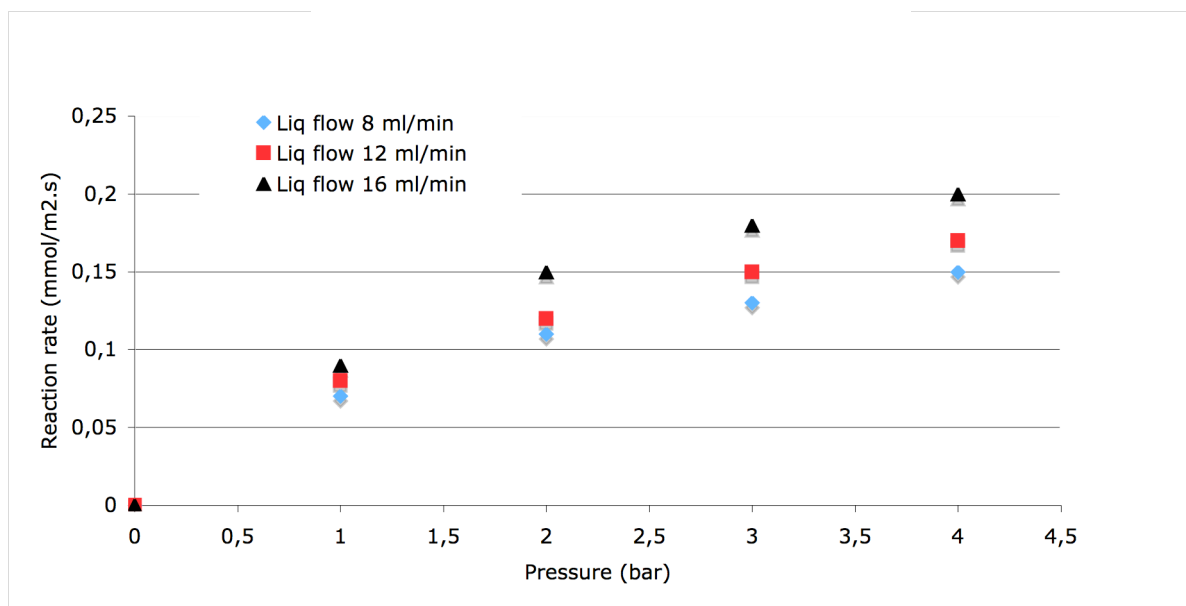
Figure 41: Effect of liquid flow rate on the formic acid reaction rate

As can be seen in figure 20, results obtained with Pt-membrane at various liquid flow rates expressed in terms of reaction rate, the effect of liquid flow rate is more remarkable at higher overpressures; the reaction rate increases as the liquid flow rate increases after pressures of 2 bars.

- Effect of temperature on the reaction rate:

The effect of reaction temperature on the reaction rate of formic acid was also tested. Results obtained with three layers Pt-membrane at various temperatures, expressed in terms of reaction rate versus transmembrane pressure are shown in figure 41.
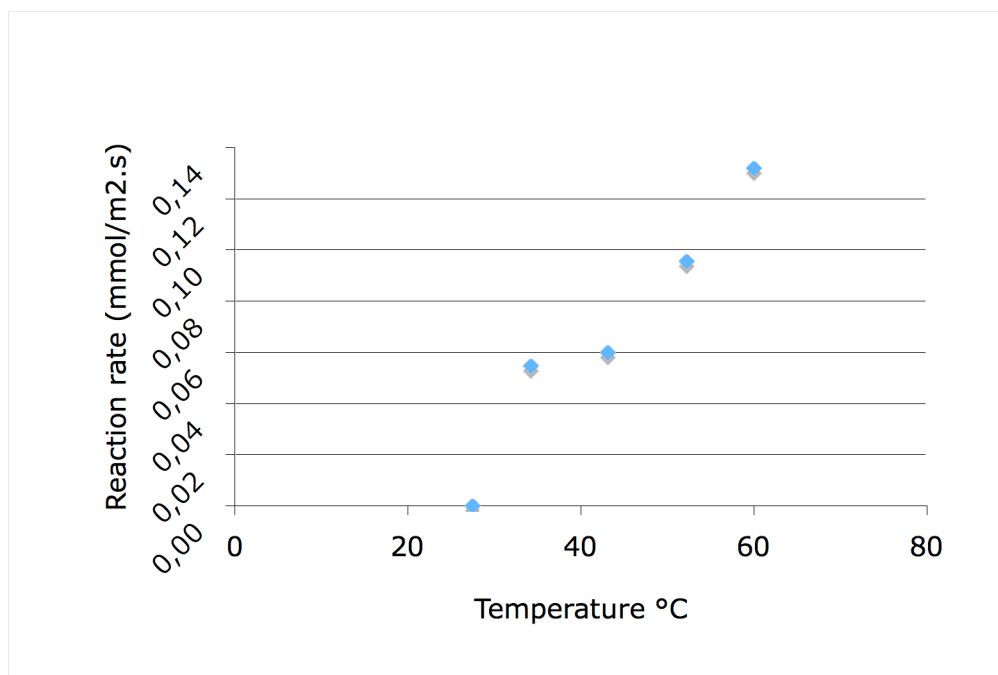
Figure 42: effect of temperature on the reaction rate at 2 bar.

The general trend with temperature is the one expected: membrane reactor performance improves (reaction rate increases) as the temperature increases.

- Activation energy:

The apparent activation energy for formic acid oxidation was estimated based on reaction rate-temperature relation, between the 25°C and 60°C, the apparent activation energy is estimated to be E_a=63.85 KJ/mol.

Results of model validation:

The results obtained during the simulation, and formic acid oxidation over Pt-membrane are depicted in figures 42 and 43
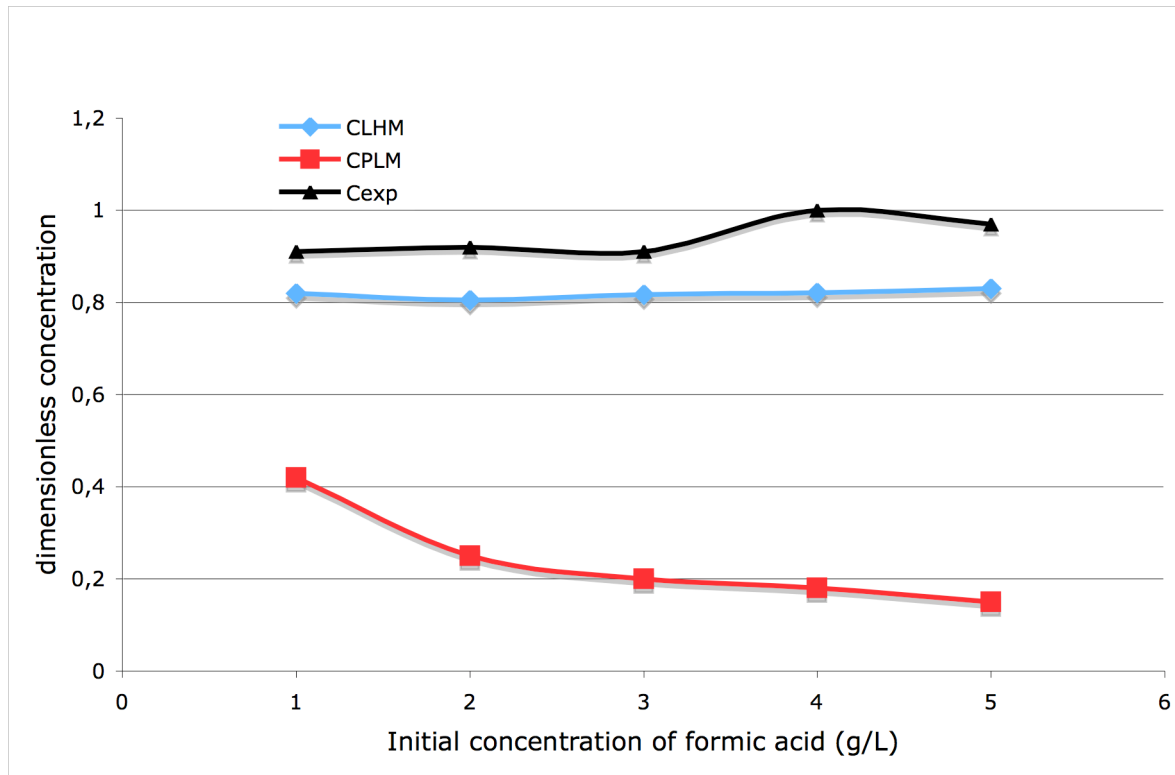
Figure 43: comparison between simulated and experimental data at

oxygen concentration = 0.0043 mol/L

As can be seen in figure 42, LHM model is more reliable than PLM model to estimate the predicted values.
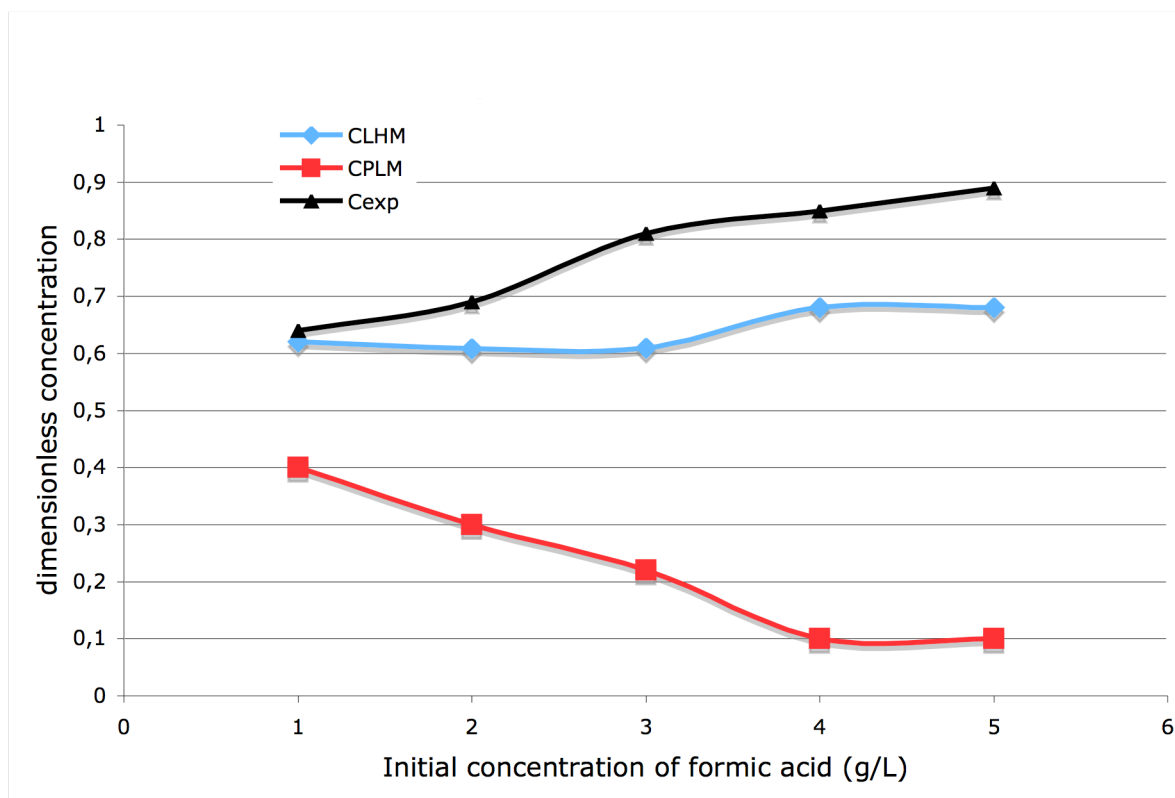
Figure 44: comparison between simulated and experimental data at

oxygen concentration = 0.0166 mol/L

As can be seen also in figure 43, LHM model is more reliable than PLM model to estimate the predicted values, but also still in fairly good areement at higher initial concentration of formic acid.

Table 26 shows the values estimated for the kinetic parameters for the oxidation of formic acid with PLM model and the values obtained for LHM model indicted in Table 27. The estimation is conducted with 25 experimental data obtained at different initial concentrations of formic acid and of oxygen.

Table 26: Estimation results PLM model

k x 10^4	n	M
2.22	0.134	0.9218

Table 27: Estimation results LHM model

k'	k"
0.0322	0.0588

Results from literature pointed out 1st order with respect to formic acid and half order with respect to oxygen.

Conclusion:

It is obvious that in both cases of kinetic models used, PLM model or LHM model, PLM model in fairly good agreement between measured and predicted values, LHM model predicted more reliable values in compared to experimental or values predicted by PLM model, which implies that the above presented assumptions, proposed mechanism, and simplification are reasonable for LHM model while is not fair for PLM model, that is in agreement with previous work reported in the literature. Eflaxias et al [31] have demonstrated that the kinetics of carboxylic acids is well established by using LHM model, while the phenol kinetics is well established by PLM model.

Parameter estimation of kinetic rate for the oxidation of formic acid in catalytic membrane reactor is not easy to be done. In fact provided the kinetics are fast enough compared with the transport of reactants, the reaction take place in limited zone inside the membrane, and any change in oxygen concentration in the gas feeds result in a shift of the reaction zone inside the membrane (Saracco et al [4]).

Nomenclature

C_A: Formic acid concentration

D_A: diffusivity of formic acid

U_A: average liquid velocity

C_A: Formic acid concentration

C_B: Oxygen concentration

C_B^*: saturation concentration of oxygen in liquid phase

D_{EA}: Effective diffusivity of formic acid

D_A: diffusivity of formic acid

τ_m : Membrane tortuosity factor

ε_m : Membrane Porosity

$D_{e,B}$: Effective diffusivity of oxygen

D_B: diffusivity of oxygen,

ε_s : Support porosity,

τ_s : Support tortuosity factor

R_A: Reaction rate of formic acid ,

R_B: Reaction rate for oxygen

$$D_{e,A} = \frac{\varepsilon}{\tau} D_A$$

$$D_{e,B} = \frac{\varepsilon}{\tau} D_B$$

References

1. Berger. J. R and Kapteijin. F, Coated-Wall Reactor Modeling-Criteria for Neglecting Radial Concentration Gradients. 1. Empty Reactor tubes, Ind. Eng. Chem. Res. 2007, 46, 3863-3870

2. Casanave. D; Ciavarella. P; Fiaty. K; Dalmon. J, Zeolite membrane reactor for isobutene dehydrogenation : experimental results and theoretical modelling, *Chem. Eng. Science*, 54 (1999) 1577-1582

3. Casanave. D, Fiaty. K, Dalmon. J. A, Computer-aided optimization of catalytic dehydrogenation in packed bed membrane reactor, Computers Chem. Engng 22 (1998) S691-S694.

4. Saracco. G and Vito Specchia, Catalytic combustion of propane in a membrane reactor with separates feed of reactants. IV. Transition from the kinetics- to the transport- controlled regime, Chem., Eng., Sci., 55 (2000) 3979-3989

5. Saracco. G, *Chem. Eng. Sci.* 1995, *50* (17), 2833-2841.

6. Cini. P and Harlod. M, Experimental study of the Tubular Multiphase Catalyst, AIChE Journal 37, no. 7, (1991), 997 – 1008.

7. Torres M; Sanchez J; Dalmon J.A; Bernauer B. and Lieto J, Modeling and simulation of a three-phase catalytic membrane reactor for nitrobenzene hydrogenation. *Ind. Eng. Chem. Res*, 33 (1994) 2421-2425

8. Vospernik, M.; Pintar, A.; Levec, J. Application of a catalytic membrane reactor to catalytic wet air oxidation of formic acid. *Chem. Eng. Process.* 2006, *45* (5), 404-414.

9. Becker. Y, Dixon. A, Moser. W, Ma. Y, Modeling of Ethylbenzene dehydrogenation in a catalytic Membrane Reactor, Journal of membrane science, 77, (1993) 233-244.

10. Costantinides. A, Mostoufi. N, Numerical Methods for Chemical Engineers with MATLAB Applications, 2nd Edition, (2000), Prentice-Hall PTR.

11. Wouwer. A, Schhiesser. W, Editorial Special Issue on the Method of Lines: dedicated to Keith Miller, Journal of Computational and Applied Mathematices 183 (2005) 241-244

12. Wouwer. A, Saucez. P, Schhiesser. W, Simulation of Distributed Parameter Systems Using a Matlab-Based Method of Lines Tool Box: Chemical Engineering Applications, Ind. Eng. Chem. Res. (2004), 43, 3469-3477.

13. Lee. H, Mathews. C, Braddock. R, Sander. G, Gandola. F, A MATLAB method of Lines template for Transport Equations, Environmental Modelling & Software, 19 (2004) 603-614.

14. Penny. J, Lindfield. J, Numerical Methods using MATLAB, 1st Edition, (1995), Ellis Horwood Limited.

15. Hines. A. L, Maddox. R. N, Mass Transfer Fundamental and Applications , 1st edition (1985), Prentice-Hall International Series

16. Levenspiel.O, Chemical Reaction Engineering, 2nd edition (1972), Mc-Graw Hill Book Company,

17. Smith. J. M, Chemical Engineering Kinetics, 3rd edition (1981), Mc-Graw Hill Book Company

18. Fogler. H. S, Elementary of Chemical Reaction Engineering, 3rd edition (1999), Prentice-Hall International Series

19. Mandowara. A, Bhattacharya. P, Membrane Contactor as degaser Operated under vacuum for Ammonia removal form Water: Numerical Simulation of Mass Transfer for Laminar flow Conditions, Computers Chem. Eng 33 (2009) 1123-1131.

20. Wu. Q, and Hu. X, kinetics study on catalytic wet air of phenol, Chem., Eng., Sci., 58 (2003) 923-928

21. Warana. J, Salmi. T, Dynamic Modelling of Catalytic Three Phase Reactors, Computers Chem. Eng 1 (1996) 39-47.

22. Hermann. C, Quicker. P, Dittmeyer. R, Mathematical Simulation o Catalytic Dehydrogenation of Ethyl benzene to Styrene in a Composite Palladium Membrane Reactor, Journal of Membrane science 136 (1997) 161-172

23. Katz. S, Chemical Reactions catalysed on tube Wall, Chem., Eng., Sci., 10 (1959) 202-211

24. Weisz. P, and Hicks. J, The behaviour of porous catalyst particles in view of internal mass and heat diffusion effects, Chem., Eng., Sci., 17 (1962) 265-275.

25. Sabate. J, Anderson. A, Kikkawa. H, Eduards. M, Hill. C, A kinetic study of the photo catalytic degradation of 3-chlorosalicyclic acid over Tio2 catalyst supported on glass, journal of catalysis 127 (1991) 167-177

26. Larsoon. M, Henriksson. N, and Andersson. B, Investigation of the kinetics of a deactivating system by Transient experiments. Applied Catalyses A: General, 166 (1998) 9-19

27. Elnashaie S. S. H., B. K. Abdallah, S. S. Elshishini, S. Alkhowaiter, M. B. Noureldeen, T. Alsoudani, On the link between intrinsic catalytic reaction kinetics and the development of catalytic processes – Catalytic dehydrogenation of ethyl benzene to styrene, Catalysis Today 64 (2001) 151-162.

28. Baldi. G, Goto. S, Chow. C, Smith. J, Catalytic Oxidation of Formic Acid in Water. Interparticle Diffusion in Liquid-Filled Pores, Ind. Eng. Chem. Process. Des. Develop, 13 no. 4 (1974), 447-452

29. Claudel, B., Nueilati., M., Andrieu., J., Oxidation of Formic Acid in Aqueous Solution by Palladium Catalysts, Applied Catalysis, 11 (1984) 217 – 225.

30. Harmsen. J, Jelemensky. L, Scheffr. P, Kuster. B, Marin. G, kinetic Modelling for wet air oxidation of Formic Acid on a carbon supported platinum catalyst, Applied Catalyses A: General, 165 (1997) 499-509

31. Eftaxias. A, Catalytic Wet Air Oxidation of Phenol in a Trickle Bed Reactor. Kinetices and Reactor Modelling, Doctoral Thesis, University Rovira I Virgili, Tarragona, Spain (2002)

32. Berecic. G, Pintar. A, Levec. J, Positioning of reaction zone by coupling results of mass transport and chemical reaction study, Catalysis Today 105 (2005) 589-597.

33. Reid R.C. , Prausnitz J.M., Poling B.E., The properties of gases and liquids,4th ed., McGraw-Hill, New York, 1987

34. Viegas R.M.C., Rodriguez M., Luque S., Alvarez J.R. Coelhoso I.M., Crespo J.P.S.G., Mass transfer correlations in membrane extraction: Analysis of Wilson-plot methodology", J. Membr. Sci., 145(1998)129-142

35. Benson B.B., Jr Krause D.,The concentration and isotopic fractionation of gases dissolved in freshwater in equilibrium with the atmosphere. 1. Oxygen, Limnol. Oceanogr., 25(4)(1980)662-671

36. Gunal T.L., Mahajani V.V., An insight Ru/TiO2 catalyzed wet air oxidation of N-ethylethanolamine in an aqueous solution, Chem. Eng. Journal, 159(2010)17-23

5 CONCLUSION AND PROPECTS

The application of catalytic membrane reactors for oxidation of model compound solutions at room temperature and moderate pressures is one milestone of this work.

The CWAO process employing several active phase metals loaded on ceramic membranes and a catalytic membrane reactor was proven to be effective for partial degradation of moderately concentrated aqueous model pollutants of short chain carboxylic acids and phenols.

In catalytic membrane reactors, a separation of the catalyst from the product is not required as the catalyst is loaded as nanoparticles in the porous media of the membrane structure.

The treatment of carbonaceous species that formed due to acetic acid oxidation reaction on Pt containing membrane, by soaking the membrane in bleach water (2.6 % liquid chlorine) for a period of 4-6 hrs. The residual washing solution is dark but after a period of time, the black species that already suspended in the residual washing solution start to settle down in the bottom of the beaker up to precipitated completely. The membrane then has washed by pure water in dead end flow mode, and then the membrane has dried under nitrogen at 100°C for 4-6 hrs and reactivated under Hydrogen at 200°C for 4hrs.

 Results of catalytic membrane reactor performance by using monometallic catalyst for degradation of model pollutants are beneficial, because it can be obtain a significant degree of organic acids, or phenol conversion at room temperature and low pressures which was not achieved in conventional reactors.

From acetic acid oxidation we confirmed that interfacial three phases catalytic membrane reactors operated at rather low mass transfer resistance even with the calcitrat behaviour of acetic acid.

The treatment of catalytic membrane deactivations that applied in this work can be divided into two ways, the first way in primary stages of membrane preparations before catalytic test by trying to prepare bimetallic catalysts, which recently proved as one way to avoid rapid catalyst deactivation, the second way after catalytic test, and the deactivation has occurred as in oxidation of acetic acid on Pt containing membrane where the formation of carbonaceous species has been observed.

At all tos, there is no noticeable metal leaching of all model compound solutions (formic acid, acetic acid, oxalic acid and phenol) with monometallic or bimetallic noble metal catalysts (Pt, Pd, and Ru). At all tos, there is noticeable metal leaching of monometallic or bimetallic transition metal catalysts (Cu, Ni, Zn) with phenol model compound solution, there is no metal leaching of phenol solutions with bimetallic Fe-Co and Cu-Pd but Fe-Co have higher activity for phenol oxidation.

The catalytic activity in CMR depends on the catalyst deposition method and metal loading. The use of layer-by-layer (LBL) deposition method for catalytic membrane preparation improves the reactor performance for oxidation of formic acid, acetic acid, and phenols at room temperature and mild pressures.

The limitation to the LBL method is the low loading of active phase metal. Since the support is quiet expensive, the cost of even noble metals is not as much of a concern as in other systems; however active phase metal cost cannot be disregarded. LBL deposition method is quiet versatile and could also be applied to polymeric hollow fibre supports, which are much less expensive than ceramic membranes.

The specific active phase metal mass loaded on the ceramic membrane is not directly affect the activity as usual in conventional catalysts, due to the multilayered structure of the membranes, the position of the gas liquid interface is moved as near as possible to the catalytic zone where a small part of the deposited metal is contribute to activate the reaction.

The catalytic activity and membrane reactor performance depends on the membrane pre-treatment before catalytic test. Optimization of wetting method vacuum wetting improves the activity by allowing overcoming the inhernt shortcomings ascribed to normal wetting by removing the air stored in the membrane pores.

Concerning the reactor modelling, it is obvious that in both cases of kinetic models used, PLM model or LHM model, the comparison between the predicted values and the experimental data is very poor with the PLM, LHM model predicted more reliable values. The proposed mechanism, and simplification with the presented assumptions are reasonable for LHM model but need to be improve. This trend is in agreement with previous work reported in the literature. Parameter estimation of kinetic rate for the oxidation of formic acid in catalytic membrane reactor is not easy to be done.

In fact provided the kinetics are fast enough compared with the transport of reactants, the reaction take place in limited zone inside the membrane, and any change in oxygen concentration in the gas feeds result in a shift of the reaction zone inside the membrane.

6 APPENDIXES

APPENDIX A: THE COMPLETE SET OF THE MEMBRANE REACTOR MODEL EQUATIONS AFTER DESCRITIZATION BY FINITE DIFFERENCE

THE FINITE DIFFERENCE EQUATIONS:

1- for liquid side:

j=1

$$\frac{\partial \theta^I{}_A}{\partial \tau} = A_1 \cdot \frac{(\theta^I{}_{A,2} - 2\theta^I{}_{A,1} + \theta^I{}_{A,0})}{\Delta \xi^2} - A_2 \cdot \frac{(\theta^I{}_{A,1} - \theta^I{}_{A,0})}{\Delta \xi} + 2.A_3 \frac{(\theta^I{}_{A,1} - \theta^{II}{}_{A1,1})}{\Delta r_m}$$

2≤ j ≤ nz-1

$$\frac{\partial \theta^I{}_A}{\partial \tau} = A_1 \cdot \frac{(\theta^I{}_{A\,j+1} - 2\theta^I{}_{A\,j} + \theta^I{}_{A\,j-1})}{\Delta \xi^2} - A_2 \cdot \frac{(\theta^I{}_{A\,j} - \theta^I{}_{A\,j-1})}{\Delta \xi} + 2.A_3 \frac{(\theta^I{}_{A\,j} - \theta^{II}{}_{A\,j,1})}{\Delta r_m}$$

j =nz

$$\frac{\partial \theta^I{}_A}{\partial \tau} = A_1 \cdot \frac{(\theta^I{}_{A\,nz+1} - 2\theta^I{}_{A\,nz} + \theta^I{}_{A\,nz-1})}{\Delta \xi^2} - A_2 \cdot \frac{(\theta^I{}_{A\,nz} - \theta^I{}_{A\,nz-1})}{\Delta \xi} + 2.A_3 \frac{(\theta^I{}_{A,nz} - \theta^{II}{}_{A\,nz,1})}{\Delta r_m}$$

2-for membrane:

For first component:

j=1

$$\frac{\partial \theta^{II}{}_A}{\partial \tau} = A_9 \cdot \left\{ \frac{(\theta^{II}{}_{A2} - 2\theta^{II}{}_{A1} + \theta^{II}{}_{A1})}{\Delta r_m{}^2} - \frac{e_m}{e_m.r_m(j) + R_1} \cdot \frac{(\theta^{II}{}_{A1} - \theta^{II}{}_{A0})}{\Delta r_m} \right\} + \frac{t_0}{C_{A,0}} R_A^{*v}$$

2≤ j ≤ nm-1

$$\frac{\partial \theta^{II}{}_A}{\partial \tau} = A_9 \cdot \left\{ \frac{(\theta^{II}{}_{A\,j+1} - 2\theta^{II}{}_{A\,j} + \theta^{II}{}_{A\,j-1})}{\Delta r_m{}^2} - \frac{e_m}{e_m.r_m(j) + R_1} \cdot \frac{(\theta^{II}{}_{A\,j} - \theta^{II}{}_{A\,j-1})}{\Delta r_m} \right\} + \frac{t_0}{C_{A,0}} R_A^{*v}$$

j=nz

$$\frac{\partial \theta^{II}{}_A}{\partial \tau} = A_9 \cdot \left\{ \frac{(\theta^{II}{}_{A\,nm+1} - 2\theta^{II}{}_{A\,nm} + \theta^{II}{}_{A\,nm-1})}{\Delta r_m{}^2} - \frac{e_m}{e_m.r_m(j) + R_1} \cdot \frac{(\theta^{II}{}_{A\,nm} - \theta^{II}{}_{A\,nm-1})}{\Delta r_m} \right\} + \frac{t_0}{C_{A,0}} R_A^{*v}$$

Membrane

For second component

J=1

$$\frac{\partial \theta^{II}{}_B}{\partial \tau} = A_{10} \cdot \left\{ \frac{(\theta^{II}{}_{B2} - 2\theta^{II}{}_{B1} + \theta^{II}{}_{B2})}{\Delta r_m{}^2} - \frac{e_m}{e_m.r_m(j) + R_1} \cdot \frac{(\theta^{II}{}_{B1} - \theta^{II}{}_{B0})}{\Delta r_m} \right\} + \frac{t_0}{C_{B,0}} R_B^{*v}$$

2≤ j ≤ nm-1

$$\frac{\partial \theta^{II}{}_{B}}{\partial \tau} = A_{10} \cdot \left\{ \frac{(\theta^{II}{}_{B\,j+1} - 2\theta^{II}{}_{B\,j} + \theta^{II}{}_{B\,j-1})}{\Delta r_m{}^2} - \frac{e_m}{e_m \cdot r_m(j) + R_1} \cdot \frac{(\theta^{II}{}_{B\,j} - \theta^{II}{}_{B\,j-1})}{\Delta r_m} \right\} + \frac{t_0}{C_{B,0}} R_B^{*v}$$

For   j =nm

$$\frac{\partial \theta^{II}{}_{B}}{\partial \tau} = A_{10} \cdot \left\{ \frac{(\theta^{II}{}_{B\,nm+1} - 2\theta^{II}{}_{B\,nm} + \theta^{II}{}_{B\,nm-1})}{\Delta r_m{}^2} - \frac{e_m}{e_m \cdot r_m(j) + R_1} \cdot \frac{(\theta^{II}{}_{B\,nm} - \theta^{II}{}_{B\,nm-1})}{\Delta r_m} \right\} + \frac{t_0}{C_{B,0}} R_B^{*v}$$

3- for support.

For j=1

$$\frac{\partial \theta^{III}{}_{B}}{\partial \tau} = A_{11} \cdot \left\{ \frac{(\theta^{III}{}_{B\,2} - 2\theta^{III}{}_{B\,1} + \theta^{III}{}_{B\,0})}{\Delta r_s{}^2} - \frac{e_s}{e_s \cdot r_s(j) + R_2} \cdot \frac{(\theta^{III}{}_{B\,1} - \theta^{III}{}_{B\,0})}{\Delta r_S} \right\}$$

For 2≤ j ≤ ns-1

$$\frac{\partial \theta^{III}{}_{B}}{\partial \tau} = A_{11} \cdot \left\{ \frac{(\theta^{III}{}_{B\,j+1} - 2\theta^{III}{}_{B\,j} + \theta^{III}{}_{B\,j-1})}{\Delta r_s{}^2} - \frac{e_s}{e_s \cdot r_s(j) + R_2} \cdot \frac{(\theta^{III}{}_{B\,j} - \theta^{III}{}_{B\,j-1})}{\Delta r_S} \right\}$$

For   j =ns

$$\frac{\partial \theta^{III}{}_{B}}{\partial \tau} = A_{11} \cdot \left\{ \frac{(\theta^{III}{}_{B\,ns+1} - 2\theta^{III}{}_{B\,ns} + \theta^{III}{}_{B\,ns-1})}{\Delta r_s{}^2} - \frac{e_s}{e_s \cdot r_s(j) + R_2} \cdot \frac{(\theta^{III}{}_{B\,ns} - \theta^{III}{}_{B\,ns-1})}{\Delta r_S} \right\}$$

4- for gas side

For j=1

$$\frac{\partial \theta_B{}^{IV}}{\partial \tau} = gam \cdot \frac{(\theta^{IV}{}_{B\,2} - 2\theta^{IV}{}_{B\,1} + \theta^{IV}{}_{B\,0})}{\Delta \xi^2} - A_2 \cdot \frac{(\theta^{IV}{}_{B\,1} - \theta^{IV}{}_{B\,0})}{\Delta \xi} + 2 \, delt \frac{(\theta^{III}{}_{B\,1} - \theta^{IV}{}_{B\,1,1})}{\Delta r_s}$$

For 2≤ j ≤ nz-1

$$\frac{\partial \theta_B{}^{IV}}{\partial \tau} = gam \cdot \frac{(\theta^{IV}{}_{B\,j+1} - 2\theta^{IV}{}_{B\,j} + \theta^{IV}{}_{B\,j-1})}{\Delta \xi^2} - A_2 \cdot \frac{(\theta^{IV}{}_{B\,j} - \theta^{IV}{}_{B\,j-1})}{\Delta \xi} + 2 \, delt \frac{(\theta^{III}{}_{B\,j} - \theta^{IV}{}_{B\,j,1})}{\Delta r_s}$$

For   j =nz

$$\frac{\partial \theta_B{}^{IV}}{\partial \tau} = gam \cdot \frac{(\theta^{IV}{}_{B\,j+1} - 2\theta^{IV}{}_{B\,j} + \theta^{IV}{}_{B\,j-1})}{\Delta \xi^2} - A_2 \cdot \frac{(\theta^{IV}{}_{B\,nz} - \theta^{IV}{}_{B\,nz-1})}{\Delta \xi} + 2 \, delt \frac{(\theta^{III}{}_{B\,nz} - \theta^{IV}{}_{B\,nz,1})}{\Delta r_s}$$

APPENDIX B: MATLAB program for solving membrane reactor model equations (MAIN PROGRAM)

```matlab
%    Main Program ....................................................
%                    HYDRODYNAMIC MODELLING
%   OF INTERFACIAL MEMBRANE REACTOR WITH SEPARATE FEED REACTANTS
%        ..............................................
%                         REACTION
%            WET AIR OXIDATION OF FORMIC ACID
%          ON CATALYZED WALL  TUBUALR CERAMIC MEMBRANE
%            VERSION  ALI ABUSALOUA 06/05/2010
% -------------------------------------------------------------------------
clc, close all, clear all, rehash
global phi2 alpha drm drs dz nm nz  ns bet gam delt tmax R1 R2 R3 R4
global es em rm rs Pe1 Pe4 DAme DBme DAse DBse cA0 cB0 DA DB u1 Po2 t0 kal
global kBov u4 n m RG Temp L z tspan  y0 k0 k1 k1dash k2 H kBg
% ========================================================================
  disp(' membrane reactor modelling ')
  disp  ('by coupling reation kinetics and')
  disp('reactor hydrodynamics')
% -------------------------------------------------------------------------
% Temp=input('Reaction temperature in K')
Temp=308; %K
RG=0,0082
%RG=1.987; % Gas constant in (bar.L/mol/K)
% -------------------------------------------------------------------------
%      Input of initial concentrations of formic acid and oxygen
cA0=input('Initial concentration of formic acid in (g/L)');
P=input('Gas transmembrane pressure in (bar) ='); yo2=0.2; Po2=yo2*P;
cB0=Po2/RG/Temp;
%t0=input(' Input t0 '); %t0=1;
% -------------------------------------------------------------------------
```

```
%                        Membrane reactor dimensions

% ----------------------------------------------------------------------242

L=25;%cm

em=0.025;%cm

es=0.150;%cm

R0=0;

R1=0.35;%cm

R2=R1+em;%cm

R3=R2+es;%cm

R4=1.2;%cm

porosm=0.4; taum=2.5; poross=0.26; taus=1.5;

%QL=input(' Liquid flow rate (ml/min')

Q1=10/60;%ml/s

%Qg=input(' Gas flow rate (ml/min')

Q4=25/60;%ml/s

S1=pi*R1^2; u1=Q1/S1; S4=pi*(R4^2-R3^2); u4=Q4/S4;

Vme=18; %volume molaire de l'eau en ml/mol

%C20=1.e-3*(exp(-171.2542+8391.24/Temp)+23.24323*log(Temp))*Po2*Vme;

%C10=.2;%g/L

%P=1;%en bar

% ----------------------------------------------------------------------

%Estimation of diffusion coefficient for O2 in water by Wilke-Chang formula

Me=18; %g/mol

phie=2.26;%facteur de correction

Temp=308; %K

visce=1.; %en cP

Vco=73.4 ; %volume critique

Vo=0.285*Vco^1.048;  %volume molaire du solute

DB=(7.48e-8)*((phie*Me)^0.5)*Temp/(visce*(Vo^0.6));  %en cm2/s

% ----------------------------------------------------------------------
```

```
% Estimation of diffusion coefficient for HCOOH in water by   Hayduk-Minhas

% formula

% Vcac=128; %volume critique

% Vac=0.285*Vcac^1.048; %volume molaire de l'acide formique

Vac=42; a=9.58/Vac-1.12; %règle de Schroeder: Reid and Prausnitz

DA=1.25e-8*((Vac^(-0.19))-0.292)*(Temp^1.52)*(visce^a);%cm2/s

DAme=porosm*DA/taum; DBme=porosm*DB/taum;

DAse=poross*DA/taus; DBse=poross*DB/taus;

% --------------------------------------------------------------------

%          Estimation of the mass transfer coefficients in different reactor

%                                 zones

% ====================================================================

    di=7/10; do=10/10; dlm=(do-di)/log(do/di);

%  di=Inner diameter of the tubular membrane in (mm)

%  do=Outer diameter of the tubular membrane in (mm)

%  dlm= is the logarithmic mean diameter of the membrane

%  ---------------------------------------------------------------------

%

delt=DAse*L*tmax/es/u4*(R3/(R4^2-R3^2)); Pe4=u4*L/DB; Pe1=u1*L/DA;

%====================================================================

RG=1.987; dpore=25e-6; thick=1.5/1000; MO2=32; Do2air=0.000352;


%====================================================================

kBgpore=(poross*thick/taus)/((3/dpore)*(pi*MO2/8/RG/Temp)^(1/2)+1/Do2air)

%====================================================================


H=4.36e3/101.3; % Henery's constant for oxygen

%  kBov= Overall mass transfer coeffiecient in the membrane porous media

kBov=1/(di*(1/kal/di+1/H/kBgpore/dlm+1/kBg/do))

%load Data_PLM.txt -ascii;
```

243

```
% -----------------------------------------------------------------------
 k0=1.4e-3/60; m=1; n=0.5; %(1/s)
 %k=input('rate constant in (1/min)')
 %m=input(' formic acid concentration power')
 %n=input(' Oxygen concentration power')
%cfa=Data_PLM(:,1);
%tmax=em^2/DAme;
%  ------------------   tmax   ------------------------------
%t0=input(' Input t0 ');
%t0=1;
tmax=pi*R1^2*L/(Q1*60) % min
tmaxsec=pi*R1^2*L/(Q1) % sec
t0=tmax;
%tmax=em^2/DAme;
%tmax=em^2/*DAme;t0=tmax;
phi2=k0*em^2*(cA0^0.5)/DAme; alpha=cA0/cB0; bet=(DAse/DAme)*(em/es)^2;
gam=DA*tmax/u1/L;
delt=DAse*L*tmax/es/u1*(R3/(R4^2-R3^2))
 %rexp=Data_PLM(:,2);


% -----------------------------------------------------------------------
oxy1=0.0217 % [mol/L]
display( '- 1 -')
%paramètre de discrétisation
nz=10; ns=5; nm=5; dz=L/(nz-1); drs=es/(ns-1); drm=em/(nm-1);
% dz= cm, drs=cm, drm =cm
z(1)=0; rm(1)=0; rs(1)=0;
h = waitbar(0,'Please wait...');
for i=1:100, % computation here %
waitbar(i/100)
```

244

```matlab
end
close(h)
for i=2:nz;
    z(i)=z(i-1)+dz;
end
for i=2:nm;
    rm(i)=rm(i-1)+drm;
end
for i=2:ns;
    rs(i)=rs(i-1)+drs;
end
% ----------------------------------------------------------
% ----------------------------------------------------------
%          Définition des concentrations initiales
% ----------------------------------------------------------
    CA0(1)=cA0;
    CB0(1)=cB0;
for i=2:nz-1;
    CA0(i)=cA0;
    CB0(i)=cB0;
end
 CA0(nz)=cA0;
    CB0(nz)=cB0;
for i=1:nz;
    for j=1:nm-1;
        CmA0(i,j)=0.001;
    end
    for j=1:nm-1;
        CmB0(i,j)=0.001;
    end
```

```
    CmB0(i,1)=0.001;

    CmB0(i,nm)=0.001;

    %Po2/4.36e3/101.3;

    for j=1:ns-1;

        Cs0(i,j)=0.001;

    end

end

% ----------------------------------------------------------------------

%       time - tspan entering to handle function

% ----------------------------------------------------------------------

%tspan = [0   0.01 0.05 ];

% -------------------------------------------------------------

k=1;

% Enternal Compartiment:  Formic acid

for i=1:nz;

    y0(k)=CA0(i);

    k=k+1;

end


%  ==== Membrane Layer = formic acid-1

for i=1:nz;

    for j=1:nm-1;

        y0(k)=CmA0(i,j);

        k=k+1;

    end

end

%  ==== Membrane Layer = Oxygen-2

for i=1:nz;

    for j=1:nm;

        y0(k)=CmB0(i,j);
```

```matlab
            k=k+1;

        end

end

% ==== Support Layer: Oxygen

for i=1:nz;

    for j=1:ns-1;

        y0(k)=Cs0(i,j);

        k=k+1;

    end

end

% ===== External Compartiment:  Oxygen

for i=1:nz;

    y0(k)=CB0(i);

    k=k+1;

end

% ------------------------------------------------------------------------

%      time - tspan entering to handle function

% ------------------------------------------------------------------------

disp('Hello get-started')

tspan = [0 1];

% ------------------------------------------------------------------------

%tspan = [0  0.01 0.05 ];

% ------------------------------------------------------------------------

% ------------------------------------------------------------------------

%                Input rate equation parameters   k m   n

% ------------------------------------------------------------------------------

 %k=input('rate constant in (1/min)')

 k0=0.2;

 %m=input(' formic acid concentration power')

 m=1;
```

```matlab
%n=input(' Oxygen concentration power')

 n=0.5;

[CPLM]=PLM05mai(k0,m,n,y0,tspan)

%load Data_LHHW.txt -ascii;

% ------------------------------------------------------------------------

%               Input rate equation parameters   k1  k2  k1dash

% ------------------------------------------------------------------------

 %k=input('rate constant in (1/min)')

 k1=0.2;

 %m=input(' formic acid concentration power')

 k2=0.3;

 %n=input(' Oxygen concentration power')

 k1dash=0.1;


%cfa=Data_LHHW(:,1);


% rexp=Data_LHHW(:,2);


% ------------------------------------------------------------------------

oxy1=0.0217 % [mol/L]

display( '- 2 -')

[CLHHW]=LHM05mai(k1,k2,k1dash,y0,tspan)
```

```matlab
%     .....................................................
%      (PLM)          VERSION   ALI ABUSALOUA 06/05/2010
% ....................................................
function [CPLM]=PLM05mai(k0,m,n,y0,tspan)
global phi2 alpha drm drs dz nm nz  ns bet gam delt tmax R1 R2 R3 R4
global es em rm rs Pe1 Pe4 DAme DBme DAse DBse cA0 cB0 DA DB u1 Po2 t0 kal
global kBov u4 n m RG Temp L  tspan  y0 k0  H kBg z
%k1 k1dash k2
% -------------------------z------------------------------
options=odeset('RelTol',1e-5,'AbsTol',1e-5);
[t,y]=ode15s('FPLM200410',tspan,y0,options);


disp('hello again')
% ----------------------------------------------------------
%sauvegarde des concentrations
% ----------------------------------------------------------
k=1;
%compartiment enternbe: acide formique
for i=1:nz;
    CA(:,i)=y(:,k);
    k=k+1;
end
%membrane
%acide formique
for i=1:nz;
    for j=1:nm-1;
        CmA(:,i,j)=y(:,k);
        k=k+1;
    end
end
```

249

```matlab
%oxygène

for i=1:nz;

    for j=1:nm;

        CmB(:,i,j)=y(:,k);

        k=k+1;

    end

end

%support: acide formique

for i=1:nz;

    for j=1:ns-1;

        Cs(:,i,j)=y(:,k);

        k=k+1;

    end

end

%compartiment externbe: oxygene

for i=1:nz;

    CB(:,i)=y(:,k);

    k=k+1;

end

CAPLM=CA

%

%conversion=1-

%slengthZ=length(z)

%ssizeCmA=size(CA)

%=======================================================================

convA=1-CA;

convB=1-CB;

%=======================================================================

figure;

plot(t,CA(:,end),'-')
```

```matlab
xlabel('time t');

ylabel('concentration CA ');

legend('CA LHHW')

Title(' Concentration profile With time by LHHW model')

% ========================================================================

figure;

plot(t,CB(:,end),'-')

xlabel('time t');

ylabel('concentration CB ');

legend('CB LHHW')

Title(' Concentration profile With time by LHHW model')

figure,

plot(t,CA(:,5),'-.',t,CA(:,nz),'.')

xlabel('time t');

ylabel('concentration C ');

legend('CA5 LHHW','CAnz LHHW')

Title(' Concentration profile at different lengths by LHHW model')

%figure;

%plot(t,CmA(:,1),'-',t,CmA(:,3),'-.',t,CmA(:,nm),'.')

figure;

plot(z,CA(end,:),'-')

xlabel('length Z');

ylabel('concentration CA ');

legend('CA LHHW')

Title(' Concentration profile with length by LHHW model')

%========================================

figure;

plot(z,CB(end,:),'-')

xlabel('length Z');

ylabel('concentration CB ');
```

```matlab
legend('CB LHHW')

Title(' Concentration profile with length by LHHW model')

%==========================================


%figure,

%plot(z,CA(end,:),'-')

%==========================================

figure;

plot(t,convA(:,end),'-')

xlabel('time t');

ylabel('convA ');

legend('convA LHHW')

Title(' ConvA profile With time by LHHW model')

% =======================================================================

figure;

plot(t,convB(:,end),'-')

xlabel('time t');

ylabel('convB ');

legend('convB LHHW')

Title(' ConvB profile With time by LHHW model')

figure;

plot(t,CA(:,end),'-')

xlabel('time t');

ylabel('concentration CA ');

legend('CA PLM')

Title(' Concentration profile  with time by PLM model')

% =======================================================================

figure,

xlabel('time t');

ylabel('concentration CA ');
```

```matlab
legend('CA1 PLM', 'CA5 PLM','CAnz PLM')

Title(' Concentration profile  with time by PLM model')

plot(t,CA(:,1),'-',t,CA(:,5),'-.',t,CA(:,nz),'.')

%figure;

%plot(t,CmA(:,1),'-',t,CmA(:,3),'-.',t,CmA(:,nm),'.')

figure;

plot(z,CA(end,:),'-')

xlabel('length Z');

ylabel('concentration CA ');

legend('CA PLM')

Title(' Concentration profile zith length of reactor ')

%==========================================

CPLM=CA;
```

```
% ------------------------------------------------------------
%    (LHHW)              VERSION  ALI ABUSALOUA 06/05/2010
% ............................................................
function [CLHHW]=LHM05mai(k1,k2,k1dash,y0,tspan)
global phi2 alpha drm drs dz nm nz  ns bet gam delt tmax
global R1 R2 R3 R4 es em rm rs Pe1 Pe4 DAme DBme DAse DBse cA0 cB0 DA DB
global u1 L Po2 t0 kal kBov u4 n m k0 k1 k1dash k2 z tspan y0 H kBg RG


% --------------------------------------------------------
%options=odeset('RelTol',1e-5,'AbsTol',1e-5);
[t,y]=ode15s('FLHM05mai',tspan,y0);%,options
disp('hello again')
% --------------------------------------------------------
%sauvegarde des concentrations
% --------------------------------------------------------


k=1;
%compartiment enternbe: acide formique
for i=1:nz;
    CA(:,i)=y(:,k);
    k=k+1;
end
%membrane
%acide formique
for i=1:nz;
    for j=1:nm-1;
        CmA(:,i,j)=y(:,k);
        k=k+1;
    end
end
```

254

```matlab
%oxygène

for i=1:nz;

    for j=1:nm;

        CmB(:,i,j)=y(:,k);

        k=k+1;

    end

end

%support: acide formique

for i=1:nz;

    for j=1:ns-1;

        Cs(:,i,j)=y(:,k);

        k=k+1;

    end

end

%compartiment externbe: oxygene

for i=1:nz;

    CB(:,i)=y(:,k);

    k=k+1;

end

%CALHHW= CA

%position

convA=1-CA;

convB=1-CB;

%slengthZ=length(z)

%ssizeCmA=size(CA)

%=========================================================================

figure;

grid on

plot(t,CA(:,end),'-')

xlabel('time t');
```

```matlab
ylabel('concentration CA ');

legend('CA LHHW')

Title(' Concentration profile With time by LHHW model')

% ========================================================================

figure;

grid on

plot(t,CB(:,end),'-')

xlabel('time t');

ylabel('concentration CB ');

legend('CB LHHW')

Title(' Concentration profile With time by LHHW model')

figure,

plot(t,CA(:,5),'-.',t,CA(:,nz),'.')

xlabel('time t');

ylabel('concentration C ');

legend('CA5 LHHW','CAnz LHHW')

Title(' Concentration profile at different lengths by LHHW model')

%figure;

%plot(t,CmA(:,1),'-',t,CmA(:,3),'-.',t,CmA(:,nm),'.')

figure;

plot(z,CA(end,:),'-')

xlabel('length Z');

ylabel('concentration CA ');

legend('CA LHHW')

Title(' Concentration profile with length by LHHW model')

%figure,

%plot(z,CA(end,:),'-')

%=========================================

figure;

plot(z,CB(end,:),'-')
```

```matlab
xlabel('length Z');

ylabel('concentration CB ');

legend('CB LHHW')

Title(' Concentration profile with length by LHHW model')

%=========================================
figure;

plot(t,convA(:,end),'-')

xlabel('time t');

ylabel('convA ');

legend('convA LHHW')

Title(' ConvA profile With time by LHHW model')

% =======================================================================
figure;

plot(t,convB(:,end),'-')

xlabel('time t');

ylabel('convB ');

legend('convB LHHW')

Title(' ConvB profile With time by LHHW model')

%======================================================================
figure;

plot(t,CA(:,end),'-')

xlabel('time t');

ylabel('concentration C ');

legend('CA LHHW')

Title(' Concentration profile With time by LHHW model')

% =======================================================================
figure,

xlabel('time t');

ylabel('concentration C ');

legend('CA1 LHHW','CA5 LHHW','CAnz LHHW')
```

```matlab
Title(' Concentration profile at different lengths by LHHW model')

plot(t,CA(:,1),'-',t,CA(:,5),'-.',t,CA(:,nz),'.')

%figure;

%plot(t,CmA(:,1),'-',t,CmA(:,3),'-.',t,CmA(:,nm),'.')

figure;

plot(z,CA(end,:),'-')

xlabel('length Z');

ylabel('concentration CA ');

legend('CA LHHW')

Title(' Concentration profile with length by LHHW model')

%figure,

%plot(z,CA(end,:),'-')

%==========================================

CLHHW=CA;

 function [dy] = FPLM05mai(tmax,y)

global phi2 alpha drm drs dz nm nz  ns bet gam delt tmax

global R1 R2 R3 R4 es em rm rs Pe1 Pe4 DAme DBme DAse DBse cA0 cB0 DA DB u1
L

global Po2 t0 kal kBov u4 n m k0 k1 k1dash k2  z tspan y0 H kBg RG Temp

% ========================================================================

% --------------------------------------------------------

%        Definition of the concentrations

% --------------------------------------------------------

k=1;

% ===== Enternal compartiment: Formic acid

for i=1:nz;

    cA(i)=y(k);

    k=k+1;

end

% ====== Membrane Layer =====  1- Formic acid

for i=1:nz;
```

```matlab
    for j=1:nm-1;

        cmA(i,j)=y(k);

        k=k+1;

    end

end

% ==== Membrqne layer ==== 2- Oxygen

for i=1:nz;

    for j=1:nm;

        cmB(i,j)=y(k);

        k=k+1;

    end

end

% ==== Support Layer:  Oxygen

for i=1:nz;

    for j=1:ns-1;

        cs(i,j)=y(k);

        k=k+1;

    end

end

% ====== External compartiment: Oxygen

for i=1:nz;

    cB(i)=y(k);

    k=k+1;

end

% -------------------------------------------------------------------------

%    Equations over Liquid-side - Formic acid

% -------------------------------------------------------------------------


%t0=tmax;
```

```matlab
A1=DA*t0/L^2; Pe1=(u1*L/DA); A3=u1*t0/L; A5=2*DAme*t0/(em*R1);

A6=DAme*t0/L^2; A7=DAme*t0/L/u1; A8=2*DAme*t0/R1; s=DAme/kal/em/drm;

saq=s+1

if saq==0;

    s==1;

else

end

% -------------------------------------------------------------------------

cmA(1,1)=(cA(1)-s*cmA(1,1))/(1+s);

% cmA(1,1) in the left side is the interfacial concentration =cmA(0,1)

% cmA(1,1) in the right side is the concentration t first point =cmA(1,1)

% -------------------------------------------------------------------------


dcA(1)=A1*((cA(2)-cA(1))/dz^2+Pe1*(1-cA(1))/dz)...

    +A3*((1-cA(1))*Pe1)+A5*(cA(1)-cmA(1,1))/drm;

 % -------------------------------------------------------------------------

cmA(i,1)=(cA(i)-s*cmA(i,1))/(1+s);

% cmA(i,1) in the left side is the interfacial concentration =cmA(i-1,1)

% cmA(i,1) in the right side is the concentration t first point =cmA(i,1)

% -------------------------------------------------------------------------

for i=2:nz-1;

 while (cA(i)<0)

dcA(i)=A6*(cA(i+1)-2*cA(i)+cA(i-1))/dz^2 -A3*(cA(i)-cA(i-1))/dz...

+A5*(cA(i)-cmA(i,1))/drm;

 end

end

% -------------------------------------------------------------------------

cmA(nz,1)=(cA(nz)-s*cmA(nz,1))/(1+s);

% cmA(nz,1) in the left side is the interfacial concentration =cmA(nz,1)

% cmA(nz,1) in the right side is the concentration at first point
=cmA(nz,1)
```

260

```matlab
% -------------------------------------------------------------------
dcA(nz)=-A6*(cA(nz)-cA(nz-1))/dz+A7*(cA(nz-1)-cA(nz))/dz^2 ...

+A8*(cA(nz)-cmA(nz,1))/drm;



% ------------------------------------------------------
%       Equations over  Membrane-Layer - Formic acid-1
% ------------------------------------------------------
% ------------------------------------------------------
A9=(DAme*t0/em^2);

for i=1:nz;

    % ...........................................
    %    PLM modeL  #1 ----- rcal=k.*co2.^m*fa^n;
    %    ..........................................;




cmA(i,nm)=cmA(i,nm-1);
dCmA(i,1)=A9*((cmA(i,2)-cmA(i,1))/drm^2-(DAme*ka1/drm^2)*...
    (cmA(i,2)-cmA(i,1))/drm^3+ (em/(em*rm(j)+R1))*(cmA(i,2)-cmA(i,1))...
    /drm)- k0*em^2*cA0^m*cB0^(n-1)*cmA(i,1)^m*cmB(i,1)^n/DAme;



for j=2:nm-1;
    while (cmA(i,j)<0)
    dcmA(i,j)=A9*((em/(em*rm(j)+R1))*(cmA(i,j)-cmA(i,j-1))/drm +...
    (cmA(i,j+1)-2*cmA(i,j)+cmA(i,j-1))/drm^2)-k0*em^2*cA0^m*cB0^(n-1)*...
    cmA(i,j)^m*(cmB(i,j)^n)/DAme;
    end
end
dcmA(i,nm)=A9*((em/(em*rm(nm)+R1))*ka1/DAme*(cmA(i,2)-cmA(i,1))/drm...
    +(cmA(i,nm-1)-cmA(i,nm))/drm^2)-k0*em^2*cA0^m*cB0^(n-1)*cmA(i,nm)^m...
```

261

```matlab
    *(cmB(i,nm)^n)/DAme;


% ----------------------------------------------------------

%       Equations over  Membrane-Layer  - Oxygene- 2

% ----------------------------------------------------------

% ---------------------------------------------------------------------------

%

A10=(DBme*t0/em^2);

cmB(i,nm)=cs(i,1);


dcmB(i,1)=A10*((cmB(i,2)-cmB(i,1))/drm^2)+...

    -2*k0*em*2*cA0^m*cB0^(n-1)*cmA(i,j)^m*(cmB(i,j)^n)/DAme;


for j=2:nm-1;

    while (cmB(i,j)<0)

    dcmB(i,j)=A10*((em/(em*rm(j)+R1))*(cmB(i,j)-cmB(i,j-1))/drm+...

    (cmB(i,j+1)-2*cmB(i,j)+cmB(i,j-1))/drm^2)-2*k0*em*2*cA0^m*cB0^(n-1)*...

    cmA(i,j)^m*(cmB(i,j)^n)/DAme;

    end

end

%dcmB(i,nm)=0.;

dcmB(i,nm)=A10*((em/(em*rm(j)+R1))*kBov/DBme*(cs(i,2)-cs(i,1))/drs+...

    (cmB(i,2)+DBme/kBov*(cmB(i,nm-1)+cmB(i,2))-2*cmB(nm)+cmB(nm-
1))/drm^2)...

    -2*k0*em*2*cA0^m*cB0^(n-1)*cmA(i,j)^m*(cmB(i,j)^n)/DAme;


% ---------------------------------------------------------------------------

% ----------------------------------------------------------

%       Equ1ations over  Support-Layer -  Oxygen

% ----------------------------------------------------------
```

```matlab
PB(i)=cB(i)*RG*Temp;

Vme=18;

xg=1.e-3*(exp(-171.2542+8391.24/Temp)+23.24323*log(Temp))

%cB=Po2/(R*Temp); %g/L

% ------------------------------------------------------------------------

A11=DBse*t0/em^2;

bet=es*DBme/em/drs/drm*DBme;

cs(i,ns)=xg*PB(i)*Vme;




dcs(i,1)=A11*(cs(i,2)-cs(i,1))/drs^2-DBse/kBov*(cmB(i,nm-1)-cs(i))/...

drm^2+(es/(es*rs(1)+R2)*(DBse/kBov)*(cmB(i,nm-1)-cs(i,1))/drs);


for j=2:ns-1;

    while (cs(i,j)<0)

    dcs(i,j)=A11*((cs(i,j+1)-2*cs(i,j)+cs(i,j-1))/drs^2 + ...

    (es/(es*rs(j)+R2))*(cs(i,j)-cs(i,j-1))/drs);

    end

end


dcs(i,ns)=A11*(cs(i,ns-1)-cs(i,ns))/drs^2 + ...

es/(es*rs(j)+R2)*(cs(i,1)-cmB(i,nm-1))+ es/(es*rs(j)+R2)*...

(cs(i,ns)-cs(i,ns-1))/drs;

end



% -------------------------------------------------------

%       Equations over External compartiment  = Oxygen

% -------------------------------------------------------

Pe4=(u4*L/DB);

tmaxmin=t0
```

```matlab
tmaxsec=t0*60

f=kBg*drs/DBse

cs(i,ns-1)=(f+1)*H/PB(i)-f*cB(i)

dcB(1)=((Pe4+t0/dz)*(1-cB(1))+gam*(cB(2)-cB(1))/dz^2 ...

-2*delt*(cB(1)-cs(1,ns-1))/drs)*RG*Temp;


for i=2:nz-1;

    while (cB(i)<0)
dcB(i)=(-(cB(i)-cB(i-1))/dz+gam*(cB(i+1)-2*cB(i)+cB(i-1))/dz^2 ...

-2*delt*(cB(i)-cs(i,ns-1))/drs)*RG*Temp;

    end

end


dcB(nz)=(-(cB(nz)-cB(nz-1))/dz+gam*(cB(nz-1)-cB(nz))/dz^2 ...

-2*delt*(cB(nz)-cs(nz,ns-1))/drs)*RG*Temp;

% -------------------------------------------------------

%  Defination of the Concentration Functions on derivative form

% -------------------------------------------------------


k=1;

% Enternal Compartiment:  Formic acid

for i=1:nz;

    dy(k)=dcA(i);

    k=k+1;

end

  %==== Membrane Layer = formic acid-1

for i=1:nz;

    for j=1:nm-1;

        dy(k)=dcmA(i,j);

        k=k+1;
```

```matlab
        end

    end

%==== Membrane Layer = Oxygen-2

for i=1:nz;

    for j=1:nm;

        dy(k)=dcmB(i,j);

        k=k+1;

    end

end

% ==== Support Layer: Oxygen

for i=1:nz;

    for j=1:ns-1;

        dy(k)=dcs(i,j);

        k=k+1;

    end

end

% ===== External Compartiment:  Oxygen

for i=1:nz;

     dy(k)=dcB(i);

     k=k+1;

end

dy=dy';

return

end
```

APPENDIX C: MATLAB PROGRAM FOR KINETIC PARAMETER ESTIMATIONS OF FORMIC ACID OXIDATION IN MEMBRANE REACTOR

```matlab
% =============================================================================
%
%                        MAIN PROGRAM - (2)
%               KINETIC MODELLING OF FORMIC ACID OXIDATION
%                    IN CATALYTIC MEMBRANE REACTOR
%
%               ---------------------------------------
%
%                        Parameter estimation
%                   PLM model
%
%
%                   Ali ABUSALOUA   DATE: 28 OCTOBRE 2009
%
% ----------------------------------------------------------------------


load Data_FA1PM.txt -ascii;

ko=0.01;

no=0.5;

mo=1.0;

%cfa=Data_OXY1(:,1);

 co2 =Data_FA1PM(:,1);

 cexp=Data_FA1PM(:,2);

 %global rexp,cfa,o2,rcal

% ----------------------------------------------------------------------

FA1=0.0217 % [mol/L]

display( '- 1 -')

[stdFA1]=OXYGFA1(FA1,ko,no,mo,co2,rexp)
```

```matlab
% --------------------------------------------------------------------
load Data_FA2PM.txt -ascii;
ko=0.01;
no=0.5;
mo=1.0;
%cfa=Data_OXY1(:,1);
 co2 =Data_FA2PM(:,1);
 cexp=Data_FA2PM(:,2);
 %global rexp,cfa,o2,rcal
% --------------------------------------------------------------------
FA2=0.0217 % [mol/L]
display( '- 1 -')
[stdFA2]=OXYGFA2(FA2,ko,no,mo,co2,rexp)
% --------------------------------------------------------------------
load Data_FA3PM.txt -ascii;
ko=0.01;
no=0.5;
mo=1.0;
%cfa=Data_OXY1(:,1);
 co2 =Data_FA3PM(:,1);
 cexp=Data_FA3PM(:,2);
 %global rexp,cfa,o2,rcal
% --------------------------------------------------------------------
FA3=0.0217 % [mol/L]
display( '- 1 -')
[stdFA3]=OXYGFA3(FA3,ko,no,mo,co2,rexp)
% --------------------------------------------------------------------
load Data_FA4PM.txt -ascii;
ko=0.01;
no=0.5;
```

```matlab
mo=1.0;

%cfa=Data_OXY1(:,1);

 co2 =Data_FA4PM(:,1);

 cexp=Data_FA4PM(:,2);

 %global rexp,cfa,o2,rcal

% ----------------------------------------------------------------------

FA4=0.0217 % [mol/L]

display( '- 1 -')

[stdFA4]=OXYGFA4(FA4,ko,no,mo,co2,rexp)

% ----------------------------------------------------------------------

load Data_FA5PM.txt -ascii;

ko=0.01;

no=0.5;

mo=1.0;

%cfa=Data_OXY1(:,1);

 co2 =Data_FA5PM(:,1);

 cexp=Data_FA5PM(:,2);

 %global rexp,cfa,o2,rcal

% ----------------------------------------------------------------------

FA5=0.0217 % [mol/L]

display( '- 1 -')

[stdFA5]=OXYGFA5(FA5,ko,no,mo,co2,rexp)

% ----------------------------------------------------------------------



% ======================================================================

%

%                         MAIN PROGRAM - (3)

%              KINETIC MODELLING OF FORMIC ACID OXIDATION

%                 IN CATALYTIC MEMBRANE REACTOR

%                 ----------------------------------------
```

```
%
%                        Parameter estimation based on
%                    Langmuir.Hinshelwood reaction rate model
%
%
%
%                    Ali ABUSALOUA   DATE: 28 OCTOBRE 2009
% ----------------------------------------------------------------------


load Data_FA1LM.txt -ascii;
ko=0.01;
k1dash0=0.5;
k20=1.00;
%cfa=Data_OXY1(:,1);
 co2 =Data_FA1LM(:,1);
 rexp=Data_FA1LM(:,2);
 %global rexp,cfa,o2,rcal
% ----------------------------------------------------------------------
FA1=0.0217 % [mol/L]
display( '- 1 -')
[stdFA1LH]=OXYGFA1LH(FA1,ko,k1dash0,k20,co2,rexp)
% ----------------------------------------------------------------------
load Data_FA2LM.txt -ascii;
ko=0.01;
k1dash0=0.5;
k20=1.00;
%cfa=Data_OXY1(:,1);
 co2 =Data_FA2LM(:,1);
 rexp=Data_FA2LM(:,2);
 %global rexp,cfa,o2,rcal
```

```
% --------------------------------------------------------------------

FA2=0.0217 % [mol/L]

display( '- 1 -')

[stdFA2LH]=OXYGFA2LH(FA2,ko,k1dash0,k20,co2,rexp)



% --------------------------------------------------------------------

load Data_FA3LM.txt -ascii;

ko=0.01;

k1dash0=0.5;

k20=1.00;

%cfa=Data_OXY1(:,1);

 co2 =Data_FA3LM(:,1);

 rexp=Data_FA3LM(:,2);

 %global rexp,cfa,o2,rcal

% --------------------------------------------------------------------

FA3=0.0217 % [mol/L]

display( '- 1 -')

[stdFA3LH]=OXYGFA3LH(FA3,ko,k1dash0,k20,co2,rexp)

% --------------------------------------------------------------------

load Data_FA4LM.txt -ascii;

ko=0.01;

k1dash0=0.5;

k20=1.00;

%cfa=Data_OXY1(:,1);

 co2 =Data_FA4LM(:,1);

 rexp=Data_FA4LM(:,2);

 %global rexp,cfa,o2,rcal

% --------------------------------------------------------------------

FA4=0.0217 % [mol/L]

display( '- 1 -')
```

```matlab
[stdFA4LH]=OXYGFA4LH(FA4,ko,k1dash0,k20,co2,rexp)

% -------------------------------------------------------------------

load Data_FA5LM.txt -ascii;

ko=0.01;

k1dash0=0.5;

k20=1.00;

%cfa=Data_OXY1(:,1);

 co2 =Data_FA5LM(:,1);

 rexp=Data_FA5LM(:,2);

 %global rexp,cfa,o2,rcal

% -----------------------------------------------------------------

FA5=0.0217 % [mol/L]

display( '- 1 -')

[stdFA5LH]=OXYGFA5LH(FA5,ko,k1dash0,k20,co2,rexp
```

271

6. COMMUNICATIONS AND PUBLICATIONS

6.1.1 Publications

•M. Dotzauer. M., Abusaloua A., Miachon S., Dalmon J-A, Bruening. L., Wet air oxidation with tubular ceramic membranes modified with polyelectrolyte/Pt nanoparticle films, Applied catal. B:Environ. 91 (2009) 180-188.

• M. Alame, A. Abusaloua, M. Pera-Titus, N. Guilhaume, K. Fiaty, A. Giroir-Fendler, High-performance catalytic wet airoxidation (CWAO) of organic acids and phenol in interfacial catalytic membrane contactors under optimized wetting conditions, CatalysisToday xxx (2010) xxx–xxx, article in press.

• A. Abusaloua, E. Iojoiu, K. Fiaty, A. Giroir-Fendler, Bimetallic catalysts for wet air oxidation of model compound solutions in membrane reactors, article in preparation.

• A. Abusaloua, K. Fiaty, A. Giroir-Fendler, Membrane reactor modelling by coupling reaction kinetics and reactor hydrodynamics, article in preparation.

6.1.2 Communications

• A. Abusaloua, M. Alame, M. Pera-Titus, N. Guilhaume, A. Giroir-Fendler, S. Miachon, K. Fiaty, J-A. Dalmon Catalytic Membrane Reactors for Wastewater Treatment, Poster presentation, Tomorrow… toward a selected chemistry, 3rd edition:' Catalysis and sustainable Development, CPE-Lyon, France, 19-20 November 2008.

• A. Abusaloua, M. Alame, M. Pera-Titus, N. Guilhaume, A. Giroir-Fendler, S. Miachon, K. Fiaty, J-A. Dalmon, High performance Wet Air Oxidation (WAO) of organic pollutants using a Catalytic membrane reactor. KeyNote presentation, 9th International Congress on Catalytic Membrane Reactors (ICCMR-9), Lyon, France, 28th June - 2nd July 2009.

•M. Alame, A. Abusaloua, M. Pera-Titus, N. Guilhaume, A. Giroir-Fendler, S. Miachon, K. Fiaty, J-A. Dalmon, High performance Wet Air Oxidation (WAO) of organic pollutants using a Catalytic membrane reactor. KeyNote presentation, Congress of EUROMEMBRANE2009, Montpellier, France, 6-10 September 2009.

• M. Alame, A. Abusaloua, M. Pera-Titus, N. Guilhaume, A. Giroir-Fendler, S. Miachon, K. Fiaty, J-A. Dalmon, Effect of wetting on the Catalytic performance of membrane reactor for Wet Air Oxidation (WAO) of organic pollutants. Oral presentation, 6th world Congress on oxidation catalysis, Lille, France, July 2009

Titre de la thèse :

Réacteur catalytique membranaire pour le traitement d'effluents liquides.

Catalytic membrane reactor for waste water treatments

Résumé:

L'objectif de cette étude portait sur la mise en oeuvre de réacteur catalytique membranaire pour une application dans le traitement d'effluents liquides contaminés par des polluants organiques. Des phases catalytiques ont été déposées au sein des structures poreuses par différentes techniques afin de bien maîtriser la localisation des phases actives. L'optimisation des conditions opératoires a ensuite été réalisée. Ces matériaux sont actifs pour l'oxydation de polluants présents dans les effluents liquides et la configuration en mode contacteur a permis d'accroître l'efficacité et la stabilité des phases catalytiques pour ces réactions de dégradation grâce à un meilleur contact entre les réactifs et les sites actifs.

Mot-clés : Oxydation catalytique, OVH, réacteur membranaire, catalyseurs métaux supportés

Abstract

The aim of this study was to evaluate catalytic membrane reactor for wet oxidation efficiencies of pollutants in waste water. In a first part, we have prepared catalytic membrane using several techniques of deposition in order to well control the position of the active phase in the porous structure. After optimisation of the experimental parameters, the study of pollutant degradation has showed that catalytic membrane reactor, in contactor configuration present highest efficiency than conventional reactor due to optimized contacts between reactants and active sites.

Keywords: Catalytic oxidation, CWAO, membrane reactor, supported metal catalysts

Discipline: Chimie

Intitulé et adresse du laboratoire : Institut de Recherches sur la Catalyse et l'environnement de Lyon (IRCELyon), 2 avenue Albert Einstein. 69626 Villeurbanne Cedex